

UNIVERSITY OF CALGARY

Structure-Function Analysis of the Human Telomerase Reverse Transcriptase

by

Haley Doris Myskiw Wyatt

A THESIS

SUBMITTED TO THE FACULTY OF GRADUATE STUDIES  
IN PARTIAL FULFILMENT OF THE REQUIREMENTS FOR THE  
DEGREE OF DOCTOR OF PHILOSOPHY

DEPARTMENT OF BIOCHEMISTRY AND MOLECULAR BIOLOGY

CALGARY, ALBERTA

SEPTEMBER, 2009

© Haley Doris Myskiw Wyatt 2009



UNIVERSITY OF  
CALGARY

The author of this thesis has granted the University of Calgary a non-exclusive license to reproduce and distribute copies of this thesis to users of the University of Calgary Archives.

Copyright remains with the author.

Theses and dissertations available in the University of Calgary Institutional Repository are solely for the purpose of private study and research. They may not be copied or reproduced, except as permitted by copyright laws, without written authority of the copyright owner. Any commercial use or re-publication is strictly prohibited.

The original Partial Copyright License attesting to these terms and signed by the author of this thesis may be found in the original print version of the thesis, held by the University of Calgary Archives.

Please contact the University of Calgary Archives for further information:

E-mail: [uarc@ucalgary.ca](mailto:uarc@ucalgary.ca)

Telephone: (403) 220-7271

Website: <http://archives.ucalgary.ca>

## Abstract

Telomeres are essential nucleoprotein structures that protect chromosome ends and maintain genome stability. Telomerase is the cellular reverse transcriptase (RT) that synthesizes telomeric DNA at chromosome 3'-ends. The minimal components for enzyme activity *in vitro* are a catalytic protein subunit, the telomerase reverse transcriptase (TERT), encoded by the *TRT* gene, and an RNA subunit, the telomerase RNA (TR). Telomerase is unique among the RT proteins in its ability to processively synthesize telomeric repeats, which is facilitated by DNA-binding domains in TERT called anchor sites.

We developed the first DNA-binding assay to characterize interactions between hTERT and ssDNA primers *in vitro*. Our results were the first to show that hTERT interacts sequence-specifically with telomeric ssDNA in the absence of hTR. We also identified several hTERT variants that bind, but do not extend, telomeric ssDNA primers. Our studies uncovered multiple anchor regions in hTERT that may co-operate during primer binding and extension.

Structural and biochemical studies indicate that an anchor region resides in the TERT N-terminus. A phylogenetically-conserved Gln is critical for telomerase anchor site function in lower eukaryotes. We determined the biochemical and cellular significance of this residue in human telomerase (hTERT Q169). Our studies uncovered an essential role for Q169 in telomerase activity *in vitro* and *in vivo*. We provided the first evidence that Q169 regulates conformational changes in the hTERT N-terminus that

facilitate nucleotide incorporation. Collectively, our results indicate that Q169 resides in an evolutionarily-conserved anchor region.

Mutations in the human *TRT* gene have been identified in patients with the disease dyskeratosis congenita and variants thereof. These patients have telomeres that are significantly shorter than age-matched controls, suggesting that the underlying disease mechanism is telomerase deficiency. We performed biochemical studies to understand specifically how these mutations affect telomerase function *in vitro*. Our results have provided fundamental insight into hTERT structure and function and may ultimately lead to novel therapeutic strategies for patients afflicted with dyskeratosis congenita.

## Preface

### **Publications included as part of this thesis:**

**Chapter 3: Wyatt HDM, Lobb DA, and Beattie TL.** Characterization of physical and functional anchor site interactions in human telomerase. *Mol Cell Biol* 2007; 27(8):3226-3240.

**Chapter 4: Wyatt HDM, Tsang AR, Lobb DA, and Beattie TL.** Human telomerase reverse transcriptase (hTERT) Q169 is essential for telomerase function *in vitro* and *in vivo*. *PLoS ONE* 2009; In Press: Manuscript # 09-PONE-RA-11510.

### **Contributions to thesis work:**

**Haley Wyatt** designed, analyzed, and interpreted the experiments presented in this thesis and wrote all of the manuscripts with support from **Dr. Tara Beattie**. The candidate performed most of the experiments and has demonstrated the ability to perform the experimental techniques described herein. The contribution of other individuals to the data presented in this thesis is described below:

**Deirdre Lobb** performed the standard conventional telomerase activity assays described in Chapters 3, 4, and 5.

**Allison Tsang** performed the pulse-chase conventional telomerase activity assays and performed and analyzed the terminal restriction fragment studies described in Chapter 4.

## Acknowledgements

I would first like to thank my supervisor, Tara Beattie, for accepting me into her lab and giving me the opportunity to pursue my interest in telomerase biochemistry. I have learned how to be an efficient and independent researcher. This will be an invaluable asset to my future scientific career.

Thank you to my supervisory committee for their time, advice, support, and interests in my research and future career: Dr. George Chaconas, Dr. Karl Riabowol, and Dr. Susan Lees-Miller. I would also like to thank each of you and your lab members for allowing me to use various reagents and instruments during the course of my graduate work. Furthermore, I want to thank all of the professors that were involved in my candidacy and thesis examinations: Dr. Katherine Friedman, Dr. Ebba Kurz, and Dr. Greg Moorhead. I sincerely appreciate your willingness to contribute to my education. I would also like to acknowledge and thank Dr. Christopher Counter for various reagents, scientific methods, and technical advice.

I would next like to acknowledge past and present members of the Beattie lab for their support and advice on scientific and personal matters: Allison, Brant, Deirdre, Denise, Chris, Nick, and Paul, I owe each of you many thanks for your contributions to my research, scientific training, and for lots of laughs during tough times. I would like to thank Brant for his work on the initial stages of the primer binding assay. I want to offer a very special thanks to Allison for being such a remarkable friend and person. I would also like to say thank you to my past lab-mates Dr. Ebba Kurz, Jason, and Danielle, for taking

the time to teach me about various scientific matters and for providing an enthusiastic, friendly, and enjoyable environment.

Thank you to Dr. Tanya Dahms, Dr. Carmela Jackson-Lepage, and Greg Whittle for everything that you have taught me about science and life. You are truly great mentors and friends and I have been inspired by each of you. Thank you for believing in me and for helping me to believe in myself.

I would like to express my gratitude to Tiz Reiter and Aerin Caley for all of their help with administrative forms and various aspects of my graduate work. I also want to thank my graduate program co-ordinator, Judy Gayford, for answering all of my program-related inquiries and for ensuring that I completed all the documentation required for my degree.

Finally, and most importantly, thank you to my family for their love, encouragement, and support: Mom, Dad, Ashley, Grandpa and Grandma Myskiw, Grandma Wyatt, Aunty Patty and Uncle Jim, Aunty Kathy and Uncle David, and Lyndsay and Brandon. I want to acknowledge my Grandad Wyatt, whom I believe would have offered me the same love and support if he had been with me during this incredible journey. Thank you all for believing in me and for giving me the courage to follow my dreams. And how could I ever forget my wonderful pets, past and present, who give me unconditional love: George I and II, Smoochy, Pete, Rambo, Gypsy, Phoenix, Waffles, Shoelace, Truffles, Roy, and Jigger.

## **Dedication**

*To my parents, Gordon and Maurena,  
and my sister, Ashley.  
Thank you for believing in me.*

## Table of Contents

Abstract.....	ii
Preface.....	iv
Acknowledgements.....	v
Dedication.....	vii
Table of Contents.....	viii
List of Tables.....	xii
List of Figures and Illustrations.....	xiv
List of Symbols, Abbreviations and Nomenclature.....	xviii
CHAPTER ONE: INTRODUCTION.....	1
1.1 Telomeres.....	1
1.1.1 Subtelomeres.....	1
1.1.2 Telomeric double-stranded DNA.....	5
1.1.3 Telomeric single-stranded DNA.....	7
1.1.4 The telomere loop.....	7
1.1.5 Telomere-associated proteins.....	10
1.2 Telomeres and the DNA Damage Response.....	15
1.2.1 The telomere damage response.....	15
1.2.2 Repression of the DNA damage response at telomeres.....	17
1.2.3 The fate of dysfunctional telomeres.....	17
1.2.3.1 Non-homologous end joining.....	18
1.2.3.2 Homologous recombination.....	18
1.2.4 Minimal requirements for telomere function.....	23
1.3 Telomere Replication and Regulation.....	24
1.3.1 Semi-conservative telomere replication.....	24
1.3.2 The end replication problem.....	25
1.3.3 Telomerase-dependent telomere maintenance.....	26
1.4 The Telomerase Ribonucleoprotein.....	30
1.4.1 Discovery.....	31
1.4.2 The telomerase reverse transcriptase subunit.....	33
1.4.2.1 Structure.....	33
1.4.2.2 DAT domains.....	39
1.4.2.3 Cellular expression and localization.....	40
1.4.3 The telomerase RNA subunit.....	41
1.4.3.1 Structure.....	41
1.4.3.2 Cellular expression and localization.....	44
1.4.4 Telomerase-associated proteins.....	45
1.4.4.1 The core TR H/ACA-binding proteins: Dyskerin, NHP2, and NOP10.....	45
1.4.4.2 Pontin and reptin.....	46
1.4.4.3 TCAB1.....	47
1.5 Telomerase RNP Biogenesis, Assembly, and Localization.....	48
1.5.1 Biogenesis.....	48
1.5.2 Assembly.....	51
1.5.3 Subcellular Localization.....	53

1.6 The Telomerase Reaction Cycle and Telomere Synthesis.....	53
1.6.1 An overview of the telomerase reaction cycle .....	54
1.6.2 Repeat addition processivity.....	57
1.6.3 Telomerase anchor sites .....	58
1.6.3.1 Primer recognition .....	58
1.6.3.2 Primer elongation.....	60
1.6.3.3 An evolutionarily-conserved anchor region in the TEN domain.....	61
1.7 Telomeres, Telomerase and Human Disease .....	62
1.7.1 Cellular senescence and aging.....	62
1.7.2 Cellular immortalization and cancer .....	66
1.7.3 Telomere maintenance without telomerase .....	68
1.7.4 Telomerase deficiency and human disease.....	69
1.8 Objectives .....	72
CHAPTER TWO: MATERIALS AND METHODS .....	74
2.1 Reconstitution of Human Telomerase .....	74
2.1.1 Cloning of hTERT constructs.....	74
2.1.1.1 Expression vectors .....	74
2.1.1.2 Enzymes and bacteria .....	74
2.1.1.3 Full Length (FL) hTERT .....	75
2.1.1.4 hTERT truncations.....	75
2.1.1.5 FL hTERT mutants .....	80
2.1.2 hTR synthesis and purification.....	86
2.1.3 In vitro synthesis of human telomerase .....	87
2.2 Cell Culture.....	87
2.2.1 Cell lines and culture conditions .....	87
2.2.2 Generation of 293T stable cell lines.....	88
2.2.3 Retroviral infections for generation of BJ stable cell lines .....	89
2.2.4 Harvesting cells .....	90
2.2.5 Cell lysis .....	91
2.2.6 $\beta$ -galactosidase staining.....	91
2.2.7 Indirect immunofluorescence .....	92
2.3 DNA Analysis.....	93
2.3.1 Oligonucleotide sequences and synthesis.....	93
2.3.2 Oligonucleotide radiolabelling .....	93
2.3.3 Terminal restriction fragment analysis.....	95
2.3.3.1 Synthesis of molecular weight marker DNA.....	95
2.3.3.2 Synthesis of telomeric DNA probe.....	95
2.3.3.3 In-gel hybridization.....	96
2.3.3.4 Quantification of telomere length.....	97
2.4 Protein Analysis.....	97
2.4.1 Limited proteolysis of radiolabelled hTERT.....	97
2.4.2 anti-FLAG immunoprecipitation.....	98
2.4.3 Western blotting .....	99
2.4.4 Coimmunoprecipitation of hTERT-hTR complexes .....	100
2.4.4.1 Synthesis of [ $\alpha$ - <sup>32</sup> P]UTP-labelled hTR .....	100
2.4.4.2 <i>In vitro</i> reconstitution of radiolabelled human telomerase .....	101

2.4.4.3 Coimmunoprecipitation .....	101
2.5 Primer Binding Assay .....	103
2.5.1 Synthesis of radiolabelled hTERT .....	103
2.5.2 DNA-binding .....	103
2.5.3 Quantification .....	105
2.5.4 Statistical analysis .....	107
2.6 Telomerase Activity Assays .....	107
2.6.1 Telomere repeat amplification protocol .....	107
2.6.2 Conventional telomerase activity assay .....	108
2.6.3 Pulse-chase conventional telomerase activity assay .....	111
2.6.4 Quantification of conventional telomerase activity assay data .....	112
2.6.5 Statistical analysis of conventional telomerase activity assay data .....	114
CHAPTER THREE: CHARACTERIZATION OF PHYSICAL AND FUNCTIONAL ANCHOR SITE INTERACTIONS IN HUMAN TELOMERASE .....	115
3.1 Preface .....	115
3.2 Summary .....	115
3.3 Results .....	116
3.3.1 hTERT interacts sequence-specifically with telomeric ssDNA in the absence of hTR .....	116
3.3.2 Investigating the relationship between physical and functional hTERT- DNA interactions .....	126
3.3.3 Primer binding can be functionally uncoupled from primer utilization .....	127
3.3.4 Identification of hTERT regions required for stable interaction with telomeric ssDNA .....	132
3.3.5 Identification and characterization of hTERT primer grip regions .....	143
3.3.6 hTERT DAT regions are involved in primer binding and utilization .....	153
3.4 Discussion .....	160
3.4.1 hTERT interacts with telomeric ssDNA in the absence of hTR .....	160
3.4.2 Primer binding can be functionally uncoupled from primer utilization .....	161
3.4.3 Evidence for multiple DNA-binding sites in hTERT .....	163
3.4.4 Contribution of a specific region within the hTERT N-terminus to primer recognition and utilization .....	164
3.4.5 hTERT primer grip regions are involved in primer binding and utilization .....	165
3.4.6 Not all DATs are created equal .....	166
3.4.7 Perspectives .....	168
CHAPTER FOUR: HUMAN TELOMERASE REVERSE TRANSCRIPTASE (hTERT) Q169 IS ESSENTIAL FOR TELOMERASE FUNCTION <i>IN VITRO</i> AND <i>IN VIVO</i> .....	171
4.1 Preface .....	171
4.2 Summary .....	171
4.3 Results .....	172
4.3.1 Q169 mediates the polymerase function of human telomerase in vitro .....	172
4.3.2 Biochemical characterization of hTERT Q169 .....	180
4.3.3 hTERT Q169A, Q169D, and Q169N retain sequence-specific ssDNA- binding activity .....	188

4.3.4 The hTERT TEN domain does not stably associate with ss telomeric DNA in vitro .....	201
4.3.5 Q169 mediates the ability of truncated hTERT proteins to interact with ssDNA.....	201
4.3.6 Q169 mediates the cellular functions of human telomerase.....	205
4.4 Discussion.....	216
4.4.1 hTERT Q169 is needed to reconstitute robust human telomerase activity in vitro.....	216
4.4.2 Q169 mediates conformational flexibility of the hTERT N-terminus .....	220
4.4.3 hTERT Q169 mutants physically interact with hTR.....	221
4.4.4 Q169 mediates ssDNA-binding activity in hTERT.....	222
4.4.5 Conceptual model to describe the catalytic phenotype of hTERT Q169 mutants.....	224
4.4.6 Perspectives .....	226
 CHAPTER FIVE: <i>IN VITRO</i> ANALYSIS OF NATURALLY-OCCURRING HTERT MUTANTS .....	
5.1 Preface .....	227
5.2 Results.....	227
5.2.1 Characterization of hTERT mutants found in patients with dyskeratosis congenita.....	227
5.2.2 Characterization of hTERT mutants found in patients with idiopathic pulmonary fibrosis .....	238
5.3 Discussion.....	245
5.3.1 Discussion of hTERT mutants associated with dyskeratosis congenita.....	245
5.3.2 Discussion of hTERT mutants associated with idiopathic pulmonary fibrosis.....	250
5.3.3 Perspectives .....	254
 CHAPTER SIX: FUTURE DIRECTIONS AND CONCLUSIONS.....	
6.1 General Discussion .....	255
6.2 Future Directions .....	256
6.2.1 Contribution of the telomerase RNA subunit and telomerase-associated proteins to ssDNA-binding .....	256
6.2.2 Understanding hTERT mutations in relation to the telomerase holoenzyme.....	258
6.2.3 Cellular significance of naturally-occurring hTERT mutants .....	258
6.3 Conclusions and Perspectives.....	259
 REFERENCES .....	 262

## List of Tables

Table 1.1: Examples of telomeric simple-sequence repeats in select organisms .....	3
Table 1.2: Shelterin proteins in select organisms .....	12
Table 1.3: Examples of human telosome proteins .....	13
Table 1.4: Examples of telomerase-associated proteins in select organisms.....	49
Table 2.1 Description of ssDNA primers used in primer binding studies, conventional telomerase activity assays, and the telomere repeat amplification protocol. ....	94
Table 3.1: Description of ssDNA primers used in primer binding studies and conventional telomerase activity assays. ....	117
Table 3.2: Quantification of activity and repeat addition processivity observed for human telomerase reconstituted with hTERT primer grip mutants.....	151
Table 3.3: Quantification of DNA synthesis and repeat addition processivity observed for human telomerase reconstituted with hTERT DAT mutants. ....	159
Table 3.4: Summary of the primer binding and conventional telomerase activity assay results obtained with the hTERT constructs and bio-TELO18 or bio-TELO6.....	169
Table 4.1: Quantification of DNA synthesis and repeat addition processivity observed for telomerase Q169 mutants with primer bio-TELO18.....	176
Table 4.2: Description of ssDNA primers used in the primer binding studies of hTERT Q169, Q169A, Q169D, and Q169N.....	195
Table 4.3: Effect of hTERT Q169A on bulk telomere length in 293T transformed human embryonic kidney cells. ....	212
Table 4.4: Effect of hTERT Q169A on bulk telomere length in BJ fibroblasts. ....	215
Table 5.1: Quantification of DNA synthesis and repeat addition processivity observed for telomerase mutants associated with DC.....	233
Table 5.2: Description of ssDNA primers used in the primer binding studies and conventional telomerase activity assays of disease-associated hTERT mutations. ....	235
Table 5.3: Quantification of DNA synthesis and repeat addition processivity observed for telomerase mutants associated with IPF.....	242
Table 5.4: Summary of the <i>in vitro</i> DNA synthesis, repeat addition processivity, and ssDNA-binding activities of hTERT mutants associated with DC.....	246

Table 5.5: Summary of the *in vitro* DNA synthesis, repeat addition processivity, and ssDNA-binding activities of hTERT mutants associated with IPF. .... 252

## List of Figures and Illustrations

Figure 1.1: Human telomere architecture. ....	2
Figure 1.2: Subtelomere structure and variation. ....	4
Figure 1.3: T-loops and D-loops. ....	8
Figure 1.4: Human telomere-associated proteins. ....	11
Figure 1.5: Shelterin composition. ....	14
Figure 1.6: The telomere damage response. ....	16
Figure 1.7: Telomere-sister chromatid exchange. ....	20
Figure 1.8: T-loop homologous recombination. ....	21
Figure 1.9: Telomere recombination with interstitial telomeric DNA. ....	22
Figure 1.10: The end-replication problem and telomere processing. ....	27
Figure 1.11: Linear architecture of the human telomerase reverse transcriptase. ....	34
Figure 1.12: Secondary structure of the vertebrate telomerase RNA. ....	42
Figure 1.13: The telomerase reaction cycle. ....	55
Figure 1.14: The relationship between telomerase, telomere length, and cellular lifespan. ....	64
Figure 2.1: Schematic of the primer binding assay. ....	106
Figure 2.2: Schematic of the telomere repeat amplification protocol. ....	109
Figure 2.3: Schematic of the conventional telomerase activity assay. ....	110
Figure 3.1: Optimizing the primer binding assay. ....	119
Figure 3.2: hTERT interacts sequence-specifically with telomeric ssDNA <i>in vitro</i> . ....	120
Figure 3.3: hTERT binds 5'-biotinylated primers containing different lengths telomeric ssDNA. ....	122
Figure 3.4: Telomerase extends 5'-biotinylated ssDNA primers containing different lengths of telomeric DNA <i>in vitro</i> . ....	124
Figure 3.5: hTERT D712A binds telomeric ssDNA as efficiently as WT hTERT. ....	128

Figure 3.6 Human telomerase reconstituted with hTERT D712A is catalytically inactive.....	130
Figure 3.7: Schematic summary of the hTERT truncation mutants tested in the primer binding assay.....	133
Figure 3.8: hTERT deletion constructs are stably expressed <i>in vitro</i> . ....	134
Figure 3.9: Identification of hTERT N-terminal regions required to support a stable and sequence-specific interaction with telomeric ssDNA. ....	136
Figure 3.10: The hTERT N-terminus is important for telomeric ssDNA-binding activity <i>in vitro</i> . ....	138
Figure 3.11: Contribution of the hTERT CTE and RT domain to telomeric ssDNA-binding activity <i>in vitro</i> . ....	140
Figure 3.12: Conservation of the telomerase reverse transcriptase domain. ....	144
Figure 3.13: Amino acid sequence of hTERT indicating the locations of the primer grip regions within the N-terminus and RT domain. ....	146
Figure 3.14: hTERT primer grip regions are involved in regulating the strength and sequence-specificity of interactions with telomeric ssDNA. ....	147
Figure 3.15: hTERT primer grip regions are important for primer extension. ....	149
Figure 3.16: hTERT DAT regions are involved in primer binding. ....	155
Figure 3.17: hTERT DAT regions are involved in primer utilization. ....	157
Figure 4.1: <i>In vitro</i> activity of telomerase reconstituted with hTERT Q169 mutants. ....	174
Figure 4.2: hTERT Q169 mutants exhibit defects in overall DNA synthesis. ....	175
Figure 4.3: Repeat addition processivity of hTERT Q169 mutants.....	178
Figure 4.4: Substitution of hTERT Q169 does not alter protein stability <i>in vitro</i> . ....	181
Figure 4.5: hTERT Q169 mutants show subtle differences in the proteolytic cleavage pattern following treatment with chymotrypsin.....	182
Figure 4.6: Q169 modulates hTERT conformation in an hTR-independent manner. ....	183
Figure 4.7: Time-course proteolytic digestion of hTERT WT and Q169 mutants in the absence of hTR. ....	184
Figure 4.8: Time-course proteolytic digestion of telomerase reconstituted with hTR and hTERT WT or Q169 mutants.....	186

Figure 4.9: Time-course proteolytic digestion of 1-300 hTERT WT and Q169 mutants in the absence of hTR. ....	189
Figure 4.10: Time-course proteolytic digestion of telomerase reconstituted with hTR and 1-300 hTERT WT or Q169 mutants. ....	191
Figure 4.11: Substitution of Q169 does not abrogate hTERT-hTR interactions. ....	193
Figure 4.12: hTERT WT and Q169 mutants physically interact with telomeric ssDNA. ....	196
Figure 4.13: hTERT Q169 mutants do not exhibit altered sequence-specific ssDNA-binding activity <i>in vitro</i> . ....	199
Figure 4.14: The hTERT TEN domain does not interact with human telomeric ssDNA at levels that exceed background binding. ....	202
Figure 4.15: hTERT 1-300 WT and Q169 mutants physically interact with human telomeric ssDNA. ....	203
Figure 4.16: hTERT 1-300 Q169 mutants exhibit reduced primer binding with certain ssDNA primers <i>in vitro</i> . ....	206
Figure 4.17: hTERT Q169 is required for telomerase activity in transformed human cells. ....	209
Figure 4.18: hTERT Q169A is not excluded from the nucleus in human cells. ....	210
Figure 4.19: hTERT Q169 is required for telomere elongation in transformed human embryonic kidney cells. ....	211
Figure 4.20: hTERT Q169 is required for telomerase activity in primary human fibroblasts. ....	213
Figure 4.21: hTERT Q169 is required for telomere length maintenance in primary human fibroblasts. ....	214
Figure 4.22: Q169 is required for the biological activities of hTERT in primary human cells. ....	217
Figure 4.23: Primary human cells expressing hTERT Q169A enter replicative senescence. ....	218
Figure 5.1: Linear architecture of the human telomerase reverse transcriptase showing the locations of various naturally-occurring mutations. ....	228
Figure 5.2: <i>In vitro</i> activity of telomerase reconstituted with distinct hTERT mutants identified in DC patients. ....	231

Figure 5.3: Analysis of the activity and repeat addition processivity of telomerase mutants associated with DC.....	232
Figure 5.4: Analysis of the telomeric ssDNA-binding activity of hTERT mutants associated with DC <i>in vitro</i> .....	236
Figure 5.5: <i>In vitro</i> activity of telomerase reconstituted with distinct hTERT mutants identified in patients afflicted with IPF.....	239
Figure 5.6: Analysis of the activity and repeat addition processivity of telomerase mutants associated with IPF.....	240
Figure 5.7: Analysis of the telomeric ssDNA-binding activity of hTERT mutants associated with IPF <i>in vitro</i> .....	243

## List of Symbols, Abbreviations and Nomenclature

### Units of Measure

bp	base pair
Ci	curie
cm	centimetre
CO <sub>2</sub>	carbon dioxide
cpm	counts per minute
× g	units of gravity
g	gram
h	hour
Kb	kilobase
mM	millimolar
min	minute
M	molar
mm	millimetre
mmol	millimole
mL	millilitre
mCi	millicurie
mpd	mean population doubling
ng	nanogram
nm	nanometre
nt	nucleotide
p	probability
pmol	picomole
s	second
SEM	standard error of the mean
U	units
µg	microgram
µL	microlitre
µm	micrometer
V	volt
vol/vol	mL solute per 100 mL solution
wt/wt	g solute per 100 g solution
wt/vol	g solute per 100 mL solution
°C	degrees celsius
%	percent

### Materials and Methods

bio	biotin
CaCl	calcium chloride
CHAPS	3-[(3-cholamidopropyl)dimethylammonio]-1-propanesulfonate
coIP	co-immunoprecipitation
DAPI	4',6-diamidino-2-phenylindole
DMEM	Dulbecco's modified Eagle's medium

EDTA	ethylenediaminetetraacetic acid
ECL	enhanced chemiluminescence
EGTA	ethylene glycol-bis-(2-aminoethyl)-N,N,N', N'-tetraacetic acid
EMEM	Eagle's minimum essential medium
HCl	hydrochloric acid
HEPES	4-(2-hydroxyethyl)-1-piperazineethanesulfonic acid
IP	immunoprecipitation
KCl	potassium chloride
KOAc	potassium acetate
MgCl <sub>2</sub>	magnesium chloride
NaCl	sodium chloride
NaOH	sodium hydroxide
NFDM	nonfat dry milk
NP-40	nonyl phenoxy polyethoxyethanol
PCR	polymerase chain reaction
PBS	phosphate-buffered saline
Pr	primer
SDS-PAGE	sodium dodecyl sulphate-polyacrylamide gel electrophoresis
SSC	saline sodium citrate
TBS	tris-buffered saline
TRITC	tetramethyl rhodamine iso-thiocyanate
tRNA	transfer RNA
Tris	tris(hydroxymethyl)aminomethane
UV/Vis	ultraviolet/visible
VSN	viral supernatant

### **Nucleic Acids**

ATP	adenosine triphosphate
ADP	adenosine diphosphate
BBP	backbone primer
cDNA	complementary DNA
dATP	deoxyadenosine triphosphate
dCTP	deoxycytidine triphosphate
dGTP	deoxyguanosine triphosphate
DNA	deoxyribonucleic acid
dNTP	deoxynucleotide triphosphate
dTTP	deoxythymidine triphosphate
GTP	guanosine triphosphate
RNA	ribonucleic acid
scaRNA	small cajal body RNA
snoRNA	small nucleolar RNA
TERRA	telomeric repeat containing ribonucleic acid
TR	telomerase RNA

UTP

uridine triphosphate

**Proteins**

ATM

Ataxia telangiectasia mutated

ATPase

Adenosine triphosphate hydrolase

ATR

ATM and Rad3-related

BLM

Bloom's syndrome, RecQ helicase-like

BSA

Bovine serum albumin

Ccq1

Coiled-coil quantitatively-enriched protein 1

Cdc13

Cell division cycle 13

CHK1/2

Checkpoint kinase 1/2

c-myc

Cellular myelocytomatosis

DNA-PK

DNA-dependent protein kinase

ERCC1

Excision repair cross-complementing rodent repair deficiency group 1

Est1/2/3p

Ever shorter telomeres 1/2/3 protein

E2F1

E2F transcription factor 1

GNL3L

Guanine nucleotide-binding protein-like 3-like protein

GTPase

Guanosine triphosphate hydrolase

HIV-1

Human immunodeficiency virus-1

hnRNP

Heterogeneous nuclear ribonucleoprotein

HPV E6

Human papillomavirus E6

HSP<sub>x</sub>(40, 70, 82, 90)

Heat shock protein of *x* kilodaltons

KIP

DNA-PK catalytic subunit-interacting protein derived from the first two letters of a patient's name

Ku

MDC1

Mediator of DNA damage checkpoint protein 1

MRN

MRE11-RAD50-NBS1

MKRN1

Makorin ring finger 1

NAF1

Nuclear assembly factor 1

NAT10

N-acetyltransferase 10

NHP2

Non-histone chromosome protein 2

NOP10

Nucleolar protein 10

p<sub>x</sub>(16, 21, 23, 53, 73)

Protein of *x* kilodaltons

PARP2

Poly(ADP-ribose) polymerase 2

PKC

Protein kinase C

POT1

Protection of telomeres 1

Poz1

Pot1-associated in *Schizosaccharomyces pombe*

pRB

Retinoblastoma protein

RAP1

Repressor activator protein 1

RAS

Rat sarcoma virus

Rat1p

Ribonucleic acid trafficking 1 protein

Rif1/2

RAP1 interacting factor 1/2

RNase

Ribonuclease

RPA1

Replication protein A1

RT	Reverse transcriptase
SMAD3	SMA and MAD-related protein 3
SMG1	Suppressor with morphological effect on genitalia 1
SMN	Survival of motor neuron
SP1	Specificity protein 1
STAT3	Signal transducer and activator of transcription 3
Stn1	Suppressor of CDC13
Taz1	TRF1 homolog in <i>Schizosaccharomyces pombe</i>
Tbf1	Telomere repeat binding factor 1
TCAB1	Telomerase cajal body protein 1
TDM	Telomeric-DNA containing double minute
TEBP $\alpha/\beta$	Telomere end-binding protein ( $\alpha$ and $\beta$ subunit)
Tel1	Telomere length regulation protein 1
Ten1	Telomeric pathways with STN1
TERT	Telomerase reverse transcriptase
TIN2	TRF1-interacting nuclear protein 2
TPP1	TINT1-PTOP-PIP1
Tpz1	TPP1 homolog in <i>Schizosaccharomyces pombe</i>
TRF1/2	TTAGGG repeat-binding factor 1/2
WRN	Werner syndrome, RecQ helicase-like
WT1	Wilms tumour 1
XPF	Xeroderma pigmentosum complementation group F
XRCC3/4	X-ray repair cross-complementing rodent repair deficiency group 3/4
$\gamma$ -H2AX	Serine 139-phosphorylated histone family 2A member X
53BP1	p53 binding protein 1
<b>General</b>	
AA	aplastic anemia
ALT	alternative lengthening of telomeres
APB	ALT-associated promyelocytic leukaemia body
ANOVA	analysis of variance
CAB	cajal body (localization sequence)
CB	cajal body
CEN	centromere
CR	conserved region
CTE	carboxy terminal extension
DAT	dissociates the biological and catalytic activities of telomerase
DC	dyskeratosis congenita
DDR	DNA damage response
d-loop	displacement-loop
ds	double-stranded
DSB	double-strand break
DTR	degenerate telomeric repeat

EM	electron microscopy
FL	full length
G	generation
G1	gap phase 1
G2	gap phase 2
HH	Hoyeraal-Hreidarsson
HJ	Holliday junction
HR	homologous recombination
IPF	idiopathic pulmonary fibrosis
LTR	long terminal repeat
M1	mortality stage 1
M2	mortality stage 2
MoMuLV	Moloney murine leukemia virus
N	no
ND	not determined
NHEJ	non-homologous end joining
NTE	amino terminal extension
RAP	repeat addition processivity
RNP	ribonucleoprotein
RRL	rabbit reticulocyte lysate
S	synthesis phase
SCE	sister chromatid exchange
SD	segmental duplication
ss	single-stranded
SS	satellite sequence
STR	subtelomeric repeat
TEL	telomere
TEN	TERT essential N-terminal domain
TIF	telomere dysfunction-induced foci
t-loop	telomere-loop
T-NHEJ	telomere-non-homologous end joining
TRBD	telomerase ribonucleic acid binding domain
T-SCE	telomere-sister chromatid exchange
WT	wild type
Y	yes

## Chapter One: Introduction

### 1.1 Telomeres

Telomeres are essential nucleoprotein structures that form a protective cap for the terminal segments of linear chromosomes. The DNA component can be divided into three distinct regions: 1) double-stranded (ds) subtelomeric repeats; 2) internal arrays of ds species-specific telomeric repeats; and 3) a terminating single-stranded (ss) 3'-overhang (Figure 1.1). Telomeric DNA is invariably rich in guanine and thymine bases, although the exact sequence is species-specific (Table 1.1). The sequence composition imparts telomeres with the ability to recruit specific proteins and form unique secondary structures, both of which are critical for telomere stability and function. In the following sections, I will discuss the general architecture and function of telomeres.

#### *1.1.1 Subtelomeres*

In humans, subtelomeric DNA is located proximal to terminal ds (TTAGGG)<sub>n</sub> repeats and comprises approximately 80 % of the most distal 800 kilobases (kb) of each chromosome arm [1]. Subtelomere architecture varies from telomere to telomere, depending on the content and organization of four structural elements: 1) subtelomeric repeats, defined as segments of duplicated DNA that occur in more than one subtelomeric region and are generally less than 1000 base-pairs long; 2) segmental duplications, which are blocks of duplicated genomic DNA that have high sequence identity and are greater than 1000 base-pairs in length; 3) satellite sequences; and 4) internal degenerate (TTAGGG)<sub>n</sub> repeats such as TTCGGG (Figure 1.2) [1,2].

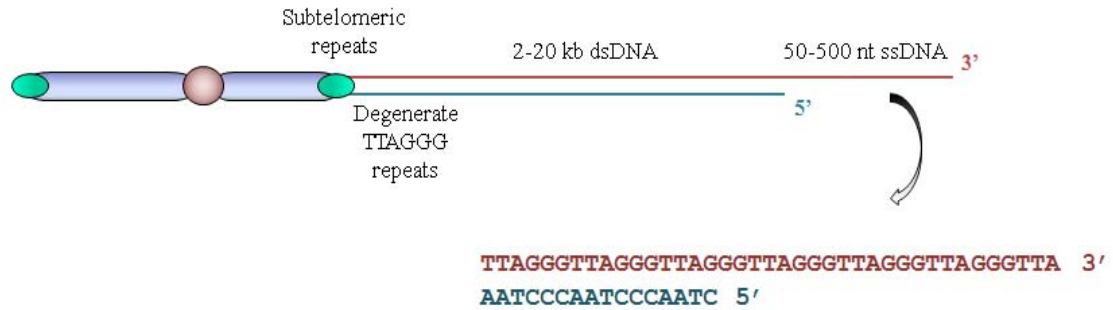


**Figure 1.1: Human telomere architecture.**

This figure shows a schematic of a human chromosome (not drawn to scale) with an emphasis on the telomeric region at one end of the chromosome. The centromere is shown in pink and the telomeres in green. The relative lengths of the double-stranded (ds) and single-stranded (ss) telomeric DNA components are indicated. These regions are comprised of multiple copies of the repeat unit 5'-TTAGGG-3' (top strand) and 5'-AATCCC-3' (bottom) strand. The nucleotide (nt) sequence of the telomere end is expanded in the lower portion of the figure.

**Table 1.1: Examples of telomeric simple-sequence repeats in select organisms**

<b>Organism</b>	<b>Telomere Sequence<sup>§</sup></b>	<b>Telomere Length</b>
<b>Protozoa</b>		
<i>Tetrahymena</i>	T <sub>2</sub> G <sub>4</sub>	100-500 bp <sup>*</sup>
<i>Euplotes</i>	T <sub>4</sub> G <sub>4</sub>	20 bp <sup>*</sup>
<i>Oxytricha</i>	T <sub>4</sub> G <sub>4</sub>	20 bp <sup>*</sup>
<b>Fungi</b>		
<i>Saccharomyces cerevisiae</i>	G <sub>2-3</sub> (TG) <sub>1-6</sub>	350-500 bp
<i>Schizosaccharomyces pombe</i>	T <sub>2</sub> AC(A)(C)G <sub>2-8</sub>	250-500 bp
<b>Nematodes</b>		
<i>Caenorhabditis elegans</i>	T <sub>2</sub> AG <sub>2</sub> C	2-4 kb
<b>Plants</b>		
<i>Arabidopsis thaliana</i>	T <sub>3</sub> AG <sub>3</sub>	2-9 kb
<i>Nicotiana</i>	T <sub>3</sub> AG <sub>3</sub>	40-160 kb
<b>Vertebrates</b>		
<i>Homo sapiens</i>	T <sub>2</sub> AG <sub>3</sub>	10-15 kb
<i>Mus musculus</i>	T <sub>2</sub> AG <sub>3</sub>	10-100 kb
<i>Felis catus</i>	T <sub>2</sub> AG <sub>3</sub>	5-27 kb

§ Telomeric DNA sequence is written 5' to 3'.

\* Macronuclear chromosomes.

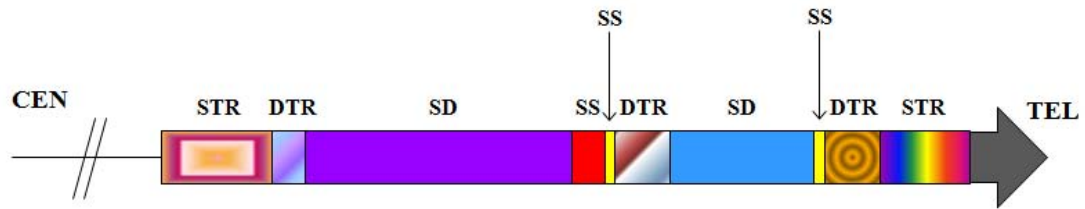


**Figure 1.2: Subtelomere structure and variation.**

This figure shows an example of the architecture observed in the subtelomeric region of human chromosomes (not drawn to scale). The polarity is from the centromere (CEN) to the telomere (TEL) at one end of the chromosome. Two examples of subtelomeric repeats (STR) are shown as pink and rainbow-filled boxes. Degenerate telomeric repeats (DTR) are illustrated in different colors to emphasize the sequence variation that is observed in these regions. Satellite sequences (SS) are shown as red or yellow rectangles and segmental duplications (SD) are indicated by violet and blue rectangles. The sequence content, size, and organization of these four elements varies significantly between chromosomes [2].

In terms of evolution, subtelomeres are plastic genome compartments that have the potential to generate new gene families. These regions are preferential sites for DNA breakage and repair, recombination, and genetic instability [1,3,4]. Consistent with this, chromosomal rearrangements in these regions have been linked to various diseases, such as neurodegenerative and immunodeficiency disorders [5].

Subtelomeres are rich in genetic information and contain both known and predicted protein-encoding genes, pseudogenes, and non-functional transcripts [1,2]. Functional gene products include immunoglobulin heavy chains, cytokine receptors, and zinc finger proteins [2]. Furthermore, subtelomeric (and telomeric) regions are transcribed into non-coding TELomeric Repeat RNA (TERRA) molecules [6]. TERRA molecules are associated with (sub)telomeric regions throughout the cell cycle and are regulated by the SMG proteins in humans [6] and the Rat1p exonuclease in yeast [7]. The current model is that telomere-bound TERRA prevents telomere elongation, although the cellular significance and regulation of TERRA is not fully understood.

### ***1.1.2 Telomeric double-stranded DNA***

The first telomeric DNA to be sequenced was that of the ciliated protozoan *Tetrahymena thermophila* [8]. Ciliates are unicellular eukaryotes that contain two distinct nuclei: 1) the macronucleus, which is transcriptionally active and required for vegetative growth; and 2) the micronucleus, which is transcriptionally inert and required for sexual reproduction (conjugation) [9]. Following conjugation, the micronucleus is fragmented into thousands of linear chromosomes that are ‘healed’ *de novo* with telomeric DNA [10].

The abundance of telomere-capped molecules was instrumental for the initial sequencing of telomeric DNA. The termini of these molecules were found to contain variable copies of the hexanucleotide unit, CCCCAA/GGGGTT [8].

Over the next ten years, telomeric DNA was isolated and sequenced from additional ciliates [11], protozoa [12,13], yeast [14,15], plants [16], and vertebrates [17-19]. One universal feature of telomeric DNA is the organization into a C/A-rich strand and a G/T-rich strand that is orientated 5' to 3' towards the physical end of the chromosome. Furthermore, telomeric DNA almost always contains tandem repeats of simple, species-specific sequences that are six to eight base-pairs long (Table 1.1). The telomeres of some strains of yeast (e.g. *Saccharomyces cerevisiae*) are a notable exception in that they contain a more complex and degenerate pattern of repeats [14,20]. In contrast to the conserved DNA sequence, telomere length varies dramatically from species to species, between organisms of the same species, and between telomeres of individual cells. The longest known telomeres are found in rats and in some strains of *Mus musculus*, ranging in length from 30 to 150 kb [21,22]. Human cells contain telomeres that range in size from 2 to 30 kb, depending on the cell type and replicative age; telomeres are approximately 10 kb at birth and gradually shorten during consecutive cell divisions in the absence of a telomere length-maintenance mechanism (Sections 1.3.3 and 1.7.3) [17,18,23-27].

### ***1.1.3 Telomeric single-stranded DNA***

Eukaryotic telomeres terminate in a ss 3'-protrusion of the G-rich strand, referred to as the 3'-overhang (Figure 1.1). As discussed below, the ubiquitous G-rich overhang is an essential feature required to maintain telomere structure and stability [11,28-32]. The 3'-overhang varies remarkably in length between species; ciliate telomeres possess 12 to 16 nucleotide (nt) overhangs [11,28] whereas human telomeres harbour variably-sized overhangs that can range from 100 to 600 nt [30,31,33,34]. The mean length of the G-rich overhang is positively correlated with overall telomere length in normal, transformed, and cancer-derived human cells [35], and shortens with increasing replicative age [33,36]. The cellular processes involved in the generation of these structures are discussed in Section 1.3.

### ***1.1.4 The telomere loop***

The ubiquitous nature of the 3'-overhang immediately suggested an essential role for this element in telomere function. In 1999, Jack Griffith and Titia de Lange identified a lariat-like structure at mammalian telomeres, which they termed the telomere-loop (t-loop) (Figure 1.3) [37]. Electron Microscopy (EM) analysis of psoralen cross-linked human and mouse telomeric DNA revealed large looped structures containing thousands of TTAGGG repeats [37]. The authors postulated that these structures were formed by invasion of the ss 3'-overhang into the duplex repeat array. In addition to t-loops, smaller lariat-like structures that contained a few hundred nucleotides of ssDNA were observed [37]. The ss loops, called displacement-loops (d-loops), were proposed to form if the

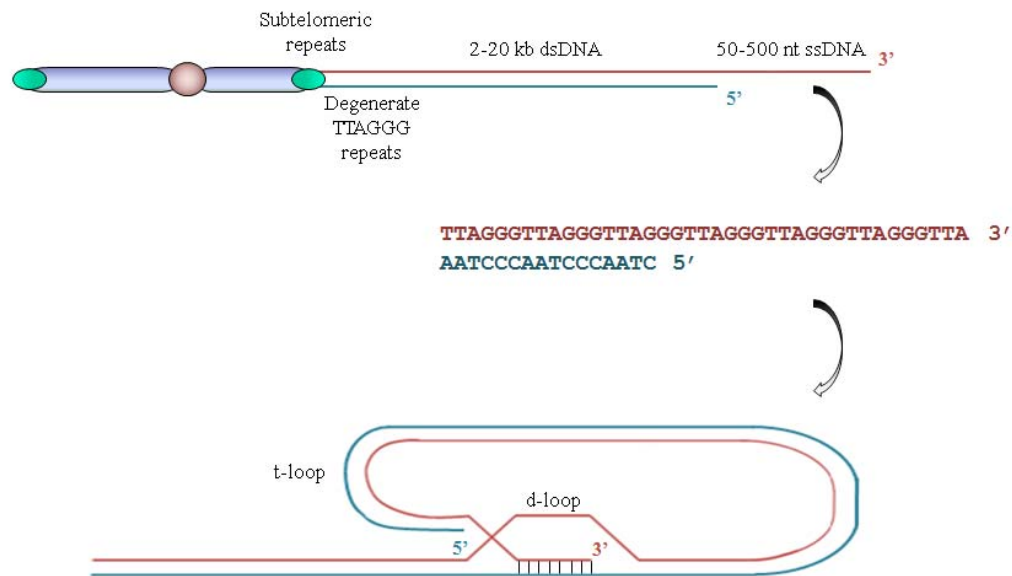


**Figure 1.3: T-loops and D-loops.**

This figure shows a schematic of a human chromosome (not drawn to scale) with an emphasis on the telomeric region at one end of the chromosome. The centromere is shown in pink and the telomeres in green. The relative lengths of the double-stranded (ds) and single-stranded (ss) telomeric DNA components at one end of the chromosome are indicated. Telomeres are comprised of multiple copies of the repeat unit 5'-TTAGGG-3' (top strand) and 5'-AATCCC-3' (bottom) strand. The nucleotide (nt) sequence of the telomere end is expanded in the middle portion of the figure and the predicted structure of a telomere-loop (t-loop) is shown at the bottom. This figure also illustrates a displacement-loop (d-loop).

invading 3'-overhang hybridized with the complementary C-strand and displaced the resident G-strand (Figure 1.3). Importantly, telomeric chromatin isolated from the nuclei of chicken erythrocytes and mouse splenocytes forms t-loop structures, suggesting that the native interphase conformation is a closed chromatin loop [38].

The key feature of t-loops is the sequestration of the ss chromosome end [37]. The current model is that t-loops provide a unique architectural cap that protects chromosome ends from degradation, recombination, and fusion with other pieces of DNA. Consistent with this, t-loop-like structures appear to be an evolutionarily-conserved phenomenon and have been identified in trypanosomes [39], ciliates [40], plants [41], nematodes [42], and some strains of yeast [43,44]. However, relatively little is known about the formation and regulation of t-loops. Biochemical studies have shown that t-loops can be reconstituted from model telomeric dsDNA containing at least one ss-TTAGGG repeat at the 3'-end in the presence of the telomere-binding protein TRF2 [37,45]. The mechanism by which TRF2 facilitates t-loop formation is thought to involve TRF2-induced modifications to DNA topology that stimulate strand invasion. This model has been deduced by the ability of TRF2 to stimulate invasion of ssDNA into plasmids containing duplex telomeric DNA *in vitro* [46]. Furthermore, the DNA-binding domain of TRF2 was recently shown to mediate the flexibility and strand invasion capacity of reconstituted nucleosomal array fibers *in vitro* [47]. An important future challenge will be to determine how the full length TRF2 modifies DNA topology in the context of telomeric chromatin and telomere-associated proteins. Furthermore, the molecular mechanisms by which t-

loops are resolved and reconstructed during specific stages of the cell cycle remain to be elucidated.

### ***1.1.5 Telomere-associated proteins***

The bulk of telomeric DNA in higher eukaryotes is organized into tightly packed nucleosomes [48]. However, the higher organization of telomeric chromatin and the roles of nucleosomes and epigenetic modifications in telomere structure are not fully understood. Nonetheless, it is well-established that telomeres are associated with a plethora of histone and non-histone proteins (Figure 1.4). The non-histone proteins are classified as shelterin or telosome proteins; shelterin components are telomere-specific proteins whereas telosome proteins have cellular functions beyond telomere maintenance [49]. The identity and proposed functions of shelterin and telosome proteins is summarized in Tables 1.2 and 1.3, respectively. In mammalian cells, there are six telomere-specific proteins that comprise shelterin: TRF1, TRF2, POT1, RAP1, TIN2, and TPP1 (Figure 1.5) [49]. The analogous proteins and protein complexes in yeast and ciliates are listed in Table 1.2 and illustrated in Figure 1.5. As discussed below, shelterin governs the architecture of telomeric DNA and provides cells with mechanisms to distinguish natural chromosome ends from *bona fide* DNA breaks and regulates telomerase-dependent telomere synthesis.

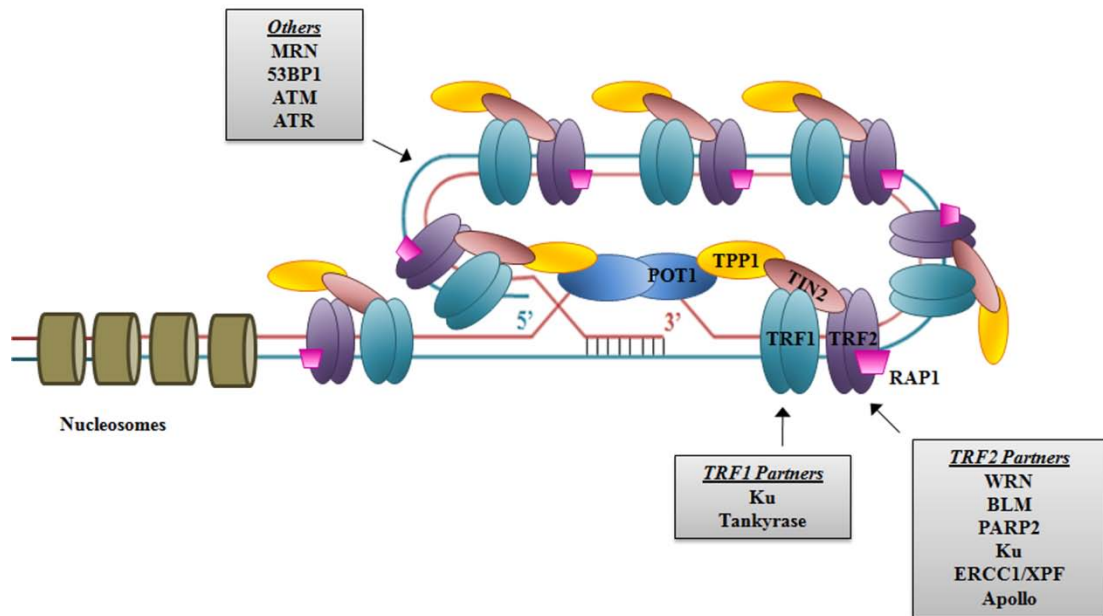


**Figure 1.4: Human telomere-associated proteins.**

This figure shows a schematic of the t-loop and d-loop in association with histone proteins (nucleosomes), telosome proteins (listed in grey boxes), and shelterin proteins (POT1, TPP1, TIN2, TRF1, TRF2, and RAP1). See also Tables 1.2 and 1.3 [50].

**Table 1.2: Shelterin proteins in select organisms**

<i>Organism &amp; Shelterin Protein</i>	<i>Function</i>	<i>Telomeric Recruitment</i>
<i>Homo sapiens</i>		
TRF1	Negative regulator of TL	dsDNA
TRF2	T-loop formation; End-protection	dsDNA
POT1	Positive & negative regulator of TL; End-protection	ssDNA; TPP1
RAP1	?	TRF2
TPP1	POT1 recruitment; Tethers POT1 to TRF1; Telomerase activation	TIN2, POT1,
TIN2	Shelterin assembly and stability	TRF1, TRF2, TPP1
<i>Schizosaccharomyces pombe</i>		
Tbf1	Negative regulator of TL	dsDNA
Taz1	Positive & negative regulator of TL; End-protection	dsDNA
Pot1	End-protection	ssDNA
Rap1	Negative regulator of TL	Taz1
Tpz1	Tethers Pot1 to Taz1	Pot1
Ccq1	Positive regulator of TL	Tpz1
Poz1	Negative regulator of TL	Tpz1
Stn1/Ten1	End-protection	ssDNA
<i>Saccharomyces cerevisiae</i>		
Rap1	Telomeric silencing; Negative regulator of TL	dsDNA
Rif1/2	Telomeric silencing; Negative regulator of TL	Rap1
Cdc13	End-protection; Positive & negative regulator of TL	ssDNA
Stn1/Ten1	End-protection	Cdc13
<i>Oxytricha nova</i>		
TEBP $\alpha/\beta$	End-protection; TL regulator	ssDNA

**Abbreviations:** h, Human; TL, telomere length. Reviewed in reference [50].

**Table 1.3: Examples of human telosome proteins**

<b>Protein/Protein Complex</b>	<b>Non-Telomeric Function</b>	<b>Telomeric Activity</b>	<b>Telomeric Recruitment</b>
MRN	Endo-exonuclease; DNA damage sensor	T-loop formation, resolution, & homologous recombination	TRF1, TRF2/RAP1
ERCC1/XPF	3'-flap endonuclease; NER	3'-overhang processing after TRF2 inhibition	TRF2
Apollo	5'-exonuclease	Telomere protection during replication	TRF2/RAP1
RPA	Binds ssDNA & prevents strand annealing reactions	Prevents strand annealing	ssDNA
Tankyrase	Poly(ADP)-ribosylation; role in mitosis	Positive regulator of TL <i>via</i> TRF1 inhibition	TRF1
PARP2	Poly(ADP)-ribosylation; BER	Negative regulator of TRF2 <i>via</i> poly(ADP)-ribosylation	TRF2
Ku	NHEJ	End-protection	dsDNA, TRF1, TRF2/RAP1
WRN Helicase	Branch migration; Resolution of G-quadruplex DNA	Unwinding dsDNA; resolving recombination intermediates	dsDNA, TRF2, POT1(?)
BLM Helicase	Branch migration	Unwinding dsDNA	TRF1, TRF2, POT1(?)

**Abbreviations:** BER, Base Excision Repair; NER, Nucleotide Excision Repair; NHEJ; Non-Homologous End-Joining; TL, Telomere Length. Reviewed in reference [50].



## **1.2 Telomeres and the DNA Damage Response**

The pioneering work of Henry Muller and Barbara McClintock revealed that broken chromosomes were unstable and needed to be protected from recombination and fusion with other broken chromosomes [51-53]. As discussed below, the shelterin complex is the basis of this protective mechanism. In the absence of shelterin, telomeres lose their end-protection and activate the canonical DNA Damage Response (DDR). There are two main mechanisms that induce telomere dysfunction: 1) progressive telomere attrition that eventually results in a ‘critically short’ telomere, and 2) perturbation of shelterin components that leads to telomere ‘de-capping’. In the following sections, I will discuss how telomeres respond to the loss of shelterin, the mechanisms by which shelterin represses the canonical DDR at natural chromosome ends, the cellular fate of dysfunctional telomeres, and the minimal requirements for telomere function.

### ***1.2.1 The telomere damage response***

As illustrated in Figure 1.6, several proteins involved in the DDR accumulate at damaged telomeres, including  $\gamma$ -H2AX, 53BP1, MDC1, and ATM [54-56]. This response generates distinct nuclear foci, referred to as TIFs (Telomere dysfunction-Induced Foci), which extend hundreds of kilobases beyond the telomere [54,55,57]. The telomere damage signal is transduced through the ATM and/or ATR kinase pathways and ultimately induces replicative senescence or apoptosis, depending on the cellular context and insult [55,56,58-61]. Consistent with the activation of these pathways, cells harbouring damaged telomeres contain elevated protein levels of total and Ser15-

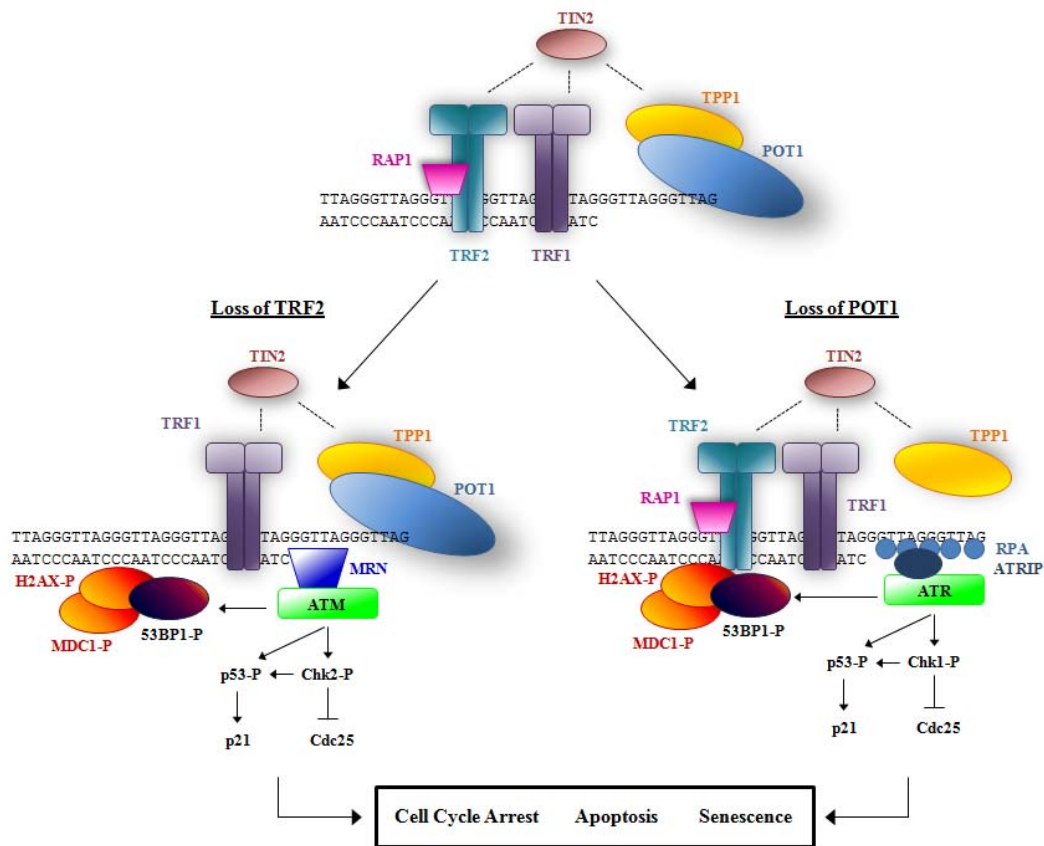


**Figure 1.6: The telomere damage response.**

This figure illustrates the cellular response, in humans, to the loss of the shelterin proteins TRF2 (shown on the left) or POT1 (shown on the right). The telomere is recognized as a *bona fide* DNA break and becomes associated with several DNA damage response proteins, some of which are shown in the middle portion of the figure. The ATM kinase signalling pathway is activated in the absence of TRF2 and the ATR pathway is induced in the absence of POT1. As shown at the bottom of the figure, these signalling pathways can induce a reversible cell cycle arrest, cell death (apoptosis), or an irreversible cell cycle arrest (senescence) [50].

phosphorylated p53, p21, and phosphorylated CHK1 and CHK2 [55]. The p53 and p16<sup>INK4a</sup>-pRB tumour suppressors are pivotal for the induction and maintenance of growth arrest upon telomere damage [55,56,59,60].

### ***1.2.2 Repression of the DNA damage response at telomeres***

One important question in telomere biology is how natural chromosome ends repress the canonical DDR. Recent studies indicate that TRF2 and POT1 function independently to repress the activation of ATM and ATR, respectively [61,62]. Telomere-bound POT1 is thought to inhibit ATR activation by preventing an interaction between RPA and telomeric ssDNA [61,63]. The mechanism by which TRF2 inhibits ATM is less clear. In one model, TRF2 is needed to form and maintain t-loops, which block upstream sensory proteins from binding the ss-overhang and recruiting the ATM kinase [50]. Similarly, t-loops might prevent changes in local chromatin structure that are otherwise sensed as broken DNA ends [50]. An alternative model is that the physical interaction between TRF2 and ATM is sufficient to repress ATM kinase activity, and thus, prevent downstream signalling events [64]. However, it remains to be determined if endogenous telomere-bound TRF2 interacts with ATM and how this interaction is modified by other telomere-associated proteins.

### ***1.2.3 The fate of dysfunctional telomeres***

Dysfunctional telomeres are processed similarly to DNA double-strand breaks (DSB) and typically activate the Non-Homologous End Joining (NHEJ) or Homologous

Recombination (HR) pathways, although less efficient ‘back-up’ repair pathways exist. The result is a range of chromosomal abnormalities that are a defining feature of cancer cells [65]. More specifically, Telomeric-NHEJ (T-NHEJ) generates covalent telomere fusions and dicentric chromosomes [66]. Recombination-based pathways can delete large segments of telomeric DNA, produce extrachromosomal telomeric circles, and promote Telomere Sister-Chromatid Exchanges (T-SCE). These pathways are summarized below.

#### 1.2.3.1 Non-homologous end joining

The T-NHEJ pathway operates predominantly in G1 [67] and requires many of the same factors that mediate NHEJ at non-telomeric sites, including DNA-PK, DNA ligase IV and XRCC4 [66,68,69]. Telomere fusions are unique, however, because of the long ssDNA 3'-overhang that requires processing prior to the end-joining reaction. The ERCC1/XPF nuclease, which is best-known for its role in nucleotide excision repair, is responsible for degrading the 3'-overhang when the T-NHEJ pathway is intact [70,71]. Recently, the nuclease activity of XPF has been implicated in telomere remodelling to facilitate TRF2 binding [72]. This observation has led to the suggestion that XPF and TRF2 form a complex that prevents telomere fusions, although the mechanism by which this occurs is unknown.

#### 1.2.3.2 Homologous recombination

There are three types of HR that can occur at dysfunctional telomeres: 1) intertelomeric recombination/T-SCE (Figure 1.7); 2) intratelomeric recombination,

referred to as t-loop HR (Figure 1.8); and 3) recombination of telomeres with interstitial telomeric DNA (Figure 1.9). TRF2 is involved in suppressing each of these pathways, emphasizing its key role in the regulation of telomere structure and function.

The telomeres of sister chromatids have the potential to recombine and exchange genetic information after DNA replication (Figure 1.7) [50]. In the case of unequal exchange, T-SCE yields elongated and shortened individual telomeres, which are then propagated to the next generation. Assuming that telomerase is absent, the daughter cell that receives the short telomere will have a reduced replicative lifespan. Data collected from various mouse models collectively indicate that TRF2, Ku70, and the WRN helicase are required to suppress T-SCEs [71,73]. It is expected that POT1 will also have an important role in suppressing T-SCEs, since WRN and POT1 physically interact and POT1 stimulates the helicase activity of WRN [74].

A second type of HR that can occur at telomeres is t-loop HR. As illustrated in Figure 1.8, t-loop HR is thought to involve the formation and resolution of a Holliday junction (HJ) structure at the base of the t-loop. This structure results in the deletion of t-loop-sized segments of DNA and the *de novo* appearance of t-loop sized circular extrachromosomal elements, which are believed to represent detached t-loops [75]. In addition to TRF2, the MRN complex and XRCC3 have been implicated in t-loop HR [75]. The current model is that TRF2 establishes a network of protein-protein interactions that suppress t-loop HR, although the mechanistic details are obscure.

The genome of many vertebrates contains interstitial sequences of telomere and telomere-like DNA. Recombination between telomeres and interstitial telomeric DNA

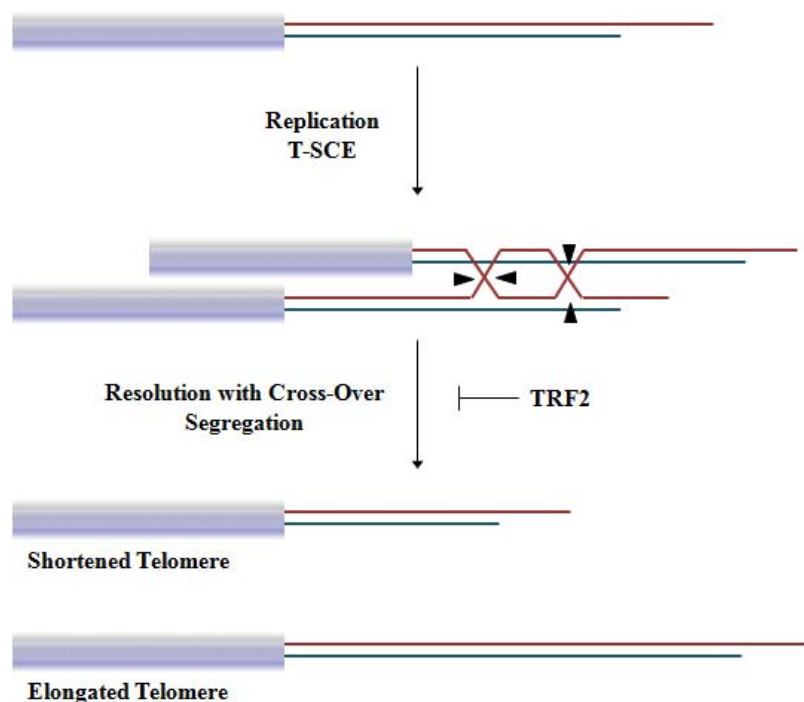


**Figure 1.7: Telomere-sister chromatid exchange.**

This figure shows a schematic of unequal telomere-sister chromatid exchange (T-SCE), which is normally suppressed by TRF2-mediated t-loop formation. The telomeric region is indicated by red (5'-3' strand) and blue (3'-5' strand) lines. The subteleric region is indicated by the grey boxes. After DNA replication, the sister telomeres can recombine and exchange genetic information. Resolution of the Holliday junction structure (indicated by arrowheads) can produce elongated and shortened telomeres, one of which is segregated to each daughter cell [50].

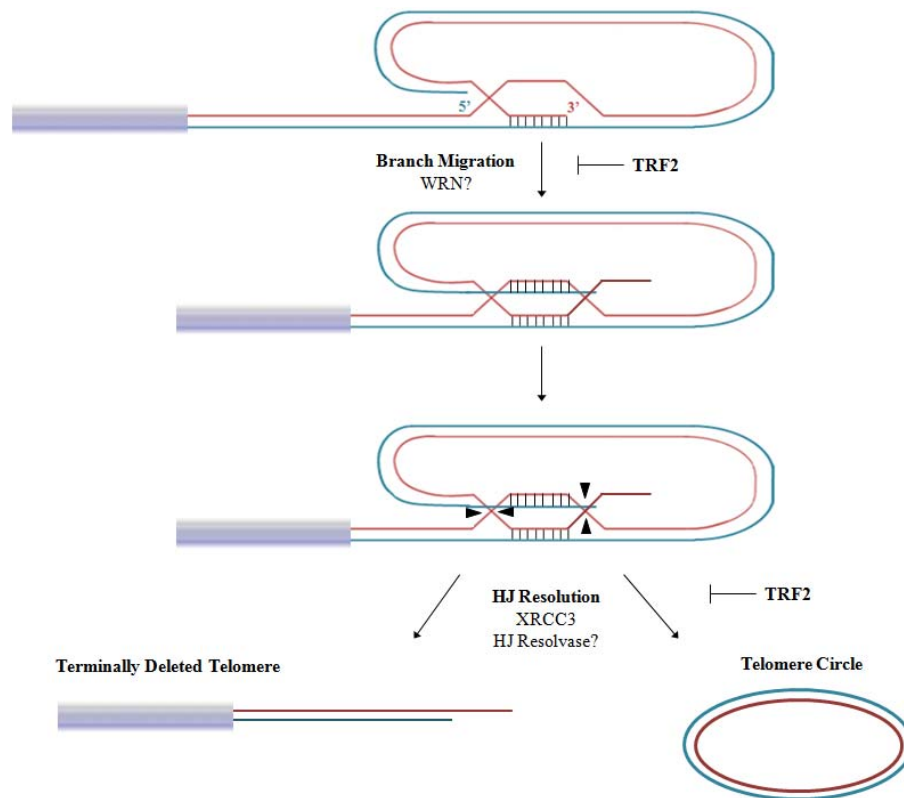


**Figure 1.8: T-loop homologous recombination.**

This figure shows a schematic of t-loop homologous recombination, which is believed to be suppressed by TRF2 and its associated proteins (not shown). The telomeric region is indicated by red (5'-3' strand) and blue (3'-5' strand) lines. The subtelomeric region is indicated by grey boxes. T-loop homologous recombination is thought to involve WRN-catalyzed t-loop migration (branch migration), which ultimately produces a Holliday junction (HJ). HJ resolution (indicated by arrowheads) can result in the deletion of large segments of telomeric DNA (terminally deleted telomere; bottom left figure) and the formation of telomere circles that represent detached t-loops (bottom right figure) [50].

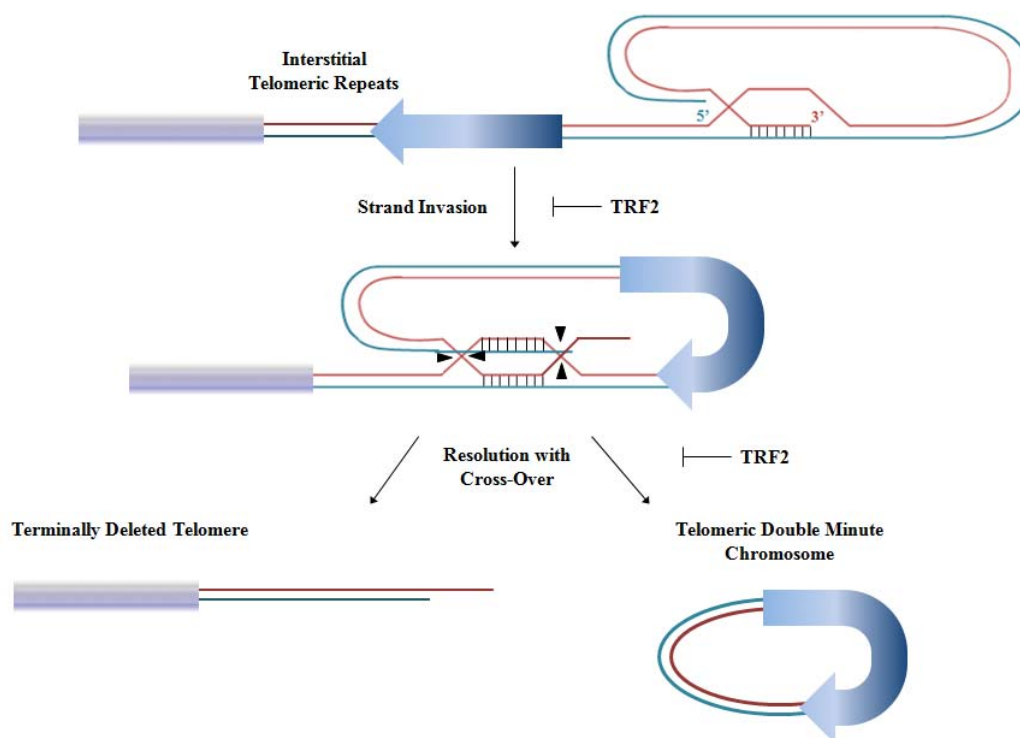


**Figure 1.9: Telomere recombination with interstitial telomeric DNA.**

This figure shows a schematic of recombination between terminal and interstitial telomeric DNA repeats. The thick blue arrows and grey boxes represent two regions of subtelomeric DNA. These regions are separated by a interstitial TTAGGG repeats (interstitial telomeric repeats). The telomere is indicated by red (5'-3' strand) and blue (3'-5' strand) lines. TRF2 is required for t-loop formation. In the absence of TRF2, the terminal segment of telomeric DNA can invade the interstitial telomeric DNA to produce a Holliday junction (HJ) (middle portion of figure). Resolution of the HJ (indicated by arrowheads) can result in the deletion of large segments of telomeric DNA (terminally deleted telomere; bottom left figure) and the formation of telomeric double-minute chromosomes (bottom right figure) [50].

can lead to chromosome inversions, deletions, and translocations, depending on the orientation of the interstitial repeat [50]. ERCC1<sup>-/-</sup> murine embryonic fibroblasts accumulate circular extrachromosomal elements comprised of telomeric and non-telomeric DNA [70]. These products are referred to as Telomeric DNA-containing Double Minute (TDM) chromosomes and are the outcome of recombination between a telomere and an interstitial telomere sequence in direct orientation on the same chromatid arm (Figure 1.9) [70]. Terminally deleted chromosomes are also expected to arise during this recombination event. Mammalian XPF/ERCC1 [70], POT1 [76,77], and the WRN helicase [73] have been implicated in repressing these events by resolving intermediate structures that arise during telomere strand-invasion into interstitial telomere sequences. The mechanisms that prevent XPF/ERCC1 from cleaving the base of the t-loop and factors that operate downstream of this nuclease, however, are currently unknown.

#### ***1.2.4 Minimal requirements for telomere function***

Telomere dysfunction has deleterious cellular consequences and is linked to human disease (Section 1.8). Therefore, it is critical to determine the threshold requirements for telomere function. Recent biochemical studies have shown that a tandem array of at least twelve canonical human telomeric repeats effectively inhibits T-NHEJ *in vitro* [78]. Another study showed that telomeres containing fewer than thirteen repeats were dysfunctional and susceptible to telomere fusion in human cells containing abrogated p53- and pRB-checkpoints [79]. However, another group reported that telomerase-positive human cells with compromised checkpoints contained a distinct class

of extremely short telomeres called t-stumps [80]. These authors demonstrated that t-stumps contained telomeric repeat variants and at least seven canonical repeats. Thus, the minimal length threshold for telomere function seems to depend on the cellular context. An important area of future research will be to investigate the minimal number of repeats required to suppress the DDR at telomeres in human cells with intact checkpoints.

### **1.3 Telomere Replication and Regulation**

#### ***1.3.1 Semi-conservative telomere replication***

Conventional semi-conservative replication accounts for the majority of telomere synthesis. Early studies in budding yeast demonstrated that telomerase activity requires passage of the replication fork through telomeres [81,82]. However, telomeric chromatin is difficult to replicate because of its highly repetitive, G-rich DNA sequence and abundance of associated proteins. Consistent with this, telomeres are particularly susceptible to fork-stalling and interactions between replication fork components and telomere-associated proteins appear to have an important role in fork progression through telomeric chromatin [83]. For example, the WRN helicase is required for efficient replication of lagging-strand telomeres in mammalian cells [84]. *In vitro*, TRF2 and POT1 interact with WRN and stimulate its helicase activity [74,85,86]. This observation suggests that shelterin recruits and/or stimulates proteins that are needed to resolve structures that arise during semi-conservative telomere replication. The current model is that stalled replication forks and the associated recombination intermediates stimulate telomeric HR [83]. This could explain why telomeres undergoing replication transiently

associate with DDR proteins involved in HR, including ATR, RPA, and XRCC3, but do not elicit a checkpoint-mediated cell cycle arrest [87,88]. An alternative, but likely related proposal, is that some of these proteins are required to reconstruct the t-loop after replication and prevent the telomere from being sensed as a DSB during G1. As discussed below, the transient recruitment of DDR proteins may also be necessary for telomerase recruitment to the telomere.

### ***1.3.2 The end replication problem***

In the early 1970's, Alexei Olovnikov [89,90] and James Watson [91] predicted that the semi-conservative DNA replication machinery was not sufficient to replicate the 3'-ends of linear chromosomes (the end replication problem). As illustrated in Figure 1.10, conventional DNA polymerases require a free 3'-hydroxyl group to initiate DNA synthesis, which is usually supplied by a short polynucleotide primer [92]. Once synthesis is initiated, the primer is degraded and the resulting gap is filled in with polynucleotides by the action of the replicating polymerase. However, the removal of the 5'-most terminal primer will leave a gap in one of the daughter strands because there is not enough room to lay down another primer (Figure 1.10). Olovnikov and Watson postulated that the progressive loss of chromosome 3'-ends incurred during consecutive cell divisions would eventually terminate cellular lifespan [89-91]. Importantly, telomeres evolved to circumvent the loss of genetic information and almost all eukaryotes rely on an enzyme called telomerase to synthesize telomeric DNA (discussed below).

The model described above predicts that only lagging-strand telomeres contain short ss 3'-overhangs (Figure 1.10). However, telomeric 3'-overhangs are simultaneously present on the leading- and lagging-strand telomeres in various eukaryotes, which suggests post-replicative strand processing [31,93]. This prediction is supported by the demonstration that human telomere 5'-ends are well-defined and nearly always terminate with the sequence ATC-5' [94]. Importantly, 3'-overhangs are generated independently of telomerase activity in ciliates, yeast, and mammals [31,32,93,95,96]. The most likely candidate for post-replicative processing of telomeric DNA is nuclease-mediated resection of the complementary C-rich strand (Figure 1.10) [31]. Thus, the overall length of the 3'-overhang is thought to be governed by the opposing actions of replication- and nuclease-associated attrition and telomerase- or recombination-mediated elongation. An important question to be resolved in the future is the identity of the nuclease that catalyzes post-replicative telomere processing.

### ***1.3.3 Telomerase-dependent telomere maintenance***

Telomerase-dependent telomere synthesis is governed by a negative feed-back loop that senses the length of telomeric DNA, transduces this information to the ss 3'-end, and regulates the ability of telomerase to access its substrate. Shelterin is the key component of negative regulation and senses telomere length by its accumulation on telomeric DNA. The current model is that POT1 is recruited to the telomere *via* TRF1-TPP1 and TRF2 complexes, which promotes POT1 binding to telomeric ssDNA [50]. The accumulation of POT1-TPP1 complexes occludes the 3'-end and prevents telomerase

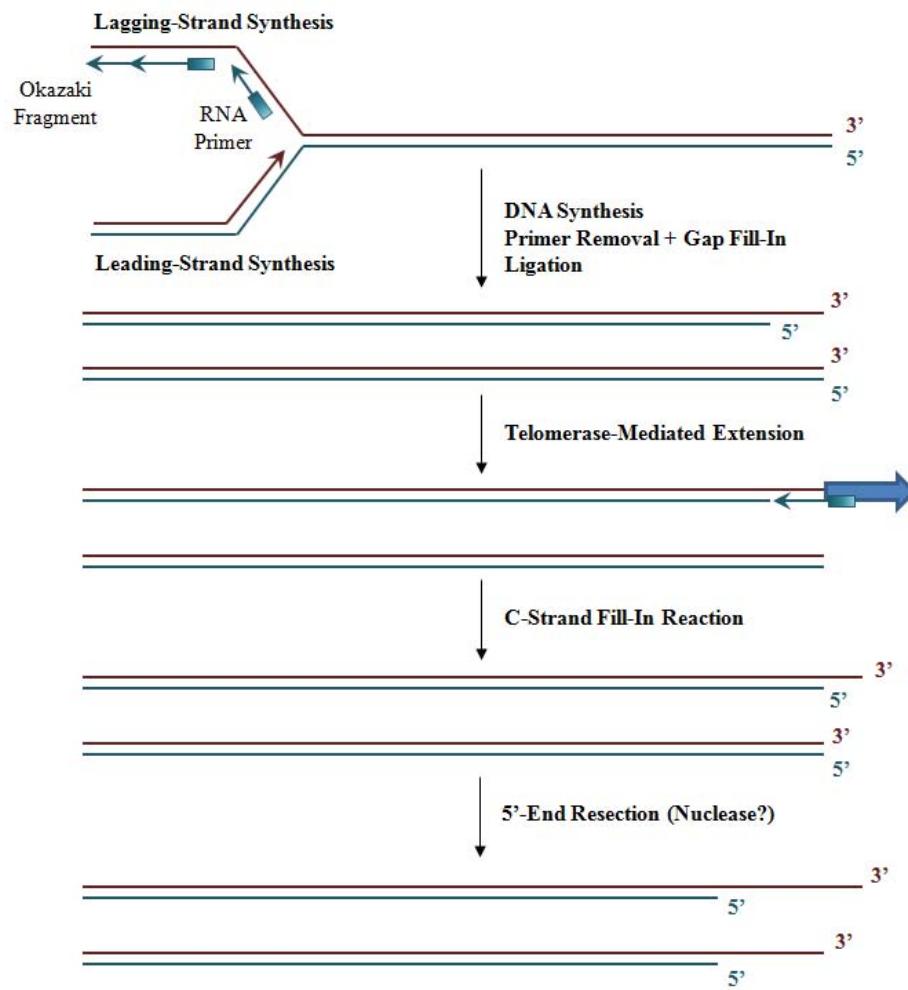


**Figure 1.10: The end-replication problem and telomere processing.**

**Figure 1.10: The end-replication problem and telomere processing.**

This figure illustrates the end-replication problem and telomere processing events that are proposed to occur during the semi-conservative replication of linear human chromosomes. A single replication fork and only one end of the leading and lagging daughter strands is shown for clarity. The leading strand is replicated as a continuous molecule of DNA from a single RNA primer (primer not shown). The lagging strand is synthesized discontinuously (Okazaki fragments) from multiple short RNA primers that are subsequently removed so the adjacent Okazaki fragments can be joined (top portion of the figure). Removing the final RNA primer leaves a short segment of ssDNA on the lagging strand that is insufficient for another priming event. Telomerase is thought to extend the ssDNA 3'-end (telomerase-mediated extension step; blue arrow) to a length that is sufficient for another priming event. The RNA primer (green box) is subsequently extended by the semi-conservative replication machinery (C-strand fill-in reaction) and then removed. A 5'-3' nuclease has been proposed to generate the ssDNA overhang at the 3'-end of the leading strand, as well as catalyze resection of the lagging strand 5'-end (5'-end resection step). As shown in the bottom portion of the figure, the ssDNA 3'-end of the leading strand has been reported to be shorter than the lagging strand [94].

from accessing the ssDNA substrate (negative regulation) [97,98]. During consecutive rounds of cell division, the TPP1-POT1 complexes gradually dissociate from continually-shortening telomeres and eventually grant telomerase access to the 3'-end. However, telomere-bound POT1-TPP1 complexes are also involved in recruiting telomerase to the telomere and enhancing telomere-synthesis (positive regulation) [99,100]. This apparent paradox is believed to provide cells with a mechanism to recruit a low abundance enzyme (telomerase) to an equally low abundant substrate (telomeric ssDNA) [101,102]. More specifically, since shelterin components are abundant (~ 100 to 1000 copies per telomere), an interaction between TPP1 and TERT would enrich telomerase at telomeric DNA *in vivo* [50].

Multiple studies have demonstrated that telomerase is preferentially recruited to the shortest telomeres in cells [103-106]. Recent work with budding yeast has provided insight into the mechanism by which short telomeres are 'marked' for elongation. These studies show that in addition to telomerase, Tel1p (the budding yeast ATM ortholog) and Est1p, which stimulates yeast telomerase activity, are preferentially recruited to the shortest telomeres [105-107]. The current model is that short telomeres are transiently recognized as a DNA break, which triggers Tel1p recruitment and subsequently, telomerase recruitment and activation. Interestingly, the recruitment of murine telomerase to short telomeres is independent of ATM, suggesting that ATR may be involved in regulating the mammalian pathway [108]. It is not clear, however, if short telomeres induce a complete DDR. Identification of downstream proteins is expected to provide critical insight into the signalling pathway that marks short telomeres for elongation.

Distinct protein complexes assemble at the telomere and regulate telomere homeostasis at various stages of the cell cycle. The mechanisms that control the association and dissociation of these complexes, however, are not well-characterized. To this end, very recent work in budding yeast indicates that the heat shock protein chaperone Hsp82 mediates the switch between extendible and non-extendible telomere states by modulating the DNA-binding activity of Cdc13 (functional ortholog of mammalian POT1) *in vitro* [109]. The working model is that Hsp82, by virtue of its ability to interact with different proteins, displaces proteins bound at the extreme 3'-end to permit telomerase-telomere association. This study illustrates telomere homeostasis as a dynamic multistep pathway that utilizes high-affinity interactions between low-abundance components (telomerase and telomeric ssDNA) and low-affinity interactions between abundant proteins (shelterin and chaperone proteins) to control the transition between extendible and non-extendible telomere states [109]. It will be interesting to determine if higher eukaryotes use a similar mechanism to regulate telomere accessibility.

#### **1.4 The Telomerase Ribonucleoprotein**

Telomerase is a unique ribonucleoprotein (RNP) reverse transcriptase (RT) that is responsible for the synthesis of telomeric DNA in almost all eukaryotes. As discussed below, the enzyme contains at least two essential core components: a catalytic protein subunit, the Telomerase Reverse Transcriptase (TERT), and an integral RNA subunit, the Telomerase RNA (TR). Telomerase reverse transcribes a small template region within the

RNA component to synthesize telomeric DNA. In this section, I will review the experiments that led to the discovery of telomerase and discuss the biochemical and cellular properties of its core components, TERT and TR.

#### ***1.4.1 Discovery***

In 1985, Carol Greider and Elizabeth Blackburn discovered a telomere-specific terminal transferase activity in *T. thermophila* cell-free extracts that was subsequently named telomerase [110]. In their pioneering experiments, Greider and Blackburn showed that the terminal transferase was sensitive to proteinase K, micrococcal nuclease, and RNase A and that a 159 nt RNA subunit co-purified with telomerase activity over five fractionation steps [110,111]. These experiments provided strong biochemical evidence that the terminal transferase was a *bona fide* cellular ribonucleoprotein reverse transcriptase. Importantly, a 5'-CAAACCCCAA-3' region was identified in the RNA gene component and proposed to serve as the template for telomere synthesis [112]. This hypothesis was confirmed by the demonstration that the RNA and telomerase activity were sensitive to RNase H after preincubation with antisense oligonucleotides mimicking the telomere sequence [112]. Moreover, the telomeres of *T. thermophila* cells transformed with telomerase RNA alleles harbouring mutations in the putative template sequence were complementary to the mutant telomerase RNA [113]. This provided the first evidence that the telomerase RNA contained the template for telomere synthesis *in vivo*.

The first telomerase catalytic protein subunits were identified through genetic screens in yeast [114] and biochemical purification of *Euplotes aediculatus* telomerase [115,116]. The *E. aediculatus* protein was found to be a homolog of the yeast protein and sequence comparison with prototypical RTs revealed an evolutionarily-conserved RT domain in both proteins [116]. Substitution of residues within the RT motifs of the yeast protein caused telomere shortening and cellular senescence, indicating that the RT domain was required for telomere synthesis *in vivo* [116]. TERT homologs were subsequently identified in humans, rodents, and ciliates [117-122].

The first direct evidence that TERT was the catalytic subunit of telomerase came from studies showing that telomerase activity could be reconstituted *in vitro* by co-expressing wild type TERT and TR in rabbit reticulocyte lysates (RRL) [121,123,124]. Further evidence was provided by the demonstration that mutations in the catalytic RT domain abolished *in vitro* telomerase activity [123]. The RRL reconstitution system is a cell-free transcription-translation assay in which T7 promoter-driven gene constructs are transcribed into mRNA by the T7 RNA polymerase and subsequently translated by the RRL protein synthesis machinery. Human telomerase is reconstituted by the addition of *in vitro* transcribed hTR and plasmid DNA that contains the T7 promoter and intronless hTERT sequence. Enzyme activity is measured using *in vitro* activity assays that rely on the addition of telomere repeats to the 3'-end of a telomeric ssDNA primer. This *in vitro* system has been used extensively to identify regions of TERT and TR that are important for enzyme activity, processivity, fidelity, and substrate specificity.

## ***1.4.2 The telomerase reverse transcriptase subunit***

### **1.4.2.1 Structure**

As illustrated in Figure 1.11, the architecture of TERT can be divided into three main regions: 1) a long N-terminal extension (NTE) that contains conserved DNA- and RNA-binding domains and an unstructured ‘linker’ region; 2) a central catalytic RT domain with seven evolutionarily-conserved RT motifs; and 3) a short C-terminal extension (CTE) that contains blocks of conserved amino acids. Although this organization defines almost all TERT proteins, there are a few notable exceptions. First, certain insect and nematode TERTs harbour a truncated NTE that does not contain the Telomerase Essential N-terminal (TEN) domain [125,126]. Secondly, the CTE is absent in *Giardia lamblia* and nematode TERTs [126]. Third, *Plasmodium falciparum* TERT contains an abundance of hypervariable insertions between the conserved domains and is at least three times larger than all other TERT proteins [127]. It will be interesting to determine if other TERT domains and/or cellular proteins compensate for the missing TERT domains *in vivo*.

A major advance in our understanding of TERT architecture has come from the recent atomic-resolution structure of full length *Tribolium castaneum* TERT in complex with an 18 nt telomeric ssDNA primer [128]. Notably, *T. castaneum* TERT lacks a significant portion of the NTE that is critical for telomerase activity in ciliates, yeast, and humans [128,129]. The crystal structure reveals a ring-like structure held together by extensive hydrophobic interactions between the CTE and N-terminus [128]. This is in good agreement with previous biochemical studies of human and *Euplotes crassus* TERT

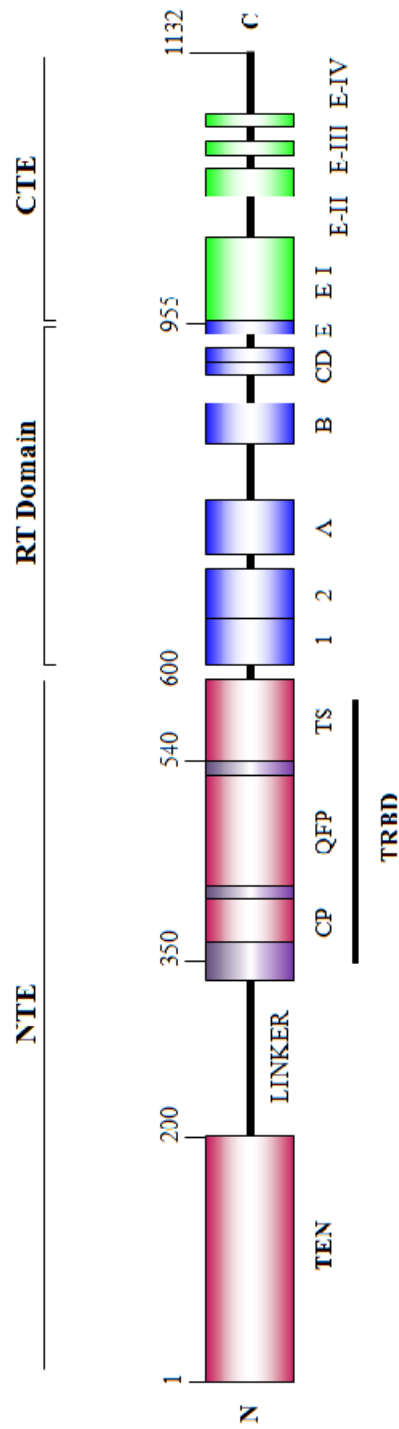


**Figure 1.11: Linear architecture of the human telomerase reverse transcriptase.**

**Figure 1.11: Linear architecture of the human telomerase reverse transcriptase.**

This figure illustrates the predicted structural organization of the human telomerase reverse transcriptase (hTERT). The protein encompasses a long N-terminal extension (NTE), a central catalytic reverse transcriptase (RT) domain, and a short C-terminal extension (CTE). Pink boxes are used to indicate the predicted locations of the telomerase essential N-terminal (TEN) domain and the telomerase-specific motifs CP, QFP, and TS. The purple box indicates the telomerase RNA-binding domain (TRBD). An unstructured linker region connects the TEN domain and TRBD. Blue boxes represent the seven evolutionarily-conserved motifs in the RT domain (1, 2, A, B, C, D, E). The CTE contains four blocks of conserved amino acids, which are shown as green boxes (E-I, E-II, E-III, E-IV). The approximate positions of amino acids are indicated above the coloured boxes. Reviewed in reference [129].

that revealed interactions between the NTE and CTE [130-132]. The interior dimensions of the ring indicate that it can accommodate seven or eight bases of double-stranded nucleic acid [128], consistent with previous biochemical studies demonstrating that the RNA-DNA heteroduplex is maintained at a constant length of seven to eight base-pairs [133,134]. Furthermore, the ring's interior is lined with amino acids that have been previously shown to mediate protein-nucleic acid interactions, nucleotide binding, and DNA synthesis in yeast [135-138] and human [139,140] TERT. An important future challenge will be to determine the high-resolution structure of TERT in complex with its integral RNA subunit. An equally important challenge will be to solve the crystal structure of full length TERT from higher eukaryotes.

#### 1.4.2.1.1 The TERT N-terminal extension

An extensive number of biochemical and genetic studies collectively indicate that the NTE of most TERT proteins contains two structurally-conserved domains, the TEN and TRBD (Figure 1.11). Separating these domains is a relatively long and unstructured linker region that is likely important for conformational changes within the holoenzyme. The NTE also contains several conserved telomerase-specific motifs, including the CP, QFP, and TS motifs (Figure 1.11) [141,142].

High-resolution structures of the *T. thermophila* TEN [143] and TRBD [128,144] domains indicate that both of these regions represent novel protein folds and are involved in binding single-stranded nucleic acids. The TEN domain is involved in TERT localization, multimerization, enzyme activity and processivity, and ssDNA-binding. The

TEN domain also displays a weak sequence non-specific RNA-binding activity, although the significance of this interaction is not clear [143]. It is possible that the TEN and TRBD co-operate to ensure optimal TR-binding and positioning required for RNP formation.

As shown in Figure 1.11, the TRBD is organized into two asymmetric lobes that contain residues from the CP and TS motifs [144]. The two halves of the TRBD are connected by extended loops that impart the domain with structural flexibility [144]. Hydrophilic and hydrophobic CP and TS residues form an extended RNA-binding groove on the surface of the domain. The dimensions of this cavity reveal a relatively wide hydrophilic pocket (CP pocket) that could accommodate dsRNA and a narrow hydrophobic pocket (T pocket) that could accommodate ssRNA [144]. In the context of full length TERT, the RNA-binding groove is located on the side of the ring and faces the interior of the ring in close proximity to the active site [128]. This placement is believed to permit the RNA 5'-end to enter the ring's interior where the active site is located. The structural data are supported by biochemical studies that have identified the CP and TS motifs as being critical for TR-binding, telomerase activity and processivity, and telomere elongation [123,141,145-153].

#### 1.4.2.1.2 The TERT RT domain

The TERT catalytic domain contains all seven of the evolutionarily-conserved RT motifs, which are required for telomerase function *in vitro* and *in vivo* (Figure 1.11) [116,117,119,123,124,137,154-156]. The RT domain is organized into two subdomains

that structurally resemble the ‘fingers’ and ‘palm’ subdomains of prototypical RT enzymes [128]. These regions are connected by a loop that contains the conserved ‘primer grip’ region of RT motif E. Molecular modelling predicts that the loop makes direct contacts with the RNA-DNA hybrid and the DNA 3'-end, suggesting that the primer grip region could be involved in positioning the ssDNA 3'-end in the enzyme active site [128]. As discussed in Chapter 3, this model is supported by biochemical studies of yeast [157] and human [158] TERT that have identified an important role for this region in ssDNA-binding and processive telomere synthesis *in vitro* and *in vivo*.

The enzyme active site consists of three invariant Asp residues from motifs A and C [128]. These residues are shared by all RTs and form a catalytic triad that participates directly in nucleotide addition *via* a two-metal ion mechanism [116,117]. Alanine mutations of these residues result in the complete loss of telomerase activity *in vitro* and *in vivo*, supporting the conclusion that they are essential for telomerase function [119,123,149,154,155]. Conserved residues from motifs 1, 2, A, B, C, and D form the nucleotide-binding pocket at the interface between the palm and fingers subdomains [128]. Two conserved surface-residues from motifs A and C (Tyr and Val, respectively) form a hydrophobic patch that is predicted to bind the base of the nucleotide substrate. This interaction would facilitate nucleotide positioning in the active site for co-ordination with a metal ion and the 3'-end of the DNA primer [128]. This model is supported by biochemical studies of ciliate [156], yeast [157], and human [159] TERT that have implicated these residues in nucleotide insertion rate, polymerase fidelity, and enzyme processivity.

#### 1.4.2.1.3 The TERT C-terminal extension

In contrast to the NTE and RT domains, the TERT CTE has weak sequence conservation, suggesting that the precise function of this region is likely species-specific. Interestingly, the CTE is essential for telomerase activity in *T. thermophila* [150] and humans [147,148], but is dispensable for telomerase activity in yeast [141]. The CTE is a helical bundle that contains several surface-exposed loops that are thought to contribute to the formation and stabilization of an RNA-DNA heteroduplex in the enzyme active site [128]. Mutations in the CTE affect nucleotide and repeat addition processivity [135,139,157], telomere length maintenance *in vivo* [140], and hTERT subcellular localization [160]. Furthermore, the addition of an epitope tag to the hTERT CTE abolishes telomere elongation *in vivo* [161].

#### 1.4.2.2 DAT domains

The TERT NTE and CTE contain unique DAT domains, which dissociate the biological and catalytic activities of telomerase [140,141,162]. Mutations in these domains have little or no effect on the ability of human telomerase to elongate partially-telomeric ssDNA primers *in vitro* yet abolish telomere length maintenance *in vivo* [140,162,163]. In yeast, certain mutations in the yeast Est2p DAT domain cause telomere over-elongation *in vivo* without apparent defects in DNA-binding or catalytic activity *in vitro* [164]. Notably, hTERT DAT mutants show no apparent defects in nuclear localization, hTR-binding, or protein multimerization [140,162]. These observations have led to the suggestion that the DAT domain has a critical role in telomerase-telomere

interactions and/or protein-protein interactions that recruit telomerase to the telomere. Consistent with the latter model, a subset of the hTERT DAT mutants can be rescued by direct fusion to TRF2 or POT1, which artificially targets telomerase to the telomere [165,166]. Nonetheless, some DAT mutants exhibit activity and processivity defects *in vitro* when tested with completely telomeric ssDNA primers [158,163,167]. As discussed in Chapter 3, we have found that certain DAT mutations can also impair the ability of hTERT to bind telomeric ssDNA *in vitro*. Collectively, these observations demonstrate that the DAT domains are not functionally equivalent.

#### 1.4.2.3 Cellular expression and localization

Expression of the TERT protein is positively correlated with telomerase activity and is the rate-limiting component for telomerase activity in most cells [118]. Human telomerase activity is robust in embryonic stem cells and germ line cells but is absent or present at very low levels in most somatic cells, with the notable exceptions being activated leukocytes and the cells of some highly proliferative tissues (e.g. epithelial tissue, hair follicles, and gut) [118,168]. Robust telomerase activity is also a hallmark of many cancer cells [169]. However, even in telomerase-positive cells, endogenous hTERT is a low abundance protein at approximately 20-50 molecules per cell [101].

The subcellular localization of hTERT is at least partly dependent on nucleolar-targeting sequences in the NTE [170,171] and CTE [172]. Various proteins have also been reported to regulate the intracellular distribution of hTERT. The 14-3-3 proteins enhance the nuclear localization of hTERT by masking a nuclear export signal in the

hTERT C-terminus [160]. Nucleolin, a major nucleolar phosphoprotein that shuttles cellular components between the nucleolus, nucleoplasm, and cytoplasm, concentrates hTERT in nucleoli [173]. Furthermore, the nucleolar protein PINX1 binds hTERT and represses telomerase activity [174,175]. Collectively, these studies suggest that telomerase activity is negatively regulated by nucleolar sequestration of hTERT. This model is supported by the observation that hTERT is localized to the nucleolus in G1 and redistributed to the nucleoplasm and unidentified nuclear foci in S phase, the time when telomeres are elongated by telomerase [176-178].

### ***1.4.3 The telomerase RNA subunit***

#### ***1.4.3.1 Structure***

The TR subunit has been identified in several different ciliates, yeast, and vertebrates. In contrast to TERT, the TR subunit has undergone significant evolutionary divergence in terms of size, primary sequence composition, and biogenesis. For example, the size varies from approximately 150 nt in ciliates, to around 500 nt in vertebrates, and more than 1300 nt in fungi [112,179-190]. The larger size of yeast and vertebrate TR subunits likely reflects the acquisition of structural elements that recruit various factors required for RNA processing and/or localization. Despite this variance, phylogenetic comparisons and computational structure predictions indicate that TR has a common core secondary structure within each phyla and that there two universally-conserved core elements [179,180,183,187,188,190-195]. First, TR invariably contains a short species-specific ss region that templates telomere synthesis. Second, the TR template is flanked

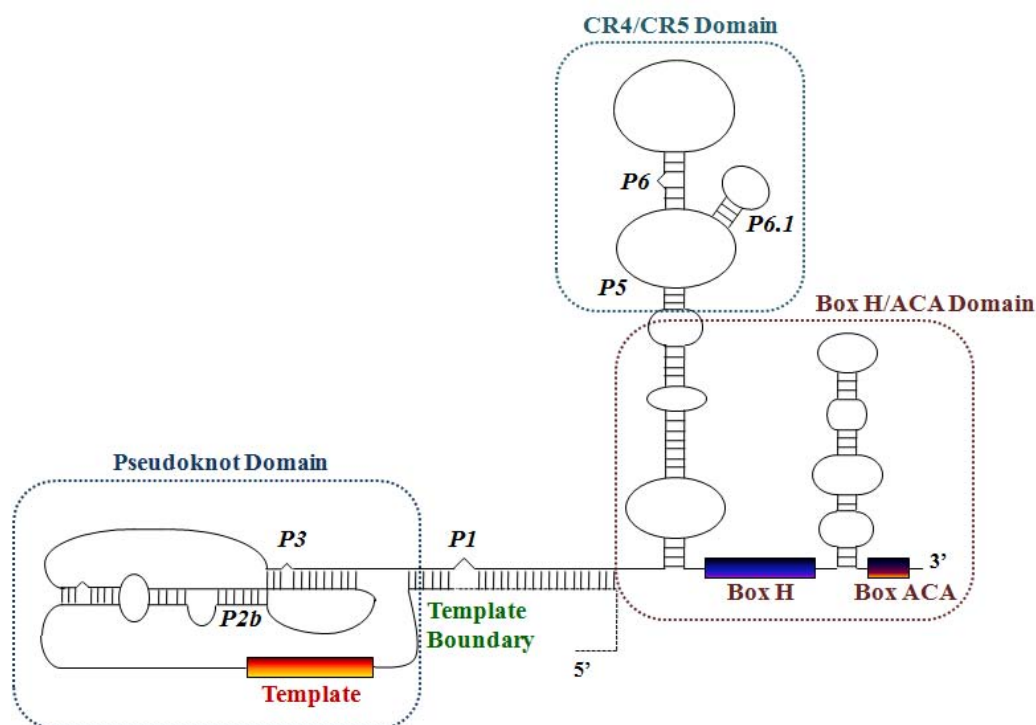


**Figure 1.12: Secondary structure of the vertebrate telomerase RNA.**

This figure is a schematic of the secondary structure for the vertebrate telomerase RNA subunit. The predicted locations of three evolutionarily conserved regions (CR) are indicated with hatched boxes (the pseudoknot/template core domain, the CR4-CR5 domain, and the box H/ACA domain). The template region, Box H, and Box ACA domains are indicated with orange, blue, and purple boxes, respectively. This figure also indicates the approximate locations of the template boundary region and various structural elements (P1, P2b, P3, P5, P6, and P6.1). Reviewed in reference [196].

by a downstream pseudoknot structure and an upstream long-range base-pairing element (helix I or P1), which are important for primer alignment, template boundary definition, and telomerase activity [197]. The template boundary regions are particularly important because they ensure that only the template region is copied into the nascent telomere.

Phylogenetic comparative analysis of the vertebrate TR subunit predicts three evolutionarily conserved structural domains: 1) the pseudoknot/template core domain; 2) the CR4/CR5 domain (for Conserved Regions 4 and 5, respectively); and 3) a box H/ACA domain (Figure 1.12) [187]. Interestingly, the CR4/CR5 and box H/ACA domains are only found in vertebrate TR and, therefore, may have species-specific roles in the biogenesis and function of vertebrate telomerase [187].

An extensive number of structure-function studies indicate that the core domain is essential for vertebrate telomerase activity *in vitro* and *in vivo* [124,147,185,198-208]. As shown in Figure 1.12, the core domain contains the template for telomere addition and 5'- and 3'-boundary elements that prevent the incorporation of non-template nucleotides [202]. This region also contains a putative TERT binding-site and a conserved pseudoknot structure [187]. Interestingly, a conserved triple-helix structure appears to participate directly in the telomerase catalytic reaction [209]. The solution structure of the pseudoknot domain, however, reveals that the catalytic moiety is sterically blocked by an hTR bulge [210]. One interpretation of these data is that the bulge serves as a hinge that regulates the accessibility of the catalytic moiety. Future studies are needed to determine the contribution of TR to enzyme catalysis.

Human telomerase activity can be reconstituted *in vitro* by co-expressing the pseudoknot/template domain and the CR4/CR5 domain in the presence of hTERT [199,200]. The TR domains work together to mediate TR-TERT interactions, nucleotide and repeat addition processivity, enzyme fidelity, and catalytic activity [201-204,206,207,211-213]. As shown in Figure 1.12, the CR4-CR5 domain contains a conserved stem-loop structure (P6.1) that is critical for TERT-binding and telomerase activity *in vitro* and *in vivo* [147,148,200,201,211,212]. The P6.1 stem-loop has also been reported to engage in long-range interactions with the template region, suggesting that intramolecular RNA-RNA interactions may play a critical role in the catalytic activity of telomerase [214].

The 3'-end of vertebrate TR contains two conserved motifs, box H and ACA elements, which serve as binding sites for proteins involved in RNA processing, stability, and subcellular localization (Figure 1.12 and Section 1.5). Although the box H/ACA domain is dispensable for telomerase activity *in vitro*, this region is essential for *in vivo* TR stability, accumulation, 3'-end processing, nuclear localization, and telomerase activity [124,199-201,211,215-221].

#### 1.4.3.2 Cellular expression and localization

The mammalian TRs are expressed at high levels (several thousand molecules per cell) in all tissues and throughout development, regardless of telomerase activity [182,222]. The subcellular localization of hTR is mediated by structural elements in the box H/ACA domains (Figure 1.12). Microinjection studies in *Xenopus* oocytes provided

the first evidence that the box H/ACA mediates hTR nuclear retention and subcellular trafficking between the nucleolus and Cajal Bodies (CB) [217,223]. Cajal bodies are dynamic intranuclear structures that mediate the biogenesis and function of several RNP complexes [224]. The box H/ACA domain of hTR contains a CAjal Body (CAB) box motif (U<sub>411</sub>GAG<sub>414</sub>) that mediates the intranuclear targeting of hTR to CBs in several different telomerase-positive cancer cell lines [142,177]. The CAB box is not sufficient for the subnuclear localization of hTR, however, and hTERT is required for the accumulation of hTR in CBs during S phase [177,225].

#### ***1.4.4 Telomerase-associated proteins***

Telomerase interacts directly or indirectly with several proteins that are known or predicted to regulate RNP biogenesis, assembly, subcellular localization, telomere recruitment, and enzyme activity. The identity of these proteins varies significantly between species and, in many cases, the functional relevance is unknown. Proteins that represent integral components of the human holoenzyme are discussed below and regulatory proteins are discussed in Section 1.5. Additional telomerase-associated proteins from various organisms are described in Table 1.4.

##### **1.4.4.1 The core TR H/ACA-binding proteins: Dyskerin, NHP2, and NOP10**

As mentioned above, hTR contains an evolutionarily-conserved box H/ACA motif that is required for end-processing and accumulation *in vivo*. The H/ACA motif is a conserved RNA structure found in H/ACA pseudouridylation guide RNAs, which post-

transcriptionally modify non-protein-encoding RNAs [226]. This family of RNAs includes small nucleolar RNAs (snoRNAs), small cajal body RNAs (scaRNAs), and the vertebrate telomerase RNAs. The H/ACA motifs interact with core set of proteins: dyskerin, NHP2, and NOP10 [227]. Dyskerin is an evolutionarily-conserved nucleolar protein that catalyzes the pseudouridylation of target RNAs. Dyskerin and NOP10 interact directly and NHP2 is recruited *via* binding NOP10 [227]. The core trimer is recruited to the site of RNA transcription by another protein, NAF1, and binds and stabilizes H/ACA-motif RNAs [228-230]. NAF1 is subsequently exchanged for a protein called GAR1, which is needed to assemble and localize the mature RNP complex [229].

Dyskerin, NHP2, and NOP10 have been identified by mass spectrometry in affinity-purified human telomerase from HeLa cells [231]. Similarly, mass spectrometric analysis of human telomerase complexes isolated by a more stringent affinity-purification strategy identified dyskerin, but not NHP2 or NOP10 [101]. This discrepancy is likely due to the increased complexity and stringency of the purification scheme used in the latter study. Consistent with this, the RNA-binding activity of dyskerin requires co-assembly with NHP2 and NOP10 [229] and all three of these proteins are required for the stability of hTR *in vivo* [231].

#### 1.4.4.2 Pontin and reptin

Mass spectrometric analysis of dual-affinity purified hTERT complexes from HeLa cells identified pontin and reptin as telomerase-associated proteins [232]. Pontin and reptin are two closely-related ATPases that are often found in the same

macromolecular complex [233]. These proteins are essential for the structural integrity and activity of several chromatin-remodelling complexes and are also involved in the stepwise assembly of nuclear complexes, transcription regulation, and DNA damage repair [233]. Biochemical studies have shown that pontin interacts directly with dyskerin and hTERT whereas reptin is recruited to the telomerase complex *via* pontin [232]. Stable depletion of pontin or reptin in human cells leads to a dramatic reduction in the accumulation of dyskerin and hTR *in vivo* and a corresponding decrease in telomerase activity *in vitro* [232]. The current model is that dyskerin, pontin, and reptin form a scaffold complex that recruits and stabilizes hTR and subsequently assembles the telomerase RNP. Once the RNP is formed, pontin and reptin are believed to dissociate and yield a catalytically-competent enzyme complex [232].

#### 1.4.4.3 TCAB1

The most recently identified telomerase-associated protein, Telomerase CAjal Body protein 1 (TCAB1), was discovered by mass-spectrometric analysis of dual affinity-purified human dyskerin complexes from HeLa cells [234]. TCAB1 has been implicated in the processing and localization of various scRNAs *via* binding the CAB and/or ACA motifs and targeting them to CBs [235]. Importantly, TCAB1 accumulates in CBs and is excluded from the nucleolus, suggesting that it might represent the protein that specifically targets RNPs to CBs *versus* nucleoli [234,235]. Immunoprecipitation experiments demonstrated that TCAB1 interacts directly with dyskerin and indirectly with hTERT *via* hTR [234]. Furthermore, immunodepletion of TCAB1 from cell extracts

severely impaired the catalytic activity of human telomerase *in vitro* [234]. Depletion of endogenous TCAB1 in telomerase-positive human cells prevented the CB-localization of hTR and impaired telomere elongation [234]. Collectively, these observations have led to the proposal that TCAB1 represents a novel component of the telomerase holoenzyme. However, since TCAB1 is not required for hTR stability, it might be more accurately defined as a regulatory protein that governs telomerase localization.

### **1.5 Telomerase RNP Biogenesis, Assembly, and Localization**

The cellular biogenesis and assembly of catalytically competent telomerase involves multiple steps, which include the following: 1) TR maturation, processing, and subcellular localization; 2) TERT transcription, translation, and post-translational modification; 3) assembly of catalytically-active telomerase RNP; and 4) delivery/recruitment of the RNP to telomeric substrates. In the following sections, I will summarize the current understanding of these pathways within the context of human telomerase.

#### ***1.5.1 Biogenesis***

The human *TR* gene (3q26) is normally single copy but is amplified in several human cancers [185,237,238]. The hTR transcript is synthesized as a 3'-extended precursor by RNA polymerase II, processed at its 3'-end to generate a mature RNA of 451 nt, and capped on its 5'-end with tri-methyl guanine [185,219,239]. The maturation and accumulation of hTR depends on the conserved H/ACA domain [215,218]. As

**Table 1.4: Examples of telomerase-associated proteins in select organisms**

<i>Organism &amp; Protein</i>	<i>Function</i> <sup>§</sup>	<i>Telomerase Interaction</i>
<i>Homo sapiens</i>		
EST1A	Telomere end-protection	TERT
EST1B	?	TERT
PKC	TERT phosphorylation; Positive regulation of TA	Telomerase
KIP	Positive regulator of TA & TL	TERT
hnRNP A1	Positive regulator of TA & TL	Telomerase
hnRNP C1/C2	Telomerase recruitment to telomeres?	TR
TOPOIII $\alpha$	Negative regulator of TA	TERT
Ku	Telomere end-protection; TL regulator	TR & TERT
<i>Saccharomyces cerevisiae</i>		
Est1p	Telomerase recruitment to telomeres; Positive regulator of TL	Tlc1 (TR)
Est3p	Positive regulator of TL	Telomerase
Sm proteins	Tlc1 stability & RNP assembly	Tlc1 (TR)
Ku	Telomerase recruitment to telomeres; Positive regulator of TA	Tlc1 (TR)
<i>Tetrahymena thermophila</i>		
p75	Positive regulator of TA	Telomerase
p65	TR stability; Initiates hierarchical assembly of telomerase RNP	TR
p45	Positive regulator of TA	Telomerase
p20	Negative regulator of TA <i>via</i> telomerase degradation?	Telomerase

<sup>§</sup> It is unclear for most proteins the mechanism(s) by which they regulate telomerase activity and/or telomere length. See [101,236] for primary references.

**Abbreviations:** h, Human; TA, Telomerase Activity; TERT, Telomerase Reverse Transcriptase subunit; TL, Telomere Length; TR, Telomerase RNA subunit.

discussed above, the H/ACA motif recruits at least four different proteins that are required for RNA accumulation *in vivo*: dyskerin, NHP2, NOP10, and GAR1. This protein complex provides biological stability to hTR and is essential for telomerase activity *in vitro* and *in vivo* [240]. The ATPases pontin and reptin have also been identified as novel factors required for hTR stabilization and the assembly of telomerase RNP complexes [232].

The human *TRT* gene (5p15) is normally a single copy gene but is frequently amplified in human cancer cells and tumour tissues [237,241,242]. Several transcriptional regulators have been identified, which include repressors (e.g. pRB, WT1, and SMAD3), activators (e.g. c-myc, HPV E6, and STAT3), and dual-function repressor/activators (e.g. E2F1, SP1, and p73) [243]. Alternatively spliced transcripts have been detected in several normal and cancer cells and tissues, indicating that post-transcriptional mechanisms regulate hTERT biogenesis [244,245]. Most of these transcripts are deletion variants that lack regions of the RT domain and at least one variant, hTERT $\alpha$ , encodes a dominant negative inhibitor of telomerase activity [246,247]. hTERT is also regulated by at least one type of post-translational modification: ubiquitylation. The E3 ubiquitin ligase MKRN1 has been shown to interact with hTERT *in vitro* and *in vivo* [248]. MKRN1 catalyzes ubiquitylation of the hTERT C-terminus and targets hTERT for proteasome-mediated protein degradation [248]. Unfortunately, the cellular signals that induce hTERT ubiquitylation and degradation have not been investigated.

### ***1.5.2 Assembly***

In ciliates, telomerase assembly is a hierarchical process initiated by a series of protein-TR interactions that induce a local conformational change in TR and promote TERT binding [249-251]. It is anticipated that a similar assembly mechanism exists for human telomerase. The chaperone proteins HSP90 and p23 were the first proteins to be identified that contribute to the assembly of catalytically active human telomerase [252]. Immunodepletion or inhibition of HSP90 or p23 impaired telomerase activity *in vitro* and *in vivo* [252-254]. In budding yeast, the HSP90 and p23 orthologs promote telomerase association and dissociation with telomeric DNA, respectively [255,256]. Likewise, there is some evidence to suggest that HSP90 is needed to maintain human telomerase in a conformation that facilitates DNA-binding [254]. These observations suggest that the HSP90-p23 chaperone complex regulates conformational changes in telomerase that are required at specific stages of the telomerase reaction cycle. In addition to HSP90 and p23, several other proteins have been identified with potential roles in the assembly of functional telomerase, including HSP70 and HSP40 [252], the RNP assembly chaperone SMN complex [257], the nucleolar acetyltransferase NAT10, and the nucleolar GTPase GNL3L [231]. The physiological significance of these interactions, however, is not fully understood.

One of the major outstanding questions regarding telomerase structure is the oligomerization state *in vitro* and *in vivo*. The ability of human [101,258], *E. crassus* [132,259], and yeast [260] telomerase to form dimers and multimers *in vitro* and *in vivo* has been deduced from gel filtration and glycerol gradient centrifugation analyses. One

potential caveat of the gel-filtration and sedimentation studies, however, is that the size of the RNP complex is determined relative to protein standards. Coprecipitation and reconstitution studies have convincingly demonstrated that TERT and TR form physical and functional dimers or multimers *in vitro* and *in vivo* [130-132,205,208,258,260,261]. However, multisubunit complexes could be artificially produced by the *in vitro* reconstitution system or by subunit over-expression in living cells. In an attempt to address these issues, single-molecule fluorescence two-color coincidence detection has been applied to recombinant human telomerase [262]. In this biophysical assay, telomerase is reconstituted *in vitro* with fluorescently-labelled hTERT and hTR. Radiometric analysis of single- and dual-colour (coincident) fluorescent intensities provides information on complex composition and stoichiometry. This technique demonstrated that hTERT-hTR monomers predominate in solution [262]. An important future study will be to apply this technique to telomerase derived from cell extracts. In this regard, dual-affinity purification of ectopically expressed telomerase suggests that the catalytic RNP exists as a monomer in human cells [263]. Finally, it is interestingly to note that telomerase from *T. thermophila* and *E. aediculatus* is active as a monomer [115,264]. It is possible that telomerase exists in monomeric and multimeric complexes that each has specialized functions during different stages of the cell-cycle or within distinct subcellular compartments. However, the cellular significance of telomerase multimerization remains unknown.

### ***1.5.3 Subcellular Localization***

The subnuclear localization of catalytically-active telomerase RNP is believed to represent an important regulatory mechanism for telomere elongation [178,265,266]. As discussed in Section 1.4, hTR and hTERT are physically sequestered in distinct nuclear compartments during G1 and G2. The highest intracellular concentration of hTR is in CBs, although minor fractions of hTR are associated with nucleoli [177,218,219]. hTERT is typically observed throughout the nucleoplasm and nucleoli [170,171,176,178]. Remarkably, hTR and hTERT are redirected to common nuclear foci during S phase [178]. Indirect immunofluorescence of telomere-binding proteins and telomere-specific oligonucleotide fluorescence *in situ* hybridization experiments revealed that these foci represent telomeres [178,266]. The current model is that CBs deliver catalytically active telomerase to a subset of telomeres for extension during S phase. It would be interesting to determine if depletion of integral CB components is associated with a reduction in telomerase activity and/or telomere elongation. Furthermore, it will be important to decipher when and where telomerase is assembled and disassembled, as well as the mechanisms of nuclear (and subnuclear) import and export.

## **1.6 The Telomerase Reaction Cycle and Telomere Synthesis**

Telomerase is an unusual reverse transcriptase because the RNA template for DNA synthesis is an integral component of the holoenzyme. Furthermore, telomerase adds hundreds of nucleotides to the same primer by catalyzing multiple rounds of template copying. This contrasts with prototypical RTs, which copy a relatively large

RNA genome into a single molecule of complementary DNA. As illustrated in Figure 1.13, the telomerase reaction cycle can be divided into three basic steps: 1) primer recognition and binding; 2) synthesis of the first telomeric repeat; and 3) translocation and realignment of the new DNA 3'-end to initiate the next round of telomere synthesis. In the following sections, I will discuss these steps and the structural features of telomerase that have key roles in the reaction cycle.

### ***1.6.1 An overview of the telomerase reaction cycle***

The telomeric ssDNA overhang is believed to be the most common primer for telomerase extension *in vivo*. However, telomerase can elongate almost any G-rich linear ssDNA primer that contains a free 3'-end *in vitro* [110,267]. Parallel intermolecular G-quadruplex substrates are also efficient substrates for ciliate telomerase *in vitro* [268-270]. Furthermore, the enzyme can also add telomeric repeats to non-telomeric ssDNA primers during chromosome healing (discussed below).

During telomere elongation, the RNA template is reverse transcribed using canonical Watson-Crick base-pairing to specify the telomeric sequence. Telomere synthesis proceeds by the sequential addition of deoxynucleotide triphosphates (dNTPs) to the free 3'-hydroxyl group of the telomeric ssDNA primer. The ability of telomerase to incorporate consecutive dNTPs without dissociating from the primer is known as nucleotide addition processivity or type I DNA synthesis [129]. During telomere elongation, the RNA-DNA hybrid is kept at a constant length of seven to eight base-pairs by melting bonds at the distal end of the template as new bonds are formed at the

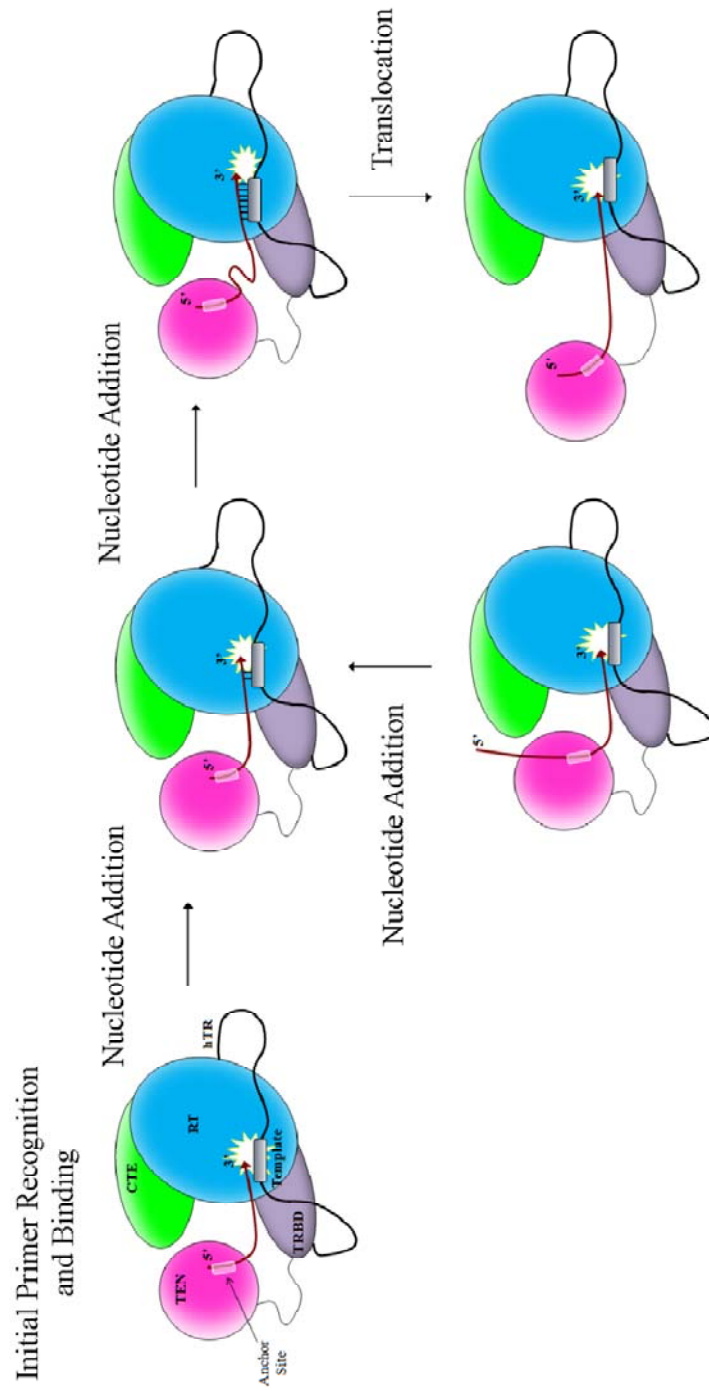


**Figure 1.13: The telomerase reaction cycle.**

**Figure 1.13: The telomerase reaction cycle.**

This figure summarizes the main steps of the telomerase reaction cycle: initial primer recognition and binding, nucleotide addition, and translocation. Telomerase contains an RNA subunit, hTR (represented by a black line that does not represent the full length subunit or secondary structure), that supplies the template for telomere synthesis (grey rectangle), and a catalytic protein subunit, hTERT. hTERT contains a telomerase essential N-terminal (TEN) domain (pink sphere), a telomerase RNA-binding domain (TRBD; purple oval), reverse transcriptase domain (RT; blue sphere), and C-terminal extension (CTE; green oval). The TEN domain contains a unique DNA-binding region called the anchor site (transparent white rectangle). An example of telomeric ssDNA is indicated by the red line. Telomerase binds the telomeric ssDNA such that the 3'-end is aligned with the hTR template in the active site (white star) and the 5'-end is positioned within the telomerase anchor site. Telomerase reverse transcribes the template region, one nucleotide at a time (nucleotide addition; top cartoons), until reaching the 5'-template boundary element (top right cartoon). At this point, a poorly-understood translocation step repositions the new DNA 3'-end within the template for a second round of telomere synthesis (bottom cartoons).

proximal end [134]. This is important because it explains why the telomerase reaction cycle does not require a high energy co-factor. When the 5'-template boundary element is reached, a poorly-understood translocation step repositions the new DNA 3'-end within the template for a second round of telomere synthesis. The ability of telomerase to catalyze more than one round of DNA synthesis while bound to the same telomeric primer is referred to as repeat addition processivity (RAP) or type II DNA synthesis. As discussed below, interactions between the 5'-end of the primer and regions of TERT outside the RT domain ('anchor sites' or 'anchor regions') are required for RAP [129].

### ***1.6.2 Repeat addition processivity***

Repeat addition processivity was first observed with *T. thermophila* telomerase [271] and subsequently for human telomerase [272]. Primer challenge experiments demonstrated that ciliate telomerase could synthesize approximately 90 telomeric repeats to a given primer in a 60 minute reaction [271]. By contrast, many rodent and fungal telomerases are relatively non-processive and catalyze short elongation products *in vitro* and *in vivo* [273-275]. Furthermore, genetic studies with mutant *T. thermophila* telomerase RNAs indicated that telomerase has limited processivity *in vivo* [10,113]. Recent *in vivo* analyses of budding yeast telomerase have provided much-needed insight into the biological significance of RAP. These studies collectively demonstrated that the RAP of *S. cerevisiae* telomerase is significantly increased at extremely short telomeres, suggesting enhanced RAP may enable cells to rapidly elongate critically short telomeres [104,276]. This model predicts that the extent of RAP depends upon telomere length and

thus, could partially explain the variance observed between telomerase RAP *in vitro* and *in vivo*.

To date, the most direct evidence that RAP is critical for telomere length maintenance comes from structure-function studies of ciliate, yeast, and human TERT. Telomerase-specific residues that mediate RAP are located in the RT domain [138,156], NTE [163,208,277-279], and CTE [139]. Mutating or deleting these amino acids in human, ciliate, or yeast TERT selectively impairs RAP *in vitro* and causes defects in telomere length maintenance *in vivo* [138,163,208,277,279]. Some of these amino acids are also required for the ability of yeast, human, and ciliate telomerase to extend partially or completely nontelomeric primers: these observations provide indirect evidence for a role in ssDNA-binding [163,208,277,279]. Mutations that specifically increase repeat addition processivity *in vitro* and cause telomere over-elongation *in vivo* have also been identified in ciliate [156] and yeast [278] TERT. This provides additional evidence that RAP is a biologically relevant property of telomerase.

### ***1.6.3 Telomerase anchor sites***

#### ***1.6.3.1 Primer recognition***

The existence of a telomerase anchor site was initially deduced from studies demonstrating that ciliate and human telomerase could efficiently elongate non-telomeric G-rich ssDNA primers *in vitro* [110,111,272,280]. Furthermore, telomerase could add telomeric repeats to chromosome break-points that contained non-telomeric DNA during *in vivo* chromosome healing [10,281]. It was subsequently shown that primers containing

almost any sequence of ssDNA could prime telomere synthesis *in vitro* if telomeric repeats were added to the 5'-end [267,282]. The sequence composition of the primer 5'-end was shown to have a dramatic effect on the catalytic rate, processivity, and apparent ssDNA-binding affinity of *T. thermophila* telomerase [283]. These observations indicated that hybridization between the DNA 3'-end and RNA template region was not absolutely required for telomerase-dependent primer elongation. This hypothesis was further supported by biochemical studies of human and yeast telomerases, which showed that the enzyme/primer complex was mainly stabilized by contacts with the catalytic protein subunit [260,284]. Interestingly, the RNA-DNA hybrid contributed minimally to complex stability [260,284]. Collectively, these studies demonstrated that telomerase interacts with DNA in a bipartite manner: 1) Watson-Crick base-pairs between the template RNA and ssDNA 3'-end in the enzyme active site; and 2) contacts between the primer 5'-end and a region of TERT outside the active site.

The first direct evidence for a telomerase anchor region was provided by photo-cross-linking studies performed with ciliate telomerase [285]. Telomerase derived from *E. aediculatus* was cross-linked to photo-reactive ssDNA primers that were aligned in the enzyme active site [285]. The authors observed that the most efficient cross-links were formed between a TERT-sized protein and residues 20 to 22 nt upstream of the 3'-end [285]. Nonetheless, it remained unclear if the TERT could interact with telomeric ssDNA in the absence of the RNA subunit. As discussed in Chapter 3, we provided the first evidence that human TERT specifically binds telomeric ssDNA independently of the human TR subunit [158]. Similar results have now been reported for *T. thermophila*

TERT, indicating that this is likely an evolutionarily-conserved feature of telomerase [270,286]. However, the telomerase RNA subunit may enhance the ability of TERT to bind telomeric ssDNA [143,277,286]. A future challenge will be to devise a method to accurately determine how TERT and TR contribute to substrate recognition *in vitro*.

### 1.6.3.2 Primer elongation

As mentioned above, telomerase anchor regions have been proposed to account for the unique ability of telomerase to catalyze processive repeat addition. A multitude of genetic and biochemical studies with ciliate, yeast, and mammalian telomerase have provided insight into regions outside the catalytic domain that are important for DNA-binding and enzyme activity [143,158,163,167,272,278-280,283,284,287,288]. Together, these studies indicate that TERT contains multiple DNA-binding regions that can be classified as either template-proximal or template-distal anchor sites. Both of these regions contribute to enzyme activity, processivity and DNA-binding, although the template-distal region is not absolutely required for RAP. Importantly, only relatively long primers ( $\geq 20$  nt) extend into the template-distal anchor region [133]. The existence of separate anchor sites is consistent with a tripartite mode of DNA-binding: 1) the primer 3'-end hybridizes with the RNA template in the active site; 2) primer nt immediately adjacent to the template-hybridizing region interact with a template-proximal anchor site; and 3) the primer 5'-end interacts with the template-distal anchor site [287]. A conformational change in the template-proximal region is believed to convert telomerase to an elongation-competent state [271]. Consistent with this idea,

recent studies with *T. thermophila* telomerase suggest that the TERT N-terminus is displaced relative to the catalytic site during telomere synthesis (Figure 1.13) [289]. This movement presumably repositions the template-proximal anchor site relative to the active site and correctly orientates the DNA primer or DNA-RNA heteroduplex in the active site during primer elongation [143,289].

### 1.6.3.3 An evolutionarily-conserved anchor region in the TEN domain

Telomerase anchor regions have been physically and functionally mapped to the TERT NTE in ciliates, yeast, and humans, although the residues that define and separate each region have not been completely elucidated (Figure 1.13) [129,158,278,279,286,289]. Importantly, conserved amino acids on the surface of the *T. thermophila* TEN domain are predicted to form a previously unrecognized ssDNA-binding channel that could represent one of the long sought-after anchor regions [143]. Photo-cross-linking studies showed that the *T. thermophila* TERT (tTERT) TEN domain exhibits telomere-sequence-specific ssDNA-binding activity *in vitro* [143,289]. Mutagenesis of key residues thought to be involved in ssDNA-binding, such as an invariant Gln (Q168 in tTERT), significantly reduced the interaction between tTERT and telomeric ssDNA and impaired enzyme activity *in vitro* [143,289]. Furthermore, mutation of the corresponding residue in *S. cerevisiae* TERT (Est2p Q146A) severely impaired telomerase activity and caused growth defects and telomere loss *in vivo* [278,290]. As described in Chapter 4, we provided the first detailed evidence regarding the biochemical and cellular roles of this residue in human telomerase, hTERT Q169. Collectively, the studies described above indicate that this Gln residue defines part of an evolutionarily-

conserved telomerase anchor site that mediates substrate recognition and orientation in the catalytic site to initiate telomere synthesis.

## **1.7 Telomeres, Telomerase and Human Disease**

### ***1.7.1 Cellular senescence and aging***

Cellular senescence, also referred to as replicative senescence, was formally defined in 1961 when Hayflick and Moorehead showed that normal human fibroblasts had a limited proliferative potential *in vitro* [291]. Pioneering experiments demonstrated that diploid human cells initially entered a phase of robust cell division, which was followed by gradual degenerative changes and decreased proliferation, ultimately leading to a complete loss of cell proliferation. The non-proliferating cells contained “bizarre nuclear forms and sizes”, yet remained viable and metabolically active [291]. This phenotype was termed cellular senescence [291]. Subsequent experiments confirmed that the proliferative capacity of normal diploid human fibroblasts was intrinsically limited [292]. These observations led to the hypothesis that cells contained an internal clock that tracked the number of cell divisions and induced replicative senescence after a predetermined number of divisions (the ‘Hayflick limit’) [292]. A connection between telomere length and replicative senescence was first reported in the early 1990s with the observation that telomeres shorten with ageing in normal human fibroblasts [24]. Furthermore, it was expected that telomere length was directly associated with telomerase activity, which was notably inactive in most somatic human cells and tissues [24,26,65,169,293,294]. These observations led to the telomere hypothesis of senescence,

which predicted that critically short telomeres cause growth arrest and chromosomal instability observed in senescent fibroblasts (Figure 1.14).

Today, it is well-established that most diploid human fibroblasts can be cultivated *in vitro* for a finite number of population doublings before entering senescence (Figure 1.14). The current view is that one or a few critically short telomeres trigger a DDR that induces replicative senescence [55,56,103,296,297]. Senescent cells are characterized by the following: 1) an inability to synthesize DNA; 2) increased expression of the cell-cycle inhibitors p16 and p21; 3) resistance to apoptosis; 4) morphological changes including a flat, extended shape and multiple abnormal nuclei; 5) senescence-associated  $\beta$ -galactosidase activity [298]; and most recently, 6) senescence-associated heterochromatic foci [299,300]. Furthermore, senescent cells display widespread changes in gene expression profiles and up-regulate genes that encode extracellular-matrix-degrading proteases, inflammatory cytokines, and growth factors [300]. The accumulation of senescent cells in aging tissues is believed to impair organ function and contribute to several age-related pathologies [300].

The *mTerc*<sup>-/-</sup> mouse model, which lacks the murine telomerase RNA component, has provided important insight into the relationship between telomerase, telomeres, senescence, and aging. Notably, first-generation mice are viable, fertile, and lack any discernable morphological defects [301]. However, successive generations demonstrate cumulative telomere shortening, which eventually manifests as defects in cell growth and renewal and organ homeostasis [301,302]. Sixth-generation (G6) *mTerc*<sup>-/-</sup> mice are sterile, show decreased regeneration of gastrointestinal and skin tissues, and exhibit

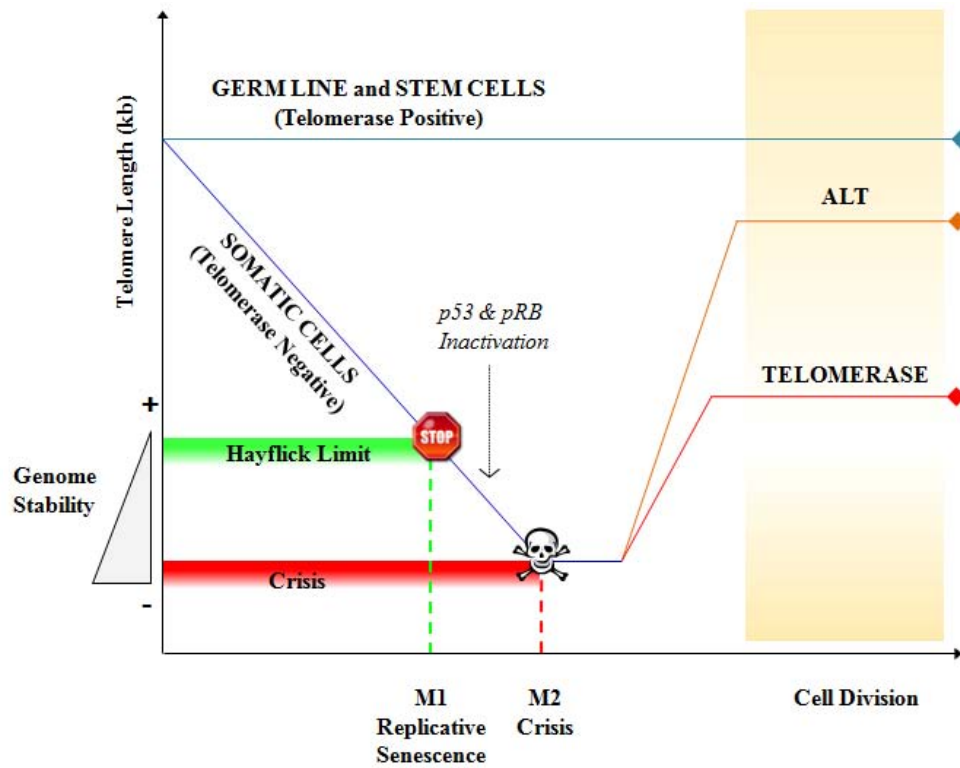


**Figure 1.14: The relationship between telomerase, telomere length, and cellular lifespan.**

**Figure 1.14: The relationship between telomerase, telomere length, and cellular lifespan.**

This figure summarizes the relationship between telomerase activity, telomere length (y-axis), and cellular lifespan/division (x-axis). The relative level of genome stability is indicated by the grey right-angle triangle: the '+' sign represents genome stability and the '-' sign reflects genome instability. Telomerase positive cells (germ line and stem cells) maintain telomeres at a steady-state length (top blue line). Somatic cells that lack telomerase activity exhibit telomere shortening during successive rounds of cell division (declining blue line). This eventually triggers a p53- and pRB-dependent growth arrest (indicated by the STOP sign cartoon), which is known as the Hayflick limit, replicative senescence, or Mortality stage (M1). Inactivation of p53 and pRB function enables cells to bypass senescence and continue proliferating, during which time telomeres continues to shorten. This continued growth eventually induce a second growth-arrest state (indicated by the skull cartoon), termed crisis or mortality stage 2 (M2), which induces massive apoptosis. However, rare clones escape crisis by activation of telomerase (red line) or an alternative lengthening of telomeres (ALT) mechanism (orange line), which enables these cells to maintain telomere length indefinitely. The orange shaded rectangle at the right end of the figure illustrates the variability in telomere length that has been observed in telomerase- or ALT-immortalized human cells [295].

defects in multiple tissue compartments, such as the hematopoietic and cardiovascular systems [302,303]. These phenotypes are associated with a significantly reduced lifespan. Many of the age-related pathologies observed in G6 *mTerc*<sup>-/-</sup> mice recapitulate age-associated human diseases. Importantly, genetic reconstitution of telomerase activity in G4 *mTerc*<sup>-/-</sup> mice is sufficient to restore telomere elongation and rescue the severe premature aging pathologies [304]. This observation emphasizes the relationship between telomere length, aging, and age-related pathologies.

### ***1.7.2 Cellular immortalization and cancer***

Telomerase expression and activity is robust in germ line and stem cells but low or absent in most somatic cells and tissues. In the absence of telomerase (or a mechanism to maintain telomere length), telomeres gradually shorten with each round of cell division until they reach a critically-short threshold (Figure 1.14). This shortening triggers a p53 and pRB-dependent DDR and induces replicative senescence, which is also referred to as M1 (Mortality stage 1) [295]. Cells harbouring inactivated p53 and pRB pathways bypass this barrier and proliferate for an additional 20 to 30 population doublings, depending on the cell type (Figure 1.14). During this period, cells exhibit increasing levels of chromosome instability and decreasing telomere lengths. This eventually triggers a second proliferative blockade, termed M2 (Mortality stage 2) or crisis [295]. At this stage, most cells exhibit extensive genome instability and telomere attrition, which triggers widespread apoptosis. However, rare cells (~ 1 in 10<sup>7</sup> cells) emerge from crisis and become immortal [295]. Immortalized cells avoid massive genetic catastrophe by up-

regulating a telomere-maintenance mechanism to stabilize their critically short telomeres (Figure 1.14).

The observations that human cancer cells have stable yet abnormal genomes, express telomerase, and are immortal collectively indicate that telomerase activation is a common pathway for cellular immortalization and transformation [65,118,169]. The causal relationship between hTERT and cell immortalization was established by a series of experiments in which human cells were transfected with vectors encoding wild type hTERT [305-307]. These studies showed that human cells expressing wild type hTERT contained robust telomerase activity, exhibited telomere elongation, and had an extended proliferative capacity. Ectopic expression of hTERT in pre-senescent [305,307] and transformed pre-crisis [161,308,309] cells permitted these cells to bypass replicative senescence and crisis, respectively. However, ectopic expression of wild type hTERT is not sufficient to immortalize all primary human cells [310] or create tumorigenic cells [311], indicating that additional mutations are required to establish the malignant phenotype. Indeed, genetic changes in at least four distinct signalling pathways are required to create human tumour cells: 1) the *Ras*-activated mitogenic response pathway; 2) inactivation of the p53 pathway; 3) abrogation of the p16/pRB pathway; and 4) up-regulation of a telomere maintenance-mechanism [311].

The relationship between hTERT, replicative lifespan, and transformation was further supported by experiments in which telomerase-negative human cells were transfected with catalytically inactive hTERT mutants harbouring amino acid substitutions in the conserved RT domain. These cells did not exhibit telomerase activity

or telomere elongation, had a finite lifespan, and did not induce tumour formation in immunodeficient mice [312]. Furthermore, when expressed in telomerase-positive human cells, the catalytically inactive mutant was observed to inhibit endogenous telomerase activity, induce telomere shortening and chromosome instability, and trigger apoptotic cell death without activating an alternative mechanism to maintain telomere length (below) [312,313]. These studies suggested that the abnormal telomerase activity observed in human cancer cells might be amenable to therapeutic intervention. Indeed, several different strategies that target and disrupt telomerase activity have been reported, including dominant negative hTERT alleles (as described above), modified oligonucleotides, or specific inhibitors [314]. Unfortunately, the efficacy and clinical application of these approaches remains limited. This is partially due to an incomplete understanding of human telomerase structure and function.

### ***1.7.3 Telomere maintenance without telomerase***

As discussed above, telomere homeostasis is a delicate balance of coordinated lengthening and shortening mechanisms. In the absence of telomerase, telomeres shorten with every cell division and eventually trigger cell cycle arrest. Inhibiting continual telomere loss by the activation of a telomere maintenance system is a hallmark of human cancers and cancer cell lines. Approximately 85 % of mammalian tumours exhibit expression of the human telomerase catalytic subunit and utilize telomerase-dependent telomere elongation to attain unlimited growth potential [169]. Some mammalian tumours and immortalized cell lines, however, lack telomerase activity and use

recombination-based mechanisms for telomere maintenance, termed Alternative Lengthening of Telomeres (ALT) pathways [315,316]. One hallmark of ALT cells is the presence of heterogeneous telomeric DNA that can range in length from less than 2 kb to greater than 50 kb [315,316]. Furthermore, the length of bulk telomeric DNA in ALT cells is generally longer than that measured in telomerase-positive transformed cells and tumours [317]. Specialized nuclear structures called ALT-associated Promyelocytic leukemia Bodies (APBs) are another defining characteristic of ALT cells. These foci contain shelterin proteins, telomeric DNA, and proteins involved in DNA replication, recombination, and repair [317]. Telomere maintenance appears to involve various recombination mechanisms [318], although the molecular details are not fully understood. ALT cells contain significantly elevated rates of telomere recombination but not global recombination [319]. The current model is that ALT cells have lost either an intrinsic ability to repress inappropriate telomere recombination or the ability to regulate HR-assisted telomere capping following telomere replication.

#### ***1.7.4 Telomerase deficiency and human disease***

The most direct evidence for a relationship between telomere shortening and age-related human pathologies comes from studies of patients inflicted with Dyskeratosis Congenita (DC). Dyskeratosis congenita is a rare, multi-system disorder that has been classified as a cancer predisposition disorder, premature aging syndrome, and bone marrow failure syndrome [320]. Clinical manifestations of DC generally appear during childhood and include a monocutaneous triad of abnormal skin pigmentation, nail

dystrophy, and oral leukoplakia [320]. These symptoms are accompanied by a spectrum of other somatic abnormalities, such as developmental delay, pulmonary disease, and premature hair loss [320]. Bone marrow failure is the principal cause of premature mortality [320]. Patients are also predisposed to developing carcinomas, lymphomas, and leukemias. At the genetic level, DC can be X-linked recessive, autosomal dominant, or autosomal recessive [320].

Accelerated telomere shortening and subsequent telomere dysfunction are the common, underlying causes of DC and DC-related diseases [320]. Inherited forms of DC exhibit anticipation, whereby successive generations exhibit earlier disease onset and present with more severe phenotypes [321,322]. The mechanism of disease anticipation in DC is thought to be caused by the inheritance of short telomeres that continue to shorten at an accelerated rate in the afflicted offspring. Mutations have been detected in five telomerase holoenzyme genes (*TERC*, *TRT*, *DKC1*, *NOP10*, and *NHP2*) and one shelterin gene, *TINF2* [320]. Heterozygous mutations in these genes have been shown to elicit the disease phenotype through haploinsufficiency [320]. Dyskerin, NOP10, and NHP2 are essential for the stability and accumulation of hTR *in vitro* and *in vivo* [323-325]. Mutations in the *TERC* gene impair hTR stability and/or telomerase catalytic activity [198,216]. Similarly, hTERT mutations have severe consequences on enzyme function *in vitro* and *in vivo* [326,327]. The telomere maintenance defects observed in cultivated human cells can be rescued by the ectopic expression of wild type hTR or hTERT, which reconstitutes telomerase activity [323,327,328]. Collectively, these observations indicate that accentuated telomere attrition occurs through a molecular

mechanism in which the mutations impair the stability and accumulation of hTR and/or adversely affect the telomerase catalytic reaction.

The most recently identified DC-associated mutation is located in the *TINF2* gene [329,330]. The protein product encoded by *TINF2* is TIN2, an integral and central component of the shelterin complex that is essential for telomere function *in vitro* and *in vivo*. Although the mechanism has not been examined in detail, it is expected that mutations in TIN2 facilitate telomere degradation directly by disrupting telomere architecture and constitutively exposing the ss 3'-end to the cell's DNA damage surveillance and repair proteins [329,330]. Consistent with this model, patients with *TINF2* mutations have telomeres that are significantly shorter than age-matched DC patients carrying mutations in any of the other known genes [329,330]. Furthermore, the majority of cases arise *de novo*, suggesting that this is a particularly severe form of DC that is largely incompatible with germ line inheritance [329,330]. The embryonic lethality of *mTin2*<sup>-/-</sup> mice further supports the severity of diseases associated with mutations in the *TINF2* gene [331].

In addition to classical DC, there are several DC-related diseases that are associated with the same genetic lesions and clinical characteristics [320]. These variants include: 1) Hoyeraal-Hreidarsson (HH) syndrome, a multisystem disorder characterized by bone marrow failure, immunodeficiency, and severe growth retardation; 2) Aplastic Anemia (AA), a hematological disorder characterized by a reduction in red blood cells of all lineages; and 3) Idiopathic Pulmonary Fibrosis (IPF), a chronic, progressive, and fatal lung disease characterized by irreversible fibrosis [320]. Mutations in *DKC1*, *TINF2*, and

*TRT* have been identified in HH patients [329,330,332,333] and heterozygous *TERC* and *TRT* mutations are associated with AA [327,334,335] and IPF [336,337]. The broad spectrum of disease phenotypes that are manifested by mutations in telomerase and telomere genes illustrates the molecular complexity of these pathways. The study of naturally-occurring mutants can provide important insight into fundamental mechanisms of protein assembly, activity, and regulation, as well as elucidate novel targets that may be amenable to therapeutic intervention. Structure-function studies of the naturally-occurring hTERT mutants will be particularly informative since there are many outstanding questions regarding the functions of telomerase in both healthy and diseased human cells.

## **1.8 Objectives**

Telomerase is an RNA-dependent DNA polymerase that has a central role in chromosome stability. Genetic and somatic mutations that disrupt the normal assembly and function of the human telomerase RNP are associated with a spectrum of disease states, including cancer and premature aging syndromes [338]. Characterization of human telomerase structure and function is required to understand the molecular mechanisms that underlie these disease states. The overall objective of my thesis work was to understand the fundamental mechanisms by which hTERT interacts with telomeric ssDNA and how these interactions contribute to telomerase function. This goal was accomplished through the following specific aims:

- 1) Identify regions of hTERT that regulate the strength and sequence-specificity of hTERT-ssDNA interactions *in vitro*.
- 2) Characterize the relationship between physical and functional telomerase-ssDNA interactions *in vitro* and *in vivo*.
- 3) Determine how hTERT mutations contribute to telomerase dysfunction in relation to human disease.

## Chapter Two: Materials and Methods

### 2.1 Reconstitution of Human Telomerase

#### 2.1.1 Cloning of *hTERT* constructs

##### 2.1.1.1 Expression vectors

The hTERT constructs described below were cloned into the *EcoRI* and *SalI* restriction sites of the vector pCI (Promega, Fisher Scientific, Ltd.). The multiple cloning site is flanked by the T7 RNA polymerase promoter, which is required for *in vitro* expression using the TNT<sup>®</sup> T7 Quick Coupled Transcription-Translation System (Promega, Fisher Scientific Ltd.). pBABE<sub>puro</sub> (courtesy Dr. C. Counter, Duke University Medical Center, Durham NC) is a retroviral mammalian expression vector that contains a multiple cloning site downstream from the Moloney Murine Leukemia Virus (MoMuLV) Long Terminal Repeat (LTR) [339]. The Simian Virus 40 (SV40) early promoter drives cellular expression of the puromycin resistance gene for selection of cells with integrated retrovirus. pCL-10A1 (courtesy Dr. C. Counter, Duke University Medical Center, Durham NC) is the helper construct used with the pBABE<sub>puro</sub> retroviral vector to package amphotropic retroviral particles [340].

##### 2.1.1.2 Enzymes and bacteria

Polymerase Chain Reaction (PCR) was performed using Platinum<sup>®</sup> Pfx DNA polymerase (Invitrogen). The *EcoRI*, *SalI*, and *SphI* restriction endonucleases and T4 DNA ligase were purchased from Invitrogen. The *DpnI* restriction endonuclease was

purchased from New England BioLabs. Bacterial transformations were performed with MAX Efficiency® DH5 $\alpha$ <sup>TM</sup> Competent Cells (Invitrogen). Plasmids from positive transformants were isolated with the use of a Mini-Prep kit (Qiagen or Fermentas).

#### 2.1.1.3 Full Length (FL) hTERT

The FL FLAG-hTERT DNA fragment (~ 3.5 kb) was excised from plasmid pBABE<sub>puro</sub>-FLAG-hTERT (a generous gift from Dr. C. Counter, Duke University Medical Center, Durham NC) using *Eco*RI and *Sal*I. The DNA fragment was subcloned into the *Eco*RI and *Sal*I sites of plasmid pCI to create a FL hTERT cDNA (~ 3.5 kb) containing an N-terminal *Eco*RI restriction site and FLAG epitope (DYKDD), and a C-terminal *Sal*I restriction site.

#### 2.1.1.4 hTERT truncations

A PCR cloning approach was used to construct hTERT truncation mutants; these mutants were selected based on previously characterized hTERT variants [131,148]. Nomenclature indicates the amino acids that comprise each hTERT truncation. Each variant was cloned to express an N-terminal FLAG epitope using primers specific for the following (written 5' to 3'):

TEN domain (amino acids 1-196) was PCR-amplified from pCI-FLAG-hTERT 1-300 with the following primers:

FLAG Forward Pr.: ggaattcatggactacaaggacgatgacgac,

1-196 Reverse Pr.: cgtgtcgactcaacgccttcgggggtccactagcg.

The PCR product corresponding to the predicted size of the FLAG-hTERT TEN domain (~ 600 bp) was purified from an agarose gel using spin columns and the QIAquick Gel Extraction kit (Qiagen) and cloned into the *EcoRI-SalI* sites of pCI.

1-300 was constructed with overlap extension PCR and the following primers:

1-300 Pr. 1: gcgtttctgataggcacctattg,

1-300 Pr. 2: gagcgcgcggcgctccttg,

1-300 Pr. 3: caaggacgacgcgccgcgctc,

1-300 Pr. 4: gctgtcgactcagcccacggatg.

First, two separate PCR products were generated from pCI-FLAG-hTERT; one using 1-300 Pr. 1 and Pr. 2 primer set (~ 200 bp) and another using the 1-300 Pr. 3 and Pr. 4 primer set (~ 900 bp). These products were gel-purified and equimolar amounts of DNA ends were re-amplified using 1-300 Pr. 1 and 1-300 Pr. 4. The PCR product corresponding to the predicted size of the FLAG-hTERT 1-300 (~ 900 bp) was gel-purified and cloned into the *EcoRI-SalI* sites of pUC19. Plasmid DNA from positive bacterial transformants (as determined visually by blue-white screening) was isolated, verified by DNA sequencing, and subcloned into the *EcoRI-SalI* sites of pCI.

1-300 Q169A was PCR-cloned from pCI-FLAG-hTERT 1-300 using site-directed mutagenesis and *DpnI* digestion with the following primers:

Q169A Reverse Pr.: ggcccgcacaccgctaggcgc,

Q169A Forward Pr.: ggcctacgcggtgtgcgggcc.

1-300 Q169D was PCR-cloned from pCI-FLAG-hTERT 1-300 using site-directed mutagenesis and *DpnI* digestion with primers specific for the following:

Q169D Reverse Pr.: ggcccgcacacgtcgtaggcgc,

Q169D Forward Pr.: ggcctacgacgtgtgcgggcc.

1-300 Q169N was PCR-cloned from pCI-FLAG-hTERT 1-300 using site-directed mutagenesis and *DpnI* digestion with the following primers:

Q169N Reverse Pr.: ggcccgcacacgtttaggcgc,

Q169N Forward Pr.: ggcctacaacgtgtgcgggcc.

1-350 was made using overlap extension PCR with the following primers:

1-350 Pr. 1: cgctttctgataggcacctattg,

1-350 Pr. 2: gagcgcgcggcgcgtcctcttg,

1-350 Pr. 3: caaggacgacgcgccgcgcgctc,

1-350 Pr. 4: gctgtcgactcacagagctgag.

First, two separate PCR products were generated from FL FLAG-hTERT; one using 1-350 Pr. 1 and Pr. 2 primer set (~ 160 bp) and another using the 1-350 Pr. 3 and Pr. 4 primer set (~ 1050 bp). These products were gel-purified and equimolar amounts of DNA ends were re-amplified using 1-350 Pr. 1 and 1-350 Pr. 4. The PCR product corresponding to the predicted size of the FLAG-hTERT 1-350 (~ 1050 bp) was gel-purified and cloned into the *EcoRI-SalI* sites of pUC19. Plasmid DNA from positive

bacterial transformants (as determined visually by blue-white screening) was isolated, verified by DNA sequencing, and subcloned into the *EcoRI-SalI* sites of pCI.

144-1132 ( $\Delta$ 144) was PCR-amplified from FL FLAG-hTERT V144M with the following primers:

$\Delta$ 144 Forward Pr.: ggaattcatggactacaaggacgacgatgacaagatgggcgacgtgctggtcacc,  
hTERT Reverse Pr. 1: gctgtcgactcagtcaggatggtctt.

The PCR product corresponding to the predicted size of the FLAG-hTERT 144-1132 (~ 3 kb) was gel-purified and cloned into the *EcoRI-SalI* sites of pCI.

301-1132 was PCR-amplified from FL FLAG-hTERT with the following primers:

$\Delta$ 300 Forward Pr.: ggaattcatggactacaaggacgacgatgacaagcgccagcaccacgcg,  
hTERT Reverse Pr. 1: gctgtcgactcagtcaggatggtctt.

The PCR product corresponding to the predicted size of the FLAG-hTERT 301-1132 (~ 2.5 kb) was gel-purified and cloned into the *EcoRI-SalI* sites of pCI.

351-1132 was PCR-amplified from FL FLAG-hTERT with the following primers:

$\Delta$ 350 Forward Pr.: ggaattcatggactacaaggacgacgatgacaggcccagcctgact,  
hTERT Reverse Pr. 1: gctgtcgactcagtcaggatggtctt.

The PCR product corresponding to the predicted size of the FLAG-hTERT 351-1132 (~ 2.3 kb) was gel-purified and cloned into the *EcoRI-SalI* sites of pCI.

928-1132 was PCR-amplified from FL FLAG-hTERT with the following primers:

$\Delta$ 928 Forward Pr.: ggaattcatggactacaaggacgacgatgacaagttcccctggtgcggc,

hTERT Reverse Pr. 1: gctgtcgactcagtccaggatgtctt.

The PCR product corresponding to the predicted size of the FLAG-hTERT 928-1132 (~600 bp) was gel-purified and cloned into the *EcoRI-SalI* sites of pCI.

967-1132 was PCR-amplified from FL FLAG-hTERT with the following primers:

$\Delta$ 967 Forward Pr.: gaattcatggactacaaggacgacgatgacaaggggaggaacatgcgtcgc,

hTERT Reverse Pr. 2: gctgtcgactcaagtccaggatgg.

The PCR product corresponding to the predicted size of the FLAG-hTERT 967-1132 (~500 bp) was gel-purified and cloned into the *EcoRI-SalI* sites of pUC19. Plasmid DNA from positive bacterial transformants (as determined visually by blue-white screening) was isolated, verified by DNA sequencing, and subcloned into the *EcoRI-SalI* sites of pCI.

505-967 was PCR-amplified from FL FLAG-hTERT with the following primers:

505 Forward Pr.: ggaattcatggactacaaggacgacgatgacaagctgcaggagctgacgtg,

967 Reverse Pr.: gctgtcgactcaccagcctgaagccg.

The PCR product corresponding to the predicted size of the FLAG-hTERT 505-967 (~2 kb) was gel-purified and cloned into the *EcoRI-SalI* sites of pUC19. Plasmid DNA from positive bacterial transformants (as determined visually by blue-white screening) was isolated, verified by DNA sequencing, and subcloned into the *EcoRI-SalI* sites of pCI.

601-927 was PCR-amplified from FL FLAG-hTERT with the following primers:

601 Forward Pr.: ggaattcatggactacaaggacgacgatgacaagctgtcggagcagagg,

927 Reverse Pr.: gctgtcgactcataggccgtgggccgg.

The PCR product corresponding to the predicted size of the FLAG-hTERT 601-927 (~2.4 kb) was gel-purified and cloned into the *EcoRI-SalI* sites of pUC19. Plasmid DNA from positive bacterial transformants (as determined visually by blue-white screening) was isolated, verified by DNA sequencing, and subcloned into the *EcoRI-SalI* sites of pCI.

#### 2.1.1.5 FL hTERT mutants

##### D712A

The *EcoRI-SalI* DNA fragment containing FLAG-hTERT D712A was subcloned from plasmid pBABE<sub>hygro</sub>-FLAG-hTERT D712A (courtesy of Dr. C. Counter, Duke University Medical Center, Durham NC) into the *EcoRI-SalI* site of plasmid pCI to create a FL hTERT cDNA expressing an N-terminal *EcoRI* restriction site and FLAG-epitope (DYKDD), and a C-terminal *SalI* restriction site.

##### DAT (+68, +98, +122, +128, and +1127)

The *EcoRI-SalI* DNA fragments containing FLAG-hTERT DAT (+68, +98, +122, +128, and +1127) were subcloned from plasmid pBABE<sub>puro</sub>-FLAG-hTERT DAT (+68, +98, +122, +128, and +1127), respectively, (generous gifts from Dr. C. Counter, Duke University Medical Center, Durham NC) into the *EcoRI-SalI* site of plasmid pCI to create



hTERT Reverse Pr. 2: gctgtcgactcaagtccaggatgg.

First, two separate PCR products were generated from FL FLAG-hTERT; one using FLAG Forward Pr. and RT-GRIP Reverse Pr. (~ 2.7 kb), and another using the RT-GRIP Forward Pr. and hTERT Reverse Pr. 2 primer set (~ 550 bp). These products were gel-purified and equimolar amounts of DNA ends were re-amplified using FLAG Forward Pr. and hTERT Reverse Pr. 2. The PCR product corresponding to the predicted size of the FL protein (~ 3.5 kb) was gel-purified and cloned into the *EcoRI-SalI* sites of pUC19. Plasmid DNA from positive bacterial transformants (as determined visually by blue-white screening) was isolated, verified by DNA sequencing, and subcloned into the *EcoRI-SalI* sites of pCI.

N&RT-GRIP was created by *EcoRI-SphI* restriction digest of pCI-FLAG-hTERT N-GRIP and pCI-FLAG-hTERT RT-GRIP, followed by ligation of the 1556 bp and 5850 bp DNA fragments recovered from digested pCI-FLAG-hTERT N-GRIP and pCI-FLAG-hTERT RT-GRIP, respectively. This ligation yielded pCI-FLAG-hTERT N&RT-GRIP with N-terminal *EcoRI* and C-terminal *SalI* restriction sites.

V144M was PCR-cloned from pCI-FL FLAG-hTERT using site-directed mutagenesis and *DpnI* digestion with the following primers:

V144M Reverse Pr.: cacgtcgtcgcccatgcccgcgacgag,

V144M Forward Pr.: ctgctgcgccgcatggcgacgacgtg.

Q169A was made by overlap extension PCR with the following primers:

FLAG Forward Pr.: ggaattcatggactacaaggacgatgacgac,

Q169A Reverse Pr.: ggcccgcacaccgcgtaggcgc,

Q169A Forward Pr.: ggcctacgcggtgtgcgggcc,

hTERT Reverse Pr. 2: gctgtcgactcaagtccaggatgg.

First, two separate PCR products were generated using pCI-FL FLAG-hTERT template; one using FLAG Forward Pr. and Q169A Reverse Pr. (~ 500 bp), and another using the Q169A Forward Pr. and hTERT Reverse Pr. 2 primer set (~ 2.9 kb). These products were gel-purified and equimolar amounts of DNA ends were re-amplified using FLAG Forward Pr. and hTERT Reverse Pr. 2 to create a FL hTERT Q169A cDNA expressing an N-terminal *EcoRI* restriction site and FLAG-epitope (DYKDD), and a C-terminal *SalI* restriction site. The PCR product corresponding to the predicted size of the FL protein (~ 3.5 kb) was gel-purified and cloned into the *EcoRI-SalI* sites of pUC19. Plasmid DNA from positive bacterial transformants (as determined visually by blue-white screening) was isolated, verified by DNA sequencing, and subcloned into the *EcoRI-SalI* sites of pCI and pBABE<sub>puro</sub>.

Q169D was PCR-cloned from pCI-FL FLAG-hTERT using site-directed mutagenesis and *DpnI* digestion with the following primers:

Q169D Reverse Pr.: ggcccgcacacgtcgttaggcgc,

Q169D Forward Pr.: ggcctacgacgtgtgcgggcc.

Q169N was PCR-cloned from pCI-FL FLAG-hTERT using site-directed mutagenesis and *DpnI* digestion with the following primers:

Q169N Reverse Pr.: ggcccgcacacgtttaggcgc,

Q169N Forward Pr.: ggcctacaacgtgtgcgggcc.

A279T was PCR-cloned from pCI-FL FLAG-hTERT using site-directed mutagenesis and *DpnI* digestion with the following primers:

A279T Reverse Pr.: ggtggcttctcggtgggtctggcagg,

A279T Forward Pr.: cctgccagaccaccgaagaagccacc.

P721R was PCR-cloned from pCI-FL FLAG-hTERT using site-directed mutagenesis and *DpnI* digestion with the following primers:

P721R Reverse Pr.: gagcctgtcctggcggatggtgcgta,

P721R Forward Pr.: tacgacaccatccgccaggacaggctc.

R865C was PCR-cloned from pCI-FL FLAG-hTERT using site-directed mutagenesis and *DpnI* digestion with the following primers:

R865C Reverse Pr.:catccaccaaacacaggagcagcccgtc,

R865C Forward Pr.: gacgggctgctcctgtgtttggtgatg.

R865H was PCR-cloned from pCI-FL FLAG-hTERT using site-directed mutagenesis and *DpnI* digestion with the following primers:

R865H Reverse Pr.: catccaccaaatacaggagcagcccgtc,

R865H Forward Pr.: gacgggctgctcctgcatttggtgatg.

K902N was PCR-cloned from pCI-FL FLAG-hTERT using site-directed mutagenesis and *DpnI* digestion with the following primers:

K902N Reverse Pr.: gaagtcaccactgtgtccgcaagttcac,

K902N Forward Pr.: gtgaacttgcggaacacagtggtaactc.

R979W was PCR-cloned from pCI-FL FLAG-hTERT using site-directed mutagenesis and *DpnI* digestion with the following primers:

R979W Reverse Pr.: gctgtgacacttcagccacaagaccccaaagag,

R979W Forward Pr.: ctctttggggtcttggctgaagtgcacagc.

F1127L was PCR-cloned from pCI-FL FLAG-hTERT using site-directed mutagenesis and *DpnI* digestion with the following primers:

F1127L Reverse Pr.: gtccaggatggtcttgaggctgagggcag,

F1127L Forward Pr.: ctgcctcagacctcaagaccatcctggac.

The identity of each hTERT construct described above was confirmed using the following methods: 1) *EcoRI* and *SalI* restriction enzyme digest and ethidium bromide-stained agarose gel electrophoresis; 2) DNA sequencing by University Core DNA Services (University of Calgary); and 3) *in vitro* expression of [<sup>35</sup>S]cysteine-labelled

hTERT (described in Section 2.5.1), followed by sodium dodecyl-sulfate polyacrylamide gel electrophoresis (SDS-PAGE) on a gel containing 8 % or 10 % (wt/vol) polyacrylamide (29:1 [wt/wt] acylamide:bisacrylamide), and overnight exposure to a high performance autoradiography film or phosphorimager screen (Cyclone<sup>®</sup> Plus, PerkinElmer, Inc.).

### ***2.1.2 hTR synthesis and purification***

hTR was synthesized *in vitro* using the MEGAscript<sup>®</sup> T7 Transcription Kit (Ambion, Inc.). hTR plasmid DNA [148] was digested with *EcoRI* to obtain linear template for the T7 transcription reaction. T7 transcription reactions (20  $\mu$ L) containing 1  $\mu$ g *EcoRI*-linearized template DNA, 1x reaction buffer, 7.5 mM ATP, 7.5 mM CTP, 7.5 mM GTP, 7.5 mM UTP, and 2  $\mu$ L enzyme mix were incubated in a 37°C water bath for 2 h and then inactivated by treating with 2 U TURBO DNase<sup>™</sup> for 15 min at 37°C. The transcription reaction products were extracted by phenol and chloroform-isoamyl alcohol (24:1), precipitated with 2.5 volumes of ethanol and one-tenth volume of sodium acetate (pH 5.2) overnight at -20°C, centrifuged at 14,175  $\times$  g for 30 min (4°C), and resuspended in nuclease-free water.

hTR was purified from a denaturing (11 M urea) sequencing gel containing 6 % (wt/vol) polyacrylamide gel (19:1 [wt/wt] acylamide:bisacrylamide) by excising the gel fragment corresponding to hTR and elution in nuclease-free water (overnight at 4°C with rocking). On the following day, the telomerase RNA elution mixture was incubated at 60°C for 30 min (with vortexing every 10 min), centrifuged at 1500  $\times$  g for 5 min,

filtered through an Acrodisc<sup>®</sup> 25 mm Syringe Filter with 0.8/0.2- $\mu$ m Supor<sup>®</sup> Membrane (Pall Corp.), precipitated with 2.5 volumes of ethanol and one-tenth volume of sodium acetate (pH 5.2), centrifuged at  $14,175 \times g$  for 30 min (4°C), dissolved in an appropriate volume of nuclease-free water, and stored at -20°C. RNA concentration was determined by measuring the absorbance at 260 nm with an Eppendorf BioPhotometer UV/Vis spectrophotometer and Eppendorf UVette<sup>®</sup> cuvettes.

### ***2.1.3 In vitro synthesis of human telomerase***

Human telomerase was reconstituted *in vitro* with the rabbit reticulocyte lysate (RRL) TNT<sup>®</sup> T7 Coupled Transcription-Translation System (Promega, Fisher Scientific Ltd.). Ten  $\mu$ L reactions were assembled on ice and contained 5  $\mu$ L TNT<sup>®</sup> RRL, 0.4  $\mu$ L TNT<sup>®</sup> reaction buffer, 0.2  $\mu$ L TNT<sup>®</sup> amino acid mixture (minus methionine), 0.2  $\mu$ L TNT<sup>®</sup> amino acid mixture (minus leucine), 8 U RNaseOUT<sup>™</sup> (Invitrogen), 100 ng hTERT plasmid DNA, 100 ng *in vitro*-transcribed hTR (Section 2.1.2), and 0.2  $\mu$ L TNT<sup>®</sup> T7 RNA polymerase. Reactions were incubated in a 30°C water bath for 1.5-2 h, snap frozen in liquid N<sub>2</sub> and stored at -80°C (no CO<sub>2</sub>) until further use.

## **2.2 Cell Culture**

### ***2.2.1 Cell lines and culture conditions***

Human cells were cultured in a ThermoForma Model 3110 Series\* CO<sub>2</sub> water jacketed incubator (Forma Scientific, Inc.) at 37°C with 5 % CO<sub>2</sub>. SV40 large T-antigen transformed human embryonic kidney cells (293T) were cultured in GIBCO<sup>®</sup> high

glucose Dulbecco's Modified Eagle's Media (DMEM) supplemented with 10 % fetal bovine serum, 50 U/mL penicillin G, and 50 µg/mL streptomycin sulfate (Invitrogen). One µg/mL puromycin (Sigma-Aldrich) was added to the growth media for stable 293T cell lines. Primary human foreskin fibroblasts (BJ cells) (courtesy of Dr. Karl Riabowol, University of Calgary, Calgary AB) were cultured in Lonza BioWhittaker\* Minimum Essential Medium Eagle (EMEM) with Earl's Balanced Salt Solution (Fischer Scientific Ltd.) supplemented with L-glutamine, 10 % fetal bovine serum, 50 U/mL penicillin G, and 50 µg/mL streptomycin sulfate. Stable cell lines were cultured in media containing 0.1-0.5 µg/mL puromycin. 293T cells were continuously passaged at 1:5 or 1:6 and BJ cells were passaged at 1:4 or 1:5 until replicative senescence or until the culture divided 2.5 times more than the vector control cell lines.

### ***2.2.2 Generation of 293T stable cell lines***

293T cells were transfected with pBABE<sub>puro</sub> constructs encoding either FL FLAG-hTERT WT or Q169A, or, as the negative control, vector only DNA. One µg of construct DNA was transfected into a 6-well dish of 293T cells using FuGENE<sup>®</sup> 6 Transfection Reagent (Roche), as per the manufacturer's instructions. Forty-eight h post-transfection, confluent cultures were split into 10 cm dishes and stable polyclonal populations were selected in medium supplemented with 1.0 µg/mL puromycin. Cell cultures were continually passaged at 1:5 or 1:6 under puromycin selection. The first 10 cm plate to reach confluence under selection was arbitrarily defined as mean population doubling (mpd) 0.

### ***2.2.3 Retroviral infections for generation of BJ stable cell lines***

Retroviral infections were used to establish polyclonal BJ cell lines that stably express pBABE<sub>puro</sub>, pBABE<sub>puro</sub>-FLAG-hTERT, or pBABE<sub>puro</sub>-FLAG-hTERT Q169A. 293T cells were used to package amphotropic retroviruses created with pCL-10A and either pBABE<sub>puro</sub>, pBABE<sub>puro</sub>-FLAG-hTERT, or pBABE<sub>puro</sub>-FLAG-hTERT Q169A plasmid DNA. Eighteen to 24 h prior to transfection, packaging cells were split to 30 % confluency in 6-well culture dishes. One  $\mu\text{g}$  of pCL-10A1 plasmid DNA and 1  $\mu\text{g}$  of the appropriate pBABE<sub>puro</sub> construct DNA were applied to cells using FuGENE<sup>®</sup> 6 Transfection Reagent (Roche), as per the manufacturer's instructions. Twenty-four h later, 293T cultures were transfected a second time and 8 h after that, the transfection medium was removed and replaced with 2 mL of fresh growth medium. At the same time, a confluent 10 cm culture dish of BJ cells at mpd 48 was split to 40 % confluency in 6-well dishes.

The first retroviral infection was performed 24 h later by collecting the viral supernatant (VSN) from transfected 293T cells, filtering it through an Acrodisc<sup>®</sup> 25 mm Syringe Filter with 0.45- $\mu\text{m}$  HT Tuffryn<sup>®</sup> Membrane (Pall Corp.), adding polybrene (Sigma-Aldrich) to a final concentration of 8  $\mu\text{g}/\text{mL}$ , and then applying 2 mL of this solution to a 6-well dish of BJ cells. At the same time, 2 mL of fresh growth medium was applied to the transfected 293T cells. The retroviral infection procedure was repeated 24 h later and the 293T packaging cells were discarded. Twelve to 24 h after the final infection, the VSN was removed from BJ cell cultures and replaced with 3 mL of fresh growth medium. Forty-eight h after the final retroviral infection, BJ cells were split 1:4

into 10 cm dishes with selective growth medium containing 0.1-0.5  $\mu\text{g/mL}$  puromycin. The mpd 0 was arbitrarily defined as the time point when the infected cells reached 80 to 90 % confluency in selective growth media. Subsequently, BJ cells were passaged at 1:4 or 1:5 under puromycin selection until the culture had divided 2.5 times more than the vector control cells or until the culture had exhausted its replicative potential. The latter stage was defined as the period when cultures failed to become confluent in a 10 cm dish within 30 days and stained positive for  $\beta$ -galactosidase at pH 6.0 [298] (Section 2.2.6).

#### ***2.2.4 Harvesting cells***

One or two 15 cm culture dishes of approximately 90 % confluent 293T were harvested by gently scraping into approximately 10 mL of culture medium. One or two 15 cm culture dishes of approximately 90 % confluent BJ cells were harvested by incubating with 5 mL of pre-warmed trypsin-EDTA (Invitrogen) at 37°C for approximately 3 min and then gently scraping into approximately 10 mL of growth medium. Cell clumps were dissociated with gentle mixing and the homogenous cell solution was transferred into a 15 or 50 mL conical tube and subsequently pelleted by centrifugation in a pre-cooled rotor at  $153 \times g$  for 3 min (4°C). The supernatant was removed by aspiration and the pellet was gently resuspended in approximately 10 volumes of PBS prior to a second centrifugation at  $153 \times g$  for 3 min (4°C). Using aspiration, the supernatant was carefully decanted and the cell pellet was frozen and stored at - 80°C until further use.

### ***2.2.5 Cell lysis***

293T and BJ cell pellets were thawed on ice, resuspended in 0.5-1.0 mL NP-40 lysis buffer (10 mM Tris-HCl, pH 7.5; 1 % [vol/vol] NP-40; 10 % [vol/vol] glycerol; 1 mM EGTA; 1 mM MgCl<sub>2</sub>; 150 mM NaCl) containing fresh  $\beta$ -mercaptoethanol (5 mM), 10 U/mL RNaseOUT™ (Invitrogen), and an appropriate amount of Complete EDTA-Free Protease Inhibitor Cocktail (Roche), incubated on ice for 30 min, and then incubated with rocking at 4°C for 30 min. Lysates were centrifuged at 12 100  $\times$  g for 30 min at 4°C to remove the insoluble debris. The soluble fraction was pre-cleared with 40-50  $\mu$ L Protein G Sepharose™ (GE Healthcare) (50 % slurry) for 30 min at 4°C with rocking and then centrifuged at 800  $\times$  g for 3 min at 4°C. The supernatant was transferred to a fresh tube and the pellet was discarded. An aliquot of the pre-cleared soluble fraction was used in the Bio-Rad Protein Detection Assay (Bio-Rad) to measure protein concentration in the lysates (absorbance at 600 nm and fitting to a standard curve). An Eppendorf BioPhotometer UV/Vis spectrophotometer and Eppendorf UVette® cuvettes were used in the quantification assay.

### ***2.2.6 $\beta$ -galactosidase staining***

Adherent BJ cells grown in 10 cm culture dishes were washed in PBS (pH 7.2), fixed for 3-5 min at room temperature in PBS (pH 7.2) containing 0.5 % glutaraldehyde (Sigma-Aldrich), washed with PBS (pH 7.2) supplemented with 1 mM MgCl<sub>2</sub>, and stained overnight at 37°C (no CO<sub>2</sub>) with fresh  $\beta$ -galactosidase staining solution: PBS (pH 6.0) containing 1 mg/mL 5-bromo-4-chloro-3-indolyl  $\beta$ -D-galactoside (X-Gal) (stock =

20 mg/mL in dimethylformamide), 1 mM MgCl<sub>2</sub>, 120 μM potassium ferricyanide, and 120 μM potassium ferrocyanide. Staining was evident the next day: stained cells were washed in PBS (pH 7.2) and visualized with bright-field microscopy.

### ***2.2.7 Indirect immunofluorescence***

The cellular localization of WT or Q169A hTERT were visualized in 293T cells that stably expressed pBABE<sub>puro</sub>, pBABE<sub>puro</sub>-FLAG-hTERT, or pBABE<sub>puro</sub>-FLAG-hTERT Q169A. Cells were seeded on poly-L-Lysine-coated coverslips (courtesy of Dr. Ebba Kurz, University of Calgary, Calgary AB), fixed in 3.7 % (w/v) formaldehyde for 10 min at room temperature, and permeabilized in PBS containing 0.5 % (v/v) Triton X-100 for 10 min at room temperature. Samples were blocked in PBS containing 1 % (w/v) bovine serum albumin (BSA) for 1 h at room temperature prior to incubation with rabbit anti-FLAG polyclonal antibody (1:2500 dilution in blocking buffer) (Sigma-Aldrich) at 4°C overnight with gentle agitation. After six washes in PBS containing 0.05 % (v/v) Tween-20, cells were incubated with tetramethyl rhodamine iso-thiocyanate (TRITC)-conjugated goat anti-rabbit IgG (1:400 dilution in blocking buffer) (Sigma-Aldrich) for 30 min at room temperature. After an additional six washes in PBS containing 0.05 % (v/v) Tween-20, nuclei were counterstained with 4',6-diamidino-2-phenylindole (DAPI) (1 μg/mL in PBS) (Sigma-Aldrich) for 10 min at room temperature, washed, and mounted using VECTASHIELD<sup>®</sup> Mounting Media (Vector Laboratories Canada, Inc.). For detection of immunofluorescence, slides were viewed using a Zeiss Axiovert 200M inverted microscope (Carl Zeiss AG Light Microscopy, Germany) at × 630

magnification. This experiment was performed once and the images are representative of approximately 80 % of the total cells scored (about 20 cells per construct).

## **2.3 DNA Analysis**

### ***2.3.1 Oligonucleotide sequences and synthesis***

All oligonucleotides were synthesized by University Core DNA Services (University of Calgary). Unless otherwise noted, oligonucleotides used in the primer binding and conventional telomerase activity assays contained a biotin molecule at the 5'-end. The oligonucleotides used in the telomere repeat amplification protocol and terminal restriction fragment analyses were non-biotinylated. Oligonucleotide sequences, written 5' to 3', are listed in Table 2.1.

### ***2.3.2 Oligonucleotide radiolabelling***

DNA oligonucleotides containing 3'-biotin molecules were 5'-end-labelled with [ $\gamma$ -<sup>32</sup>P]ATP using T4 polynucleotide kinase (Invitrogen). A typical 20  $\mu$ L reaction containing 1x exchange reaction buffer (5x stock = 250 mM imidazole-HCl [pH 6.4]; 60 mM MgCl<sub>2</sub>; 5 mM 2-mercaptoethanol; 350  $\mu$ M ADP), 200 pmol 3'-biotinylated oligonucleotide, 3-5  $\mu$ L [ $\gamma$ -<sup>32</sup>P]ATP (3000 Ci/mmol, 10 mCi/mL) (GE Healthcare), and 10 U T4 polynucleotide kinase (Invitrogen) was incubated for 30 min in a 37°C water bath. The labelling reaction was terminated by the addition of 25 mM EDTA. Unincorporated nucleotides were removed by applying the reaction to a MicroSpin™ G-25 Gel Filtration Column (GE Healthcare), which was centrifuged at 200  $\times$  g for 2 min at

**Table 2.1 Description of ssDNA primers used in primer binding studies, conventional telomerase activity assays, and the telomere repeat amplification protocol.**

Name	Length (nt)	DNA Sequence (5' to 3')
bio-TELO30	30	TTAGGG TTAGGG TTAGGG TTAGGG TTAGGG
bio-TELO24	24	TTAGGG TTAGGG TTAGGG TTAGGG
bio-TELO18	18	TTAGGG TTAGGG TTAGGG
bio-TELO12	12	TTAGGG TTAGGG
bio-TELO6	6	TTAGGG
bio-antiTELO18	18	AATCCC AATCCC AATCCC
bio-pBR	24	AGCCAC TATCGA CTACGC GATCAT
bio-BBP	24	AATCCG TCGAGC AGAAAT CCGCAA
bio- <i>Tetrahymena</i>	18	TTGGGG TTGGGG TTGGGG
bio-Yeast	15	TGTGTG GTGTGT GGG
TELO24	24	TTAGGG TTAGGG TTAGGG TTAGGG
TELO18	18	TTAGGG TTAGGG TTAGGG
TS	18	AATCCG TCGAGC AGAGTT
ACX	30	GCGCGG CTTACC CTTACC CTTACC CTAACC

These primers were tested for physical interaction with hTERT in the primer binding assay and telomerase-mediated extension in the conventional telomerase activity assay (bio-TELO18 and bio-TELO6) or telomere repeat amplification protocol (TS and ACX). Primers containing a 5'-biotin molecule are indicated with the prefix 'bio'.

room temperature and then discarded. The filtrate was diluted 1 in 100 with nuclease-free water and stored at -20°C. Approximately  $10^3$  cpm were loaded as molecular weight markers for conventional telomerase activity assays (Sections 2.6.2 and 2.6.3).

### ***2.3.3 Terminal restriction fragment analysis***

#### **2.3.3.1 Synthesis of molecular weight marker DNA**

Two  $\mu\text{g}$  *Hind*III-digested  $\lambda$  DNA (Invitrogen) was incubated at 37°C for 1 h in a 20  $\mu\text{L}$  reaction containing REact<sup>®</sup> 2 buffer (50 mM Tris-HCl [pH 8.0]; 10 mM  $\text{MgCl}_2$ ; 50 mM NaCl) (Invitrogen), 2.5 mM dATP, 2.5 mM dTTP, 2.5 mM dCTP, 5  $\mu\text{L}$  [ $\alpha$ -<sup>32</sup>P]-dGTP (3000 Ci/mmol, 10 mCi/mL) (GE Healthcare), and 5 U large fragment of DNA polymerase I (Klenow fragment) (Invitrogen). The reaction was terminated by the addition of 12.5 mM EDTA, diluted 1 in 100 with nuclease-free water, and stored at -20°C. Approximately  $10^3$  cpm were loaded as molecular weight markers for in-gel hybridization experiments (Section 2.3.3.3).

#### **2.3.3.2 Synthesis of telomeric DNA probe**

Telomeric DNA probes were synthesized from an 800 bp fragment of duplex DNA containing TTAGGG repeats (courtesy of Dr. J. Karlseder, Salk Institute for Biological Studies, La Jolla CA). Double-stranded template DNA (100 ng) was mixed with 1000 pmol random primers p(dN)<sub>6</sub> (Roche) in a 14  $\mu\text{L}$  reaction and incubated at 95°C for 3 min to denature the template DNA. The reaction was subsequently placed in ice and the following components were added (25  $\mu\text{L}$  final volume): REact<sup>®</sup> 2 buffer (50

mM Tris-HCl [pH 8.0]; 10 mM MgCl<sub>2</sub>; 50 mM NaCl) (Invitrogen), 50 μM dATP, 50 μM dTTP, 50 μM dCTP, 5 μL [ $\alpha$ -<sup>32</sup>P]-dGTP (3000 Ci/mmol, 10 mCi/mL) (GE Healthcare), and 3-9 U (1 μL) large fragment of DNA polymerase I (Klenow fragment) (Invitrogen). The assembled synthesis reaction was then incubated at room temperature for 5 h. Unincorporated nucleotides were removed by applying the reaction to a MicroSpin™ G-25 Gel Filtration Column (GE Healthcare), which was centrifuged at 200 × g for 2 min (room temperature) and then discarded. The filtrate was stored at -20°C.

#### 2.3.3.3 In-gel hybridization

Telomeres were visualized by in-gel hybridization of *HinfI* and *RsaI* restriction enzyme-digested genomic DNA (5 μg) with the telomeric DNA probe described above. Aliquots of *HinfI* and *RsaI* digested DNA were electrophoresed through a 0.6 % agarose gel at 90 V for 5 h (450 Vh) at 4 °C. Gels were denatured for 45 min in denaturation solution (0.5 M NaOH; 1.5 M NaCl), neutralized for 45 min in neutralization solution (1 M Tris, pH 8.0; 1.5 M NaCl), and dried on a piece of Whatman 3MM filter paper for 45 min at room temperature, followed by an additional 45 min at 60°C using a Model 583 Gel-Dryer (Bio-Rad). The dried gel was submerged in denaturation solution for 10 min at room temperature (with gentle rocking) and then in neutralization solution for 10 min at room temperature (with gentle rocking), prior to hybridization in 5x SSC (20x stock = 3 M NaCl; 300 mM sodium citrate) containing approximately  $4 \times 10^6$  cpm <sup>32</sup>P-labelled telomeric probe at 37°C for 20 h. Hybridized gels were washed three times in 2x SSC for 10 min (room temperature), washed once in nuclease-free water for 5 min (at room

temperature with gentle rocking), dried on a piece of Whatman 3MM filter paper for 20 min at 60°C using a Model 583 Gel-Dryer, covered in plastic wrap, and exposed to a phosphorimager screen.

#### 2.3.3.4 Quantification of telomere length

Mean telomere length was calculated from at least three independent experiments using OptiQuant™ version 5.0 software (PerkinElmer, Inc.),  $\pm$  Standard Error of the Mean (SEM). The molecular weight of telomeric bands was determined by measuring the intensity of the peak apex and comparing it to a standard curve constructed from radiolabelled DNA molecular weight markers run on the same gel.

## 2.4 Protein Analysis

### 2.4.1 *Limited proteolysis of radiolabelled hTERT*

$\alpha$ -chymotrypsin from bovine pancreas (Sigma-Aldrich) was reconstituted in 1 mM HCl containing 2 mM CaCl and diluted to the appropriate working concentration in 1x reaction buffer (10x stock = 200 mM Tris-HCl, pH 8.3; 150 mM MgCl<sub>2</sub>; 630 mM KCl; 0.5 % Tween-20; 10 mM EGTA, pH 8.0). RRL containing [<sup>35</sup>S]cysteine-labelled FLAG-hTERT (Section 2.5.1) was digested with various concentrations of chymotrypsin for a constant time or with a constant enzyme concentration for various time points. In the former experiments, RRL containing comparable amounts of radioactivity (1 or 2  $\mu$ L RRL containing [<sup>35</sup>S]cysteine-labelled hTERT) was digested in a 15  $\mu$ L reaction containing 1x reaction buffer and 10, 100, or 1000 ng/mL chymotrypsin in a 30°C water

bath for 2 min. In the latter experiments, RRL containing comparable amounts of radioactivity (1 or 2  $\mu$ L RRL containing [ $^{35}$ S]cysteine-labelled hTERT) was digested with 500 ng/mL chymotrypsin in a 30°C water bath for 30 s, 1 min, 2 min, 5 min, 10 min, 15 min, 30 min, and 45 min. In all experiments, the reactions were terminated by the addition of SDS-PAGE loading buffer and boiling (5 min) and the entire reaction was resolved by SDS-PAGE on a gel containing 12 % (wt/vol) polyacrylamide (29:1 [wt/wt] acrylamide-bisacrylamide). The gel was dried on a piece of Whatman 3MM filter paper for 30 min at 80°C using a Model 583 Gel Dryer, wrapped in plastic wrap, and exposed to a high performance autoradiography film or phosphorimager screen.

#### ***2.4.2 anti-FLAG immunoprecipitation***

FLAG-hTERT was immunoprecipitated with anti-FLAG M2 affinity resin (Sigma-Aldrich) in ice-cold IP buffer 150 (10 mM Tris-HCl, pH 7.5; 1 % [vol/vol] NP-40; 10 % [vol/vol] glycerol; 1 mM EGTA; 1 mM MgCl<sub>2</sub>; 150 mM NaCl) supplemented with 10 U/mL RNaseOUT™ (Invitrogen) and an appropriate amount of Complete EDTA-Free Proteinase Inhibitor Cocktail (Roche). Aliquots (100-200  $\mu$ L) of anti-FLAG M2 affinity resin (50 % slurry) were pre-equilibrated by washing five times in 1 mL IP buffer 150 (centrifuged at 300  $\times$  g for 30 s between washes). Soluble cell lysate (800-1000  $\mu$ g) was immunoprecipitated for 2 h at 4°C with 40-50  $\mu$ L pre-equilibrated anti-FLAG M2 affinity resin in IP buffer 150 (1 mL final volume) (end-over-end rotation). The protein-resin complex was centrifuged at 300  $\times$  g for 3 min (4°C) and washed four times with either 1 mL of ice-cold IP buffer 150 (washes 1 and 4) or IP buffer 300 (IP

buffer containing 300 mM NaCl; washes 2 and 3) with 30 s spins at  $300 \times g$  between washes. FLAG-hTERT was eluted from the anti-FLAG M2 affinity resin by competition with excess  $3 \times$  FLAG peptide (Sigma-Aldrich). The affinity resin was resuspended in 30  $\mu$ L ice-cold IP buffer 150 containing 2 mg/mL  $3 \times$  FLAG peptide, rocked for 30 min at  $4^{\circ}\text{C}$ , and then centrifuged at  $800 \times g$  for 3 min ( $4^{\circ}\text{C}$ ). The eluate containing FLAG-hTERT was transferred to a fresh tube. The resin was subjected to a second competitive elution and the eluate was combined with that from the first elution.

#### ***2.4.3 Western blotting***

Following SDS-PAGE, proteins were transferred to a polyvinylidene difluoride membrane in ice-cold transfer buffer (25 mM Tris base; 190 mM glycine; 20 % [vol/vol] methanol; pH adjusted to 8.0), fixed in methanol, air dried, and blocked with TBS (50 mM Tris-HCl, pH 7.4; 150 mM NaCl) containing 0.5 % Tween-20 and 5 % (wt/vol) nonfat dry milk (NFDM) for 1-2 h at room temperature. To detect hTERT, blocked membranes were incubated overnight at  $4^{\circ}\text{C}$  with either a 1:500 dilution of the commercially-available polyclonal anti-hTERT antibody (Rockland Immunochemicals, Inc.) or a 1:1000 dilution of the polyclonal anti-hTERT antibody (courtesy of Dr. S. Artandi, Stanford School of Medicine, Stanford, CA) [232], prepared in TBST (TBS; 0.1 % Tween-20) containing 2.5 % (wt/vol) NFDM. After probing, the blots were washed three times in TBST (15-20 min; room temperature), rinsed in TBS, and incubated with ECL<sup>TM</sup> donkey, anti-rabbit immunoglobulin G, horseradish peroxidase-linked secondary antibody (GE Healthcare) (1:2000 dilution in TBST-2.5 % [wt/vol] NFDM) for 1 h at

room temperature. The blots were subsequently washed three times in TBST (10-15 min; room temperature) and once in TBS (5-10 min; room temperature). The membrane was then incubated with enhanced chemiluminescence (ECL) reagent (GE Healthcare), covered in plastic wrap, and exposed to a high performance chemiluminescence film.

#### **2.4.4 Coimmunoprecipitation of hTERT-hTR complexes**

##### **2.4.4.1 Synthesis of [ $\alpha$ -<sup>32</sup>P]UTP-labelled hTR**

hTR was transcribed from *Eco*RI-linearized plasmid DNA [148] in the presence of [ $\alpha$ -<sup>32</sup>P]UTP with the MEGAscript T7-coupled expression system (Ambion, Inc.). Final reaction volumes contained 1  $\mu$ g template DNA, 1x transcription buffer, 500  $\mu$ M ATP, 500  $\mu$ M CTP, 500  $\mu$ M GTP, 6  $\mu$ M unlabeled UTP, 5  $\mu$ L [ $\alpha$ -<sup>32</sup>P]UTP (3000 Ci/mmol; 10 mCi/mL; GE Healthcare), 2 U/ $\mu$ L RNaseOUT™ (Invitrogen), and 1x T7 RNA polymerase enzyme mix. Reactions were incubated in a 37°C water bath for 2 h, treated with 1  $\mu$ L of TURBO DNase™, and incubated in the 37°C water bath for an additional 15 min. Unincorporated nucleotides were removed by applying the reaction to a MicroSpin™ G-25 Gel Filtration Column, which was centrifuged at 200  $\times$  g for 2 min at room temperature and then discarded. RNA concentration in the filtrate was determined by measuring the absorbance at 260 nm using an Eppendorf BioPhotometer UV/Vis spectrophotometer and Eppendorf UVette® cuvettes. A typical transcription reaction yielded approximately 100 ng/ $\mu$ L RNA. In some instances, the RNA concentration was adjusted using unlabelled *in vitro* transcribed hTR. The activity of [ $\alpha$ -<sup>32</sup>P]UTP-labelled hTR was approximately 10<sup>6</sup> cpm/pmol, as determined by scintillation counting.

#### 2.4.4.2 *In vitro* reconstitution of radiolabelled human telomerase

Human telomerase was reconstituted using the RRL TNT<sup>®</sup> T7 Coupled Transcription-Translation System (Promega, Fisher Scientific Ltd.). Ten  $\mu\text{L}$  reactions were assembled on ice and contained 5  $\mu\text{L}$  TNT<sup>®</sup> RRL, 0.8  $\mu\text{L}$  TNT<sup>®</sup> reaction buffer, 0.8  $\mu\text{L}$  TNT<sup>®</sup> amino acid mixture (minus cysteine), 8 U RNaseOUT<sup>™</sup> (Invitrogen), 0.4  $\mu\text{L}$  [<sup>35</sup>S]cysteine ( $> 1000$  Ci/mmol, 10 mCi/mL; GE Healthcare), 600 ng FLAG-hTERT plasmid DNA, 300 ng [ $\alpha$ -<sup>32</sup>P]UTP-labelled hTR, and 0.4  $\mu\text{L}$  TNT<sup>®</sup> T7 RNA polymerase. RRL reactions were incubated in a 30°C water bath for 60-90 min and either immunoprecipitated immediately (below) or snap frozen in liquid N<sub>2</sub> and stored at -80°C (no CO<sub>2</sub>) until the following day.

#### 2.4.4.3 Coimmunoprecipitation

hTERT-hTR complexes were immunoprecipitated using two methods, similar to those described previously [152]. Initial experiments were performed using the first method and later experiments were performed by slightly modifying this protocol, as detailed in the second method.

Aliquots (100-200  $\mu\text{L}$ ) of anti-FLAG M2 affinity resin (50 % slurry) (Sigma-Aldrich) were pre-equilibrated by washing five times in 1 mL ice-cold coIP buffer 150 (10 mM Tris-HCl, pH 7.5; 0.5 % [wt/vol] 3-[(3-cholamidopropyl)dimethylammonio]-1-propanesulfonate (CHAPS); 10 % [vol/vol] glycerol; 1 mM MgCl<sub>2</sub>; 150 mM NaCl) supplemented with 10 U/mL RNaseOUT<sup>™</sup> (Invitrogen), and Complete EDTA-Free Protease Inhibitor Cocktail (Roche), with 30 s spins at 300  $\times$  g (room temperature)

between washes. Forty  $\mu\text{L}$  of pre-washed affinity resin was resuspended in 1 mL ice-cold coIP buffer 150 containing blocking agents (200  $\mu\text{g}/\text{mL}$  yeast total RNA, 100  $\mu\text{g}/\text{mL}$  *Escherichia coli* tRNA, and 100  $\mu\text{g}/\text{mL}$  BSA) and rocked at 4°C overnight to block non-specific binding sites. The next day, samples were centrifuged at  $300 \times g$  for 1 min and resuspended in ice-cold coIP buffer 150 containing the blocking agents described above. RRL reactions containing human telomerase complexes were pre-cleared with Sepharose<sup>®</sup> CL-4B (Sigma-Aldrich) in coIP buffer 150 by rotating end-over-end at 4°C for 30 min. After centrifugation at  $300 \times g$  for 1 min, the supernatant was immunoprecipitated with 40  $\mu\text{L}$  pre-blocked anti-FLAG M2 affinity resin resuspended in coIP buffer 150 (1 mL final volume) for 90 min at 4°C (end-over-end rotation). Following immunoprecipitation, samples were washed four times in ice-cold coIP buffer containing either 150 mM (washes 1 and 4) or 300 mM (washes 2 and 3) NaCl, with 30 s spins at  $300 \times g$  (room temperature) between washes. For washes 2 and 3, samples were rotated end-over-end for 10 min at room temperature. After washing, 100 % of the beads were resuspended in SDS-PAGE loading buffer and 15  $\mu\text{L}$  aliquots were resolved by SDS-PAGE on a pre-cast gradient gel containing 4-15 % (wt/vol) polyacrylamide (Bio-Rad). The gel was dried on a piece of Whatman 3MM filter paper for 40 min at 80°C using a Model 853 Gel Dryer, covered in plastic wrap, and exposed to two pieces of high performance autoradiography film or a phosphorimager screen.

In the second method, 1  $\mu\text{g}$  of rabbit polyclonal anti-FLAG antibody (Sigma-Aldrich) was bound to 40  $\mu\text{L}$  Protein G-Sepharose<sup>™</sup> (50 % slurry) (GE Healthcare) by rocking at 4°C for 90 min in ice-cold coIP buffer 150 containing blocking agents (100

$\mu\text{g/mL}$  yeast total RNA,  $50 \mu\text{g/mL}$  *E.coli* tRNA, and  $50 \mu\text{g/mL}$  BSA). RRL reactions containing human telomerase complexes were pre-cleared by rotating end-over-end for 90 min at  $4^{\circ}\text{C}$  with Protein G-Sepharose<sup>TM</sup> in ice-cold coIP buffer 150 and then centrifuged at  $300 \times g$  for 1 min. The supernatant was subsequently immunoprecipitated with  $40 \mu\text{L}$  anti-FLAG Protein G-Sepharose<sup>TM</sup> in coIP buffer 150 (1 mL final volume), as described above.

## **2.5 Primer Binding Assay**

### ***2.5.1 Synthesis of radiolabelled hTERT***

hTERT proteins were synthesized in the absence of hTR using the RRL TNT<sup>®</sup> T7 Coupled Transcription-Translation System (Promega, Fisher Scientific Ltd.). Thirty  $\mu\text{L}$  reactions were assembled on ice and contained  $15 \mu\text{L}$  TNT<sup>®</sup> RRL,  $2.4 \mu\text{L}$  TNT<sup>®</sup> reaction buffer,  $2.4 \mu\text{L}$  TNT<sup>®</sup> amino acid mixture (minus cysteine), 24 U RNaseOUT<sup>TM</sup> (Invitrogen),  $2.4 \mu\text{g}$  FLAG-hTERT plasmid DNA,  $1.2 \mu\text{L}$  [<sup>35</sup>S]cysteine ( $>1000 \text{ Ci/mmol}$ , 10 mCi/mL) (GE Healthcare), and  $1.2 \mu\text{L}$  TNT<sup>®</sup> T7 RNA polymerase. For control samples, TNT<sup>®</sup> luciferase DNA was substituted for hTERT DNA. Reactions were incubated in a  $30^{\circ}\text{C}$  water bath for 1.5-2 h, snap frozen in liquid N<sub>2</sub>, and stored at  $-80^{\circ}\text{C}$  (no CO<sub>2</sub>).

### ***2.5.2 DNA-binding***

Aliquots ( $100 \mu\text{L}$ ) of Ultralink<sup>®</sup> Immobilized NeutrAvidin slurry (Pierce Biotechnology, Inc.) were pre-equilibrated with binding buffer (90.7 mM HEPES, pH

8.0; 7 mM KCl; 2.3 mM MgCl<sub>2</sub>) supplemented with fresh β-mercaptoethanol (1 mM) and an appropriate amount of Complete EDTA-Free Protease Inhibitor Cocktail (Roche). Each aliquot was washed four times in 500 μL binding buffer and centrifuged for 5 min at 3300 × g (room temperature) between washes. During the second wash, the beads were rotated end-over-end for 30 min at 4°C with 5 μL RRL containing reconstituted human telomerase to block non-specific binding sites. After the fourth wash, the beads were resuspended in 500 μL of binding buffer and kept on ice until the next step (below).

The hTERT-primer complex was assembled on ice by adding equivalent counts of [<sup>35</sup>S]cysteine-labelled hTERT (calculation described in Section 2.5.3) to a 60 μL final reaction volume containing 1x reaction buffer (10x stock = 200 mM Tris-HCl, pH 8.3; 150 mM MgCl<sub>2</sub>; 630 mM KCl; 0.5 % Tween-20; 10 mM EGTA, pH 8.0), 1000 pmol (TTTTTT)<sub>3</sub> oligonucleotide, and 600 pmol 5'-biotinylated oligonucleotide of interest. hTERT-primer complex formation was allowed to proceed for 10 min at room temperature. The reaction was subsequently incubated with 100 μL pre-equilibrated NeutrAvidin (in 500 μL binding buffer) for 3 h at 4°C with end-over-end rotation. After pull-down, the samples were centrifuged at 3300 × g for 5 min (room temperature) and washed three times with binding buffer (500 μL for washes one and three; 750 μL for wash 2) with 5 min spins at 3300 × g (room temperature) between washes. The second wash was rotated end-over-end for 15 min at room temperature with rocking. After the final wash, the beads were resuspended in 5 μL SDS-PAGE loading buffer, boiled for 5 min, and centrifuged at 16 000 × g for 5 min. 15 μL aliquots were resolved by SDS-

PAGE on a gel containing 8 % or 10 % (wt/vol) polyacrylamide (29:1 [wt/wt] acylamide:bisacrylamide). The gel was dried on a piece of Whatman 3MM filter paper for 30 min at 80°C with a Model 583 Gel Dryer, covered in plastic wrap, and exposed overnight to a high performance autoradiography film or phosphorimager screen. A schematic of this assay is shown in Figure 2.1.

The primer binding protocol was further optimized for the experiments described in Chapters 4 and 5. Specifically, the primer mix containing 1x reaction buffer, 1000 pmol (TTTTTT)<sub>3</sub> oligonucleotide, and 600 pmol 5'-biotinylated oligonucleotide was incubated on ice for 45-60 min prior to adding the RRL reaction containing [<sup>35</sup>S]cysteine-labelled hTERT proteins. All other steps were performed as described in the original protocol.

### ***2.5.3 Quantification***

To determine the amount of [<sup>35</sup>S]cysteine-labelled hTERT in each RRL reconstitution reaction, 2 µL of RRL was mixed with SDS-PAGE loading buffer, boiled (5 min), and separated with 8 % or 10 % SDS-PAGE. The gel was dried on a piece of Whatman 3MM filter paper for 30 min at 80°C using a Model 583 Gel Dryer and exposed overnight to a high performance autoradiography film (Chapter 3) or phosphorimager screen (Chapters 4 and 5). The signal intensity of bands corresponding to each hTERT construct was quantified using Bio-Rad Quantity One<sup>®</sup> version 4.5.0 software. The volume of RRL added to each primer binding reaction was adjusted so that each experiment was performed with nearly equivalent counts of radiolabelled-hTERT

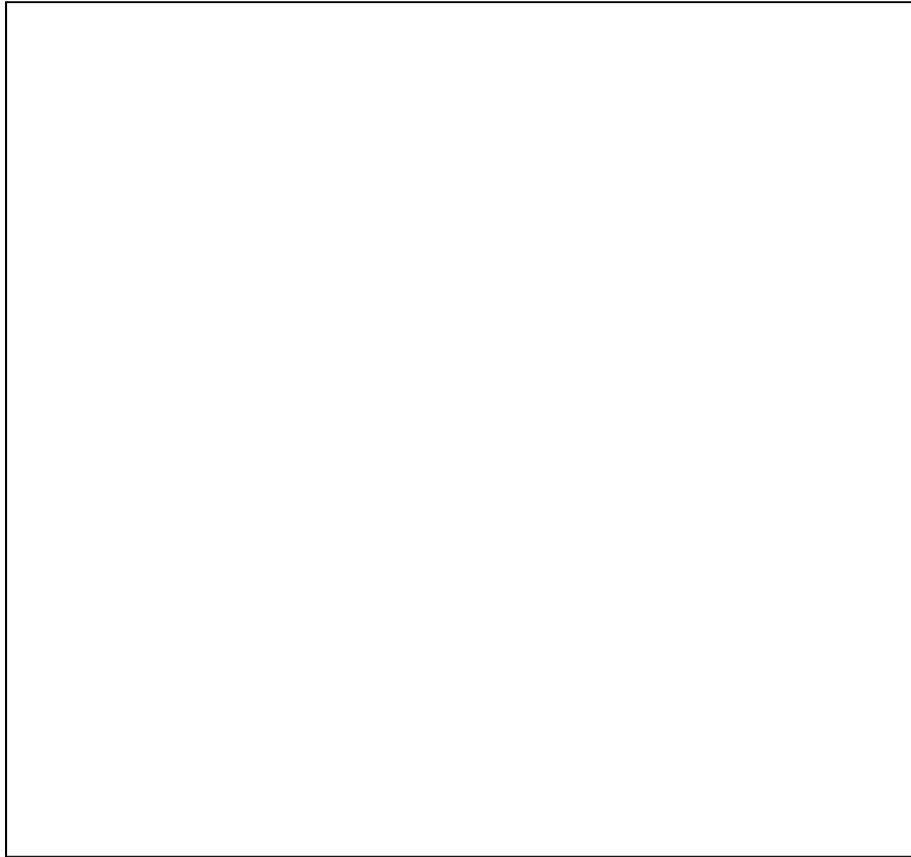


**Figure 2.1: Schematic of the primer binding assay.**

Human telomerase reverse transcriptase (hTERT; red oval) is reconstituted *in vitro* in the presence of [<sup>35</sup>S]cysteine with the rabbit reticulocyte lysate (RRL) system (step 1). RRL containing reconstituted hTERT proteins is incubated in a primer binding reaction containing excess blocking oligonucleotide, (TTTTTT)<sub>3</sub>, and a saturating amount of 5'-biotinylated oligonucleotide, such as biotin-(TTAGGG)<sub>4</sub> (step 2). The biotinylated oligonucleotide (and associated hTERT) is immobilized on NeutrAvidin resin (step 3). DNA-bound radiolabelled-hTERT is boiled off the resin, resolved by SDS-PAGE, and visualized by autoradiography or phosphorimaging (step 4).

proteins. The total protein counts in this volume were mathematically calculated and considered to represent 'input counts'. To determine the percentage of hTERT that was bound to the 5'-biotinylated ssDNA primer ('final counts'), the appropriate hTERT bands were quantified using Quantity One<sup>®</sup> version 4.5.0 software (Bio-Rad), adjusted for background binding by subtracting the non-biotinylated TELO24 oligonucleotide signal, and applied to the formula, (final counts/input counts) × 100 %. Primer binding results are reported as the mean ± SEM of at least three independent experiments.

#### ***2.5.4 Statistical analysis***

Statistical significance was assessed using GraphPad InStat version 3.00<sup>®</sup>. One-way Analysis of Variance (ANOVA) with Tukey multiple comparisons post-test or Student's two-tailed unpaired T-tests were used to calculate the levels of statistical significance observed between binding of wild type hTERT to different primers or between wild type and mutant hTERT with a given primer, respectively.

## **2.6 Telomerase Activity Assays**

### ***2.6.1 Telomere repeat amplification protocol***

Telomerase activity was detected using a modified, two-step version of the Telomeric Repeat Amplification Protocol (TRAP) [169] (Figure 2.2). In the first step (telomere extension), 1 µL of RRL or 2 µL of 3 × FLAG peptide eluate was incubated for 30 min at room temperature in a 50 µL reaction containing 1x TRAP buffer (10x stock = 200 mM Tris-HCl, pH 8.3; 150 mM MgCl<sub>2</sub>; 630 mM KCl; 0.5 % Tween-20; 10 mM

EGTA, pH 8.0), 50  $\mu$ M dATP, 50  $\mu$ M dCTP, 50  $\mu$ M dGTP, 50  $\mu$ M dTTP, 0.1  $\mu$ g TS primer (5'-AATCCGTCGAGCAGAGTT-3'), and 2 U *Taq* DNA polymerase (Invitrogen). In the second step (amplification), 0.1  $\mu$ g of ACX primer (5'-GCGCGG[CTTACC]<sub>3</sub>CTAACC-3') and 1  $\mu$ L of [ $\alpha$ -<sup>32</sup>P]dGTP (3000 Ci/mmol; 10 mCi/mL) (GE Healthcare) were added to each 50  $\mu$ L extension reaction, which was then amplified using a RoboCycler<sup>®</sup> Gradient 40 (Stratagene) PCR machine equipped with a heated lid for 20 to 25 cycles consisting of 95°C for 30 s, 50°C for 30 s, and 72°C for 90 s. 5  $\mu$ L of DNA loading dye (0.25 % [wt/vol] bromophenol blue, 0.25 % [wt/vol] xylene cyanol, and 30 % [vol/vol] glycerol) was added to each PCR reaction. TRAP reaction products (9  $\mu$ L) were electrophoresed on a native 12 % (wt/vol) polyacrylamide (29:1 [wt/wt] acrylamide-bisacrylamide) gel for 25 min at 1500 V. The gel was dried on a piece of Whatman 3MM filter paper for 30 min at 80°C with a Model 583 Gel Dryer, covered in plastic wrap, and exposed overnight to a high performance autoradiography film or phosphorimager screen.

### **2.6.2 Conventional telomerase activity assay**

The Conventional Telomerase Activity assay (CTA) was performed using a modified version of the original protocol [139] (Figure 2.3). A 24.5  $\mu$ L aliquot of RRL containing reconstituted human telomerase (Section 2.1.3) was assayed for activity in a 40  $\mu$ L final reaction volume containing 1x CTA buffer (10x stock = 500 mM Tris-HCl, pH 8.3; 500 mM KOAc; 10 mM MgCl<sub>2</sub>; 50 mM  $\beta$ -mercaptoethanol; 10 mM spermidine), 1 mM dATP, 1 mM dTTP, 1.25  $\mu$ M dGTP, 1.5  $\mu$ M 5'-biotinylated telomeric ssDNA

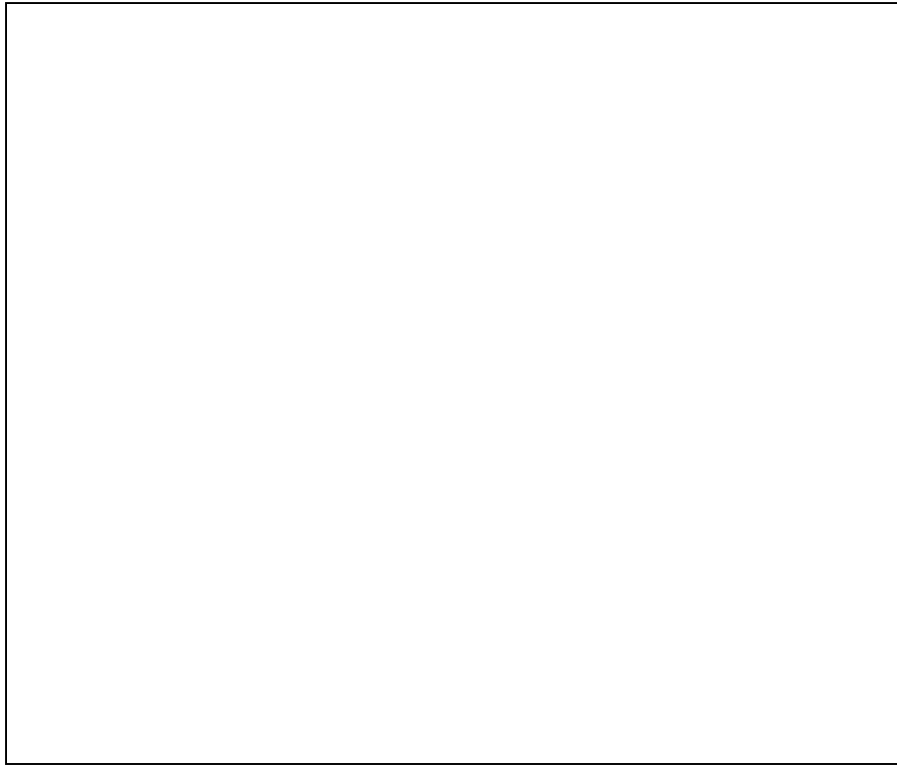


**Figure 2.2: Schematic of the telomere repeat amplification protocol.**

Human telomerase (red oval) is reconstituted *in vitro* with the rabbit reticulocyte lysate (RRL) system and incubated in a reaction containing dNTPs and a G-rich oligonucleotide ssDNA primer (green line). Telomerase extends the primer with the available dNTPs (step 1) and the extension products are subsequently amplified using the polymerase chain reaction (PCR) (step 2). The PCR reaction contains forward (TS; blue line) and reverse (ACX; black line) primers and radiolabelled dGTP (indicated by red asterisks). The PCR amplification products are resolved by PAGE and visualized by autoradiography or phosphorimaging (step 3).

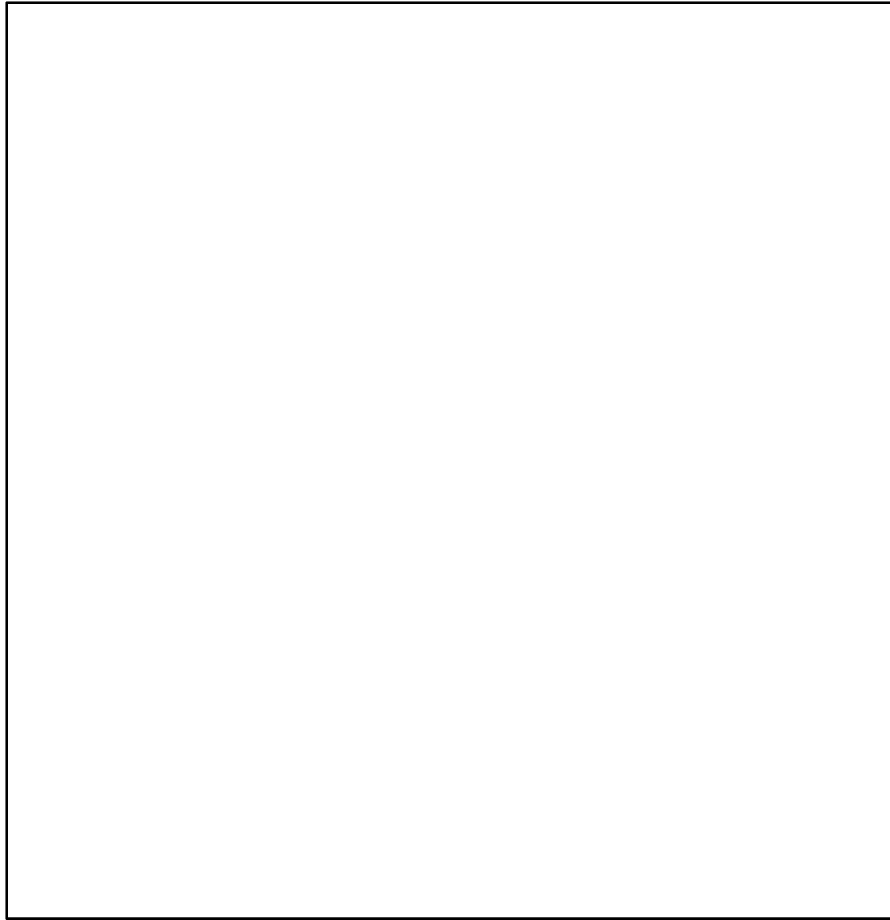


**Figure 2.3: Schematic of the conventional telomerase activity assay.**

Human telomerase (red oval) is reconstituted *in vitro* with the rabbit reticulocyte lysate (RRL) system and incubated in a reaction containing dTTP, dATP, and radiolabelled dGTP (indicated in red font and with a red asterisk) and a 5'-biotinylated telomeric ssDNA primer, such as (TTAGGG)<sub>3</sub>. Telomerase extends the biotinylated primer with the available dNTPs (step 1) and the extension products are subsequently immobilized on streptavidin resin (step 2). The extension products are boiled off the resin, resolved by denaturing PAGE, and visualized by phosphorimaging (step 3).

primer, and 6  $\mu\text{L}$  [ $\alpha$ - $^{32}\text{P}$ ]dGTP (3000 Ci/mmol, 10 mCi/mL) (GE Healthcare). The elongation reaction was incubated in a 30°C water bath for 3.5 h and then terminated by adding 50  $\mu\text{l}$  of stop buffer (10 mM EDTA; 2 M NaCl; 0.1 mg/ml RNase A) and incubating in a 37°C water bath for 15 min.

Aliquots (70  $\mu\text{L}$ ) of Streptavidin MagneSphere® paramagnetic beads (Promega, Fisher Scientific Ltd.) were pre-equilibrated by washing three times with 250  $\mu\text{L}$  buffer A (10 mM Tris-HCl, pH 7.5; 1 M NaCl; 0.5 mM EDTA). The pre-equilibrated beads were resuspended in 250  $\mu\text{L}$  buffer A and incubated with the elongation reaction (above) for 1 h at room temperature, during which time the samples were mixed by pipetting once every 10-15 min. Subsequently, the bead–elongation product complexes were washed three times with buffer A, twice with buffer B (10 mM Tris-HCl, pH 7.5), resuspended in 10  $\mu\text{l}$  loading dye (95 % [vol/vol] deionized formamide; 10 mM EDTA; 0.05 % [wt/vol] xylene cyanol; 0.05 % [wt/vol] bromophenol blue), and boiled for 30 min. Telomerase elongation products (9  $\mu\text{L}$ ) were resolved by electrophoresis through a denaturing (8 M urea) gel containing 8 % (wt/vol) polyacrylamide (19:1 [wt/wt] acrylamide-bisacrylamide) at 1500 V for 1 h 50 min. The gel was dried on a piece of Whatman 3MM filter paper for 1 h at 80°C with a Model 583 Gel Dryer, covered in plastic wrap, and exposed to a phosphorimaging screen.

### ***2.6.3 Pulse-chase conventional telomerase activity assay***

Pulse-chase CTA assays were used to determine the repeat addition processivity of human telomerase in Chapter 4, using protocols similar to those described previously

[139,208]. RRL containing reconstituted telomerase was incubated in a 40  $\mu$ L reaction containing 1x CTA buffer (10x stock = 500 mM Tris-HCl, pH 8.3; 500 mM KOAc; 10 mM MgCl<sub>2</sub>; 50 mM  $\beta$ -mercaptoethanol; 10 mM spermidine), 1.5  $\mu$ M 5'-biotinylated (TTAGGG)<sub>3</sub> primer, 1 mM dATP, 1 mM dTTP, 1.25  $\mu$ M dGTP, and 6  $\mu$ L [ $\alpha$ -<sup>32</sup>P]dGTP (3000 Ci/mmol, 10 mCi/mL) (GE Healthcare) at 30°C for 5 min ('pulse'). The pulse reaction was incubated with 200  $\mu$ M non-biotinylated (TTAGGG)<sub>3</sub> primer for 5, 15, or 30 min ('chase') and terminated by incubating with stop buffer (10 mM EDTA; 2 M NaCl; 0.1 mg/mL RNase A) at 37°C for 15 min. Elongated biotinylated pulse primers were separated from elongated non-biotinylated chase primers by immobilization on streptavidin MagneSphere<sup>®</sup> paramagnetic beads, as described above for the standard CTA.

#### ***2.6.4 Quantification of conventional telomerase activity assay data***

Telomerase activity (*i.e.* DNA synthesis) was measured using data collected with the standard CTA assay and repeat addition processivity was calculated with the data obtained in pulse-chase CTA experiments (Chapter 4) or standard CTA experiments (Chapters 3 and 5). The signal of each elongation product was quantified using Quantity One<sup>®</sup> version 4.5.0 software (Bio-Rad) and normalized to the total number of [ $\alpha$ -<sup>32</sup>P]dGTP incorporated [139].

Total DNA synthesis within the first hexameric telomeric repeat (P<sub>i</sub>) was calculated using the formula  $P_i = (T_i + T_{i+1} + \dots + T_{i+5})$ . T values correspond to the signal of the elongation product at position i. For the 18 nt telomeric primer (bio-TELO18), the

normalized values obtained at positions  $T_i \dots T_{i+5}$  in each independent experiment were added and expressed as a fraction of WT telomerase activity. For bio-TELO6, only the most intense products within the first telomeric repeat were quantified. Next, the signals at each position were summed to determine the total DNA synthesis within the first repeat. This value was expressed relative to the total DNA synthesis calculated for the wild type enzyme in the same experiment. The results of three independent experiments were averaged and the SEM was calculated.

Repeat addition processivity ( $P_i$ ) was calculated within the first three (for bio-TELO6 data) or five (for bio-TELO 18 data) hexameric repeats, using methods similar to those described previously [139,341]. The normalized signals of the +6, +12, +18, +24, +30, and +36 elongation products were applied to the formula  $P_i = (T_{i+6})/(T_i + T_{i+6})$ . First, we calculated the repeat addition processivity for each pair of elongation products separately. Next, the repeat addition processivity values at each position were summed to determine the overall processivity within the repeats that were quantified. The overall processivity results of three independent experiments were averaged ( $RAP_{x \text{ [mut or wt]}}$ ) and the SEM was calculated ( $SEM_{x \text{ [mut or wt]}}$ ). Average repeat addition processivity for mutant telomerases was expressed relative to the wild type enzyme ( $RAP_y$ ) and the SEM ( $SEM_y$ ) was calculated using the formula shown below. The final repeat addition processivity and SEM values were multiplied by 100 to report as a percent wild type telomerase repeat addition processivity  $\pm$  SEM.

$$SEM_y/RAP_y = \text{sqrt} (\{SEM_{x[wt]}/RAP_{x[wt]}\}^2 + \{SEM_{x[mut]}/RAP_{x[mut]}\}^2)$$

### ***2.6.5 Statistical analysis of conventional telomerase activity assay data***

Statistical significance was assessed using GraphPad InStat version 3.00<sup>®</sup>. Student's two-tailed unpaired T-tests were calculated to determine if DNA synthesis or repeat addition processivity was statistically different for human telomerase reconstituted with hTERT WT compared to mutant hTERT.

## **Chapter Three: Characterization of physical and functional anchor site interactions in human telomerase**

### **3.1 Preface**

As discussed previously, multiple studies have provided evidence for DNA-binding domains in TERT that reside outside the catalytic domain (anchor sites). Anchor sites are thought to bind telomeric and G-rich ssDNA primers upstream of the template-hybridizing region and confer telomerase with the property of repeat addition processivity (RAP). At the time of this study, the information available about human TERT (hTERT) anchor sites had been inferred from activity-based assays and it was not clear if hTERT could bind telomeric ssDNA in the absence of the human telomerase RNA subunit (hTR). We developed a DNA-binding assay, the primer binding assay, to identify regions in hTERT that regulate the strength and sequence-specificity of physical interactions with ssDNA *in vitro*. The primer binding assay was used in conjunction with the conventional telomerase activity assay to investigate the relationship between primer binding and primer utilization and identify separation-of-function hTERT mutants.

### **3.2 Summary**

Telomerase is a ribonucleoprotein reverse transcriptase that adds telomeric DNA to the 3'-ends of linear chromosomes and is crucial for genome stability. It is thought that the N-terminal extension (NTE) of the protein subunit, TERT, contains an anchor site that forms stable interactions with G-rich ssDNA to facilitate telomere synthesis and

RAP. According to this hypothesis, hTERT should bind telomeric ssDNA in the absence of the hTR. In this work, we developed a primer binding assay to study interactions between RRL-reconstituted hTERT and ssDNA primers *in vitro*. We provide the first detailed evidence that hTERT can form stable and sequence-specific interactions with telomeric ssDNA in the absence hTR. Our results also demonstrate that hTERT-mediated primer binding can be functionally uncoupled from telomerase-mediated primer extension. The primer binding results demonstrate that the first 350 amino acids of hTERT have a critical role in regulating the strength and specificity of protein-ssDNA interactions, supporting the presence of an anchor region in the TERT NTE. We also identified primer grip regions in the hTERT NTE and RT domain that are important for physical and functional interactions with ssDNA primers *in vitro*. Collectively, our data indicate that hTERT contains distinct anchor regions that likely co-operate to regulate the recognition and elongation of telomeric ssDNA.

### **3.3 Results**

#### ***3.3.1 hTERT interacts sequence-specifically with telomeric ssDNA in the absence of hTR***

The primer binding assay was developed to characterize physical interactions between the telomerase catalytic protein subunit, hTERT, and ssDNA oligonucleotides *in vitro*. [<sup>35</sup>S]cysteine-labelled FLAG-hTERT (simply referred to as hTERT from this point forth) was reconstituted in RRL in the absence of hTR and tested for its ability to interact with 5'-biotinylated primers comprised of telomeric or anti-telomeric ssDNA (Table 3.1).

**Table 3.1: Description of ssDNA primers used in primer binding studies and conventional telomerase activity assays.**

<b>Name</b>	<b>Length (nt)</b>	<b>DNA Sequence (5' to 3')</b>
<b>bio-TELO24</b>	24	TTAGGG TTAGGG TTAGGG TTAGGG
<b>bio-TELO18</b>	18	TTAGGG TTAGGG TTAGGG
<b>bio-TELO12</b>	12	TTAGGG TTAGGG
<b>bio-TELO6</b>	6	TTAGGG
<b>bio-antiTELO18</b>	18	AATCCC AATCCC AATCCC
<b>TELO24</b>	24	TTAGGG TTAGGG TTAGGG TTAGGG

These primers were tested for physical interaction with hTERT in the primer binding assay and telomerase-mediated extension in the conventional telomerase activity assay (bio-TELO18 and bio-TELO6). Primers containing a 5'-biotin molecule are indicated with the prefix 'bio'.

Biotinylated ssDNA primers (and associated hTERT proteins) were purified using neutravidin resin. Initial primer binding experiments were conducted using buffers that contained 24 mM, 50 mM, 90 mM, or 190 mM HEPES (Figure 3.1). Minimal levels of hTERT background-binding were observed with buffers containing 50 mM or 90 mM HEPES. Subsequent experiments were conducted with the 90 mM HEPES buffer. Using these experimental conditions, hTERT showed a strong interaction with bio-TELO24, the primer comprised of 24 nt of human telomeric ssDNA (*i.e.* four consecutive TTAGGG repeats) (Figure 3.2). In contrast, the interaction between hTERT and bio-antiTELO18, an 18 nt anti-telomeric primer containing the sequence (AATCCC)<sub>3</sub>, was markedly reduced ( $p < 0.001$ ), confirming that the hTERT-DNA interactions detected in this assay were specific for telomeric ssDNA (Figure 3.2). The 18 nt anti-telomeric primer was used as a negative control instead of a 24-mer because the interaction between hTERT and bio-TELO18 was slightly stronger than that with bio-TELO24 and human telomerase was more active with bio-TELO18 than bio-TELO24 (Figures 3.3 and 3.4, respectively). No interaction was observed when bio-TELO24 was incubated with comparable counts of *in vitro* synthesized [<sup>35</sup>S]cysteine-labelled luciferase (Figure 3.2), providing additional evidence for the specificity of the interactions between hTERT and human telomeric ssDNA. Negligible amounts of hTERT bound the neutravidin resin in the absence of an oligonucleotide or in the presence of a non-biotinylated 24 nt telomeric primer, TELO24 (Figure 3.2). To correct for non-specific background binding in subsequent primer binding experiments, we measured the signal intensity of TELO24-bound hTERT and subtracted this from the signal intensity derived from biotinylated DNA-bound hTERT.

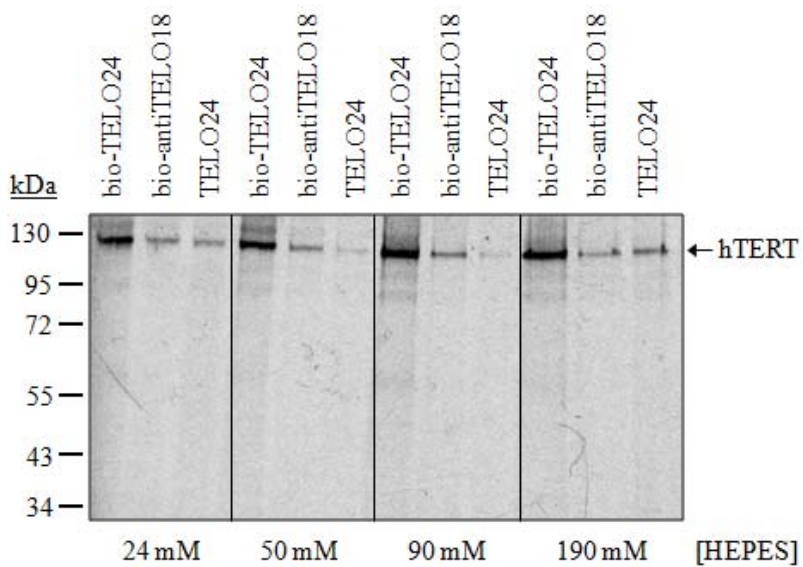


**Figure 3.1: Optimizing the primer binding assay.**

The primer binding assay was used to test for interactions between [ $^{35}\text{S}$ ]cysteine-labelled hTERT and 5'-biotinylated and non-biotinylated telomeric ssDNA (bio-TELO24 and TELO24, respectively) and 5'-biotinylated anti-telomeric ssDNA (bio-antiTELO18) in reactions that contained 24 mM, 50 mM, 90 mM, or 190 mM HEPES buffer. Reactions conducted in 90 mM HEPES buffer yielded a strong interaction between [ $^{35}\text{S}$ ]cysteine-labelled hTERT and bio-TELO24 and minimal non-sequence-specific interactions with bio-antiTELO18. Furthermore, negligible amounts of hTERT-TELO24 complexes were retained non-specifically on the neutravidin resin using the buffer that contained 90 mM HEPES. This experiment was performed twice.

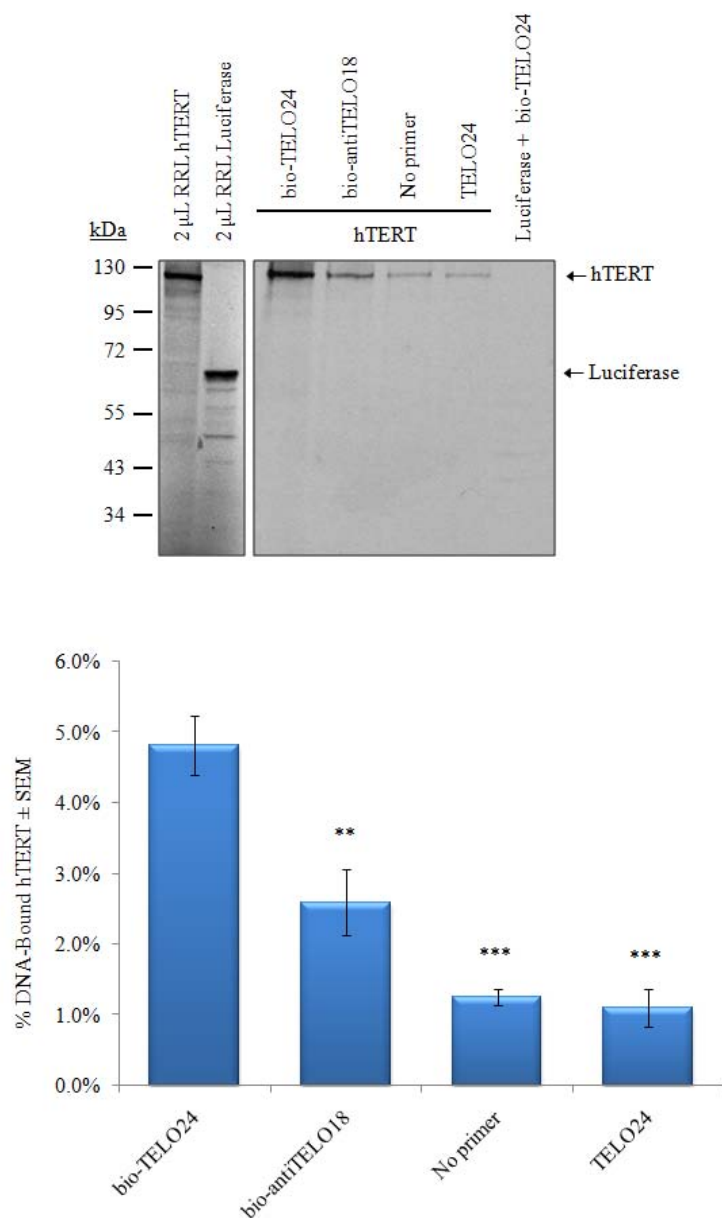


**Figure 3.2: hTERT interacts sequence-specifically with telomeric ssDNA *in vitro*.**

**Figure 3.2: hTERT interacts sequence-specifically with telomeric ssDNA *in vitro*.**

*Top*, Comparable amounts of [<sup>35</sup>S]cysteine-labelled hTERT or luciferase proteins (left panel) were tested for physical interactions with biotinylated or non-biotinylated DNA primers (right panel). [<sup>35</sup>S]cysteine-labelled hTERT bound 5'-biotinylated ssDNA primers containing 24 telomeric nt (bio-TELO24) and showed a significantly reduced interaction with 5'-biotinylated primers comprised of anti-telomeric ssDNA (bio-antiTELO18). Very low levels of [<sup>35</sup>S]cysteine-labelled hTERT were non-specifically retained on the neutravidin resin in the absence of DNA or after incubation with non-biotinylated telomeric DNA (TELO24). As the control, [<sup>35</sup>S]cysteine-labelled luciferase did not interact with bio-TELO24.

*Bottom*, Quantification and statistical analysis of the primer binding experiments is shown in graphical format. The results are reported as the mean % DNA-bound hTERT ± SEM of at least four independent experiments. Asterisks denote levels of statistical significance compared to the relative strength of the interaction between hTERT and bio-TELO24, as determined using Student's two-tailed unpaired T-tests; p < 0.01 (\*\*) and p < 0.001 (\*\*\*)

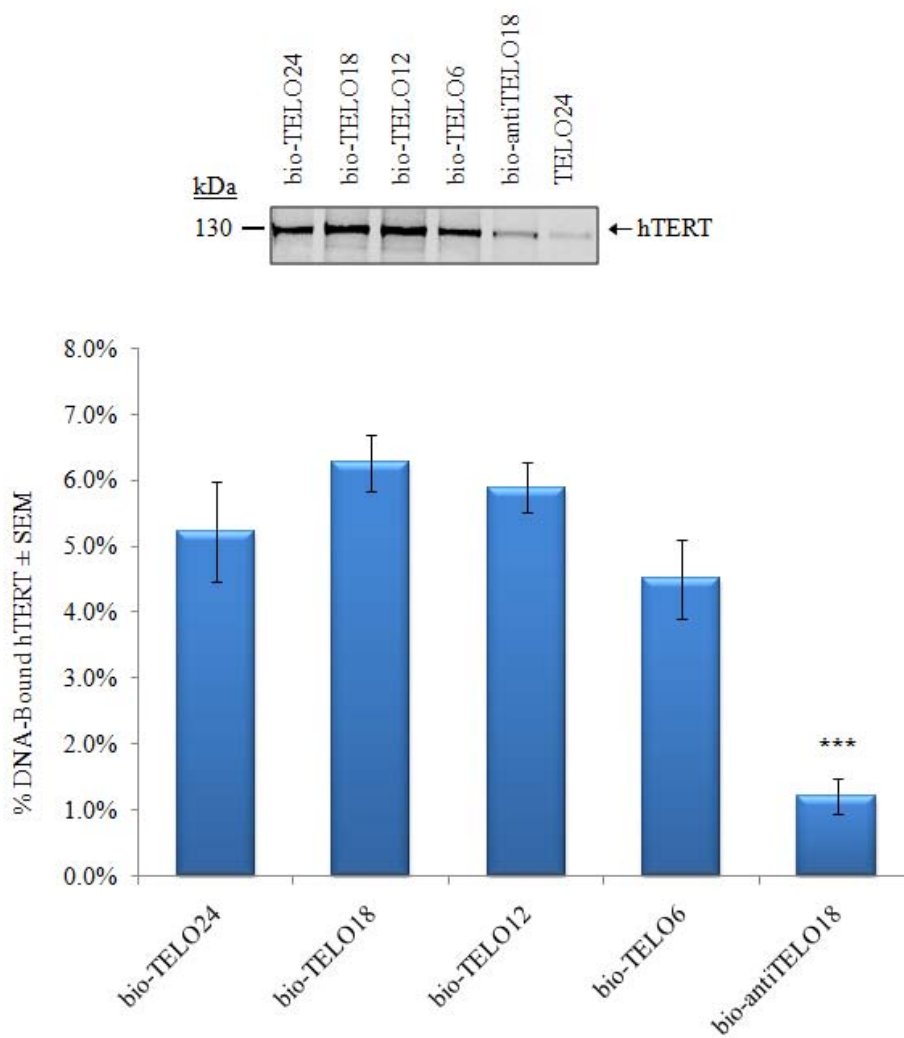


**Figure 3.3: hTERT binds 5'-biotinylated primers containing different lengths telomeric ssDNA.**

**Figure 3.3: hTERT binds 5'-biotinylated primers containing different lengths of telomeric ssDNA.**

*Top*, Approximately equivalent amounts of [<sup>35</sup>S]cysteine-labelled hTERT were incubated in a primer binding reaction containing 600 pmol of the indicated 5'-biotinylated oligonucleotide (Table 3.1). hTERT-DNA complexes were immobilized on neutravidin beads, purified, resolved by 8 % SDS-PAGE, and detected by autoradiography.

*Bottom*, Quantification and subsequent statistical analysis of the primer binding experiments is shown in graphical format. Results are reported as the mean % DNA-bound hTERT ± SEM of seven independent experiments. Asterisks denote levels of statistical significance as determined using one-way ANOVA;  $p < 0.0001$  (\*\*\*).

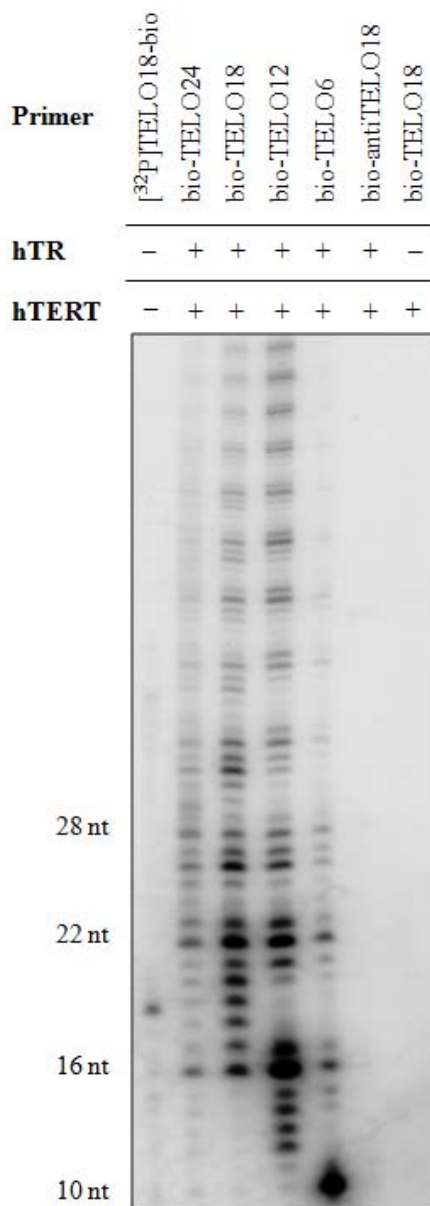


**Figure 3.4: Telomerase extends 5'-biotinylated ssDNA primers containing different lengths of telomeric DNA *in vitro*.**

**Figure 3.4: Telomerase extends 5'-biotinylated ssDNA primers containing different lengths of telomeric DNA *in vitro*.**

Human telomerase was reconstituted with hTERT and hTR and tested for its ability to extend 5'-biotinylated ssDNA primers (Table 3.1) using the conventional telomerase activity assay. Telomerase efficiently extended primers containing different lengths of telomeric ssDNA but not anti-telomeric ssDNA. The size of the elongation products, as indicated on the left side of the image, was determined based on the migration of 5'-radiolabelled TELO18 primer that contained a biotin molecule at the 3'-end.

### ***3.3.2 Investigating the relationship between physical and functional hTERT-DNA interactions***

We combined the primer binding assay with the conventional telomerase activity assay (CTA) to directly compare physical hTERT-DNA interactions with functional interactions between human telomerase and the same ssDNA primers (*i.e.* primer extension). We studied a series of primers containing different lengths of human telomeric ssDNA (Table 3.1) because telomerase elongates primers containing two or three TTAGGG repeats more efficiently than one or four TTAGGG repeats [163,272]. To determine if differences in hTERT-DNA interactions could explain the differences in primer utilization, we compared the ability of hTERT to bind biotinylated primers containing one, two, three, or four consecutive TTAGGG repeats with the ability of telomerase to elongate these DNA primers (Figures 3.3 and 3.4, respectively).

As shown in Figure 3.3, hTERT bound each telomeric ssDNA primer with similar avidity ( $p > 0.05$ ), although the primer binding assay might lack the sensitivity required to detect, with statistical confidence, subtle differences in hTERT binding to each DNA primer. We observed that one TTAGGG repeat was sufficient for a stable and sequence-specific interaction with hTERT *in vitro*, indicating that the 5'-biotin did not impede hTERT from contacting short stretches of telomeric ssDNA. The interaction between hTERT and bio-TELO12 or bio-TELO6 was significantly greater than that observed with bio-antiTELO18, providing additional evidence for the specificity of hTERT-DNA interactions measured in this assay. In contrast to the primer binding results, yet consistent with previous studies, CTA experiments showed that human telomerase was

more active on telomeric primers containing two or three TTAGGG repeats than on primers containing one or four repeat(s) (Figure 3.4) [163,272]. This result indicated that the relative strength of physical hTERT-telomeric ssDNA interactions was not the sole determinant of the efficiency with which telomerase extended these primers.

### ***3.3.3 Primer binding can be functionally uncoupled from primer utilization***

The preceding experiments suggested that the requirements for a physical interaction between hTERT and telomeric ssDNA were different than those needed for primer extension *in vitro*. We therefore investigated the DNA-binding activity of hTERT containing a D712A mutation, which disrupts the evolutionarily-conserved triad of metal-coordinating aspartic acids that are required for catalysis (D712, D868, and D869) [119,123,124]. hTERT D712A bound telomeric ssDNA primers at levels that were indistinguishable from wild type hTERT (Figure 3.5). However, as anticipated, human telomerase reconstituted with hTERT D712A was catalytically inactive (Figure 3.6). The loss of catalytic activity was not due to reduced stability of the hTERT D712A protein in RRL, as determined by comparable levels of [<sup>35</sup>S]cysteine-labelled WT and D712A hTERT (Figure 3.5, top left panel). These experiments provided evidence that primer binding could be functionally uncoupled from primer utilization in human telomerase. Further support is provided by experiments described in the following sections.

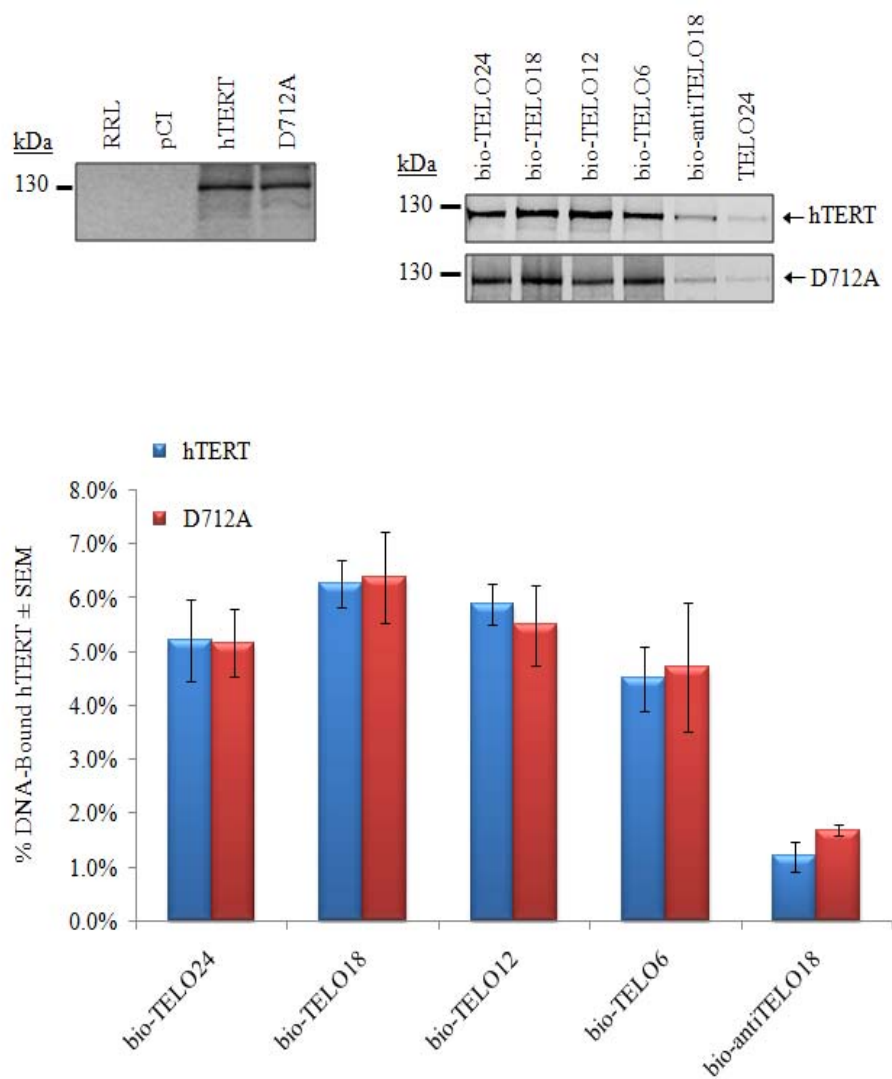


**Figure 3.5: hTERT D712A binds telomeric ssDNA as efficiently as WT hTERT.**

**Figure 3.5: hTERT D712A binds telomeric ssDNA as efficiently as WT hTERT.**

*Top*, Comparable amounts of [<sup>35</sup>S]cysteine-labelled hTERT (left panel) were tested for physical interaction with the indicated ssDNA primer (right panel). hTERT-DNA complexes were immobilized on neutravidin beads, purified, and the reaction products were separated by 10 % SDS-PAGE and visualized with autoradiography.

*Bottom*, Quantification and statistical analysis of the primer binding results is shown in graphical format. Results are reported as the mean % DNA-bound hTERT  $\pm$  SEM of at least three independent experiments. No statistically significant differences were detected between hTERT WT and D712A primer binding results, as determined using Student's two-tailed unpaired T-tests and the hTERT WT primer binding data set shown in Figure 3.3.

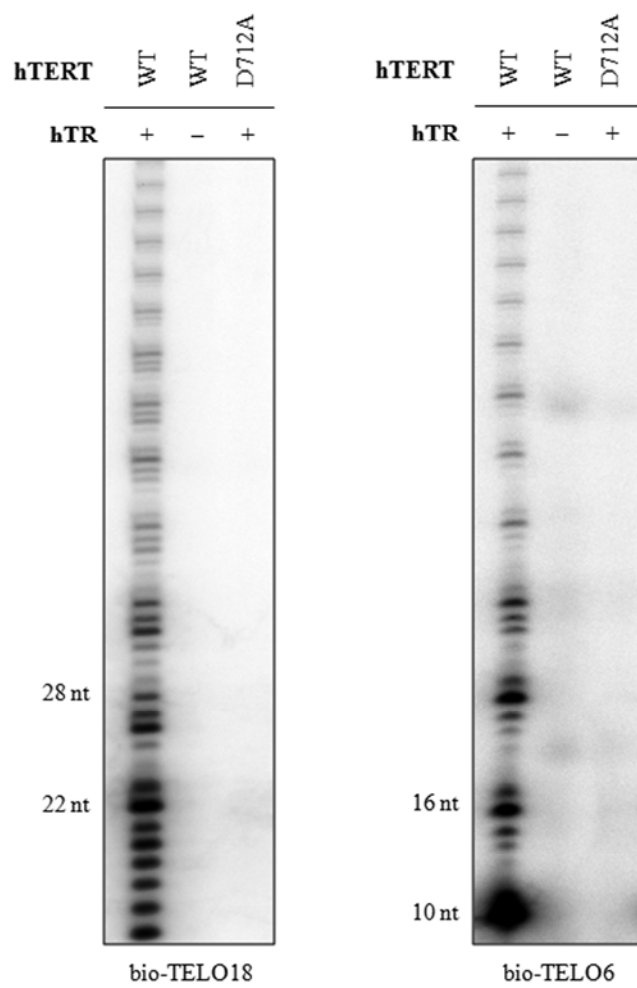


**Figure 3.6 Human telomerase reconstituted with hTERT D712A is catalytically inactive.**

**Figure 3.6 Human telomerase reconstituted with hTERT D712A is catalytically inactive.**

Human telomerase was reconstituted with hTR and hTERT or hTERT D712A and tested for its ability to extend 5'-biotinylated ssDNA primers comprised of 18 nt or 6 nt of telomeric ssDNA using the conventional telomerase activity assay (bio-TELO18 and bio-TELO6, respectively). As the control, hTERT was synthesized in the absence of hTR to demonstrate that the activity is not due to contaminating polymerases in the RRL. The positions of the 22 nt and 28 nt (bio-TELO18) or 10 nt and 16 nt (bio-TELO6) elongation products are indicated on the left side of the image.

### ***3.3.4 Identification of hTERT regions required for stable interaction with telomeric ssDNA***

We tested several hTERT truncation proteins in the primer binding assay to identify regions of hTERT that mediate the strength and sequence-specificity of interactions with telomeric ssDNA, [147,148]. As shown in Figure 3.7, this panel included N-terminal fragments (spanning residues 1-300 or 1-350), mutants that lack different regions of the N-terminus (mutants that span residues 301-1132 or 351-1132), C-terminal fragments (spanning residues 928-1132 or 967-1132), and RT domain variants (spanning residues 505-967 and 601-927). Many of these truncated proteins have previously been shown to bind hTR and the telomerase-associated protein TEP1 [148,208]. Furthermore, the proteins are not degraded when expressed in RRL or in human cells ([131,148,152,208] and Figure 3.8). Collectively, these results indicate that the truncated proteins are not grossly misfolded although we cannot rule out changes in protein conformation. Each primer binding experiment contained comparable counts of radiolabelled hTERT, as assessed by SDS-PAGE and autoradiography, to ensure an accurate comparison of different hTERT variants (Figure 3.8). Additional product bands migrating below the expected molecular mass of each hTERT construct likely represent prematurely truncated proteins and/or proteins synthesized from non-coding start sites. These products did not interact with the biotinylated primers at levels that exceeded background binding.

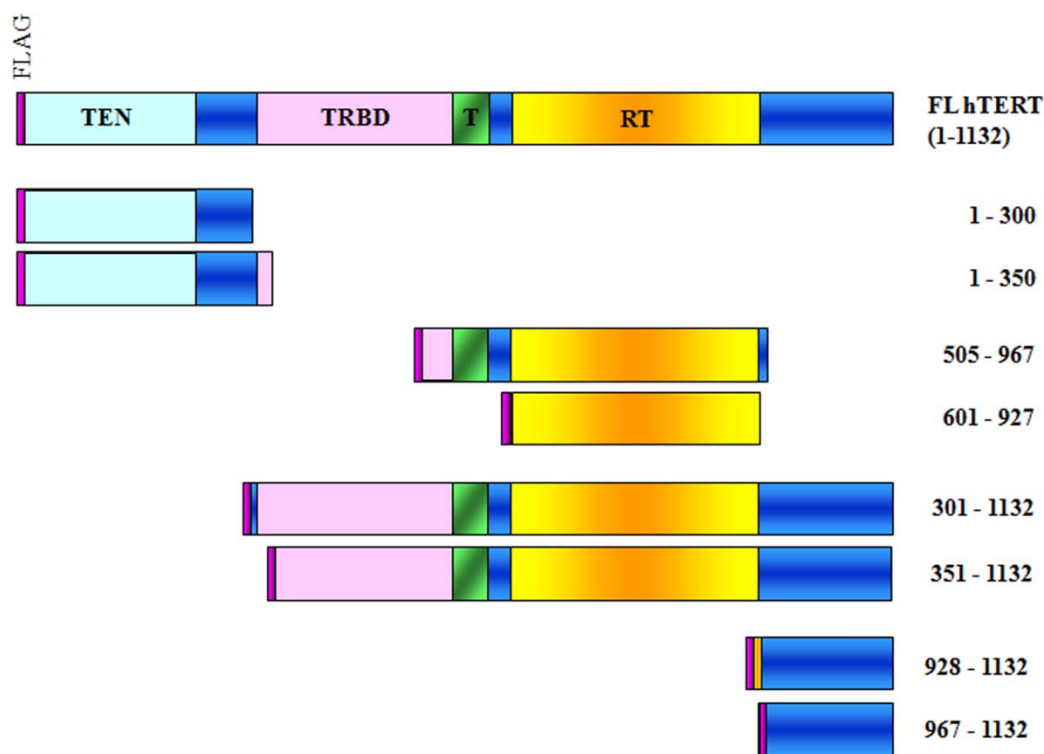


**Figure 3.7: Schematic summary of the hTERT truncation mutants tested in the primer binding assay.**

These deletion constructs were used to delineate regions of hTERT that mediate stable and human telomere sequence-specific interactions with ssDNA primers. The full length protein is represented by a blue rectangle and the N-terminal FLAG epitope is shown in purple. Specific colors are superimposed upon the full length protein to represent different protein domains. The telomerase essential N-terminal (TEN) domain is shown in cyan; the telomerase RNA-binding domain (TRBD) in pink; the telomerase specific motif (T) is shown in green; and the reverse transcriptase (RT) domain in yellow.

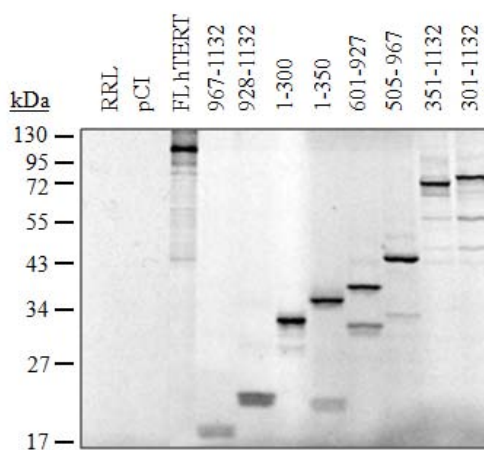


**Figure 3.8: hTERT deletion constructs are stably expressed *in vitro*.**

10 % SDS-PAGE and autoradiography was used to show that the amount of RRL added to primer binding reactions contained equivalent amounts of radiolabelled hTERT. Control reactions included RRL without protein (RRL control) and RRL containing cDNA for the pCI vector control. Bands corresponding to the molecular mass of each hTERT mutant were quantified and normalized to that of the full length protein.

We first investigated protein-DNA interactions using the N-terminal variants. The interaction between hTERT 1-300 and each telomeric primer was indistinguishable from that of full length hTERT, whereas the slightly larger fragment spanning amino acids 1-350 showed significantly reduced interactions with telomeric ssDNA ( $p < 0.05$ ) (Figure 3.9). hTERT 1-300 also showed an abnormally strong interaction with bio-antiTELO18 relative to full length hTERT ( $p < 0.01$ ) (Figure 3.9). This result suggested that the region between amino acids 300 and 350 might negatively regulate the strength of hTERT-ssDNA interactions and provide specificity for telomeric ssDNA.

To expand this observation, we assessed the DNA-binding properties of hTERT mutants that lacked either the first 300 amino acids (hTERT 301-1132) or the first 350 amino acids (hTERT 351-1132). Consistent with the above observations, hTERT 301-1132 showed a reproducible reduction in binding short telomeric ssDNA (bio-TELO12 and bio-TELO6) when compared to full length hTERT (Figure 3.10). However, hTERT 301-1132 showed a more stable interaction with bio-antiTELO18 than full length hTERT ( $p < 0.05$ ) (Figure 3.10). This might indicate that the region spanning amino acids 300 to 350 functions in *cis* with the extreme N-terminus (*i.e.* the first 300 amino acids) to provide hTERT with specificity for telomeric ssDNA (see discussion).

We next tested two protein fragments that lacked the NTE and RT domain (hTERT 928-1132 and 967-1132) to determine if the hTERT CTE was sufficient to bind telomeric ssDNA *in vitro*. Neither hTERT 928-1132 nor 967-1132 bound telomeric ssDNA primers at levels that exceeded background binding, indicating that the CTE does not contain a high affinity DNA-binding domain (Figure 3.11). Lastly, we determined if

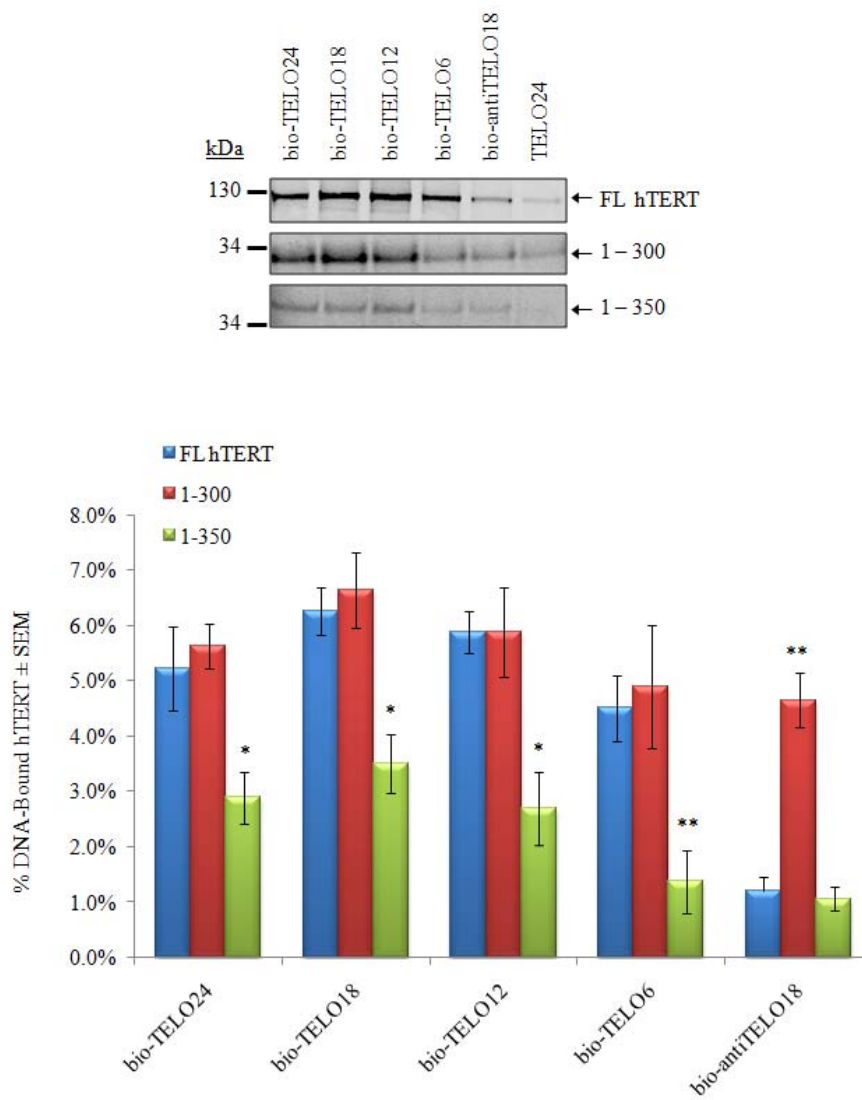


**Figure 3.9: Identification of hTERT N-terminal regions required to support a stable and sequence-specific interaction with telomeric ssDNA.**

**Figure 3.9: Identification of hTERT N-terminal regions required to support a stable and sequence-specific interaction with telomeric ssDNA**

*Top*, Approximately equivalent counts of [<sup>35</sup>S]cysteine-labelled hTERT (Figure 3.8) were tested for physical interaction with the indicated ssDNA primer (Table 3.1). hTERT-DNA complexes were immobilized on neutravidin beads, purified, and the reaction products were separated by 10 % SDS-PAGE and visualized with autoradiography.

*Bottom*, Quantification and statistical analysis of the primer binding results is shown in graphical format. Results are reported as the mean % DNA-bound hTERT  $\pm$  SEM of at least three independent experiments. Asterisks denote levels of statistical significance compared to the interaction observed between full length hTERT and the corresponding primer, as determined using Student's two-tailed unpaired T-tests and the hTERT WT primer binding data set shown in Figure 3.3;  $p < 0.05$  (\*), and  $p < 0.01$  (\*\*).

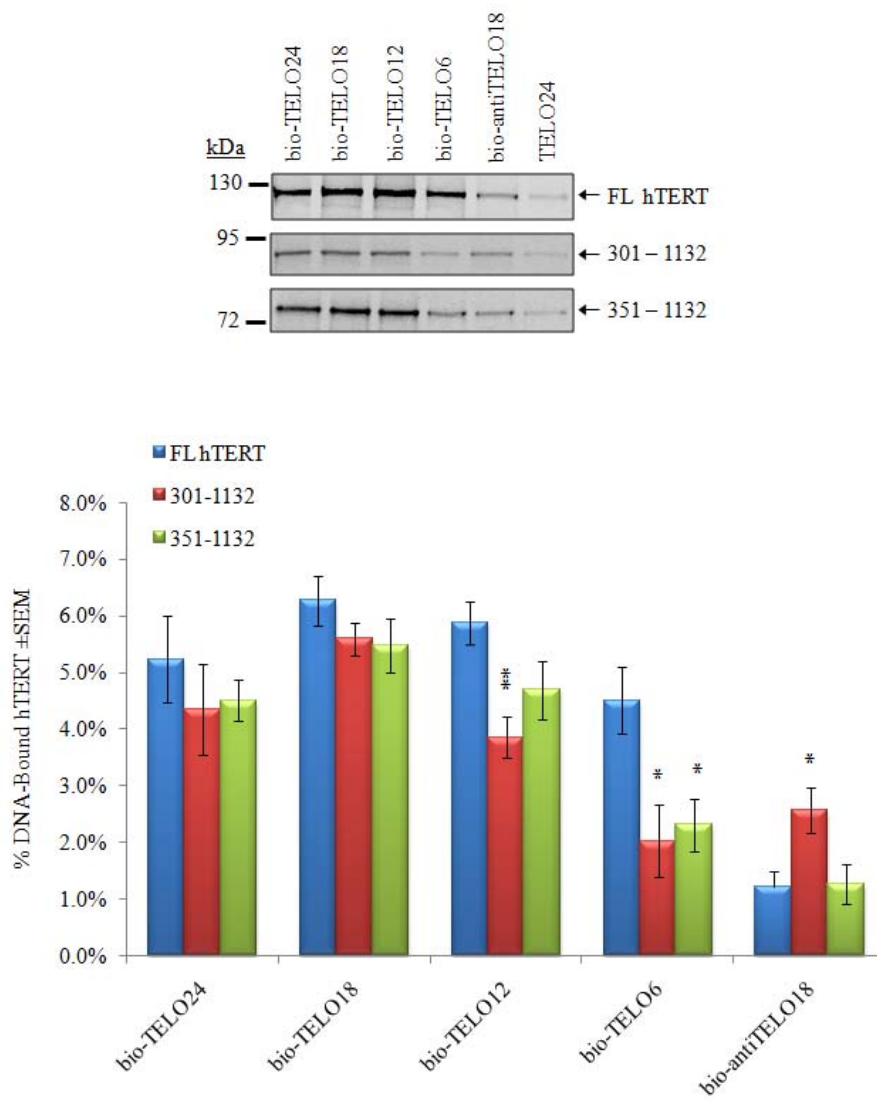


**Figure 3.10: The hTERT N-terminus is important for telomeric ssDNA-binding activity *in vitro*.**

**Figure 3.10: The hTERT N-terminus is important for ssDNA-binding activity *in vitro*.**

*Top*, Approximately equivalent amounts of [<sup>35</sup>S]cysteine-labelled hTERT (Figure 3.8) were tested for physical interaction with the indicated ssDNA primer (Table 3.1). hTERT-DNA complexes were immobilized on neutravidin beads, purified, and the reaction products were separated by 10 % SDS-PAGE and visualized with autoradiography.

*Bottom*, Quantification and statistical analysis of the primer binding results is shown in graphical format. Results are reported as the mean % DNA-bound hTERT ± SEM of at least three independent experiments. Asterisks denote levels of statistical significance compared to the interaction observed between full length hTERT and the corresponding primer, as determined using Student's two-tailed unpaired T-tests and the hTERT WT primer binding data set shown in Figure 3.3; p < 0.05 (\*) and p < 0.01 (\*\*).

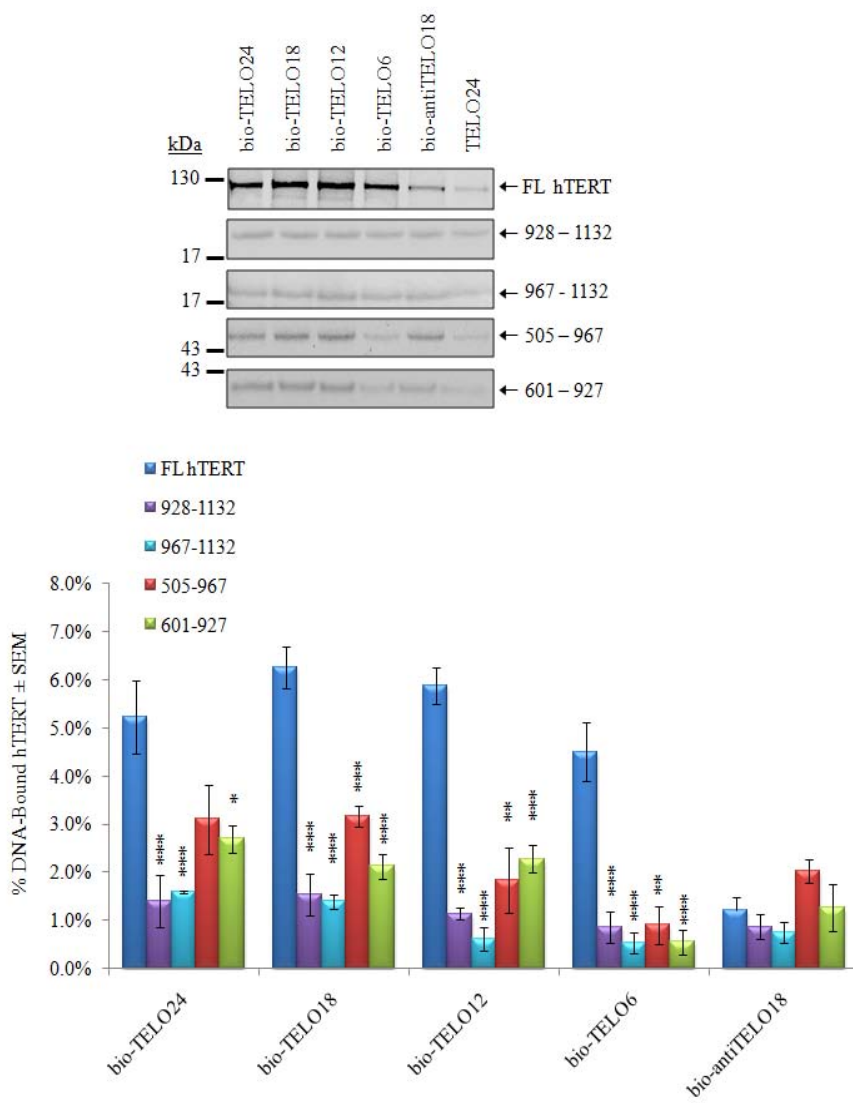


**Figure 3.11: Contribution of the hTERT CTE and RT domain to telomeric ssDNA-binding activity *in vitro*.**

**Figure 3.11: Contribution of the hTERT CTE and RT domain to telomeric ssDNA-binding activity *in vitro*.**

*Top*, RRLs containing approximately equivalent counts of [<sup>35</sup>S]cysteine-labelled hTERT (Figure 3.8) were tested for physical interaction with the indicated ssDNA primer (Table 3.1). hTERT-DNA complexes were immobilized on neutravidin beads, purified, and the reaction products were separated by 10 % SDS-PAGE and visualized with autoradiography.

*Bottom*, Quantification and statistical analysis of the primer binding results is shown in graphical format. Results are reported as the mean % DNA-bound hTERT  $\pm$  SEM of at least three independent experiments. Asterisks denote levels of statistical significance compared to the interaction observed between full length hTERT and the corresponding primer, as determined using Student's two-tailed unpaired T-tests and the hTERT WT primer binding data set shown in Figure 3.3;  $p < 0.05$  (\*),  $p < 0.01$  (\*\*), and  $p < 0.001$  (\*\*\*).

the RT domain alone could support stable interactions with telomeric ssDNA. Two different hTERT RT mutants were tested: the 601-927 variant comprises most of the RT domain, and the 505-967 mutant consists of the entire RT domain, the telomerase-specific motif, and a short stretch of residues C-terminal to the RT domain. With the exception of the interaction with bio-TELO6, we found that both RT mutants consistently bound telomeric ssDNA with greater avidity than that observed for the C-terminal fragments. In comparison to full length hTERT, however, the RT mutants exhibited a modest reduction in binding bio-TELO24 and significantly reduced interactions with bio-TELO18, bio-TELO12, and bio-TELO6 (Figure 3.11). This result indicates that the NTE makes a significant contribution to the overall stability of hTERT-DNA complexes, especially with short DNA primers (Figure 3.11). Interestingly, both RT mutants showed a slight, but reproducible, increase in the relative strength of the interaction with bio-antiTELO18, although this was not statistically significant (Figure 3.11). This could mean that the hTERT RT domain contains a length-dependent, sequence-non-specific ssDNA-binding activity whereas DNA-binding domains beyond the RT domain confer hTERT with specificity for human telomeric DNA.

### 3.3.5 Identification and characterization of hTERT primer grip regions

We speculated that the region between amino acids 927 and 967 (RT motif E) was important for the length-dependent ssDNA binding demonstrated by hTERT 505-967. This region contains a five residue primer grip sequence (W<sub>930</sub>CGLL) that is conserved in other telomerase and non-telomerase RT proteins [117] (Figures 3.12 and 3.13). In HIV-1 RT, the primer grip sequence is required for template-primer interactions and DNA polymerization [342]. Alanine substitution of the corresponding primer grip in *S. cerevisiae* Est2p impaired DNA synthesis and enzyme processivity [157]. To determine if this region was important for human telomerase activities, the putative primer grip region of full length hTERT was substituted with alanine residues. The hTERT RT-GRIP mutant was then synthesized in RRL and tested for its ability to recognize and utilize different lengths of telomeric ssDNA primers. hTERT RT-GRIP was expressed at levels similar to WT hTERT and bound bio-TELO24, bio-TELO18, and bio-TELO12 as efficiently as the WT protein (Figure 3.14). However, a statistically significant decrease in binding was observed with bio-TELO6 ( $p < 0.01$ ), suggesting that the RT primer grip stabilized the interaction between hTERT and short stretches of telomeric ssDNA. Substitution of the RT primer grip abolished telomerase activity, indicating that the RT primer grip is critical for enzyme function *in vitro* (Figure 3.15 and Table 3.2). Importantly, these experiments provided additional evidence that the requirements for primer binding could be functionally uncoupled from primer utilization.



**Figure 3.12: Conservation of the telomerase reverse transcriptase domain.**

This figure was taken from Nakamura *et al.* [117] and modified for visual clarity of the primer grip region in motif E (underlined in red).

Multiple sequence alignment of telomerase reverse transcriptases (RTs) and other RT families (Sc\_al, cytochrome oxidase group II intron 1-encoded protein from *S. cerevisiae* mitochondria; Dm\_TART, RT from *Drosophila melanogaster* TART non-LTR retrotransposable element). Residues in boldface are identical in at least three telomerase sequences in the alignment and coloured residues are highly conserved in telomerase and non-telomerase RTs. Telomerase reverse transcriptase (TRT) con and RT con indicate the consensus sequences for telomerase and non-telomerase RTs, respectively. Red arrowheads indicate some of the differences between telomerase and other RT enzymes. Numbers represent how many amino acids are located between each motif.

1 MPRAPRCKAVKSLLRSHYKEVLPALATFVRRLLGPGWRLVQRGDPAAFRALVAQCLVCPWDARPPPAAPS  
 71 FRQVSKLKELVARVLQRLCERGAKNVLAFGFALLDGGARGGPEAFTTSVRSYLPNTVTDALRGSGA**WGLL** → N-Primer  
 141 LRRVGDVLVHLLARCAALFVLVAPSCAYQVCGPPLYQLGAAIQARPPPHASGPRRRLGGERAWNHSVREA Grip  
 211 GVPGLPAPGARRRRGGSASRSILPLPKRPRRGAAPPEPERTPVGQGSWAHPGRTRGFSDRGFCVVSAPPAE  
 281 EATSEALSGTRHSHPSVGRQHHA GPPSTSRPPRPWDITCPPVYAEIKHFHLYSSGDKEQLRPSLELSSL  
 351 RPSLTGARRLVETIHLGSRPWMPGTPRRLPRLPQRYWQMRPLFELLEGNHAQCPYGVLLKTHCPLRAAVT  
 421 PAAGVCAREKPOGSAAPPEEEDTDRRLVQLLRQHSSPWQVYGFVRACLRRLVPPGLWGSRHNERRFLRN  
 491 TKKFIISLGHAKLSLQELTWKMSVRDCAWLRRSPGVGCVPAAEHRLREELAKFLHWLMSVYVVELLRSF  
 561 FYVTETTFQKNRLLFFYRKSVWSKLSQSIGRQHLKRVQLRELSEAEV RQHREARPALLSRLRFIPKPDGL  
 631 RPVNNMDYVV GAKTRRREKRAEKLTSRVKALFSVLNVERARRPGLLGASVGLDDIHRAWKTFVLRVRAQ  
 701 DPPPELYFVKVDVTGAYDTIIPQDRUTEVIAIHKPQNTYCVRRYAVVQKA AHGHVVKAFKSHVSTLTDLQ  
 771 PYMRQFVAHLQETSPLRD AVIEQSSSLEASSGLFDVFLRFMCHHAWRIIRGKSYVQCCGIPQGSILSTL  
 841 LCSLCYGDMDENKLFAGIRRDGLLRLVDDFLVTPHLTHAKTFLEKTLV RGVPEYGCVVNL RKTIVVNFVVE  
 911 DEALGGTAFV QMPAHGLFP**WCGLLLD**TKTLEVQSDYSSYAKTSIRASLTFNRGFKAGRNMRRKLFVLRRL  
 981 KCHSLFLDLQVNSLQTVCTINIKILLQAVRFAACVLQLPFHQVWKNPTFFLRFVISDTASLCYSILKAK  
 1051 NAGMSLGAKGAGPLPSEAVQWLCHQAECLKLTRHRYTVVPLLGSILKTAQTQLSRKLPGTTLTALEAAN  
 1121 PALPSDFKTLID

**Figure 3.13: Amino acid sequence of hTERT indicating the locations of the primer grip regions within the N-terminus and RT domain.**

Blue type indicates amino acid residues located within the evolutionarily-conserved RT domain and red type indicates the primer grip regions in the N-terminus and RT domain.

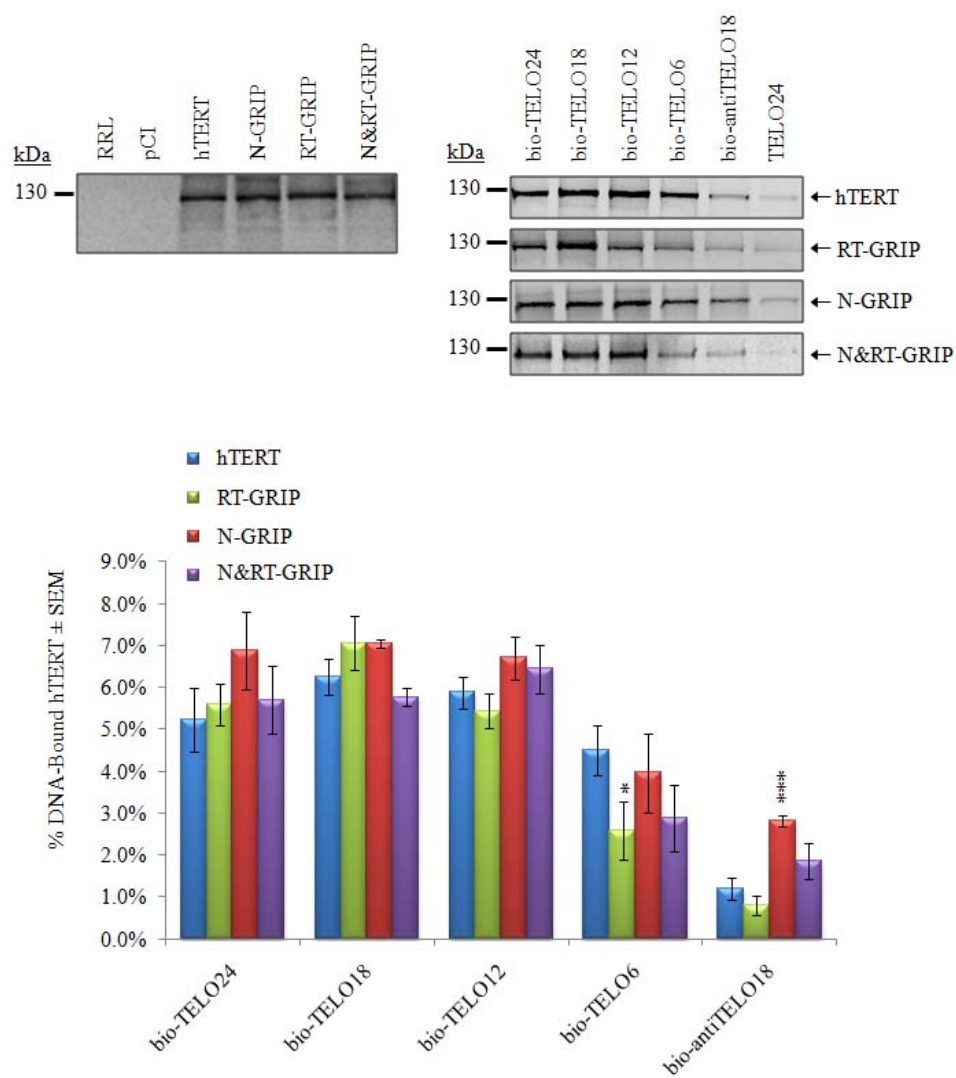


**Figure 3.14: hTERT primer grip regions are involved in regulating the strength and sequence-specificity of interactions with telomeric ssDNA.**

**Figure 3.14: hTERT primer grip regions are involved in regulating the strength and sequence-specificity of interactions with telomeric ssDNA.**

*Top*, Approximately equivalent amounts of [<sup>35</sup>S]cysteine-labelled hTERT (left panel) were tested for physical interaction with the indicated ssDNA primer (right panel). hTERT-DNA complexes were immobilized on neutravidin beads, purified, and the reaction products were separated by 10 % SDS-PAGE and visualized with autoradiography.

*Bottom*, Quantification and statistical analysis of the primer binding results is shown in graphical format. Results are reported as the mean % DNA-bound hTERT  $\pm$  SEM of at least three independent experiments. Asterisks denote levels of statistical significance compared to the interaction observed between WT hTERT and the corresponding primer, as determined using Student's two-tailed unpaired T-tests and the hTERT WT primer binding data set shown in Figure 3.3;  $p < 0.05$  (\*) and  $p < 0.001$  (\*\*\*)).

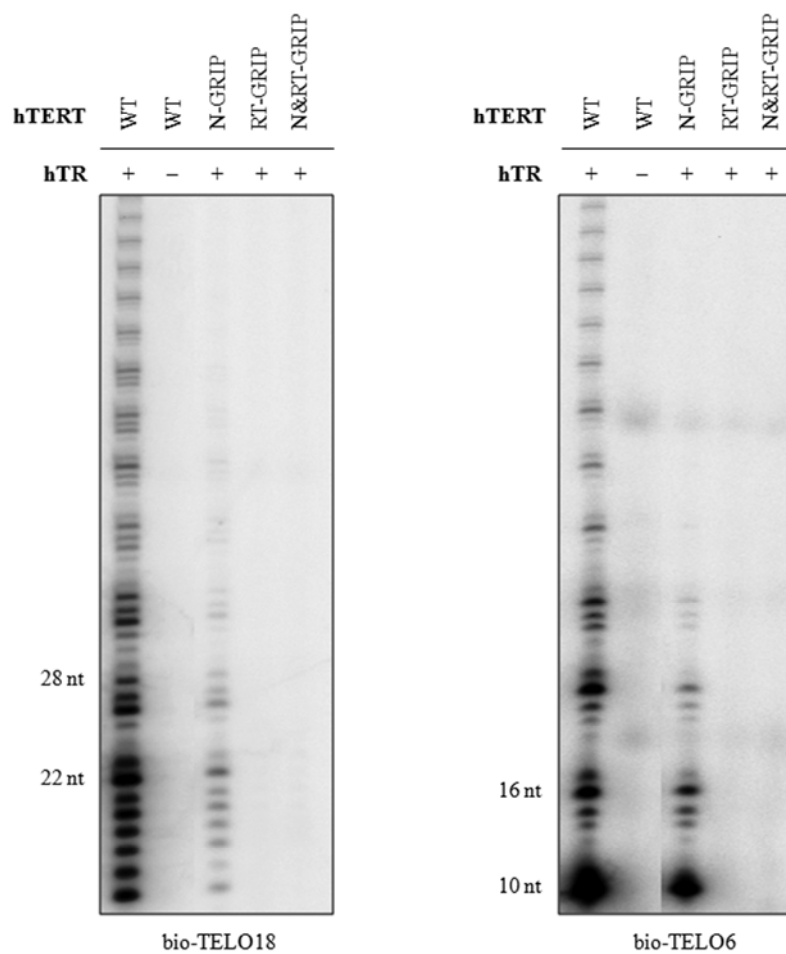


**Figure 3.15: hTERT primer grip regions are important for primer extension.**

**Figure 3.15: hTERT primer grip regions are important for primer extension.**

Human telomerase was reconstituted with hTR and hTERT WT, hTERT N-GRIP, RT-GRIP, or N&RT-GRIP and tested for its ability to extend 5'-biotinylated ssDNA primers comprised of 18 nt or 6 nt of telomeric ssDNA using the conventional telomerase activity assay (bio-TELO18 and bio-TELO6, respectively). As the control, hTERT was reconstituted in the absence of hTR to demonstrate that the DNA extension activity detected with this assay is not catalyzed by polymerases in the RRL. The positions of the 22 nt and 28 nt (bio-TELO18) or 10 nt and 16 nt (bio-TELO6) elongation products are indicated on the left side of the image. Table 3.2 shows the quantification of results obtained from at least three independent experiments.

**Table 3.2: Quantification of activity and repeat addition processivity observed for human telomerase reconstituted with hTERT primer grip mutants.**

hTERT Mutant	<u>bio-TELO18</u>		<u>bio-TELO6</u>	
	DNA Synthesis (% WT $\pm$ SEM)	Repeat Addition Processivity (% WT $\pm$ SEM)	DNA Synthesis (% WT $\pm$ SEM)	Repeat Addition Processivity (% WT $\pm$ SEM)
<b>N-GRIP</b>	19 $\pm$ 10 <sup>§</sup>	87 $\pm$ 4 <sup>*</sup>	24 $\pm$ 10 <sup>*</sup>	25 $\pm$ 4 <sup>*</sup>
<b>RT-GRIP</b>	ND	ND	ND	ND
<b>N&amp;RT-GRIP</b>	ND	ND	ND	ND

Results are reported as the mean % DNA synthesis or repeat addition processivity  $\pm$  SEM, relative to WT telomerase. DNA synthesis was calculated by measuring the signal intensity of the elongation products within the first hexameric repeat. For bio-TELO6, only the most intense products were quantified. Repeat addition processivity was determined by measuring the signal intensities of the pause products within the first five hexameric repeats (bio-TELO18) or first three hexameric repeats (bio-TELO6). Not detected (ND) indicates that telomerase was catalytically inactive. Asterisks denote statistical significance compared to WT telomerase, as determined using Student's two-tailed unpaired T-tests ( $p < 0.05$ , [\*]) and the section sign (§) indicates p values that were not statistically significant despite a reproducible decrease in total DNA synthesis compared to the wild type enzyme.

As shown in Figure 3.13, analysis of the hTERT primary sequence revealed an additional putative primer grip in the hTERT NTE (W<sub>137</sub>GLLL). We hypothesized that this region might partially account for the strong DNA-binding activity displayed by the hTERT mutant spanning amino acids 1-300. W<sub>137</sub>GLLL was substituted with A<sub>137</sub>AAAA in the context of full length hTERT (hTERT N-GRIP). The mutant was synthesized in RRL (at nearly equivalent levels to WT hTERT) and subsequently tested in the primer binding and CTA assays. Interestingly, hTERT N-GRIP bound telomeric ssDNA primers at levels similar to WT hTERT, but exhibited a relatively stronger association with bio-antiTELO18 (Figure 3.14). This suggested that the N-terminal primer grip was involved in the ability of hTERT to recognize human telomeric ssDNA. The functional importance of this region was revealed when telomerase reconstituted with hTERT N-GRIP exhibited significantly reduced levels of DNA synthesis and RAP with bio-TELO18 and bio-TELO6 (Figure 3.15 and Table 3.2). The catalytic defects were most severe with bio-TELO6, indicating that this region of the hTERT NTE is particularly important for telomerase-dependent elongation of short telomeric primers. Finally, a full length hTERT construct with alanine substitutions in both primer grips was generated. hTERT N&RT-GRIP was expressed in RRL at comparable levels to the WT protein (Figure 3.14, top left panel). The double mutant did not exhibit statistically significant alterations in its capacity to bind telomeric ssDNA (Figure 3.14). However, we did observe a reproducible reduction in the interaction with bio-TELO6 when compared to WT hTERT. Telomerase reconstituted with hTERT N&RT-GRIP was incapable of synthesizing telomeric DNA *in vitro* (Figure 3.15 and Table 3.2).

### 3.3.6 *hTERT DAT regions are involved in primer binding and utilization*

hTERT contains several DAT domains that dissociate the biological and catalytic activities of telomerase and have been implicated in physical and functional telomerase-telomere interactions [140,162,163,165-167]. We used the primer binding and CTA assays to test the DNA-binding properties and catalytic activity, respectively, of five well-characterized hTERT DAT mutants [140,162,165]. These included four N-terminal mutants (DAT +68, DAT +98, DAT +122, and DAT +128) and the lone C-terminal mutant (DAT +1127). The DAT mutations are six amino-acid NAAIRS substitutions that are reported to have negligible impact on overall protein structure because the NAAIRS peptide sequence maintains protein length and can adopt multiple conformations [162,343]. Importantly, it has previously been shown that the DAT mutants studied here interact with hTERT (multimerization) and hTR *in vitro* [140,162].

hTERT DAT mutants were synthesized as [<sup>35</sup>S]cysteine-labelled proteins in RRL at levels comparable to WT hTERT (Figure 3.16, top left panel). These proteins were tested for ssDNA-binding and enzyme activity *in vitro*. With the exception of the interaction between hTERT DAT +122 and bio-TELO24, the DAT mutants appeared to associate more weakly with telomeric ssDNA primers than WT hTERT, although this was not always statistically significant (Figure 3.16). hTERT DAT +68 and hTERT DAT +98 exhibited the weakest interactions with ssDNA primers containing 18, 12, or 6 telomeric nt ( $p < 0.05$ ). Telomerase reconstituted with these mutants also exhibited reduced levels of DNA synthesis with bio-TELO18 and bio-TELO6, indicating that impaired ssDNA-binding might contribute to the catalytic defects of these mutants

(Figure 3.17 and Table 3.3). Repeat addition processivity was unaffected with bio-TELO18 but reduced with bio-TELO6 ( $p < 0.01$ ), suggesting that the +68 and +98 DAT regions are critical for processive elongation of short telomeric primers. Telomerase reconstituted with hTERT DAT +122 showed significant reductions in DNA synthesis and RAP (bio-TELO6) (Figure 3.17 and Table 3.3). hTERT DAT +128 exhibited a general trend of weaker ssDNA-binding than WT hTERT (Figure 3.16). Interestingly, although this mutant catalyzed near wild type levels of DNA synthesis with bio-TELO18, enzyme activity was significantly impaired with the short primer, bio-TELO6 (Figure 3.17). Similar to the DAT +128 mutant, hTERT DAT +1127 exhibited a general trend of weaker ssDNA-binding than WT hTERT (Figure 3.16). However, telomerase reconstituted with this mutant demonstrated profound functional defects and was devoid of catalytic activity with bio-TELO6, indicating that the C-DAT region is critical for enzyme function (Figure 3.17 and Table 3.3). The DAT mutants studied here did not show a statistically significant interaction with bio-antiTELO18 and thus, retained sequence-specificity for human telomeric ssDNA (Figure 3.16). Overall, we did not observe a direct correlation between the magnitude of the reduction in ssDNA-binding activity and reduction in enzyme activity or processivity. These results indicate that the DAT phenotype can result from alterations in multiple aspects of telomerase biochemistry, including hTERT-ssDNA interactions.

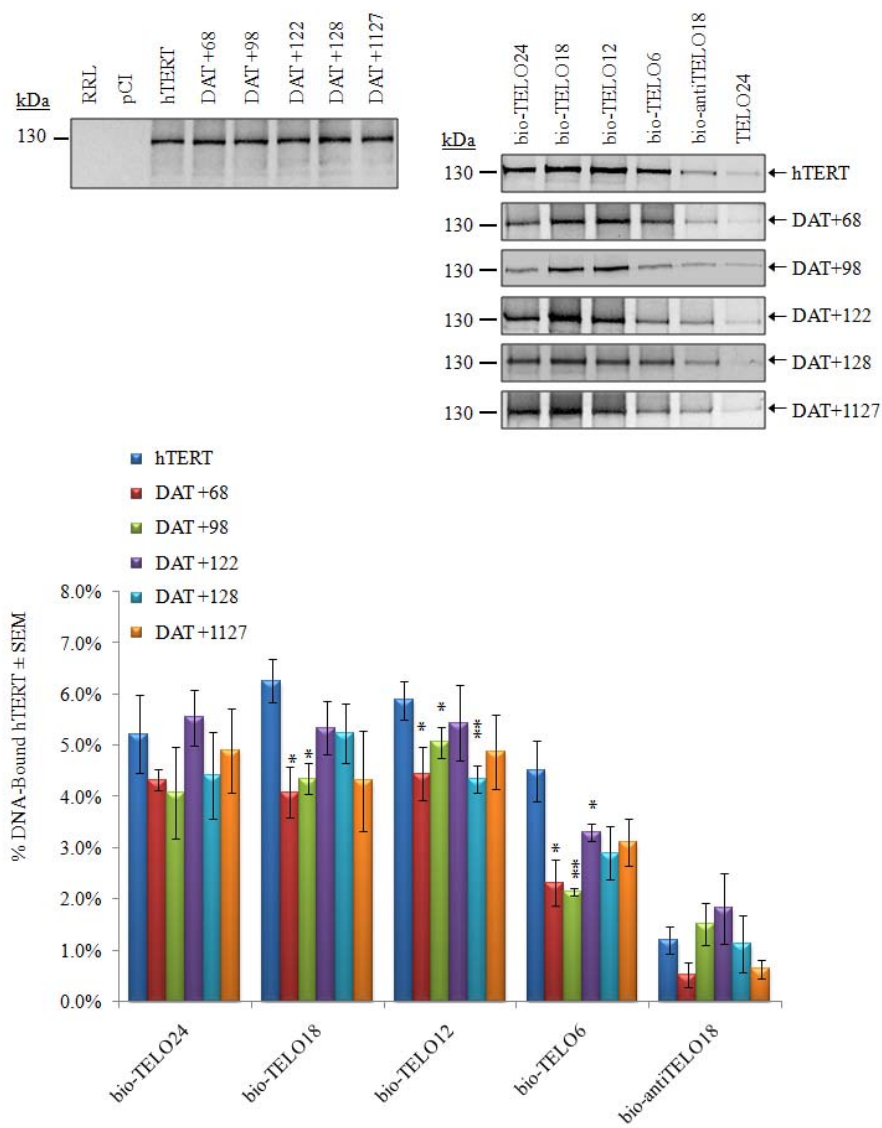


**Figure 3.16: hTERT DAT regions are involved in primer binding.**

**Figure 3.16: hTERT DAT regions are involved in primer binding.**

*Top*, Approximately equivalent amounts of [<sup>35</sup>S]cysteine-labelled hTERT (left panel) were tested for physical interaction with the indicated ssDNA primer (right panel). hTERT-DNA complexes were immobilized on neutravidin beads, purified, and the reaction products were separated by 8 % SDS-PAGE and visualized with autoradiography.

*Bottom*, Quantification and statistical analysis of the primer binding results is shown in graphical format. Results are reported as the mean % DNA-bound hTERT  $\pm$  SEM of at least three independent experiments. Asterisks denote levels of statistical significance compared to the interaction observed between hTERT WT and the corresponding primer, as determined using Student's two-tailed unpaired T-tests and the hTERT WT primer binding data set shown in Figure 3.3;  $p < 0.05$  (\*) and  $p < 0.01$  (\*\*).

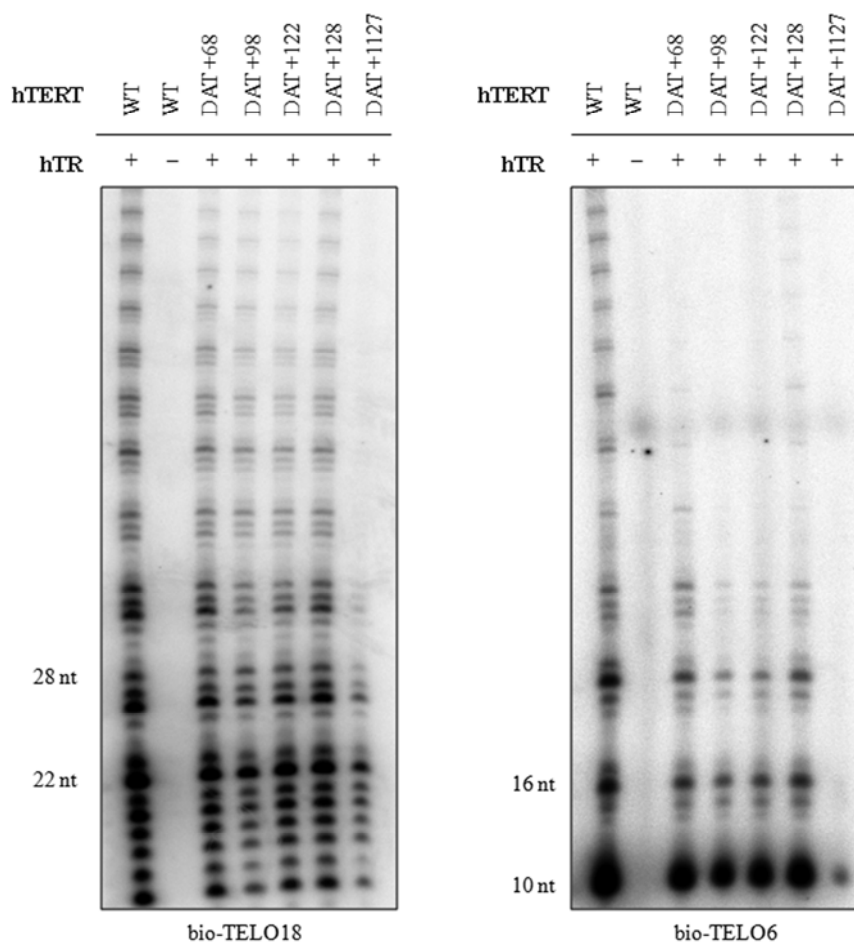


**Figure 3.17: hTERT DAT regions are involved in primer utilization.**

**Figure 3.17: hTERT DAT regions are involved in primer utilization.**

Human telomerase was reconstituted with hTR and hTERT WT, hTERT DAT +68, DAT +98, DAT +122, DAT +128, or DAT +1127 and tested for its ability to extend 5'-biotinylated ssDNA primers comprised of 18 nt or 6 nt of telomeric ssDNA using the CTA assay (bio-TELO18 and bio-TELO6, respectively). As the control, hTERT WT was reconstituted in the absence of hTR to demonstrate that the DNA extension activity detected with this assay is not catalyzed by polymerases in the RRL. The positions of the 22 nt and 28 nt (bio-TELO18) or 10 nt and 16 nt (bio-TELO6) elongation products are indicated on the left side of the image. The quantification of these results is shown in Table 3.3.

**Table 3.3: Quantification of DNA synthesis and repeat addition processivity observed for human telomerase reconstituted with hTERT DAT mutants.**

hTERT DAT Mutant	<u>bio-TELO18</u>		<u>bio-TELO6</u>	
	DNA Synthesis (% WT $\pm$ SEM)	Repeat Addition Processivity (% WT $\pm$ SEM)	DNA Synthesis (% WT $\pm$ SEM)	Repeat Addition Processivity (% WT $\pm$ SEM)
<b>+68</b>	60 $\pm$ 11 <sup>§</sup>	96 $\pm$ 5	44 $\pm$ 4 <sup>§</sup>	85 $\pm$ 1 <sup>**</sup>
<b>+98</b>	56 $\pm$ 14 <sup>§</sup>	98 $\pm$ 5	34 $\pm$ 4 <sup>*</sup>	82 $\pm$ 2 <sup>**</sup>
<b>+122</b>	38 $\pm$ 10 <sup>§</sup>	95 $\pm$ 6	34 $\pm$ 5 <sup>*</sup>	86 $\pm$ 1 <sup>**</sup>
<b>+128</b>	75 $\pm$ 24	93 $\pm$ 6	43 $\pm$ 7 <sup>*</sup>	85 $\pm$ 1 <sup>**</sup>
<b>+1127</b>	18 $\pm$ 9 <sup>*</sup>	86 $\pm$ 3	ND	ND

Results are reported as the mean % DNA synthesis or repeat addition processivity  $\pm$  SEM, relative to WT telomerase. DNA synthesis was calculated by measuring the signal intensity of the elongation products within the first hexameric repeat. For bio-TELO6, only the most intense products were quantified. Repeat addition processivity was determined by measuring the signal intensities of the pause products within the first five hexameric repeats (bio-TELO18) or first three hexameric repeats (bio-TELO6). Not detected (ND) indicates that telomerase was catalytically inactive. Asterisks denote statistical significance compared to WT telomerase, as determined using Student's two-tailed unpaired T-tests ( $p < 0.01$ , [<sup>\*\*</sup>] and  $p < 0.05$ , [<sup>\*</sup>]), and the section sign (§) indicates p values that were not statistically significant despite a reproducible decrease in total DNA synthesis compared to the wild type enzyme.

### 3.4 Discussion

#### 3.4.1 *hTERT interacts with telomeric ssDNA in the absence of hTR*

Here, we report the development of an activity-independent DNA-binding assay that was used to delineate regions of hTERT that formed stable and sequence-specific interactions with telomeric ssDNA. This assay utilizes biotinylated ssDNA oligonucleotides to test for protein-DNA interactions, similar to the methods that Snow *et al.* used to characterize interactions between telomeric ssDNA and the telomere-binding protein, hEST1A [344]. In this study, optimal reaction conditions were established to characterize *in vitro* interactions between the catalytic subunit of human telomerase, hTERT, and biotinylated ssDNA primers. We chose an *in vitro* approach to focus on hTERT-DNA interactions in the absence of cellular factors that may aid or inhibit this association *in vivo*. hTERT was synthesized in RRL in the absence of hTR to gain insight into important protein-DNA interactions that might be masked by hTR-DNA interactions. In addition, this approach was used because we could not determine how much recombinant hTERT was bound to hTR, making it impossible to distinguish between DNA-bound hTERT and DNA-bound hTERT-hTR species. Furthermore, the formation of hTERT-hTR complexes in RRL is relatively inefficient and technical difficulties have precluded the reconstitution of large quantities of purified hTERT-hTR complexes that would be needed for biochemical studies.

The primer binding assay was used to show that hTERT synthesized in RRL could form stable and telomere-sequence-specific interactions with ssDNA in the absence of hTR. These observations are in accordance with those made by Sealey and Harrington, who have also found that hTERT interacts sequence-specifically with biotinylated

telomeric ssDNA in the absence of hTR (D. Sealey and L. Harrington, personal communication). We observed that hTERT interacts very weakly with ssDNA representing the sequence of the chromosome C-strand (bio-antiTELO18 primer). This observation provided evidence that the hTR template is not required for hTERT to recognize and bind telomeric ssDNA *in vitro*. This observation is consistent with a substantial amount of functional data indicating that the primary determinant of telomere recognition is protein contacts with the 5'-end of G-rich ssDNA primers [267,282-284].

#### ***3.4.2 Primer binding can be functionally uncoupled from primer utilization***

We used the primer binding and conventional telomerase activity assays to understand the relationship between physical hTERT-DNA interactions and functional telomerase-DNA interactions (summarized in Table 3.4). This experimental approach also allowed us to: 1) determine if the interactions detected in the primer binding assay were functionally relevant, and 2) identify separation-of-function hTERT mutants (*i.e.* proteins that retained ssDNA-binding activity but did not reconstitute functional enzymes).

We concluded that physical hTERT-DNA interactions were functionally relevant because the anti-telomeric primer that showed negligible interaction with hTERT was not extended by telomerase *in vitro*. Likewise, hTERT formed stable interactions with each of the human telomeric primers that were primers for telomerase-dependent elongation. However, our studies revealed a complex relationship between the relative strength of hTERT-mediated primer binding and the efficiency of telomerase-mediated primer extension. Consistent with previous functional studies of human [163,272] and ciliate

[280,283,286,288] telomerase, we found that the catalytic activity of human telomerase was greatest with primers that contained 18 and 12 nt of telomeric DNA and much reduced with primers containing 24 and 6 nt of telomeric DNA. However, the primer binding results showed that hTERT bound each of these primers with similar avidity ( $p > 0.05$ ). One interpretation of these data is that only a small region of telomeric ssDNA is needed to form a stable hTERT-DNA complex, which is consistent with the ability of ciliate, yeast, and human telomerase to efficiently extend short telomeric primers *in vitro* [268,272,280,283,288,345]. However, we cannot rule out the possibility that the primer binding assay lacks the sensitivity that is required to measure subtle differences in protein-DNA interactions.

Primer binding results indicated that the reduced activity of human telomerase on certain telomeric primers was not due to an overall reduction in the ability of hTERT to bind these DNA primers. We speculate that the decreased activity of telomerase with bio-TELO24 may, in part, be due to the ability of telomeric primers containing four consecutive TTAGGG repeats to adopt a higher-order DNA structure known as the G-quadruplex since our reaction conditions were similar to those in which these structures can form [346,347]. Prior to telomerase-mediated elongation, the G-quadruplex would have to be unwound to allow telomerase access to the ssDNA primer. In support of this, hPOT1 has been shown to stimulate the RecQ helicases WRN and BLM to unwind telomeric dsDNA structures and, upon doing so, increases the efficiency with which telomerase extends (TTAGGG)<sub>4</sub> primers *in vitro* [74,347].

Our hypothesis that the protein requirements for telomere binding are distinct from those required for telomere elongation was supported by the finding that

catalytically inactive hTERT mutants bound telomeric primers as efficiently as WT hTERT. More specifically, we studied the relationship between primer binding and utilization using a catalytically inactive mutant containing a point mutation in the RT domain (hTERT D712A). The TERT RT domain contains an evolutionarily-conserved triad of metal-coordinating aspartic acids that are essential for catalysis *in vitro* and *in vivo* (D712, D868, and D869 in hTERT) [119,123,124]. As expected, human telomerase reconstituted with hTERT D712A was devoid of catalytic activity. However, hTERT D712A bound telomeric ssDNA-binding activity at levels that were indistinguishable from WT hTERT. This result provided evidence that physical primer binding could be functionally uncoupled from primer utilization and demonstrated the feasibility of using this approach to identify separation-of-function hTERT mutants.

### ***3.4.3 Evidence for multiple DNA-binding sites in hTERT***

Collectively, our primer binding experiments provided evidence for multiple ssDNA-binding sites in hTERT. We identified a strong DNA-binding activity within the first 300 amino acids. However, truncated hTERT mutants that lacked the first 300 amino acids also formed stable interactions with telomeric ssDNA. Furthermore, hTERT variants comprised of the RT domain alone retained weak telomeric ssDNA-binding activity *in vitro*. These results were independently supported in a recent study that used a similar primer binding assay to study TERT-DNA interactions in *T. thermophila* telomerase [286]. We found that the hTERT CTE was not sufficient to reconstitute stable hTERT-DNA interactions with telomeric ssDNA. In contrast, the CTE of *T. thermophila* TERT has been reported to be important for primer binding *in vitro* [286]. Similarly, a

weak nucleic-acid binding activity has been reported for the yeast TERT CTE [135]. These somewhat contradictory observations might be due to the different experimental approaches that were used to detect protein-DNA interactions. However, the TERT CTE has very weak sequence conservation and therefore, it is possible that this domain has evolved species-specific roles in telomere-binding.

#### ***3.4.4 Contribution of a specific region within the hTERT N-terminus to primer recognition and utilization***

Previous studies have shown that human telomerase reconstituted in RRL with hTERT 301-1132 catalyzes short elongation products in the TRAP assay whereas telomerase reconstituted with hTERT 351-1132 is devoid of catalytic activity [148]. These functional defects could not be attributed to loss of hTR-binding. Furthermore, each truncation restored wild type levels of catalytic activity to its complementary N-terminal fragment in *trans* [131,148]. However, 1-300 hTERT could not restore catalytic activity to hTERT 351-1132, identifying an important functional role for amino acids 300 to 350 [131,148]. Collectively, these studies provided the first evidence that this 50-amino acid region might facilitate primer recognition and extension by mediating protein-DNA interactions.

Our primer binding results support this hypothesis and provide novel insight into the significance of this 50-amino acid region. Specifically, we found that this region was an important determinant of the strength and sequence-specificity of hTERT-ssDNA interactions *in vitro*. The apparent strength of the interaction between hTERT 1-300 and telomeric ssDNA primers was indistinguishable from that observed with the full length

protein. However, hTERT 1-300 showed an equally strong interaction with anti-telomeric ssDNA, suggesting that this fragment interacts with ssDNA in a sequence non-specific manner. Interestingly, sequence-specificity was restored in the hTERT 1-350 mutant. This result indicates that the region between residues 300 and 350 is critical for recognition of human telomeric ssDNA. Since hTERT 301-1132 also bound ssDNA in a sequence non-specific manner, we suggest that the 50-amino acid region acts in *cis* with the extreme N-terminus of hTERT to confer specificity for telomeric ssDNA.

Interestingly, we also observed that the apparent strength of the interactions between hTERT 1-350 and telomeric ssDNA were significantly less than that observed with either full length or 1-300 hTERT. This leads us to suggest that the region between amino acids 300 and 350 may also negatively regulate the strength of the interaction between hTERT and telomeric ssDNA. We speculate that telomerase requires a negative regulatory DNA-binding domain because an exceedingly strong hTERT-DNA complex could 'lock' the enzyme into a conformation that impedes polymerization and translocation. In conclusion, we propose that hTERT contains at least two distinct, but co-operative, anchor regions that are partly regulated by the region spanning amino acids 300 to 350. Further studies will be required to fully understand how this region mediates primer binding and utilization in human telomerase.

#### ***3.4.5 hTERT primer grip regions are involved in primer binding and utilization***

In HIV-1 RT, the primer grip region in the RT domain is required for template-primer interactions, DNA polymerization, and enzyme processivity [342]. This motif is structurally conserved in the TERT proteins. In Est2p, the RT domain primer grip

regulates telomerase activity *in vitro* and is necessary for telomerase-dependent telomere length maintenance *in vivo* [157]. Here, we showed that the RT primer grip was important for the apparent strength of interactions between hTERT and short telomeric ssDNA and was essential for telomerase activity *in vitro*. We identified a putative primer grip within the hTERT NTE that was involved in regulating sequence-specificity and elongation of telomeric primers *in vitro*. We speculate that the existence of two primer grips may be explained as follows: the evolutionarily conserved RT-primer grip is needed to align the 3'-end of the ssDNA primer in the catalytic site for telomerase-mediated elongation, and the N-terminal primer grip is involved in regulating the strength and specificity of protein interactions with the primer 5'-end. Together, optimal N- and RT-primer grip interactions facilitate sequence-specific primer binding and processive elongation of telomeric primers.

#### ***3.4.6 Not all DATs are created equal***

hTERT contains several DAT domains that are required for telomerase-dependent telomere length maintenance in human cells and elongation of completely telomeric primers *in vitro* [140,162,163,167]. The DAT mutations, however, do not hinder the ability of human telomerase to elongate non-canonical telomeric primers *in vitro* and therefore, dissociate the catalytic and biological activities of telomerase [140,162,167]. Importantly, the loss of biological activity is not due to abrogated interactions with hTR, protein degradation, or nuclear exclusion [140,162]. It has thus been speculated that the DAT domains are a key determinant of protein-DNA interactions at the telomere [140,162,163,165-167]. More specifically, DAT domains are thought to be involved in

either telomerase recruitment to the telomere (physical association with telomeric DNA) or in the accurate positioning of telomerase at the chromosome 3'-overhang (termed end-positioning). Previous studies have relied on activity-based assays to gain insight into interactions between hTERT DAT mutants and telomeric ssDNA *in vitro*. The strength of our study is that we used an activity-independent DNA-binding assay to characterize physical interactions between specific hTERT DAT mutants and ssDNA primers.

The primer binding results presented here provide the first direct insight into the ssDNA-binding capacity of hTERT DAT mutants. The DAT mutants studied here demonstrated slightly less stable interactions with telomeric ssDNA than WT hTERT. In most cases, telomerase reconstituted with these mutants exhibited reduced levels of DNA synthesis (bio-TELO18 and bio-TELO6) and reduced RAP (bio-TELO6). In a related study, Autexier *et al.* reported that telomerase reconstituted with hTERT DAT +110 exhibited defects in RAP that were rescued at high primer concentrations, which provided indirect evidence for altered protein-DNA interactions [163]. Thus, it seems clear that the DAT mutations do alter the ability of hTERT to bind telomeric ssDNA. Our data indicate that there is not a direct correlation between the magnitude of the reduction in ssDNA-binding and severity of the catalytic phenotype. For example, although hTERT DAT +68 and +98 showed the weakest interactions with telomeric ssDNA, the most severe functional defect was associated with telomerase reconstituted with hTERT DAT +1127. This observation is consistent with the previous finding that extracts from human cells expressing hTERT DAT +1127 are devoid of catalytic activity [167] and provides additional evidence that the hTERT CTE has a critical role in telomerase function. Collectively, our results indicate that defects in various aspects of telomerase

biochemistry, including telomeric ssDNA-binding, can manifest the DAT phenotype. Not surprisingly, a complex interplay of interactions within the telomerase RNP complex appears to regulate the ability of the enzyme to recognize, bind, and elongate telomeric ssDNA.

### ***3.4.7 Perspectives***

We developed the first DNA-binding assay to characterize interactions between RRL-reconstituted hTERT and ssDNA primers *in vitro*. Our results provide the first evidence that hTERT can interact sequence-specifically with telomeric ssDNA in the absence of hTR. We also demonstrate that the first 350 amino acids of hTERT have a critical role in regulating protein-DNA interactions, which strengthens the hypothesis that the TERT NTE contains an anchor site. Importantly, we have uncovered an additional region within motif E of the RT domain that is involved in protein-DNA interactions and is essential for enzyme activity. Collectively, our data indicate that hTERT contains distinct anchor regions that co-operate to regulate telomerase-mediated DNA recognition and elongation.

**Table 3.4: Summary of the primer binding and conventional telomerase activity assay results obtained with the hTERT constructs and bio-TELO18 or bio-TELO6.**

hTERT Variant	Sequence Specificity	<u>bio-TELO18</u>			<u>bio-TELO6</u>		
		DNA Binding	DNA Synthesis	RAP	DNA Binding	DNA Synthesis	RAP
D712A	Y	WT	ND	ND	WT	ND	ND
1-300	N	WT	ND	ND	WT	ND	ND
1-350	Y	↓	ND	ND	↓↓	ND	ND
301-1132	N	WT	ND	ND	↓	ND	ND
351-1132	Y	WT	ND	ND	↓	ND	ND
505-967	Y	↓↓↓	ND	ND	↓↓↓	ND	ND
601-927	Y	↓↓↓	ND	ND	↓↓↓	ND	ND
928-1132	Y	↓↓↓	ND	ND	↓↓↓	ND	ND
976-1132	Y	↓↓↓	ND	ND	↓↓↓	ND	ND
RT-GRIP	Y	WT	ND	ND	↓	ND	ND
N-GRIP	N	WT	↓↓	WT	WT	↓↓	↓↓
N&RT-GRIP	Y	WT	ND	ND	WT	ND	ND
DAT +68	Y	↓ §	↓ §	WT	↓ §	↓↓ §	↓
DAT+98	Y	↓ §	↓↓ §	WT	↓↓	↓↓	↓
DAT+ 122	Y	WT	↓↓ §	WT	↓	↓↓	↓
DAT +128	Y	WT	WT	WT	↓ §	↓↓	↓
DAT +1127	Y	↓ §	↓↓↓	WT	↓ §	ND	ND

**Table 3.4: Summary of the primer binding and conventional telomerase activity assay results obtained with the hTERT constructs and bio-TELO18 or bio-TELO6.**

Results are reported relative to WT hTERT (DNA-binding) and telomerase (DNA synthesis and repeat addition processivity [RAP]). Sequence specificity refers to whether or not a stable interaction was observed between the hTERT construct and anti-telomeric ssDNA primer. Yes (Y) indicates that the construct did not interact with the anti-telomeric ssDNA primer and, thus, retained sequence-specificity and no (N) indicates that the hTERT mutant formed a relatively stable interaction with the anti-telomeric ssDNA primer and thus, was deemed to lack sequence-specificity. A wild type (WT) designation means there was no statistically significant difference between the mutant and WT enzyme. Arrows indicate the relative reduction in DNA-binding, DNA synthesis, or RAP compared to WT telomerase: small reduction ( $\downarrow$ ), moderate reduction ( $\downarrow\downarrow$ ), and dramatic reduction ( $\downarrow\downarrow\downarrow$ ). Not detected (ND) indicates that telomerase reconstituted with hTR and the hTERT mutant was catalytically inactive. The section sign (§) indicates values that are not statistically significant despite a reproducible decrease in DNA binding or total DNA synthesis compared to the WT enzyme.

## **Chapter Four: Human telomerase reverse transcriptase (hTERT) Q169 is essential for telomerase function *in vitro* and *in vivo***

### **4.1 Preface**

In 2006, the atomic-resolution structure of the *T. thermophila* Telomerase Essential N-terminal (TEN) domain was determined by X-ray crystallography [143]. Phylogenetically-conserved residues on the surface of this domain were predicted to form a previously unrecognized ssDNA-binding channel that could represent a long sought-after anchor site. Consistent with this, structure-function studies indicated that an invariant Gln was involved in ciliate and yeast telomerase anchor site function [143,278,289]. In this study, I characterized the corresponding residue in human telomerase reverse transcriptase (hTERT) to determine if the Gln residue was important for telomerase function, anchor site interactions, and telomere length maintenance in human telomerase.

### **4.2 Summary**

Telomerase is a reverse transcriptase that maintains the telomeres of linear chromosomes and preserves genomic integrity. The minimal components for enzyme activity *in vitro* are a catalytic protein subunit, the telomerase reverse transcriptase (TERT), and an RNA subunit, the telomerase RNA (TR). Telomerase is unique in its ability to catalyze processive telomere repeat addition, which is facilitated by telomere-specific DNA-binding domains in TERT called anchor sites. In lower eukaryotes, a conserved glutamine residue in the TERT N-terminus is important for anchor site

interactions. To understand the significance of this residue in human TERT (hTERT Q169), we performed site-directed mutagenesis to create neutral (Q169A), conservative (Q169N), and non-conservative (Q169D) mutant proteins. In this work, we show that these mutations severely compromise telomerase activity *in vitro* and *in vivo*. The functional defects are not due to abrogated interactions with hTR or telomeric ssDNA. However, substitution of hTERT Q169 dramatically impairs the ability of telomerase to incorporate nucleotides at the second position of the template. Furthermore, Q169 mutagenesis alters the relative strength of hTERT-telomeric ssDNA interactions, which identifies Q169 as a novel residue in hTERT required for optimal primer binding. Proteolysis experiments indicate that Q169 regulates conformational flexibility of the hTERT N-terminus, providing the first evidence that this residue maintains the hTERT NTE in a conformation that is critical for catalytic function. Collectively, our results indicate that Q169 is important for a conformation of the hTERT N-terminus that is necessary for optimal substrate-enzyme interactions and nucleotide incorporation. We show for the first time that the conserved Gln is a functionally critical residue in human telomerase and provide the first detailed evidence regarding the cellular significance of this residue in higher eukaryotes.

## 4.3 Results

### 4.3.1 *Q169 mediates the polymerase function of human telomerase in vitro*

We first sought to determine whether the evolutionarily-conserved Gln residue was required for human telomerase activity *in vitro*. Human telomerase complexes were assembled in RRL with N-terminally FLAG-tagged hTERT WT or Q169 mutant plasmid

DNA and *in vitro* transcribed hTR, and tested for enzyme activity using the Telomere Repeat Amplification Protocol (TRAP). We found that human telomerase reconstituted with either hTERT Q169A, Q169D, or Q169N exhibited a dramatic reduction in catalytic activity compared to the WT enzyme (Figure 4.1). Control reactions showed that RNase A inhibited these reactions, indicating that DNA synthesis was catalyzed by telomerase and not by contaminating polymerases present in the RRL. The Q169D substitution was particularly disruptive and largely eliminated enzymatic activity, perhaps due to electrostatic repulsion between the polyanionic DNA backbone and electronegative carboxylic acid side-chain.

The TRAP is a highly sensitive method to detect telomerase activity. However, it does not distinguish between enzymes with catalytic defects (*i.e.* impaired DNA polymerization) and non-processive enzymes with translocation defects that synthesize fewer than four telomeric repeats [169,348]. Therefore, we used the CTA to gain more insight into the catalytic defects of the hTERT Q169 mutants. Similar to the TRAP results, human telomerase reconstituted with hTERT Q169A, Q169D, or Q169N exhibited markedly reduced activity compared to the WT enzyme when tested with an 18 nt telomeric ssDNA primer, bio-TELO18 (Figure 4.2). CTA assays were performed with bio-TELO18 because human telomerase exhibits robust activity with this primer ([158] and Figure 3.4). Quantification of three independent experiments showed that telomerase reconstituted with hTERT Q169A was approximately 20 % as active as the WT enzyme ( $p < 0.001$ ) (Table 4.1). The activity defect was more severe for telomerases reconstituted with either hTERT Q169D or hTERT Q169N, which were only 11 % and 14 % as active as WT telomerase, respectively ( $p < 0.001$ ). We observed a striking defect in the ability

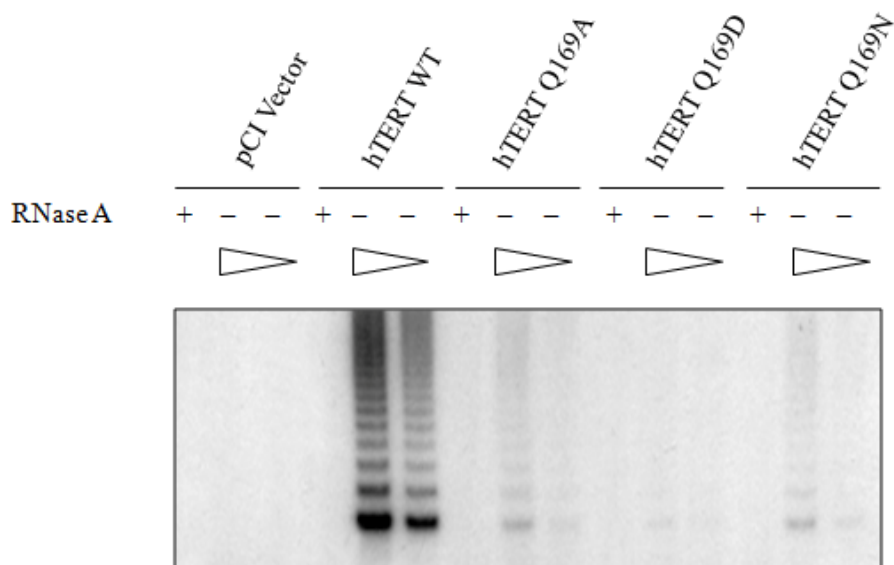


**Figure 4.1: *In vitro* activity of telomerase reconstituted with hTERT Q169 mutants.** Human telomerase was reconstituted in RRL with hTR and plasmid DNA for the pCI vector, hTERT WT, hTERT Q169A, hTERT Q169D, or hTERT Q169N and tested for *in vitro* enzyme activity using the telomere repeat amplification protocol. RRL reconstitution reactions (1  $\mu$ L) were assayed in the presence and absence of 5  $\mu$ g RNase A to show that DNA extension was catalyzed by telomerase and not by polymerases present in the RRL. The triangles represent a five-fold dilution of each reaction to confirm that the activity assays were in the linear range. This experiment was performed four times.

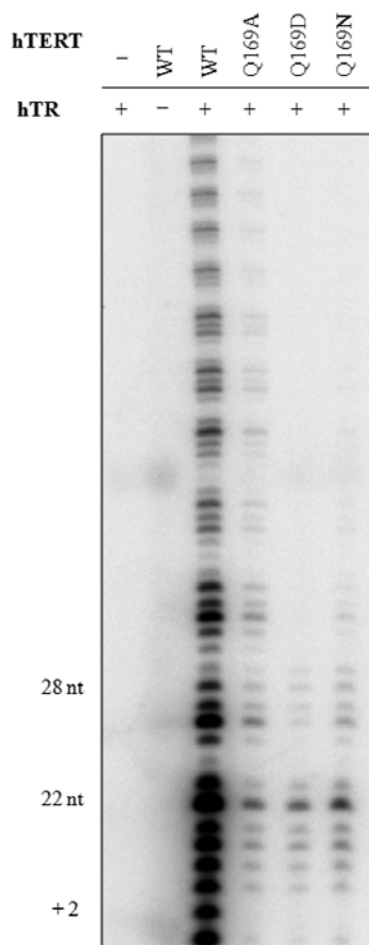


**Figure 4.2: hTERT Q169 mutants exhibit defects in overall DNA synthesis.**

Human telomerase reconstituted in RRL with hTR and hTERT WT, Q169A, Q169D, or Q169N was tested for catalytic activity with an 18 nt telomeric primer, bio-TELO18. The positions of the 22 nt and 28 nt elongation product are shown at the left of the image and were determined by comparison with the mobility of a 5'-end-radiolabelled 18 nt telomeric primer containing a 3'-biotin residue (data not shown). The nucleotide corresponding to the second position of the hTR template region is indicated as + 2. The quantification and statistical analysis of these data are shown in Table 4.1.

**Table 4.1: Quantification of DNA synthesis and repeat addition processivity observed for telomerase Q169 mutants with primer bio-TELO18.**

<b>hTERT Mutant</b>	<b>DNA Synthesis (% WT <math>\pm</math> SEM)</b>	<b>Repeat Addition Processivity (% WT <math>\pm</math> SEM)</b>
<b>Q169A</b>	21 $\pm$ 1 ***	96 $\pm$ 4
<b>Q169D</b>	11 $\pm$ 1 ***	ND
<b>Q169N</b>	14 $\pm$ 3 ***	ND

DNA synthesis was calculated using the data shown in Figure 4.3 and repeat addition processivity was determined from the data shown in Figure 4.4. Results were calculated from three independent experiments and the mean  $\pm$  SEM is reported relative to the wild type enzyme. DNA synthesis was calculated within the first hexameric repeat and repeat addition processivity was determined within the first five hexameric repeats. Not detected (ND) indicates that the signal was below the detection limit of this assay and the data were not quantified. Asterisks denote the level of statistical significance compared to wild type telomerase, as determined using Student's two-tailed unpaired T-tests:  $p < 0.0001$  (\*\*\*).

of the Q169 mutants to incorporate the second nucleotide, which corresponds to the second G in the extension product 5'-GGGTTAG-3'. This could be explained if the Q169 mutants have reduced affinity for the nucleotide that would be incorporated at this position. However, we have not been able to address this question because kinetic studies and derivation of affinity constants cannot be performed with RRL-reconstituted human telomerase. This limitation is due to the high abundance of RRL proteins and the inability to accurately quantify the concentration of functional enzyme. Similar arguments exist for FLAG-immunoprecipitated human telomerase. An alternative, but not necessarily independent explanation is that substitution of Q169 altered hTERT conformation, which prevented efficient nucleotide incorporation.

Pulse-chase CTA experiments indicated that mutation of hTERT Q169 did not affect repeat addition processivity (RAP) (Figure 4.3). These experiments were performed by allowing telomerase to bind and extend bio-TELO18 for 5 min ('pulse'), 'chasing' the enzyme with several-fold excess non-biotinylated TELO18 (TELO18), and then isolating the biotinylated extension products with streptavidin-conjugated magnetic beads. Only processive enzymes continue to extend the pulse primer (bio-TELO18) when challenged with chase DNA (TELO18). A direct correlation was observed between the length of the extended, biotinylated products and the time that WT and Q169A telomerase were incubated with chase DNA. This result indicated that telomerase remained associated with bio-TELO18 and catalyzed processive DNA synthesis. Quantification of the repeat addition processivity within the first five telomeric repeats revealed that hTERT Q169A was at least 95 % as processive as WT telomerase when pulsed with bio-TELO18 and chased with TELO18 ( $p > 0.05$ ). This data suggests that

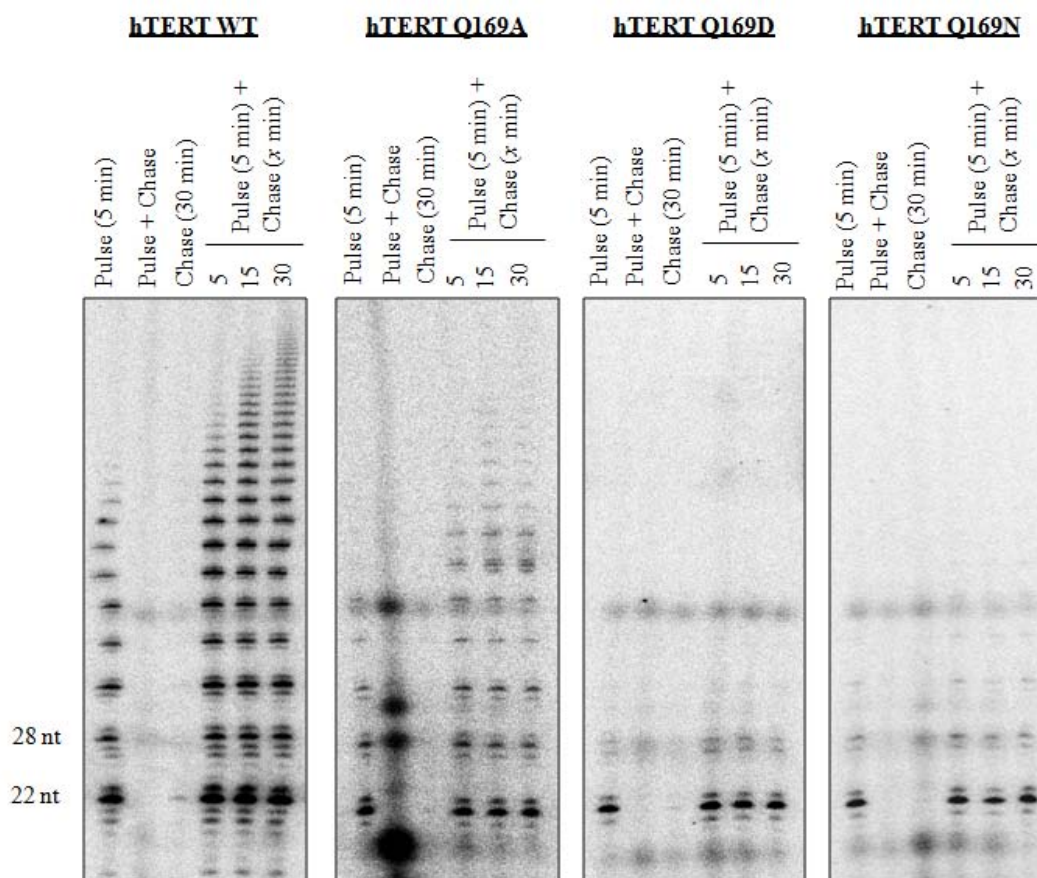


**Figure 4.3: Repeat addition processivity of hTERT Q169 mutants.**

**Figure 4.3: Repeat addition processivity of hTERT Q169 mutants.**

Pulse-chase CTA experiments were used to measure repeat addition processivity of human telomerase reconstituted in RRL with hTR and hTERT WT, Q169A, Q169D, or Q169N and bio-TELO18. The telomerase extension reaction was initiated with 1.5  $\mu$ M bio-TELO18. Telomerase was allowed to extend bio-TELO18 for 5 min and then challenged with 200  $\mu$ M chase primer (TELO18) for 5, 15, and 30 min. The first three lanes in each panel represent control reactions (left to right): pulse (5 min), reactions performed with pulse primers alone to show that telomerase can efficiently elongate this bio-TELO18; pulse + chase, pulse and chase primers added simultaneously to demonstrate the efficiency of the chase conditions; chase (30 min), reactions performed with the chase primer alone to show that the non-biotinylated reaction products are not isolated on streptavidin beads. The positions of the 22 nt and 28 nt elongation product are shown at the left of the image. The quantification and statistical analysis of these data are shown in Table 4.1.

hTERT Q169 has a critical role in the first round of DNA synthesis but is less important for subsequent rounds of DNA synthesis (*i.e.* translocation). However, we cannot rule out a potential role for Q169 in repeat addition processivity since we were unable to quantify the processivity of telomerase reconstituted with hTERT Q169D or Q169N.

#### ***4.3.2 Biochemical characterization of hTERT Q169***

To investigate the basis for the activity defects, we determined whether Q169 modulates hTERT stability, conformation, and physical interactions with hTR. There was no appreciable difference in the protein levels of [<sup>35</sup>S]cysteine-labelled hTERT WT, Q169A, Q169D, or Q169N (Figure 4.4), indicating that Q169 mutagenesis does not have a significant impact on hTERT stability *in vitro*. However, it remained possible that Q169 mutation might induce a conformational change in hTERT that inhibited enzyme activity without compromising protein stability. Therefore, RRL containing comparable levels of [<sup>35</sup>S]cysteine-labelled WT or Q169 mutated hTERT were subjected to limited proteolysis using chymotrypsin. Interestingly, the signal intensity of [<sup>35</sup>S]cysteine-labelled proteolytic fragments migrating at approximately 20 kDa was diminished in hTERT Q169A, Q169D, and Q169N. This result indicated that the hTERT Q169A, Q169D, and Q169N mutants were more susceptible to chymotrypsin digestion than hTERT WT (Figure 4.5). This was an hTR-independent effect because the proteolytic fragments derived from hTERT reconstituted in the presence of hTR were indistinguishable from those observed in its absence (Figure 4.6). This observation was confirmed with time-course proteolytic digestions of [<sup>35</sup>S]cysteine-labelled hTERT WT, Q169A, Q169D, or Q169N that were synthesized in the presence and absence of hTR (Figures 4.7 and 4.8).

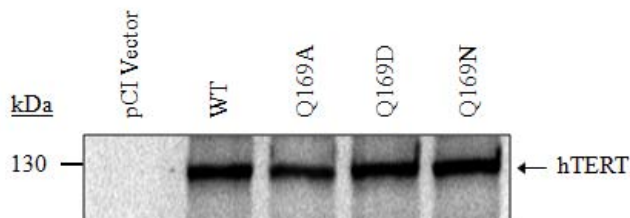


**Figure 4.4: Substitution of hTERT Q169 does not alter protein stability *in vitro*.**

SDS-PAGE and autoradiography was used to assess the expression and stability of [<sup>35</sup>S]cysteine-labelled proteins synthesized in RRL. Reconstitution reactions contained plasmid DNA for the following (left to right): pCI 'empty' vector, hTERT WT, hTERT Q169A, hTERT Q169D, and hTERT Q169N. 2  $\mu$ L of each RRL reaction were resolved by 8 % SDS-PAGE and visualized by autoradiography and phosphorimaging.

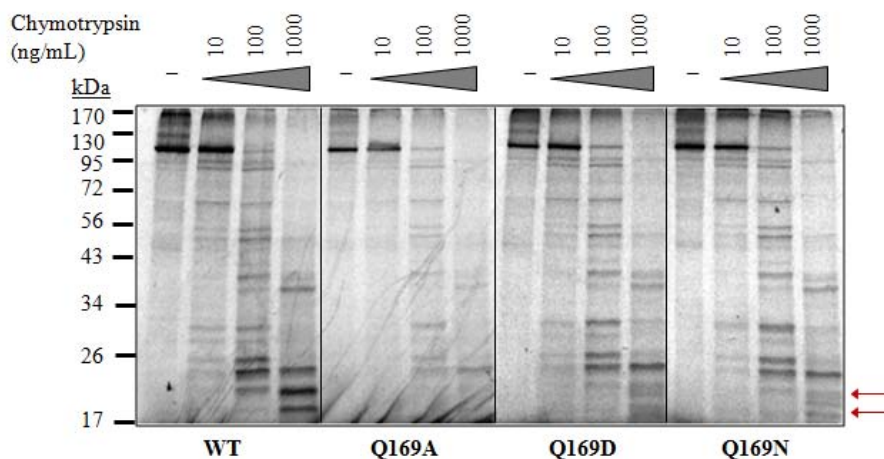


**Figure 4.5: hTERT Q169 mutants show subtle differences in the proteolytic cleavage pattern following treatment with chymotrypsin.**

Comparable amounts of [<sup>35</sup>S]cysteine-labelled hTERT WT, hTERT Q169A, hTERT Q169D, or hTERT Q169N were incubated with 0, 10 ng/mL, 100 ng/mL, or 1000 ng/mL chymotrypsin at 30°C for 2 min. Reactions were terminated by the addition of SDS-PAGE loading buffer and boiling (5 min). Following digestion, products were resolved by 12 % SDS-PAGE. Arrows indicate the proteolytic fragments that are reduced upon substitution of hTERT Q169.

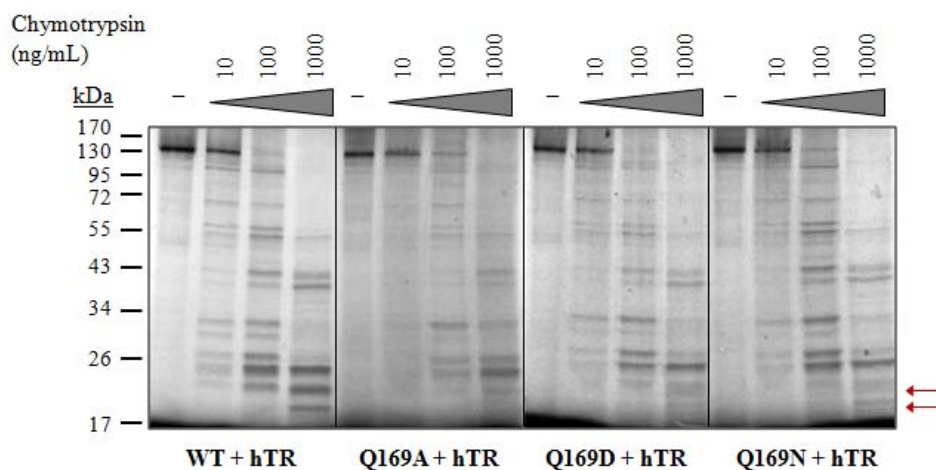


**Figure 4.6: Q169 modulates hTERT conformation in an hTR-independent manner.** Comparable counts of human telomerase reconstituted with hTR and [<sup>35</sup>S]cysteine-labelled hTERT WT, hTERT Q169A, hTERT Q169D, or hTERT Q169N were incubated with 0, 10 ng/mL, 100 ng/mL, or 1000 ng/mL chymotrypsin at 30°C for 2 min. Reactions were terminated by the addition of SDS-PAGE loading buffer and boiling (5 min). Following digestion, products were resolved by 12 % SDS-PAGE. Arrows indicate the proteolytic fragments that are reduced upon substitution of hTERT Q169.

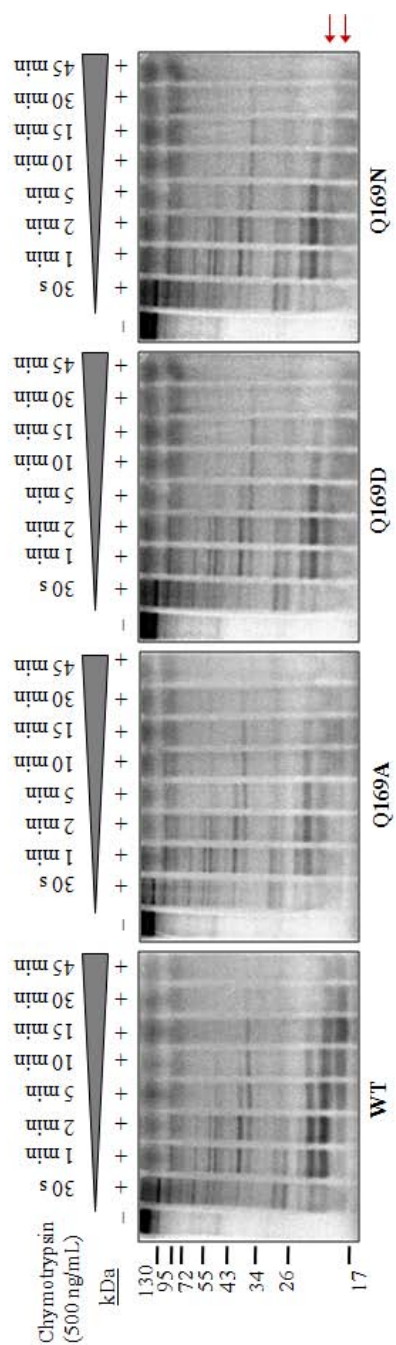


**Figure 4.7: Time-course proteolytic digestion of hTERT WT and Q169 mutants in the absence of hTR.**

**Figure 4.7: Time-course proteolytic digestion of hTERT WT and Q169 mutants in the absence of hTR.**

Comparable counts of [<sup>35</sup>S]cysteine-labelled hTERT WT, Q169A, Q169D, or Q169N were incubated with 500 ng/mL chymotrypsin at 30°C for 30 s, 1 min, 2 min, 5 min, 10 min, 15 min, 30 min, and 45 min. Reactions were terminated by the addition of SDS-PAGE loading buffer and boiling (5 min). Following digestion, products were resolved by 12 % SDS-PAGE and visualized by autoradiography and phosphorimaging. Arrows indicate the proteolytic fragments that are reduced upon substitution of hTERT Q169.

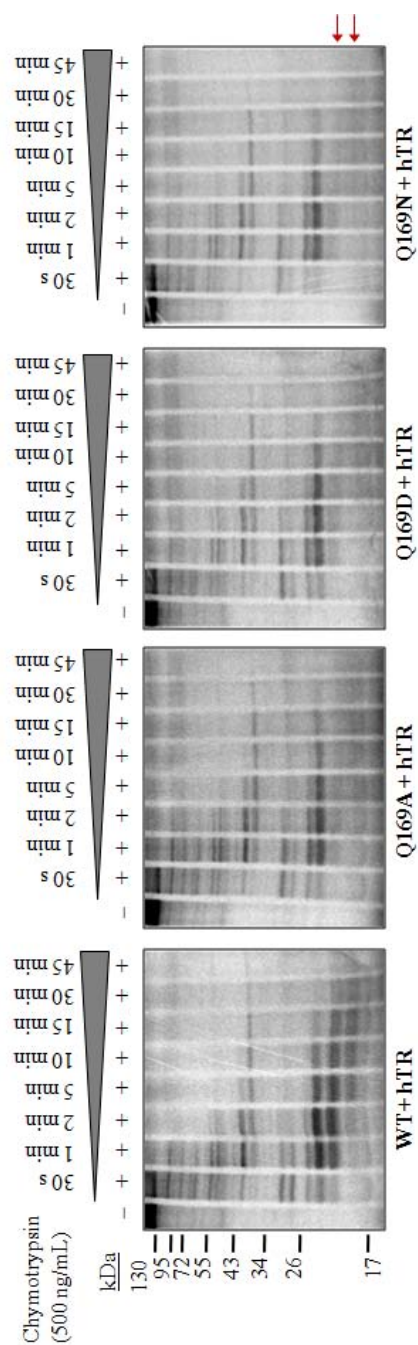


**Figure 4.8: Time-course proteolytic digestion of telomerase reconstituted with hTR and hTERT WT or Q169 mutants.**

**Figure 4.8: Time-course proteolytic digestion of telomerase reconstituted with hTR and hTERT WT or Q169 mutants.**

Comparable counts of human telomerase reconstituted with hTR and [<sup>35</sup>S]cysteine-labelled hTERT WT, Q169A, Q169D, or Q169N were incubated with 500 ng/mL chymotrypsin at 30°C for 30 s, 1 min, 2 min, 5 min, 10 min, 15 min, 30 min, and 45 min. Reactions were terminated by the addition of SDS-PAGE loading buffer and boiling (5 min). Following digestion, products were resolved by 12 % SDS-PAGE and visualized by autoradiography and phosphorimaging. Arrows indicate the proteolytic fragments that are reduced upon substitution of hTERT Q169.

To gain insight into the identity of the proteolytic fragments at approximately 20 kDa, we performed limited proteolysis on truncated hTERT proteins containing the first 300 amino acids. A comparison of the proteolytic profiles of [<sup>35</sup>S]cysteine-labelled 1 – 300 hTERT WT and Q169A, Q169D, and Q169N revealed a reduction in the 20 kDa proteolytic fragment in the Q169 mutants, similar to the results obtained with full length hTERT (Figure 4.9 and 4.10). This analysis provides the first experimental evidence that Q169 is important for the structure of the hTERT N-terminus.

Interactions between hTERT and hTR are essential for telomerase activity and some mutations in hTERT that impair hTR-binding reconstitute non-functional enzymes [131,148,152]. Thus, defects in hTERT-hTR assembly could potentially explain the loss of activity observed with the hTERT Q169 mutants. To test this possibility, human telomerase was reconstituted with [ $\alpha$ -<sup>32</sup>P]UTP-labelled hTR and [<sup>35</sup>S]cysteine-labelled-FLAG-hTERT WT, Q169A, Q169D, or Q169N. [<sup>35</sup>S]cysteine-labelled hTERT was immunoprecipitated with FLAG antibodies and analyzed for the presence of [ $\alpha$ -<sup>32</sup>P]UTP-labelled hTR. As shown in Figure 4.11, the hTERT Q169 mutants bound hTR as efficiently as hTERT WT, indicating that the functional defects observed with these mutants are not due to abrogated hTERT-hTR interactions.

#### ***4.3.3 hTERT Q169A, Q169D, and Q169N retain sequence-specific ssDNA-binding activity***

Telomeric primers need to be positioned correctly within the telomerase active site to initiate reverse transcription. In addition to RNA-DNA interactions, this requires interactions between the TERT RT domain and the 3'-end of the ssDNA primer, as well

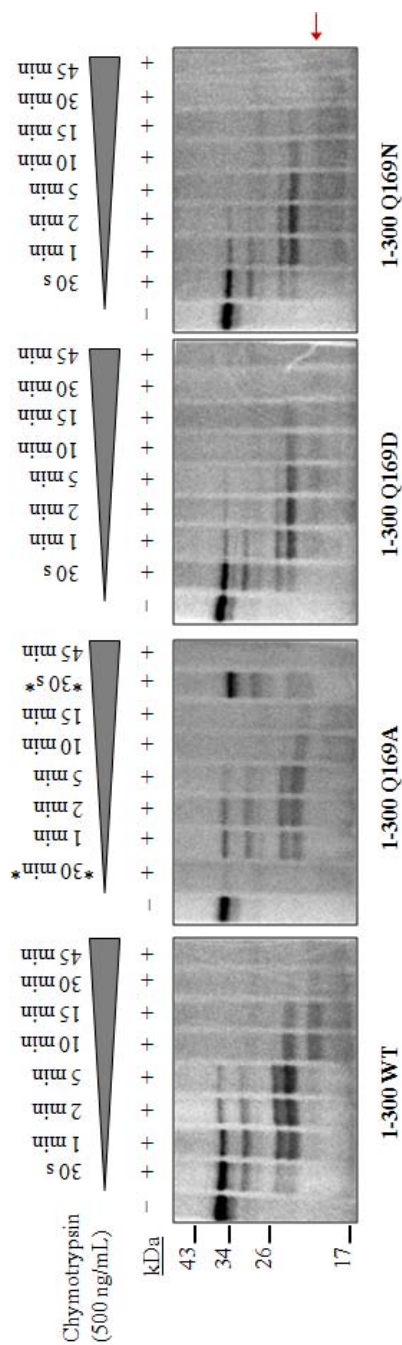


**Figure 4.9: Time-course proteolytic digestion of 1-300 hTERT WT and Q169 mutants in the absence of hTR.**

**Figure 4.9: Time-course proteolytic digestion of 1-300 hTERT WT and Q169 mutants in the absence of hTR.**

Comparable counts of [<sup>35</sup>S]cysteine-labelled 1-300 hTERT WT, Q169A, Q169D, or Q169N were incubated with 500 ng/mL chymotrypsin at 30°C for 30 s, 1 min, 2 min, 5 min, 10 min, 15 min, 30 min, and 45 min. Reactions were terminated by the addition of SDS-PAGE loading buffer and boiling (5 min). Following digestion, products were resolved by 12 % SDS-PAGE and visualized by autoradiography and phosphorimaging. Arrows indicate the proteolytic fragments that are reduced upon substitution of hTERT Q169. In 1-300 Q169A, note the inversion of the 30 s and 30 min samples.

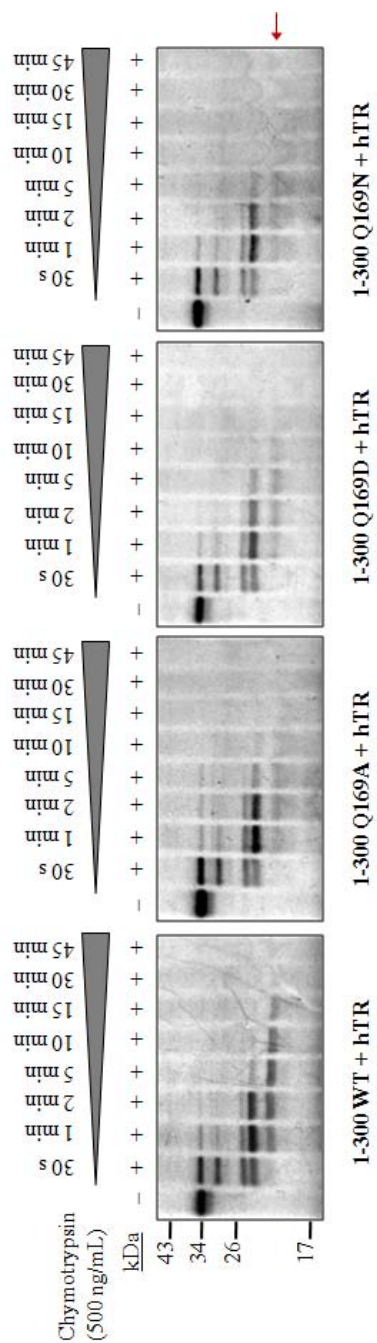


**Figure 4.10: Time-course proteolytic digestion of telomerase reconstituted with hTR and 1-300 hTERT WT or Q169 mutants.**

**Figure 4.10: Time-course proteolytic digestion of telomerase reconstituted with hTR and 1-300 hTERT WT or Q169 mutants.**

Comparable amounts of human telomerase reconstituted with hTR and [<sup>35</sup>S]cysteine-labelled 1-300 hTERT WT, Q169A, Q169D, or Q169N were incubated with 500 ng/mL chymotrypsin at 30°C for 30 s, 1 min, 2 min, 5 min, 10 min, 15 min, 30 min, and 45 min. Reactions were terminated by the addition of SDS-PAGE loading buffer and boiling (5 min). Following digestion, products were resolved by 12 % SDS-PAGE and visualized by autoradiography and phosphorimaging. Arrows indicate the proteolytic fragments that are reduced upon substitution of hTERT Q169.

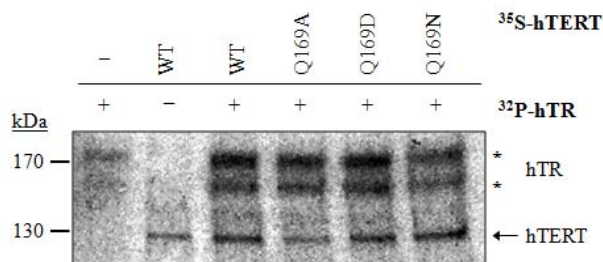


**Figure 4.11: Substitution of Q169 does not abrogate hTERT-hTR interactions.**

Human telomerase was reconstituted in RRL with [ $\alpha$ -<sup>32</sup>P]UTP-labelled hTR and [<sup>35</sup>S]cysteine-labelled FLAG-hTERT WT, Q169A, Q169D, or Q169N and immunoprecipitated with anti-FLAG antibodies. [ $\alpha$ -<sup>32</sup>P]UTP-labelled hTR (indicated by asterisks) was coimmunoprecipitated with [<sup>35</sup>S]cysteine-labelled FLAG-hTERT WT or Q169 mutants (indicated by arrow). Coimmunoprecipitates were resolved by 4-15 % SDS-PAGE and visualized by autoradiography and phosphorimaging. The signal corresponding to [ $\alpha$ -<sup>32</sup>P]UTP-labelled hTR was confirmed by placing two sheets of autoradiography film on the gel: the [<sup>35</sup>S]cysteine signal cannot penetrate the first film and therefore, only [ $\alpha$ -<sup>32</sup>P]UTP signals appeared on the second film.

as between the N-terminus (anchor region) and the primer 5'-end [129]. Thus, suboptimal interactions between hTERT and DNA primers could explain the activity defects observed with the hTERT Q169 mutants.

We used our recently-developed DNA-binding assay to characterize physical interactions between hTERT WT, Q169A, Q169D, and Q169N and 5'-biotinylated ss-oligonucleotides (Table 4.2) [158]. As described in Chapter 3, we did not detect statistically significant differences in the physical interactions between RRL-reconstituted hTERT and 5'-biotinylated ssDNA primers containing one, two, three, or four TTAGGG repeats (bio-TELO6, bio-TELO12, bio-TELO18, and bio-TELO24, respectively;  $p > 0.05$ , as determined by ANOVA). Nonetheless, we did observe a general trend in the apparent strength of hTERT-ssDNA interactions: bio-TELO18 ~ bio-TELO12 > bio-TELO24 ~ bio-TELO6 (Figure 3.3). The primer binding results reported here and in Chapter 5 reveal a more pronounced difference in the apparent strength of the interaction between hTERT and ssDNA primers containing different lengths of telomeric DNA. However, ANOVA indicates that the difference between the means is not significant ( $p > 0.05$ ). In these experiments the trend in the apparent strength of hTERT-ssDNA interactions was bio-TELO30 ~ bio-TELO18 > bio-TELO24 ~ bio-TELO12 > bio-TELO6 (Figure 4.12). This difference can be explained by the method of detection and data quantification. Specifically, the primer binding data in Chapter 3 were quantified from autoradiography film whereas the results presented here and in Chapter 5 were quantified from phosphorimager screens. The latter method is more accurate and sensitive, thereby revealing subtle differences in the strength of hTERT-ssDNA interactions.

**Table 4.2: Description of ssDNA primers used in the primer binding studies of hTERT Q169, Q169A, Q169D, and Q169N.**

<b>Name</b>	<b>Length (nt)</b>	<b>DNA Sequence (5' to 3')</b>
<b>bio-TELO30</b>	30	TTAGGG TTAGGG TTAGGG TTAGGG TTAGGG
<b>bio-TELO24</b>	24	TTAGGG TTAGGG TTAGGG TTAGGG
<b>bio-TELO18</b>	18	TTAGGG TTAGGG TTAGGG
<b>bio-TELO12</b>	12	TTAGGG TTAGGG
<b>bio-TELO6</b>	6	TTAGGG
<b>bio-antiTELO18</b>	18	AATCCC AATCCC AATCCC
<b>bio-pBR</b>	24	AGCCAC TATCGA CTACGC GATCAT
<b>bio-BBP</b>	24	AATCCG TCGAGC AGAAAT CCGCAA
<b>bio-Tetrahymena</b>	18	TTGGGG TTGGGG TTGGGG
<b>bio-Yeast</b>	15	TGTGTG GTGTGT GGG
<b>TELO24</b>	24	TTAGGG TTAGGG TTAGGG TTAGGG
<b>TELO18</b>	18	TTAGGG TTAGGG TTAGGG

These primers were tested for physical interaction with hTERT in the primer binding assay and telomerase-mediated extension in the conventional telomerase activity assay (bio-TELO18). Primers containing a 5' biotin molecule are indicated with the prefix 'bio'.

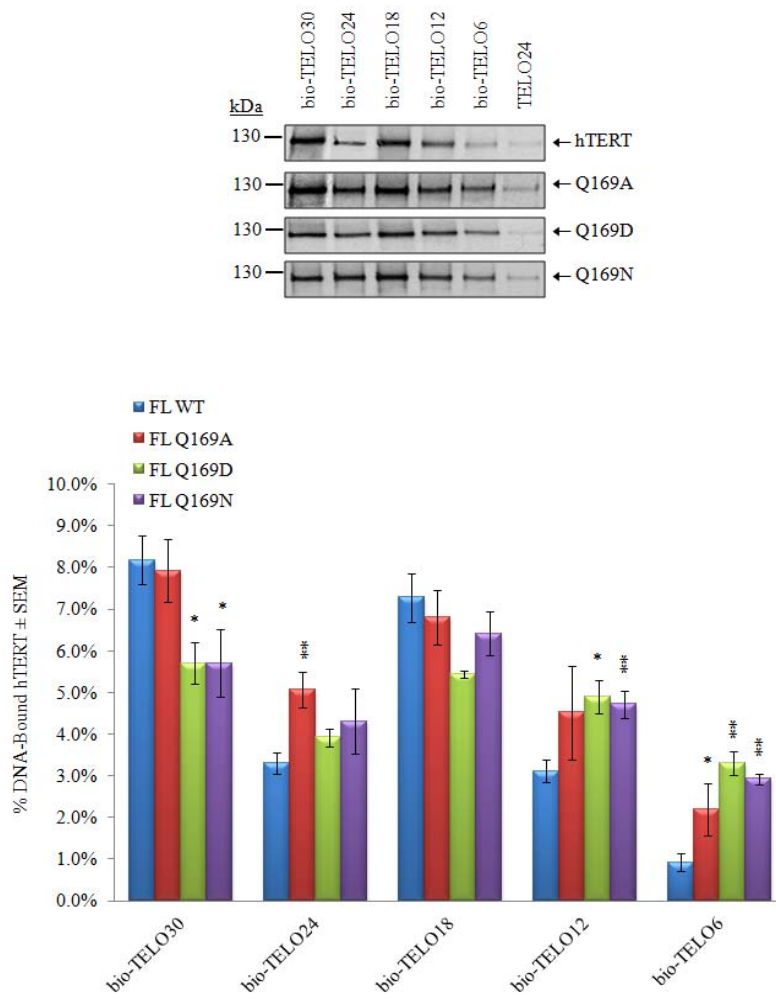


**Figure 4.12: hTERT WT and Q169 mutants physically interact with telomeric ssDNA.**

**Figure 4.12: hTERT WT and Q169 mutants physically interact with telomeric ssDNA.**

*Top*, Comparable counts of [<sup>35</sup>S]cysteine-labelled hTERT (Figure 4.5) were tested for physical interaction with biotinylated ssDNA primers containing different lengths of human telomeric DNA. A description of the oligonucleotides can be found in Table 4.2. hTERT-ssDNA complexes were immobilized on neutravidin beads, purified, separated by 8 % SDS-PAGE and visualized with autoradiography and phosphorimaging.

*Bottom*, Quantification and statistical analysis of at least three independent experiments is shown in graphical format. Results are reported as the mean % DNA-bound hTERT ± SEM. Asterisks denote levels of statistical significance compared to the interaction between hTERT WT and the corresponding primer, as determined using Student's two-tailed unpaired T-tests; p < 0.05 (\*) and p < 0.01 (\*\*).

The data shown in Figure 4.12 indicates that the Q169 mutants retained sequence-specific ssDNA-binding activity *in vitro*. When compared with hTERT WT, however, the Q169 mutants exhibited differences in their interactions with specific lengths of human telomeric DNA (Figure 4.12). The relative strength of the interaction between short telomeric primers (bio-TELO12 and bio-TELO6) and the Q169 mutants was greater than that observed for hTERT WT. This was also observed between hTERT Q169A and bio-TELO24, and may reflect tighter binding of the primers to the Q169 mutants ( $p < 0.01$ ). In contrast, the relative strength of the interaction between hTERT Q169D or Q169N and bio-TELO30, the longest primer tested, was significantly reduced ( $p < 0.05$ ).

We next tested the Q169 mutants for interactions with non-human telomeric or random ssDNA to determine whether Q169 was important for the sequence-specificity of hTERT (Table 4.2). As shown in Figures 4.12 and 4.13, hTERT Q169A, Q169D, and Q169N demonstrated sequence-specific ssDNA-binding activity that was indistinguishable from hTERT WT. The interactions between Q169 mutants and primers comprised of either 18 nt (bio-antiTELO18) or 24 nt (bio-pBR and bio-BBP) of non-telomeric DNA were not statistically different from those observed with hTERT WT ( $p > 0.05$ ). When tested with primers representing the telomeres of other organisms, hTERT WT and Q169 mutants interacted very efficiently with a primer containing 18 nt of *T. thermophila* telomeric DNA (bio-Tetrahymena) and much less efficiently with a primer containing 15 nt of *S. cerevisiae* telomeric DNA (bio-Yeast) (Figure 4.13). The interaction with bio-Tetrahymena is consistent with the ability of wild type human telomerase to elongate primers containing this G-rich sequence (TTGGGG) [272].

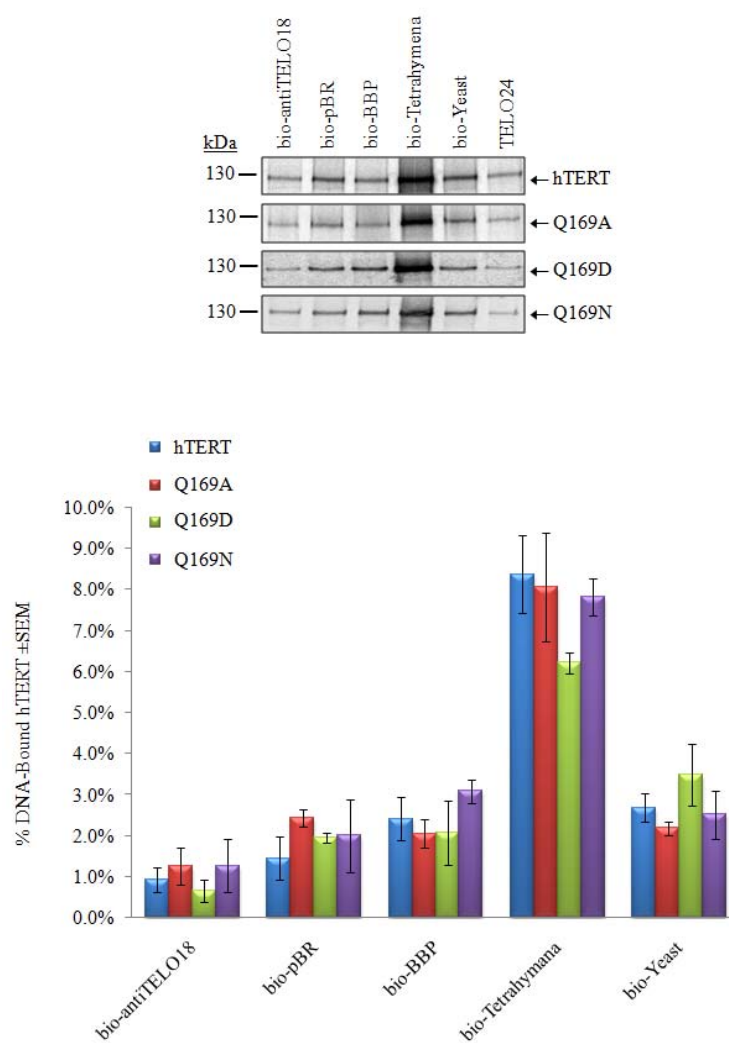


**Figure 4.13: hTERT Q169 mutants do not exhibit altered sequence-specific ssDNA-binding activity *in vitro*.**

**Figure 4.13: hTERT Q169 mutants do not exhibit altered sequence-specific ssDNA-binding activity *in vitro*.**

*Top*, Comparable counts of [<sup>35</sup>S]cysteine-labelled hTERT (Figure 4.5) were tested for physical interaction with biotinylated ssDNA primers containing non-human telomeric or random DNA. A description of the oligonucleotides can be found in Table 4.2. hTERT-ssDNA complexes were immobilized on neutravidin beads, purified, separated by 8 % SDS-PAGE and visualized with autoradiography and phosphorimaging (top panel).

*Bottom*, Quantification and statistical analysis of at least three independent experiments is shown in graphical format. Results are reported as the mean % DNA-bound hTERT ± SEM. No statistically significant differences were detected between WT hTERT and the Q169 mutants, as determined by Student's two-tailed unpaired T-tests.

#### ***4.3.4 The hTERT TEN domain does not stably associate with ss telomeric DNA in vitro***

It has been previously shown that the *T. thermophila* TEN domain photo-cross-links to telomeric ssDNA and that this interaction is compromised by a Q168A substitution [143]. To address the contribution of the isolated TEN domain to TERT-telomere interactions in human telomerase, we engineered an hTERT construct spanning amino acids 1 to 196 and tested the ability of this fragment to associate with different lengths of human telomeric ssDNA (Table 4.2). However, we could not detect stable interactions between the TEN domain and telomeric DNA that exceeded background levels (Figure 4.14), consistent with previous studies of *T. thermophila* telomerase [286]. These data support a model in which multiple DNA-binding domains within hTERT mediate overall telomere recognition and binding. Furthermore, this finding provides evidence that the hTERT TEN domain alone does not possess significant binding affinity for telomeric ssDNA.

#### ***4.3.5 Q169 mediates the ability of truncated hTERT proteins to interact with ssDNA***

As mentioned above, TERT contains multiple DNA-binding regions that make it difficult to assess how one amino acid might influence DNA binding in the full length protein. Since we were unable to detect stable interactions between the TEN domain and telomeric DNA, the Q169A, Q169D, and Q169N mutations were cloned into an hTERT fragment comprised of residues 1 to 300. We have previously shown that this hTERT variant binds telomeric DNA *in vitro* at levels that are readily apparent above background binding (Figure 3.9 and [158]). As shown in Figure 4.15, the Q169 substitutions reduced the relative strength of the interactions between hTERT 1-300 and short telomeric



**Figure 4.14: The hTERT TEN domain does not interact with human telomeric ssDNA at levels that exceed background binding.**

Approximately equivalent counts of [<sup>35</sup>S]cysteine-labelled hTERT TEN (representative sample included in the first lane on the left) were tested for physical interaction with biotinylated ssDNA primers containing different lengths of human telomeric DNA. A description of the oligonucleotides can be found in Table 4.2. hTERT-ssDNA complexes were immobilized on neutravidin beads, purified, separated by 10 % SDS-PAGE and visualized with autoradiography and phosphorimaging.

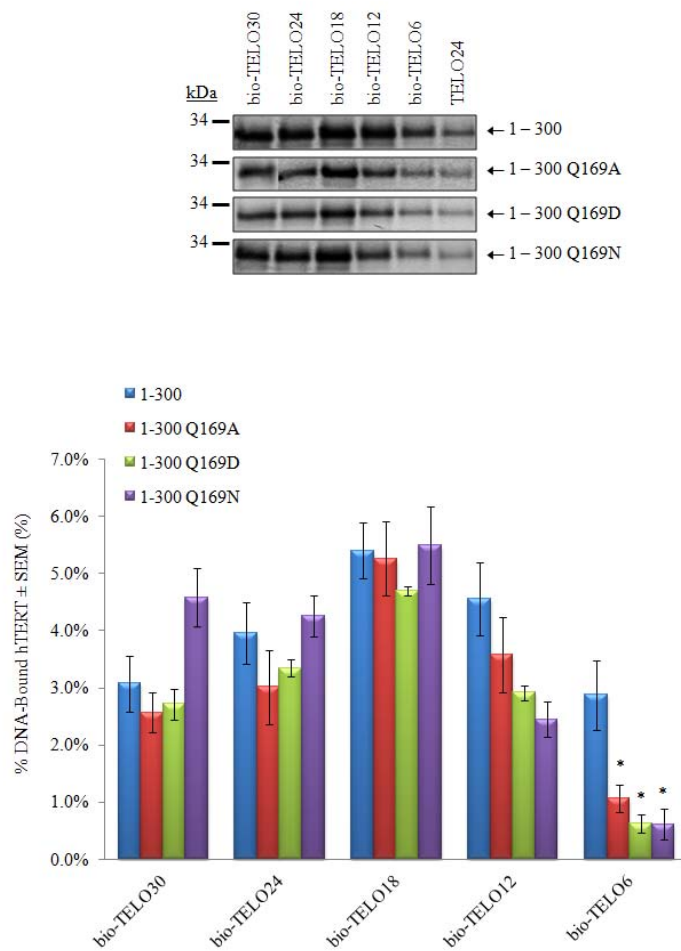


**Figure 4.15: hTERT 1-300 WT and Q169 mutants physically interact with human telomeric ssDNA.**

**Figure 4.15: hTERT 1-300 WT and Q169 mutants physically interact with human telomeric ssDNA.**

*Top*, Approximately equivalent counts of [<sup>35</sup>S]cysteine-labelled hTERT 1-300 were tested for physical interaction with biotinylated ssDNA primers containing different lengths of human telomeric DNA. A description of the oligonucleotides can be found in Table 4.2. hTERT-ssDNA complexes were immobilized on neutravidin beads, purified, separated by 10 % SDS-PAGE and visualized with autoradiography and phosphorimaging.

*Bottom*, Quantification and statistical analysis of at least three independent experiments is shown in graphical format. Results are reported as the mean % DNA-bound hTERT ± SEM. Asterisks denote levels of statistical significance compared to the interaction between hTERT 1-300 WT and the corresponding primer, as determined using Student's two-tailed unpaired T-tests;  $p < 0.05$  (\*).

primers (bio-TELO12 and bio-TELO6). This result provides an interesting contrast to that observed with full length hTERT, where mutation of Q169 increased the apparent strength of the interaction between bio-TELO12 and bio-TELO6 (Figure 4.12). In addition, the hTERT 1-300 Q169 mutants showed a marked decrease in the interaction with ss primers comprised of yeast telomere (bio-Yeast) or random (bio-pBR and bio-BBP) sequences (Figure 4.16). The relatively strong interaction between hTERT 1-300 fragments and bio-Tetrahymena can be explained by the sequence similarity between *T. thermophila* telomeres (TTGGGG) and human telomeres (TTAGGG). Taken together, the data in Figures 4.15 and 4.16 indicate that Q169 is involved in the ssDNA-binding activity of the hTERT N-terminus and thus, contributes to anchor site interactions in human telomerase.

#### ***4.3.6 Q169 mediates the cellular functions of human telomerase***

The preceding experiments demonstrated that hTERT Q169 was required for human telomerase activity *in vitro*. To extend these studies, we next determined if Q169 mediates the biological activity of telomerase in human cells. hTERT Q169A was stably expressed in telomerase positive (SV40 large T-antigen transformed human embryonic kidney cells; 293T) and telomerase negative (human foreskin fibroblasts; BJ) cells. Q169A was chosen as a representative mutant for these experiments since this substitution was the least detrimental to telomerase activity *in vitro* (Figure 4.2). Polyclonal cell populations were analyzed at various mean population doublings (mpd) for hTERT protein expression, telomerase activity, and telomere length maintenance with

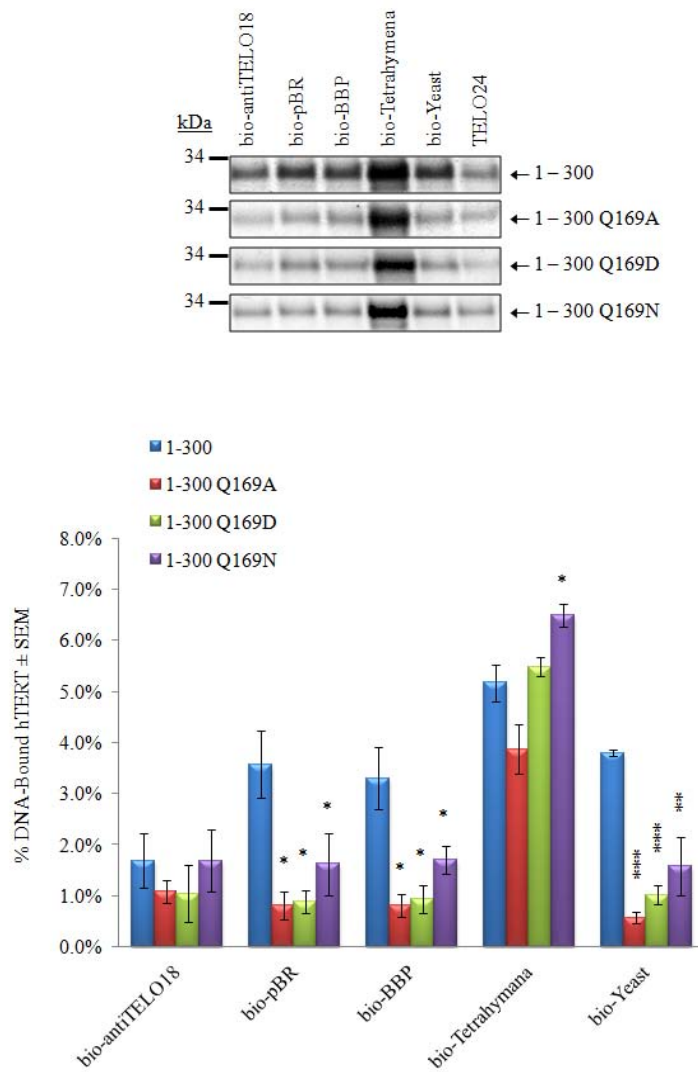


**Figure 4.16: hTERT 1-300 Q169 mutants exhibit reduced primer binding with certain ssDNA primers *in vitro*.**

**Figure 4.16: hTERT 1-300 Q169 mutants exhibit reduced primer binding with certain ssDNA primers *in vitro*.**

*Top*, Approximately equivalent counts of [<sup>35</sup>S]cysteine-labelled hTERT 1-300 were tested for physical interaction with biotinylated ssDNA primers containing non-human telomeric or random DNA. A description of the oligonucleotides can be found in Table 4.2. hTERT-ssDNA complexes were immobilized on neutravidin beads, purified, separated by 10 % SDS-PAGE and visualized with autoradiography and phosphorimaging.

*Bottom*, Quantification and statistical analysis of at least three independent experiments is shown in graphical format. Results are reported as the mean % DNA-bound hTERT ± SEM. Asterisks denote levels of statistical significance compared to the interaction between hTERT 1-300 WT and the corresponding primer, as determined using Student's two-tailed unpaired T-tests; p < 0.05 (\*), p < 0.01 (\*\*), and p < 0.001 (\*\*\*).

cell proliferation. Cells stably expressing hTERT served as the positive control and cultures expressing the vector only served as the negative control for these experiments.

We first investigated the cellular function of hTERT Q169A in 293T cells. Figure 4.17 shows that anti-FLAG-immunoprecipitated hTERT WT exhibited robust TRAP activity at various stages during culture whereas the Q169A mutant was consistently inactive. The loss of telomerase activity was not due to abrogated protein expression (Figure 4.17) or nuclear exclusion (Figure 4.18). As expected, telomere elongation was observed in 293T cells expressing hTERT WT but not in cultures expressing the catalytically inactive Q169A mutant (Figure 4.19 and Table 4.3). As mentioned above, 293T cells contain functional endogenous telomerase. This allowed us to investigate whether hTERT Q169A inhibited the action of endogenous telomerase at telomeres. Bulk telomere length in cells stably expressing hTERT Q169A was indistinguishable from that of vector-only control cells (Figure 4.19 and Table 4.3), indicating that hTERT Q169A does not function as a dominant negative protein *in vivo*.

The cellular function of hTERT Q169A was also investigated in normal diploid fibroblasts (BJ cells). Telomerase negative BJ cells provided a strong cellular contrast to the telomerase positive 293T cells and thus, provided a control for cell line-dependent phenotypes. Expression of hTERT WT, but not Q169A, conferred BJ cells with telomerase activity (Figure 4.20). The lack of telomerase activity in immunoprecipitates containing hTERT Q169A was not due to abrogated protein expression (Figure 4.20). Furthermore, stable expression of hTERT WT induced telomere elongation with cell proliferation during early passages and telomere length maintenance during later passages (Figure 4.21 and Table 4.4). These cells completed approximately three times more mean

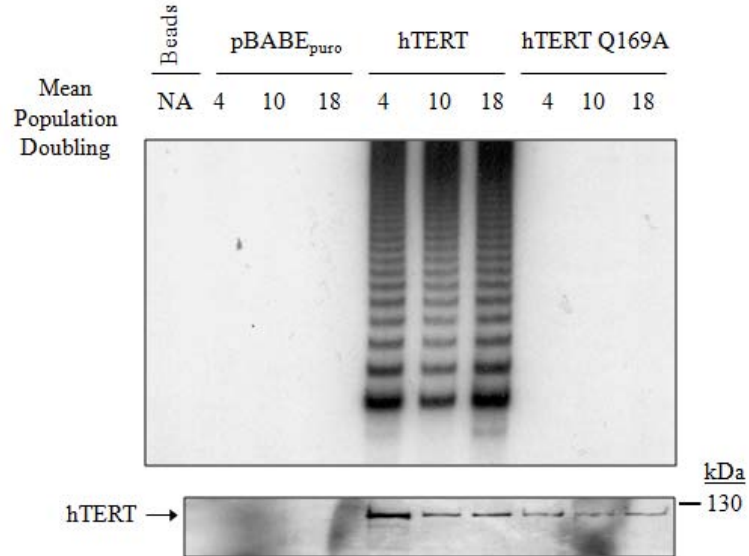


**Figure 4.17: hTERT Q169 is required for telomerase activity in transformed human cells.**

Extracts from telomerase positive 293T cells that stably expressed either pBABE<sub>puro</sub>, pBABE<sub>puro</sub>-FLAG-hTERT, or pBABE<sub>puro</sub>-FLAG-hTERT Q169A were immunoprecipitated with anti-FLAG antibodies. FLAG-hTERT was eluted from the beads by competition with excess FLAG peptide and the following experiments were performed:

*Top*, 2  $\mu$ L of eluate was tested for telomerase activity by the telomere repeat amplification protocol. Not applicable (NA).

*Bottom*, 35  $\mu$ L of eluate was examined for hTERT protein expression by Western blotting with anti-hTERT antibodies.

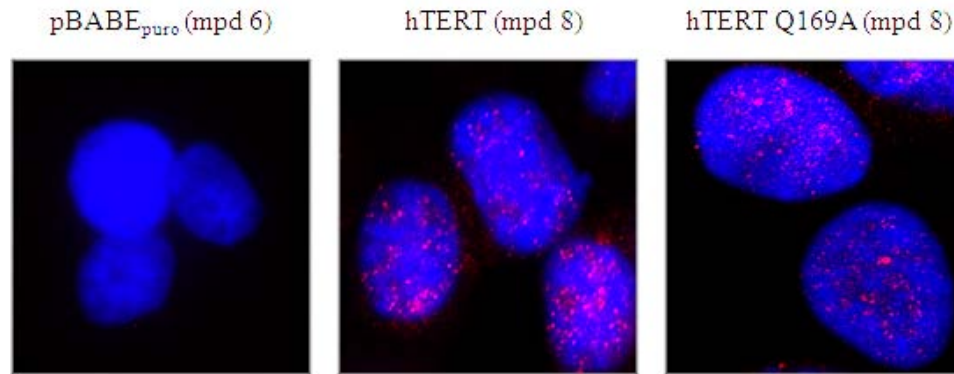


**Figure 4.18: hTERT Q169A is not excluded from the nucleus in human cells.**

Indirect immunofluorescence was used to investigate the cellular localization of hTERT and hTERT Q169A in telomerase positive 293T cells (mean population doubling [mpd] indicated in parentheses). These experiments were performed using anti-FLAG antibodies that recognize the FLAG epitope on the hTERT N-terminus and TRITC-conjugated goat anti-rabbit IgG secondary antibodies (red). Nuclei were counterstained with DAPI (blue).

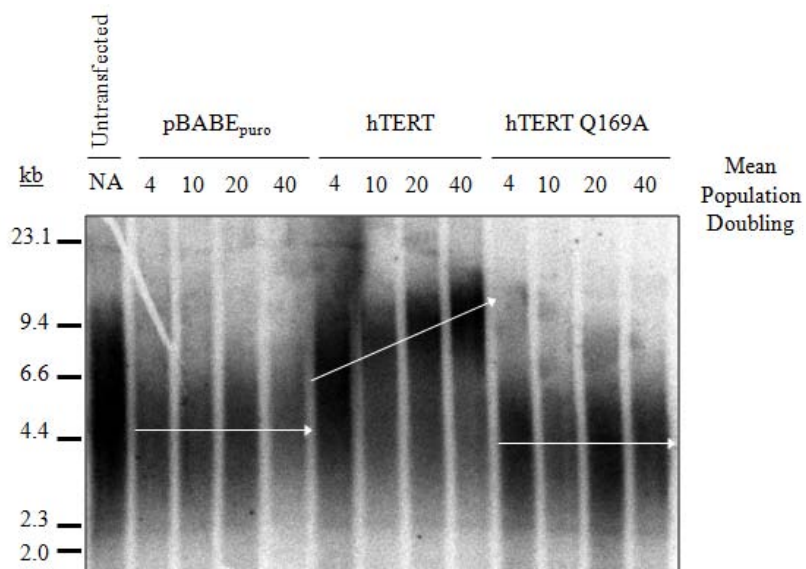


**Figure 4.19: hTERT Q169 is required for telomere elongation in transformed human embryonic kidney cells.**

Telomerase positive 293T cells that stably expressed pBABE<sub>puro</sub>, pBABE<sub>puro</sub>-FLAG-hTERT, or pBABE<sub>puro</sub>-FLAG-hTERT Q169A were tested with the terminal restriction fragment analysis to measure bulk telomere length. Arrows are included for visual clarification and represent the approximate mean bulk telomere length of each sample. Untransfected 293T cells are included as an additional control for these experiments. Not applicable (NA). The quantification of these results is shown in Table 4.3.

**Table 4.3: Effect of hTERT Q169A on bulk telomere length in 293T transformed human embryonic kidney cells.**

Mean Population Doubling	Mean Telomere Length (kb) $\pm$ SEM			
	pBABE <sub>puro</sub>	hTERT	hTERT Q169A	Untransfected 293Ts
<b>4</b>	4.5 $\pm$ 0.12	8.0 $\pm$ 0.14	4.8 $\pm$ 0.29	NA
<b>10</b>	4.6 $\pm$ 0.19	10.0 $\pm$ 0.34	4.8 $\pm$ 0.36	NA
<b>20</b>	4.8 $\pm$ 0.03	10.7 $\pm$ 0.00	4.8 $\pm$ 0.38	NA
<b>40</b>	4.9 $\pm$ 0.03	11.8 $\pm$ 0.38	5.0 $\pm$ 0.49	NA
<b>NA</b>	NA	NA	NA	5.1 $\pm$ 0.04

The terminal restriction fragment analysis was used to measure telomere length at various mean population doublings (Figure 4.19). Results are reported as the mean telomere length  $\pm$  SEM from at least three independent experiments. Untransfected 293T cells are included as additional controls for these experiments and the mean telomere length  $\pm$  SEM was calculated from four independent experiments. Not applicable (NA).

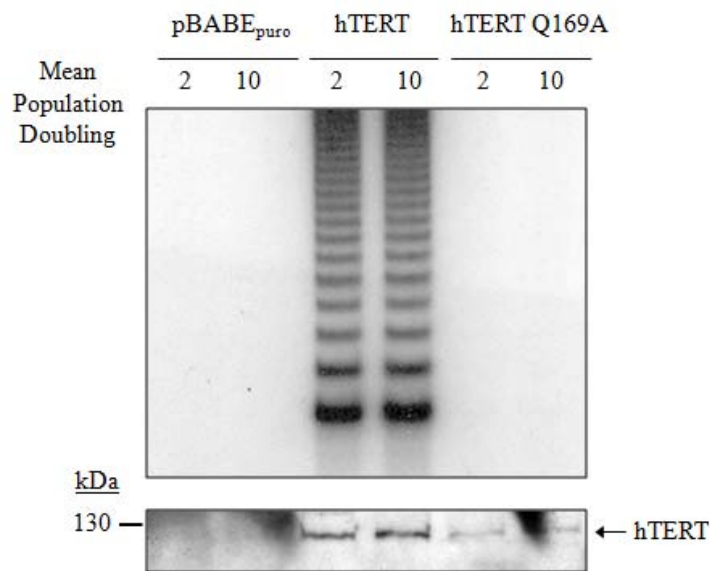


**Figure 4.20: hTERT Q169 is required for telomerase activity in primary human fibroblasts.**

Extracts from telomerase negative BJ cells that stably expressed pBABE<sub>puro</sub>, pBABE<sub>puro</sub>-FLAG-hTERT, or pBABE<sub>puro</sub>-FLAG-hTERT Q169A were immunoprecipitated with anti-FLAG antibodies. FLAG-hTERT was eluted from the beads by competition with excess FLAG peptide and tested as follows:

*Top*, 2  $\mu$ L of eluate was tested for telomerase activity by the telomere repeat amplification protocol.

*Bottom*, 35  $\mu$ L of eluate was examined for hTERT protein expression by Western blotting with anti-hTERT antibodies.

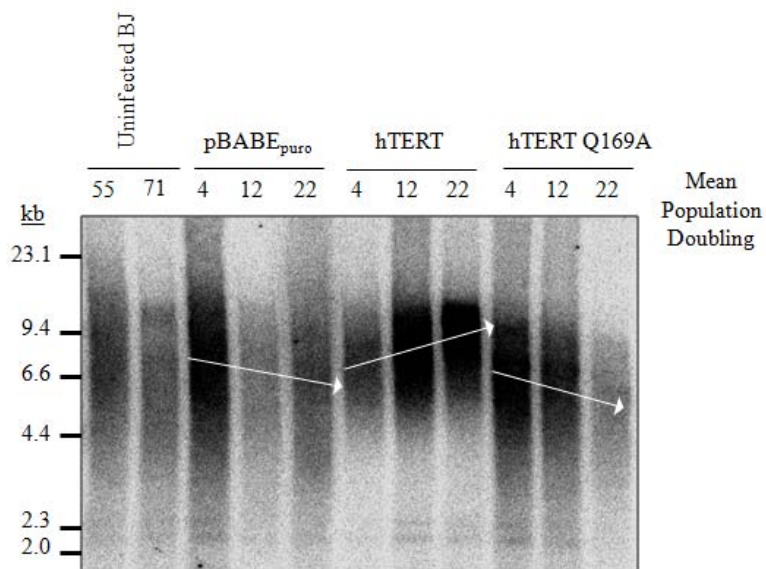


**Figure 4.21: hTERT Q169 is required for telomere length maintenance in primary human fibroblasts.**

Telomerase negative BJ cells that stably expressed pBABE<sub>puro</sub>, pBABE<sub>puro</sub>-FLAG-hTERT, or pBABE<sub>puro</sub>-FLAG-hTERT Q169A were tested in the terminal restriction fragment analysis to measure bulk telomere length. Arrows are included for visual clarification and represent the approximate mean bulk telomere length of each sample. Uninfected BJ cells at mean population doublings 55 and 71 correspond to the infected cultures at mean population doublings 4 and 22, respectively. The quantification of these results is shown in Table 4.4.

**Table 4.4: Effect of hTERT Q169A on bulk telomere length in BJ fibroblasts.**

Mean Population Doubling	Mean Telomere Length (kb) $\pm$ SEM			
	Uninfected BJs	pBABE <sub>puro</sub>	hTERT	hTERT Q169A
<b>4</b>	NA	8.7 $\pm$ 0.18	8.5 $\pm$ 0.10	7.5 $\pm$ 0.30
<b>12</b>	NA	8.0 $\pm$ 0.11	9.2 $\pm$ 0.13	6.8 $\pm$ 0.22
<b>22</b>	NA	7.5 $\pm$ 0.13	11.3 $\pm$ 0.09	6.2 $\pm$ 0.30
<b>55</b>	8.6 $\pm$ 0.27	NA	NA	NA
<b>71</b>	7.3 $\pm$ 0.15	NA	NA	NA

The terminal restriction fragment analysis was used to measure telomere length at early, mid, and late mean population doublings (Figure 4.21). Results are reported as the mean telomere length  $\pm$  SEM from four independent experiments. Uninfected BJ cells at mean population doublings 55 and 71 correspond to the infected cultures at mean population doublings 4 and 22, respectively. Not applicable (NA).

population doublings (mpd) than the vector-only control cells and did not exhibit senescence-associated  $\beta$ -galactosidase activity (Figures 4.22 and 4.23, respectively) [298]. BJ cells expressing hTERT Q169A exhibited defects in telomere length maintenance, exhausted their replicative potential after 25 mpd, and did not surmount replicative senescence (Figures 4.21, 4.22, and 4.23). Thus, mutation of hTERT Q169 inhibited human telomerase function in living cells.

#### **4.4 Discussion**

##### ***4.4.1 hTERT Q169 is needed to reconstitute robust human telomerase activity in vitro***

Important questions in telomerase biochemistry pertain to the mechanisms by which the enzyme recognizes and orientates telomeric ssDNA in the active site and catalyzes processive telomere synthesis. A long-standing notion is that telomerase has two modes of primer recognition: initial recognition of a telomere sequence and/or structure at the DNA 5'-end and subsequent identification of the 3'-terminus to prime the addition of telomeric nt [129]. Template-independent enzyme-DNA interactions are known as anchor site interactions and a subset of these are believed to confer telomerase with the property of RAP. After synthesizing a complete telomeric repeat, Watson-Crick base pairs between the DNA 3'-end and RNA template are melted so that the nascent DNA 3'-end can be repositioned with the template for the next round of telomere synthesis. During this dynamic process, the telomerase anchor site(s) remains associated with upstream nt and prevents the enzyme from dissociating from the ssDNA primer.

The crystal structure of the *T. thermophila* TEN domain revealed a ssDNA-binding groove on the surface that contained several phylogenetically-conserved residues,

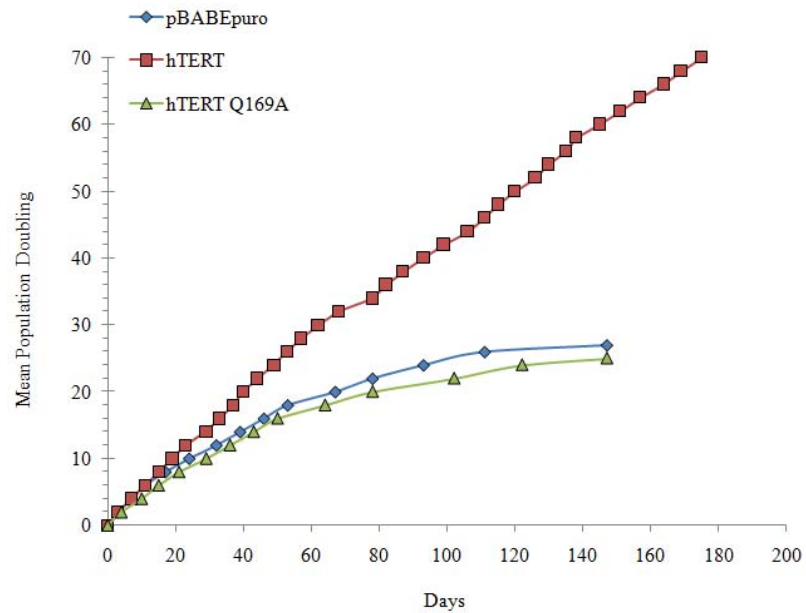


**Figure 4.22: Q169 is required for the biological activities of hTERT in primary human cells.**

Growth curves were used to monitor the proliferative potential of BJ cells that stably expressed pBABEpuro, pBABEpuro-FLAG-hTERT, or pBABEpuro-FLAG-hTERT Q169A. BJ cells that stably expressed hTERT Q169A ceased proliferation at approximately the same time point as the vector-only expressing cells (approximately 25 mean population doublings post-retroviral infection). In contrast, stable expression of hTERT WT significantly prolonged the proliferative lifespan of BJ cells.

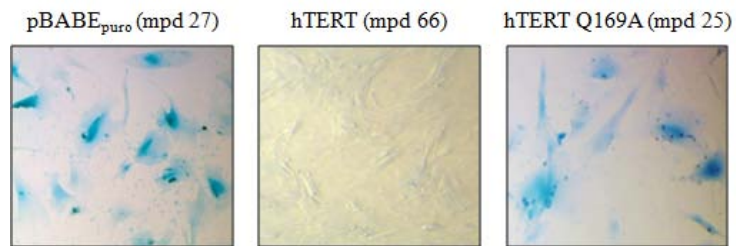


**Figure 4.23: Primary human cells expressing hTERT Q169A enter replicative senescence.**

BJ cells that stably expressed pBABE<sub>puro</sub>, pBABE<sub>puro</sub>-FLAG-hTERT, or pBABE<sub>puro</sub>-FLAG hTERT Q169A were tested for  $\beta$ -galactosidase activity at pH 6.0. The mean population doubling (mpd) of each culture is indicated in parentheses. Representative BJ cells that stably expressed the empty vector or FLAG-hTERT Q169A exhibited blue staining that coincided with the cessation of proliferation (Figure 4.23). These cells also exhibited the morphological changes associated with replicative senescence, including an increased cell size and irregular and flat shape. In contrast, cells stably expressing FLAG-hTERT WT stained negative for  $\beta$ -galactosidase activity (pH 6.0).

including the Gln residue investigated here [143,289]. Alanine mutagenesis of tTERT Q168 significantly impaired telomerase activity without affecting RAP and identified an important role for this residue in ciliate telomerase anchor site interactions [143,289]. The corresponding mutation in Est2p caused a dramatic loss of yeast telomerase activity *in vivo* [278,290]. Here, we show for the first time that human telomerase reconstituted with hTERT Q169A, Q169D, or Q169N exhibited severe defects in DNA polymerization *in vitro* and *in vivo*, indicating that the invariant Gln residue has an evolutionarily-conserved role in telomerase function. Our study provides novel insight into the role of this residue by revealing its importance for the ability of telomerase to incorporate nucleotides at the second position of the RNA template. The loss of telomerase activity *in vivo* was not due to nuclear exclusion or abrogated protein expression, although protein levels were reduced compared to hTERT WT. Similarly, yeast strains expressing endogenous Est2p Q146A exhibited a reduction in Est2p protein levels, telomere attrition, and severe growth defects [141,278,290]. Thus, it appears that living cells do not tolerate high expression of TERT proteins harboring mutations of the invariant Gln residue.

In the absence of crystallographic data of hTERT, we can only speculate on the mechanism underlying the severity of the Q169D and Q169N mutations in relation to Q169A. As mentioned previously, the non-conservative Q169D substitution could cause electrostatic repulsion between the polyanionic DNA backbone and electronegative carboxylic acid side-chain. Our observation that the conservative Q169N does not rescue the catalytic phenotype indicates that both the length and the hydrogen-bonding potential of the side chain at position 169 are critical for the activity of human telomerase. The finding that hTERT Q169A reconstitutes weak telomerase activity is likely due to the fact

that this is a neutral amino acid substitution. Although both Ala and Asn potentially eliminate important hydrogen-bonding interactions that would be normally fulfilled by Gln, the Q169N substitution is more detrimental to activity. One interpretation of this data is that the Asn substitution also introduces an unfavorable interaction whereby the shorter side chain prevents the amide group from satisfying its hydrogen-bonding potential.

Finally, we note that this residue appears to have evolved some species-specific functions. Alanine substitution of the corresponding residue in Est2p significantly impaired RAP *in vitro* [278]. One intriguing explanation for these differences might be that telomerase uses different mechanisms to interact with different sequences of telomeric DNA. It is conceivable that ciliate and human telomerase use similar mechanisms to bind and synthesize telomeric DNA because of the high degree of telomere sequence similarity (TTGGGG and TTAGGG, respectively). In contrast, yeast telomeres are degenerate (*e.g.* G<sub>2-3</sub>(TG)<sub>1-6</sub> in *S. cerevisiae*) [20] and different molecular mechanisms might be used for telomere length maintenance in this organism.

#### ***4.4.2 Q169 mediates conformational flexibility of the hTERT N-terminus***

Telomerase is thought to contain template-distal and template-proximal anchor sites [129]. It has been speculated that a conformational change in the template-proximal anchor site is required for telomerase to transition into an elongation-competent complex [129]. Structure-function studies with *T. thermophila* telomerase suggested that the ssDNA-binding groove on the surface of the TEN domain formed part of a template-proximal anchor site [143,289]. Photo-cross-linking studies with tTERT and short

telomeric ssDNA suggested that the TEN domain was displaced relative to the catalytic site during telomere synthesis [143,289]. It was proposed that this movement was needed to reposition the template-proximal anchor site relative to the active site and correctly orientate the DNA primer or DNA-RNA heteroduplex in the active site during primer elongation [143,289].

In this work, we investigated the structural significance of hTERT Q169 directly by using limited proteolysis to monitor the conformational flexibility of mutant proteins. Importantly, our results indicated that the overall conformation of hTERT Q169A, Q169D, and Q169N was intact. However, the NTE of the Q169 mutants was more sensitive to chymotrypsin proteolysis than hTERT WT. This is interpreted as evidence that Q169 is important for the conformation of the hTERT N-terminus. We believe that a small fraction of the mutant proteins attained WT conformation because there was not a complete loss of the 20 kDa fragments. It is possible that these Q169 mutants are catalytically competent and thus, are responsible for the low levels of processive telomerase activity we observe *in vitro* (see below).

#### ***4.4.3 hTERT Q169 mutants physically interact with hTR***

TERT contains an essential and universally-conserved telomerase RNA-binding domain (TRBD) that makes extensive contacts with TR and represents the major TR-binding domain [144,208]. It seemed unlikely that substitution of hTERT Q169 would disrupt hTERT-hTR interactions since this residue is not located in the TRBD. We confirmed here that hTERT Q169 is not involved in critical hTERT-hTR interactions. However, we cannot rule out the possibility that Q169 substitution causes small changes

in hTR-binding that are masked in the context of the full length protein. Similarly, Q169 could regulate conformational changes in hTR or the RNP complex that are required for telomerase activity.

#### ***4.4.4 Q169 mediates ssDNA-binding activity in hTERT***

We showed here for the first time that hTERT proteins containing Q169A, Q169D, or Q169N mutations retained telomere sequence-specific ssDNA-binding activity *in vitro*. However, when compared to hTERT WT, the Q169 mutants exhibited subtle differences in the relative strength of the interactions with telomeric ssDNA. In parallel, we investigated the DNA-binding properties of hTERT 1-300 variants containing the Q169 substitutions. hTERT 1-300 Q169A, Q169D, and Q169N also retained telomeric ssDNA-binding activity and demonstrated subtle differences in the relative strength of protein-DNA interactions when compared to 1-300 WT. Although the presence of multiple DNA-binding sites in TERT complicates the interpretation of these data [158,286], our studies clearly indicate that Q169 is involved in protein-telomeric DNA interactions, thereby identifying a novel residue in hTERT that regulates ssDNA-binding activity. Future studies are required to determine if Q169 substitution has a direct or indirect effect on DNA-binding.

Interestingly, the hTERT Q169 mutations cause an increase in the relative strength of the interaction between the full length protein and short telomeric ssDNA primers whereas the mutations decrease the interactions between hTERT 1-300 and these ssDNA primers. We have previously identified multiple DNA-binding regions throughout the hTERT protein, including the N-terminus, RT domain, and C-terminus

[158]. Similar results have now been reported for ciliate TERT [286]. Importantly, the DNA-binding regions appear to co-operate during telomeric ssDNA-binding *in vitro* and establish a dynamic 'DNA-binding equilibrium' in which the primer can interact with any or all of the DNA-binding domains [158,286]. Our primer binding studies indicate that the Q169 mutations have disrupted an important DNA-binding domain in the hTERT N-terminus thereby favouring an interaction with the remaining DNA-binding domains. Our observation that short ssDNA primers interact with the full length Q169 mutants to a greater extent than wild type hTERT implies that in the context of full length hTERT, Q169 negatively regulates the overall strength of the interaction with short telomeric primers. The apparent decrease in the strength of the interaction between bio-TELO30 and hTERT Q169D and Q169N, however, implies that Q169 may also be required to stabilize interactions with longer stretches of telomeric ssDNA. In contrast to full length hTERT, mutation of Q169 decreases the interaction between short telomeric primers and hTERT 1-300. One explanation for this decrease is that the 1-300 mutants lack many of the previously identified DNA-binding regions in hTERT. Thus, Q169 has an important role in stabilizing the interactions that occur between the hTERT N-terminus and short telomeric ssDNA primers *in vitro*. Importantly, we have previously shown that the hTERT 1-300 fragment has a strong non-sequence-specific ssDNA-binding activity *in vitro* [158]. We interpreted this to mean that the hTERT N-terminus contains a strong ssDNA-binding activity but regions beyond the N-terminus are important for TTAGGG-specific ssDNA-binding. We show here that substitution of Q169 in the context of hTERT 1-300 causes a significant decrease in the ability of this fragment to bind ssDNA primers comprised of random or yeast telomeric ssDNA. This identifies a previously

unrecognized role for Q169 in stabilizing the interactions between the hTERT NTE and ssDNA primers that lack the human telomeric sequence, providing further evidence that the first 300 amino acids of hTERT have little sequence-specificity for telomeric DNA [158]. Our data support previous studies that identified a potential role for Q168 in mediating ciliate telomerase's affinity for telomeric ssDNA [143,289]. Collectively, these studies indicate that the Gln residue has an evolutionarily-conserved role in regulating TERT-telomeric ssDNA interactions (*i.e.* anchor site interactions).

#### ***4.4.5 Conceptual model to describe the catalytic phenotype of hTERT Q169 mutants***

Recently, Zaug *et al.* proposed a model for telomerase activity in which the catalytic cycle is regulated by a series of conformational changes [279]. It was suggested that telomerase initiates DNA synthesis when the TEN domain is in close proximity to the remainder of the RNP ('closed state') (Figure 1.13, top cartoons). This conformation is regulated by an intramolecular protein-protein interaction between the TEN domain and an as yet unidentified residue [279]. Once the first round of telomere synthesis is completed, this interaction is broken and the TEN domain is displaced relative to the catalytic site, which relaxes the RNP into an 'open state' (Figure 1.13, translocation step). Displacement of the TEN domain repositions the template-proximal anchor site and template region and restores base-pairing between the DNA 3'-end and template 5'-end. It is thought that the DNA 5'-end slides through the ssDNA-binding groove on the TEN domain, which signals the RNP to return to the closed state for the next round of telomere synthesis (Figure 1.13, bottom left cartoon). This model invokes conformation changes within telomerase that are similar to those described for bacterial and eukaryotic RNA

polymerases during the transition from transcription initiation to elongation (reviewed in [349,350]). For example, the initial loading of promoter DNA onto RNA polymerase II triggers a series of structural changes that includes the closure of an evolutionarily-conserved ‘clamp’ over the template and transcript. Clamp closure converts the enzyme from an open to a closed state that is required for transcription elongation. It is intriguing to speculate that the TEN domain could be involved in processes that are similar to the RNA polymerase clamp structure.

We interpret the increased protease-sensitivity of full length and 1-300 hTERT Q169 mutants as evidence that the N-terminus adopts a conformation that is more accessible to chymotrypsin than WT hTERT (*i.e.* greater conformational flexibility). We speculate that the mutants cannot easily convert between open and closed states, which alters critical telomerase-DNA interactions and causes severe catalytic defects *in vitro* and *in vivo*. This conformational change seems particularly important for the ability of human telomerase to incorporate nucleotides at the second position of the hTR template. We suggest that the minimal activity observed with Q169 mutants *in vitro* stems from a small population of enzymes that correctly orientate the DNA primer and/or DNA-RNA hybrid in the catalytic site to initiate DNA synthesis. It is possible that a small fraction of mutant proteins fold into the WT conformation and initiate telomere synthesis. According to the model proposed by Zaug *et al.*, Q169 is not directly involved in RAP [279], which is consistent with our observation that hTERT Q169A demonstrates normal RAP. We propose that the mechanism by which Q169 regulates telomerase activity involves conformational changes that promote optimal enzyme-primer-substrate interactions and

facilitate the efficient incorporation of nucleotides during the first round of telomere synthesis.

#### ***4.4.6 Perspectives***

In summary, we show that Q169 is a functionally critical residue in human telomerase and provide the first detailed evidence regarding the biochemical and cellular significance of this evolutionarily-conserved Gln residue in higher eukaryotes. The intimate relationship between telomerase and human disease underscores the importance for structure-function studies that elucidate regions in hTERT that could be amenable to therapeutic intervention. Our studies are necessary, but not sufficient, for a complete understanding of how the TEN domain contributes to telomerase structure, activity, and telomere length maintenance in higher eukaryotes.

## Chapter Five: *In vitro* analysis of naturally-occurring hTERT mutants

### 5.1 Preface

Mutations in the human *TRT* gene have been identified in patients with dyskeratosis congenita (DC) (Figure 5.1). Dyskeratosis congenita is a multifaceted disorder that has several disease variants, including idiopathic pulmonary fibrosis (IPF) [320]. The common link between these diseases is telomere length: patients have telomeres that are significantly shorter than age-matched controls [338]. This observation implies that the underlying disease mechanism is telomerase deficiency. However, a detailed description of how these mutations affect telomerase structure and function is still lacking. To this end, I engineered several of the naturally-occurring hTERT mutants and tested the mutant proteins for the ability to bind telomeric ssDNA and reconstitute human telomerase activity *in vitro*. This work forms provides a platform for future studies to examine further the biochemical and cellular consequence of several disease-associated hTERT variants.

### 5.2 Results

#### 5.2.1 *Characterization of hTERT mutants found in patients with dyskeratosis congenita*

We studied five hTERT variants to gain insight into the mechanism by which *TRT* mutations might contribute to the short telomere phenotype of DC patients: A279T, P721R, K902N, R979W, and F1127L. The locations of these residues are as follows: 1) A279 resides in the N-terminal linker region; 2) P721 and K902 are located in the RT domain; and 3) R979 and F1127 reside in the C-terminal domain (Figure 5.1).

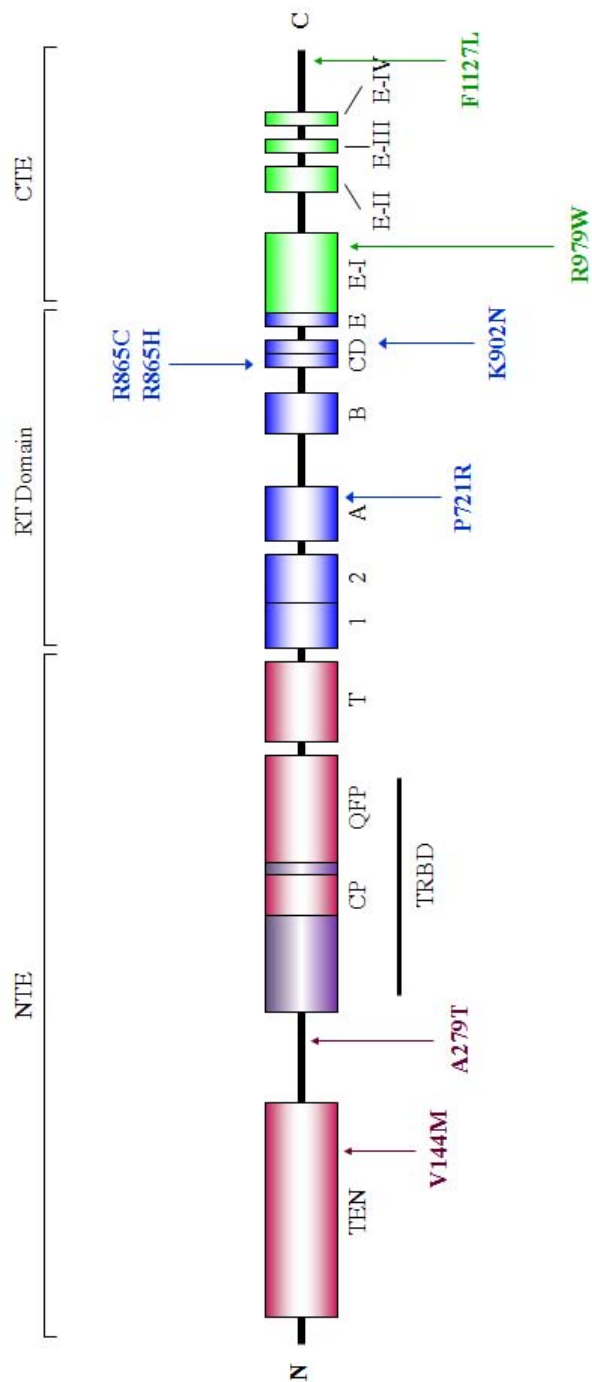


**Figure 5.1: Linear architecture of the human telomerase reverse transcriptase showing the locations of various naturally-occurring mutations.**

**Figure 5.1: Linear architecture of the human telomerase reverse transcriptase showing the locations of various naturally-occurring mutations.**

This figure illustrates the predicted structural organization of the human telomerase reverse transcriptase (hTERT) and the approximate positions of the disease-associated mutations characterized in this study. The hTERT protein encompasses a long N-terminal extension (NTE), a central catalytic reverse transcriptase (RT) domain, and a short C-terminal extension (CTE). Pink boxes are used to indicate the predicted locations of the telomerase essential N-terminal (TEN) domain and the telomerase-specific motifs CP, QFP, and TS. The purple box indicates the telomerase RNA-binding domain (TRBD). An unstructured linker region connects the TEN domain and TRBD. Blue boxes represent the seven evolutionarily-conserved motifs in the RT domain (1, 2, A, B, C, D, E). The CTE contains four blocks of conserved amino acids, which are shown as green boxes (E-I, E-II, E-III, E-IV).

The hTERT A279T mutation has been identified in patients suffering from aplastic anemia (AA), a variant of classical DC [326]. Interestingly, this mutation has also been detected in apparently healthy individuals [326]. The F1127L mutation was identified in a patient demonstrating symptoms associated with Hoyeraal-Hreidarsson (HH) syndrome, another disease variant of classical DC [326].

We first sought to understand how these mutations affect the catalytic activity of telomerase. Human telomerase was reconstituted in RRL with hTR and either hTERT WT, A279T, P721R, K902N, R979W, or F1127L and tested for *in vitro* activity with the TRAP assay. As shown in Figure 5.2, telomerase reconstituted with hTERT P721R, R979W, or F1127L showed nearly wild type levels of TRAP activity, whereas telomerase reconstituted with hTERT A279T exhibited a notable defect in this assay. The hTERT K902N mutation abolished catalytic activity, indicating that that this residue is essential for telomerase function *in vitro* (Figure 5.2). With the exception of the A279T mutation (see discussion), our results corroborate the TRAP activity detected in lysates prepared from VA13 human cells transfected with the hTERT variants [327].

As mentioned previously, the TRAP is a highly sensitive method to detect telomerase activity. However, it does not distinguish between enzymes with catalytic defects and enzymes with defects in repeat addition processivity. Therefore, we used the CTA to gain more insight into the catalytic defects of the DC-associated hTERT mutants. Unexpectedly, hTERT A279T exhibited wild type levels of DNA synthesis and RAP when tested with telomeric ssDNA primers containing 18 nt or 6 nt (Figure 5.3). The quantification of at least three independent experiments is shown in Table 5.1. One interpretation of these data is that the catalytic defect of these mutants is only unveiled in

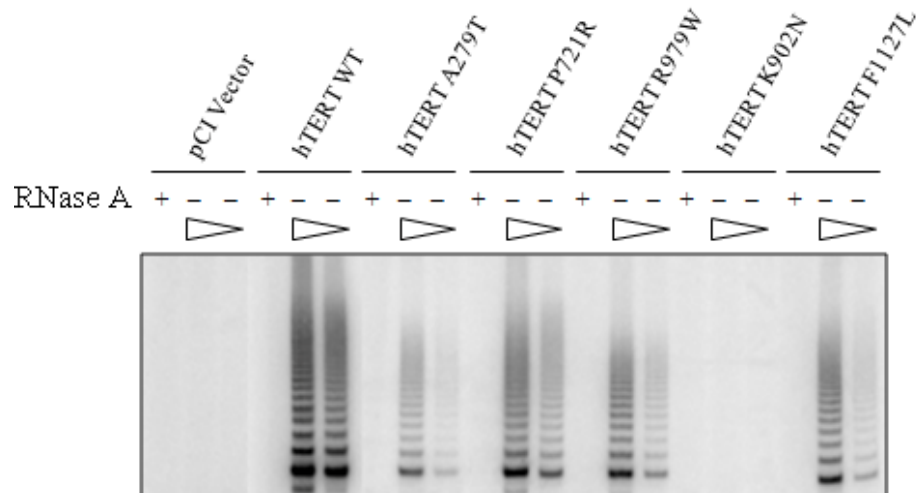


**Figure 5.2: *In vitro* activity of telomerase reconstituted with distinct hTERT mutants identified in DC patients.**

Human telomerase reconstituted in RRL with hTR and plasmid DNA for the pCI vector, hTERT WT, A279T, P721R, R979W, K902N, or F1127L was tested for *in vitro* enzyme activity using the telomere repeat amplification protocol. RRL reconstitution reactions (1  $\mu$ L) were assayed in the presence and absence of 5  $\mu$ g RNase A to show that DNA extension was catalyzed by telomerase and not by polymerases present in the RRL. The triangles represent a five-fold dilution of each reaction to confirm that the activity assays were in the linear range. This experiment was performed four times.

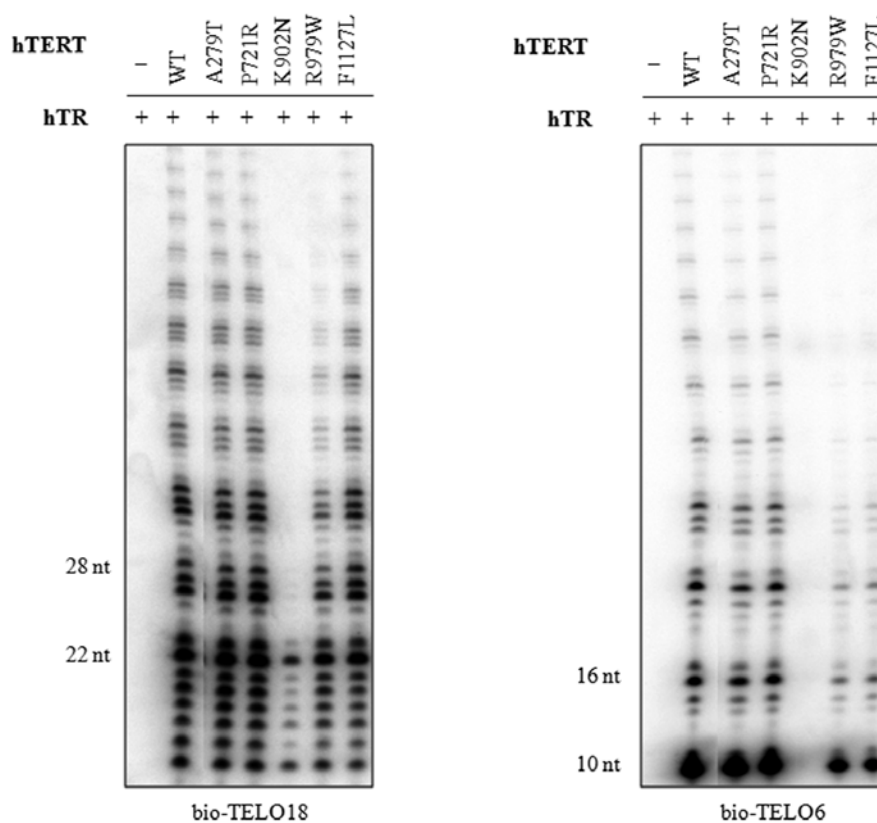


**Figure 5.3: Analysis of the activity and repeat addition processivity of telomerase mutants associated with DC.**

Human telomerase reconstituted in RRL with hTR and hTERT WT, A279T, P721R, K902N, R979W, or F1127L was tested for catalytic activity and repeat addition processivity with an 18 nt telomeric primer, bio-TELO18, and a 6 nt telomeric primer, bio-TELO6. The positions of the 22 nt and 28 nt elongation product are shown at the left of the image and were determined by comparison with the mobility of a 5'-end-radiolabelled 18 nt telomeric primer containing a 3'-biotin molecule (not shown). The quantification and statistical analysis of these data is shown in Table 5.1.

**Table 5.1: Quantification of DNA synthesis and repeat addition processivity observed for telomerase mutants associated with DC.**

<b>hTERT Mutant</b>	<b><u>bio-TELO18</u></b>		<b><u>bio-TELO6</u></b>	
	<b>DNA Synthesis (% WT <math>\pm</math> SEM)</b>	<b>Repeat Addition Processivity (% WT <math>\pm</math> SEM)</b>	<b>DNA Synthesis (% WT <math>\pm</math> SEM)</b>	<b>Repeat Addition Processivity (% WT <math>\pm</math> SEM)</b>
<b>A279T</b>	106 $\pm$ 16	98 $\pm$ 8	95 $\pm$ 5	95 $\pm$ 7
<b>P721R</b>	97 $\pm$ 16	99 $\pm$ 9	116 $\pm$ 5	91 $\pm$ 6
<b>K902N</b>	12 $\pm$ 1 **	ND	ND	ND
<b>R979W</b>	54 $\pm$ 11 *	78 $\pm$ 8	26 $\pm$ 4 *	87 $\pm$ 10
<b>F1127L</b>	44 $\pm$ 2 *	91 $\pm$ 8	23 $\pm$ 2 *	87 $\pm$ 10

DNA synthesis and repeat addition processivity were determined from the data shown in Figure 5.3. Results were calculated from three independent experiments and the mean  $\pm$  SEM is reported relative to the wild type enzyme. DNA synthesis was calculated within the first hexameric repeat and repeat addition processivity was determined within the first five hexameric repeats. Not detected (ND) indicates that the signal was below the detection limit of this assay and the data were not quantified. Asterisks denote the level of statistical significance compared to wild type telomerase, as determined using Student's two-tailed unpaired T-tests;  $p < 0.01$  (\*\*) and  $p < 0.05$  (\*).

the presence of a partially telomeric ssDNA primer, such as that used in the TRAP assay (see discussion). Interestingly, hTERT P721R also exhibited wild type levels of DNA synthesis and RAP in the CTA (Figure 5.3). However, telomerase reconstituted with hTERT R979W or F1127L exhibited defects in DNA synthesis when tested with long and short telomeric primers. We observed that the activity defects were more severe with the short ssDNA primer, bio-TELO6 (Figure 5.3 and Table 5.1). The R979W and F1127L mutations do not appear to disrupt RAP. Lastly, telomerase reconstituted with hTERT K902N exhibited severe activity defects when tested with bio-TELO18 and was devoid of activity in the presence of bio-TELO6 (Figure 5.3). The severe catalytic defect observed with bio-TELO18 prevented the determination of RAP.

We used the primer binding assay to determine if any of the mutations had disrupted the ability of hTERT to bind primers containing different lengths of telomeric ssDNA (Table 5.2). As shown in Figure 5.4, each hTERT variant retained the ability to interact with different lengths of ssDNA *in vitro*. The interaction between hTERT K902N and bio-TELO18, however, was significantly reduced compared to the wild type protein ( $p < 0.05$ ). This reduction in ssDNA-binding could be a contributing factor to the inability of hTERT K902N to elongate bio-TELO18 in the CTA (Figure 5.3). Interestingly, the interaction between bio-TELO12 and hTERT A279T or F1127L was significantly greater than that observed for hTERT WT ( $p < 0.05$ ). These mutants also showed a reproducibly stronger interaction with bio-TELO6, although this was not statistically significant (Figure 5.4). The DC-associated hTERT mutants did not form stable interactions with bio-antiTELO18, indicating that these mutants retained specificity for telomeric ssDNA *in vitro* (Figure 5.4).

**Table 5.2: Description of ssDNA primers used in the primer binding studies and conventional telomerase activity assays of disease-associated hTERT mutations.**

<b>Name</b>	<b>Length (nt)</b>	<b>DNA Sequence (5' to 3')</b>
<b>bio-TELO24</b>	24	TTAGGG TTAGGG TTAGGG TTAGGG
<b>bio-TELO18</b>	18	TTAGGG TTAGGG TTAGGG
<b>bio-TELO12</b>	12	TTAGGG TTAGGG
<b>bio-TELO6</b>	6	TTAGGG
<b>bio-antiTELO18</b>	18	AATCCC AATCCC AATCCC
<b>TELO24</b>	24	TTAGGG TTAGGG TTAGGG

These primers were tested for physical interaction with hTERT in the primer binding assay and telomerase-mediated extension in the conventional telomerase activity assay (bio-TELO18 and bio-TELO6). Primers containing a 5' biotin molecule are indicated with the prefix 'bio'.

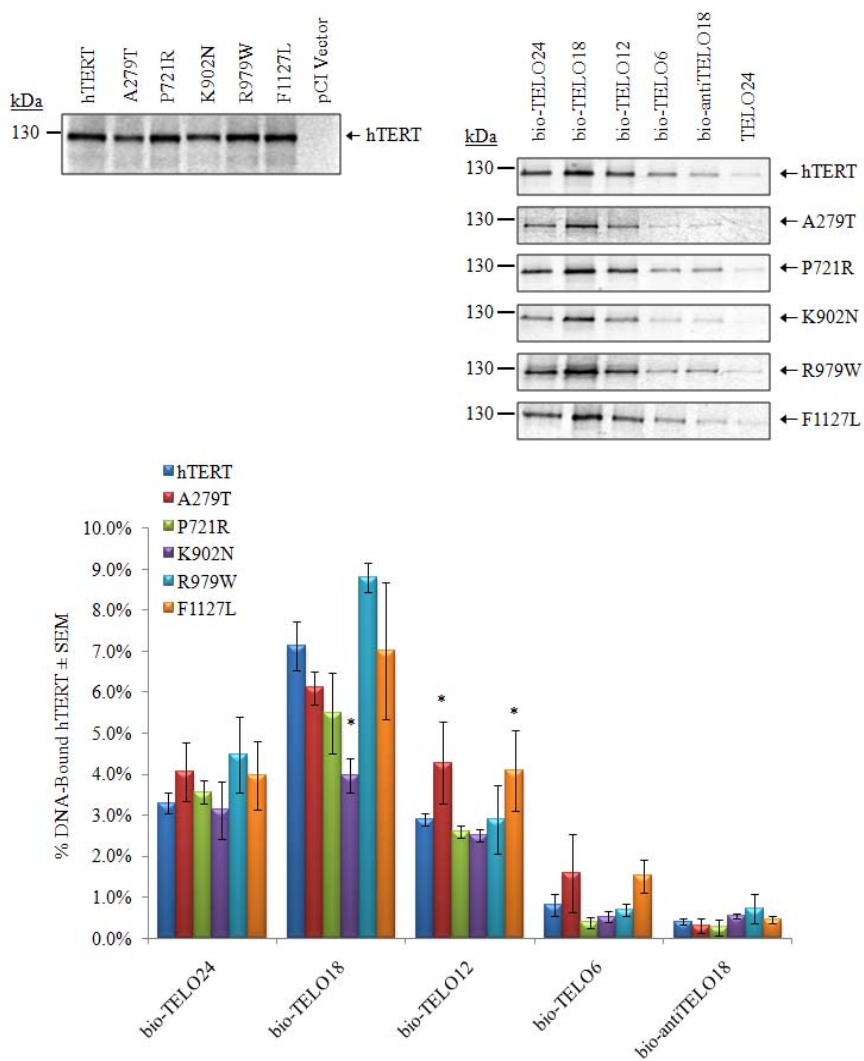


**Figure 5.4: Analysis of the telomeric ssDNA-binding activity of hTERT mutants associated with DC *in vitro*.**

**Figure 5.4: Analysis of the telomeric ssDNA-binding activity of hTERT mutants associated with DC *in vitro*.**

*Top*, Comparable counts of [<sup>35</sup>S]cysteine-labelled hTERT (left panel) were tested for physical interaction with biotinylated ssDNA primers containing different lengths of human telomeric DNA (right panel). A description of the oligonucleotides can be found in Table 5.2. hTERT-ssDNA complexes were immobilized on neutravidin beads, purified, separated by 8 % SDS-PAGE and visualized with autoradiography and phosphorimaging.

*Bottom*, Quantification and statistical analysis of at least three independent experiments is shown in graphical format. Results are reported as the mean % DNA-bound hTERT ± SEM. Asterisks denote levels of statistical significance compared to the interaction between hTERT WT and the corresponding primer, as determined using Student's two-tailed unpaired T-tests;  $p < 0.05$  (\*).

### 5.2.2 Characterization of hTERT mutants found in patients with idiopathic pulmonary fibrosis

To understand how hTERT mutations contribute to IPF, we focused on three distinct full length hTERT variants: V144M, R865C, and R865H. These residues are located within the TEN and RT domains, respectively (Figure 5.1). We also investigated a truncated protein lacking the first 144 amino acids because it was not clear if the V144M mutant was translated as a full length protein or if translation was initiated from the novel internal methionine.

We first determined whether these mutants could form a functional telomerase complex. Human telomerase was reconstituted in RRL with hTR and hTERT WT,  $\Delta$ 144, V144M, R865C, or R865H and tested for enzyme activity *in vitro* with the TRAP assay. Human telomerase reconstituted with hTERT V144M exhibited a minor reduction in enzyme activity compared to the wild type enzyme (Figure 5.5). The catalytic defect was more pronounced when telomerase was reconstituted with hTERT R865C and R865H. Strikingly, telomerase reconstituted with hTERT  $\Delta$ 144 was devoid of catalytic activity, which reveals for the first time that these 144 amino acids are essential for telomerase activity *in vitro* (Figure 5.5). Control reactions showed that RNase A inhibited these reactions, indicating that DNA synthesis was catalyzed by telomerase and not by contaminating polymerases present in RRL (Figure 5.5).

We next tested wild type and mutant telomerase in the CTA to gain more detailed information on the catalytic properties of these enzymes. As expected, human telomerase reconstituted with hTERT  $\Delta$ 144 was devoid of enzyme activity (Figure 5.6). Human telomerase reconstituted with hTERT V144M exhibited nearly wild type levels of total

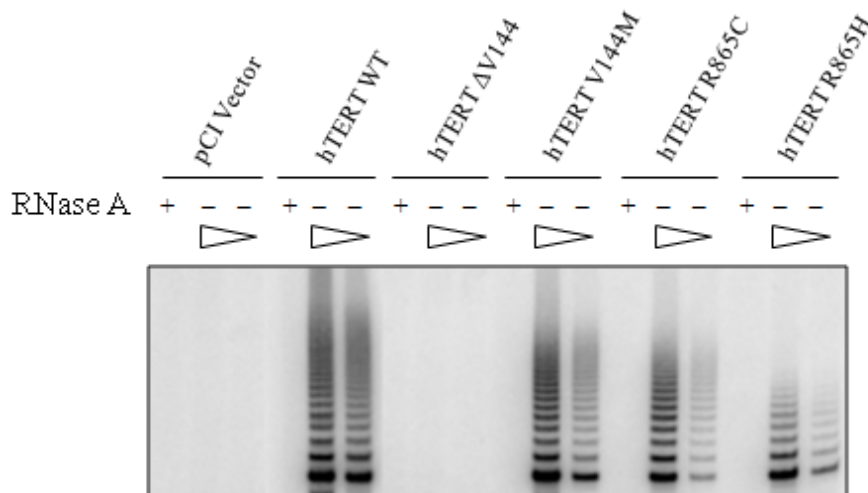


**Figure 5.5: *In vitro* activity of telomerase reconstituted with distinct hTERT mutants identified in patients afflicted with IPF.**

Human telomerase reconstituted in RRL with hTR and plasmid DNA for the pCI vector, hTERT WT,  $\Delta 144$ , V144M, R865C, or R865H was tested for *in vitro* enzyme activity using the telomere repeat amplification protocol. RRL reconstitution reactions (1  $\mu$ L) were assayed in the presence and absence of 5  $\mu$ g RNase A to show that DNA extension was catalyzed by telomerase and not by polymerases present in the RRL. The triangles represent a five-fold dilution of each reaction to confirm that the activity assays were in the linear range. This experiment was performed four times.

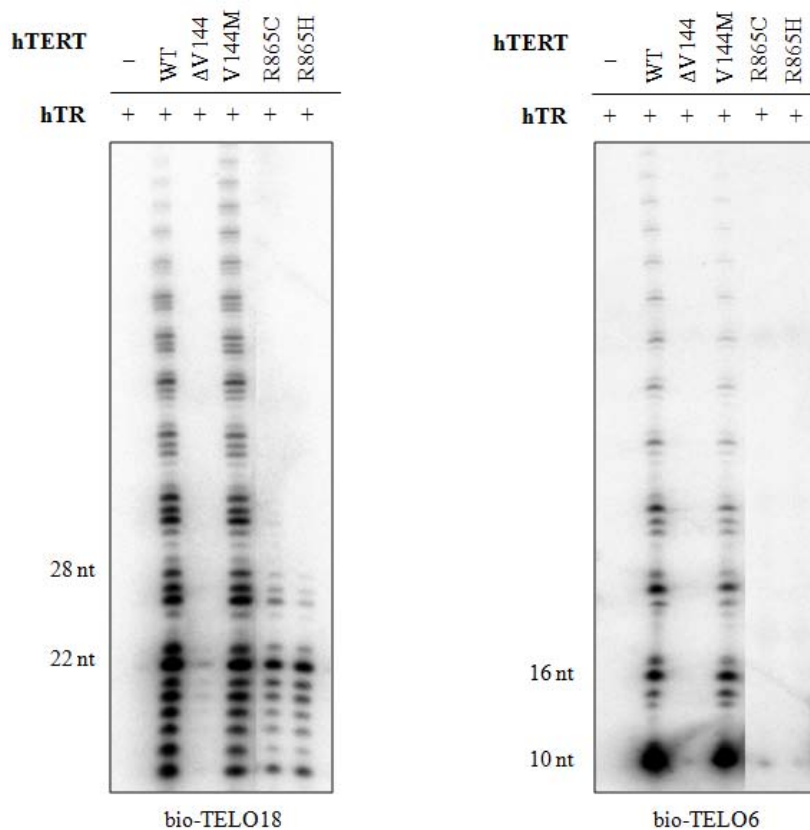


**Figure 5.6: Analysis of the activity and repeat addition processivity of telomerase mutants associated with IPF.**

Human telomerase reconstituted in RRL with hTR and hTERT WT,  $\Delta$ 144, V144M, R865C, or R865H was tested for catalytic activity and repeat addition processivity with an 18 nt telomeric primer, bio-TELO18, and a 6 nt telomeric primer, bio-TELO6. The positions of the 22 nt and 28 nt elongation product are shown at the left of the image and were determined by comparison with the mobility of a 5'-end-radiolabelled 18 nt telomeric primer containing a 3'-biotin molecule (not shown). The quantification and statistical analysis of these data is shown in Table 5.1.

DNA synthesis and RAP when tested with 18 nt and 6 nt telomeric ssDNA primers (bio-TELO18 and bio-TELO6, respectively) (Figure 5.6). By contrast, the hTERT R865C and R865H mutations were associated with severe defects in total DNA synthesis and RAP with bio-TELO18 and bio-TELO6 (Figure 5.6). Quantification of three independent experiments showed that telomerase reconstituted with hTERT R865C and R865H were approximately 20 % as active as the WT enzyme when tested with bio-TELO18 (Table 5.3). We were unable to detect any activity with the shorter ssDNA primer, bio-TELO6. Furthermore, the R865 mutations caused significant defects in RAP, indicating that these residues are required for efficient DNA synthesis and processive repeat addition (Figure 5.6 and Table 5.3).

We next tested the ability of the mutant proteins to interact with telomeric ssDNA to determine if the catalytic defects were caused by impaired protein-DNA interactions. Figure 5.7 shows that the hTERT mutants did not form a stable interaction with bio-antiTELO18 and thus, retained sequence-specific ssDNA-binding activity *in vitro*. When compared with hTERT WT, however, the IPF mutants exhibited differences in their interactions with specific lengths of human telomeric ssDNA (Figure 5.7). Interestingly, the relative strength of the interaction between bio-TELO18 and each of the R865 mutants was significantly less than that observed for hTERT WT (Figure 5.7). This result suggests that impaired protein-DNA interactions could contribute to the activity and RAP defects of telomerase reconstituted with hTERT R865C and R865H. The R865H mutant, which exhibited the most severe defects in DNA synthesis and RAP, also showed a relatively weak interaction with bio-TELO12 and bio-antiTELO18. The increased strength of the interaction between hTERT V144M and bio-TELO24 may reflect tighter

**Table 5.3: Quantification of DNA synthesis and repeat addition processivity observed for telomerase mutants associated with IPF.**

<b>hTERT Mutant</b>	<b><u>bio-TELO18</u></b>		<b><u>bio-TELO6</u></b>	
	<b>DNA Synthesis (% WT <math>\pm</math> SEM)</b>	<b>Repeat Addition Processivity (% WT <math>\pm</math> SEM)</b>	<b>DNA Synthesis (% WT <math>\pm</math> SEM)</b>	<b>Repeat Addition Processivity (% WT <math>\pm</math> SEM)</b>
<b><math>\Delta</math>V144</b>	ND	ND	ND	ND
<b>V144M</b>	65 $\pm$ 13	105 $\pm$ 9	92 $\pm$ 6	94 $\pm$ 19
<b>R865C</b>	24 $\pm$ 3 *	14 $\pm$ 4 **	ND	ND
<b>R865H</b>	20 $\pm$ 4 **	ND	ND	ND

DNA synthesis and repeat addition processivity was determined from the data shown in Figure 5.3. Results were calculated from three independent experiments and the mean  $\pm$  SEM is reported relative to the wild type enzyme. DNA synthesis was calculated within the first hexameric repeat and repeat addition processivity was determined within the first five hexameric repeats. Not detected (ND) indicates that the signal was below the detection limit of this assay and the data was not quantified. Asterisks denote the level of statistical significance compared to wild type telomerase, as determined using Student's two-tailed unpaired T-tests;  $p < 0.05$  (\*) and  $p < 0.01$  (\*\*).

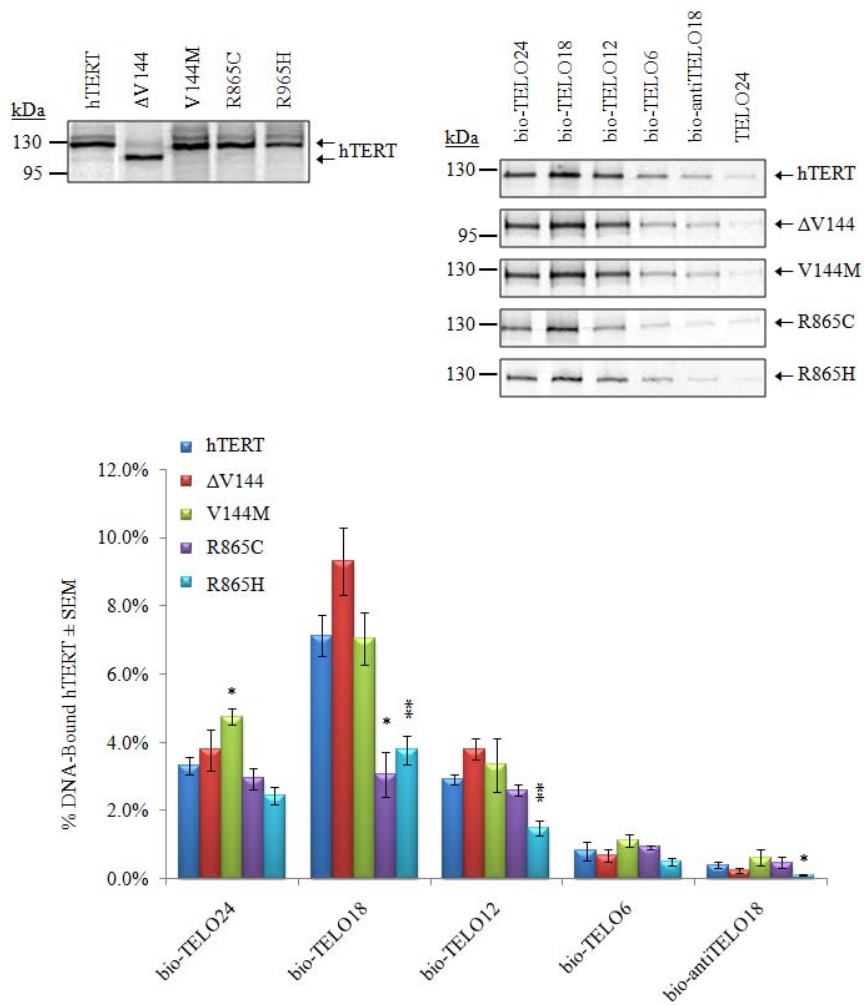


**Figure 5.7: Analysis of the telomeric ssDNA-binding activity of hTERT mutants associated with IPF *in vitro*.**

**Figure 5.7: Analysis of the telomeric ssDNA-binding activity of hTERT mutants associated with IPF *in vitro*.**

*Top*, Comparable counts of [<sup>35</sup>S]cysteine-labelled hTERT (left panel) were tested for physical interaction with biotinylated ssDNA primers containing different lengths of human telomeric DNA (right panel). A description of the oligonucleotides can be found in Table 5.2. hTERT-ssDNA complexes were immobilized on neutravidin beads, purified, separated by 8 % SDS-PAGE and visualized with autoradiography and phosphorimaging.

*Bottom*, Quantification and statistical analysis of at least three independent experiments is shown in graphical format. Results are reported as the mean % DNA-bound hTERT ± SEM. Asterisks denote levels of statistical significance compared to the interaction between hTERT WT and the corresponding primer, as determined using Student's two-tailed unpaired T-tests and the hTERT WT primer binding data set shown in Figure 5.4; p < 0.05 (\*) and p < 0.01 (\*\*).

binding of the primers to this mutant. Interestingly, the catalytically inactive hTERT  $\Delta 144$  bound the telomeric ssDNA primers as efficiently as WT hTERT (Figure 5.7). This observation is consistent with the studies described in Chapter 3, which indicate primer binding can be functionally uncoupled from primer utilization.

## 5.3 Discussion

### 5.3.1 Discussion of *hTERT* mutants associated with *dyskeratosis congenita*

Dyskeratosis congenita is a rare, multi-system disorder that generally presents during childhood [320]. Accelerated telomere shortening due to telomerase deficiency is the general underlying cause of DC and DC-related diseases [320]. Inherited forms of DC exhibit anticipation, whereby successive generations exhibit earlier disease onset and present with more severe phenotypes [321,322]. The mechanism of disease anticipation in DC is thought to be caused by the inheritance of short telomeres that continue to shorten at an accelerated rate in the afflicted offspring. Mutations have been detected in five telomerase holoenzyme genes (*TERC*, *TRT*, *DKC1*, *NOP10*, and *NHP2*) and one shelterin gene, *TINF2* [320]. In this study, we sought to gain insight into the mechanisms by which specific *TRT* mutations contribute to this disease. We determined the effects of five different hTERT mutants on overall telomerase activity, RAP, and telomeric ssDNA-binding activity *in vitro*. None of the hTERT substitutions altered protein expression or stability in RRL. The results of these experiments are summarized in Table 5.4 and discussed below.

**Table 5.4: Summary of the *in vitro* DNA synthesis, repeat addition processivity, and ssDNA-binding activities of hTERT mutants associated with DC.**

hTERT Mutant	TRAP Activity	<u>bio-TELO18</u>			<u>bio-TELO6</u>		
		DNA Binding	DNA Synthesis	Repeat Addition Processivity	DNA Binding	DNA Synthesis	Repeat Addition Processivity
<b>A279T</b>	↓↓	WT	WT	WT	WT	WT	WT
<b>P721R</b>	WT/↓	WT	WT	WT	WT	WT	WT
<b>K902N</b>	↓↓↓	↓	↓↓↓	ND	WT	ND	ND
<b>R979W</b>	WT/↓	WT	↓	WT	WT	↓↓	WT
<b>F1127L</b>	WT/↓	WT	↓↓	WT	WT	↓↓	WT

A wild type (WT) designation is given to mutants that did not show a difference compared to wild type telomerase or hTERT. Not detected (ND) indicates that the signal was below the detection limit of this assay and the data were not quantified. The number of arrows indicates the relative level of change compared to wild type telomerase or hTERT: minor decrease (↓), moderate decrease (↓↓), and severe decrease (↓↓↓).

The hTERT A279T mutation is particularly interesting because it has been identified in both diseased and apparently healthy individuals [326]. This residue forms part of the N-terminal linker region that separates the TEN and TRB domains and has species-specific roles in telomerase activity and TR-binding *in vitro* [142,145,152]. The length and sequence of the linker region varies significantly between species, although vertebrate TERTs contain a small block of conserved residues in the extreme C-terminal portion of the linker [152]. Based on the observation that A279 resides in a poorly conserved region that exhibits structural flexibility, we speculate that the conservative A279T mutation could be well-tolerated, thereby explaining its presence in apparently healthy individuals. Nonetheless, Thr is physically larger and more polar than Ala, indicating that the substitution could affect TERT structure and/or function. Consistent with this, we found that telomerase reconstituted with hTERT A279T exhibited reduced levels of TRAP activity compared to the wild type enzyme (Figure 5.2). By contrast, the mutant enzyme catalyzed wild type levels of DNA synthesis and RAP in the CTA (Figure 5.3). The most obvious explanation for this difference is the sequence composition of the ssDNA primer: the TRAP assay utilizes a G-rich primer that does not contain canonical TTAGGG repeats whereas the CTA uses primers comprised entirely of telomeric repeats. Thus, the A279T mutation seems to affect the ability of telomerase to elongate non-telomeric G-rich ssDNA primers *in vitro*. Consistent with this is our observation that hTERT A279T interacts with ssDNA primers containing 24 nt or 18 nt of telomeric DNA *in vitro* as efficiently as wild type hTERT (Figure 5.4). Interestingly, another group has shown that human telomerase reconstituted *in vivo* with hTERT A279T exhibits wild type levels of TRAP activity [327]. The most likely explanations for this difference are: 1) the

reconstitution system (RRL vs human VA13 cells); 2) sample origin (crude RRL vs total cell lysate); and/or 3) the number of PCR cycles used to amplify telomerase-extension products variations, which we have found strongly affect the observed TRAP activity of certain hTERT mutants.

Two of the amino acid substitutions investigated in this study are located within the hTERT RT domain: P721R and K902N. These residues form part of the highly conserved RT motifs A and D, respectively [116,117]. We expected that the P721R substitution would have a significant impact on telomerase structure and function because of its non-conservative nature and the general importance of Pro residues in protein folding. However, telomerase reconstituted with hTERT P721R showed wild type levels of DNA synthesis and RAP *in vitro* (Figure 5.3). Furthermore, hTERT P721R bound telomeric ssDNA primers as efficiently as wild type hTERT (Figure 5.4). Our TRAP corroborates a previous demonstration that human telomerase reconstituted with hTERT P721R *in vivo* exhibits nearly wild type levels of TRAP activity [327]. In light of these data, it would be useful to know the telomere lengths of patients that carry this mutation because it appears that this mutation does not lead to telomerase deficiency. If these patients do in fact harbour short telomeres then it would be interesting to determine the cellular localization of hTERT P721R and whether it is targeted to telomeric DNA *in vivo*. Furthermore, motif A of the hTERT RT domain has been shown to be required for an efficient interaction with the ATPase pontin, suggesting that the P721R mutation could have disrupted the ability of pontin to stabilize the telomerase complex *in vivo* [232].

Telomerase reconstituted with hTERT K902N was devoid of catalytic activity in the TRAP assay (Figure 5.2). The mutant enzyme also exhibited severe activity defects when tested in the CTA with an 18 nt telomeric primer and was catalytically inactive with the 6 nt primer (Figure 5.3). Our results are consistent with previous observations regarding the effect of this mutation on human telomerase activity *in vitro* and *in vivo* [322,327] and collectively indicate that hTERT K902N is a loss-of-function mutant. hTERT K902 forms part of the evolutionarily-conserved motif D within the catalytic RT domain [116,117]. The high-resolution structure of flour beetle TERT reveals that motif D forms a loop beneath the active site [128]. The positively charged Lys side-chain is believed to position and/or stabilize the triphosphate group of the incoming dNTP during catalysis [128]. This model is supported by biochemical studies of the corresponding residue in HIV-1 RT, which have identified an important role for this residue in nucleotide binding [351]. We propose that the non-conservative K902N mutation directly impairs dNTP-binding and/or positioning in the enzyme active site, thereby explaining the loss of catalytic activity associated with this mutation.

We studied the effects of two C-terminal amino acid substitutions (R979W and F1127L) on telomerase function *in vitro*. Although the CTE is not as well-characterized as other regions in TERT, it is important for the activity and processivity of human telomerase *in vitro* and *in vivo* [139,140]. Interestingly, hTERT F1127 resides in the CTE DAT domain, which is required for telomerase-mediated telomere elongation in human cells [140]. We found that human telomerase reconstituted with either hTERT R979W or F1127L exhibited nearly wild type levels of activity in the TRAP assay and did not demonstrate any RAP defects in the CTA (Figure 5.3). However, both mutants

demonstrated a significant reduction in overall DNA synthesis when tested with 18 and 6 nt telomeric primers in the CTA (Figure 5.3). Importantly, our studies have uncovered a previously unrecognized role for these residues in mediating the first round of DNA synthesis. The observation that hTERT R979W retains wild type levels of ssDNA-binding is consistent with our previous finding that the CTE does not contain a major DNA-binding domain (Chapter 3) [158].

### ***5.3.2 Discussion of hTERT mutants associated with idiopathic pulmonary fibrosis***

Idiopathic pulmonary fibrosis is a progressive and often fatal lung disease that typically presents after the fifth decade [338]. There are no medical therapies that prolong life expectancy and the mean survival is three years after initial diagnosis [338]. The disease is characterized by extensive damage to the lung parenchyma due to a combination of dysfunctional epithelial repair processes, fibrosis, and inflammation. Another distinguishing feature of IPF is the unknown etiology, although recent genetic studies have provided insight into the culprit genes. More specifically, heterozygous *TRT* mutations have been identified in patients afflicted with familial IPF [337,352]. The telomeres of these patients are significantly shorter than the telomeres of age-matched family members without these mutations [337,352]. Telomerase deficiency is considered the underlying cause of this phenotype. However, a detailed description of how these mutations affect telomerase structure and function is still lacking. To gain a more detailed insight into how hTERT mutations contribute to IPF, we investigated the effects of four different hTERT mutations on telomerase activity, RAP, and telomeric ssDNA-binding activity *in vitro*. Notably, none of the hTERT substitutions altered protein expression or

stability in RRL (Figure 5.7). The results of these experiments are summarized in Table 5.5 and discussed below.

We observed that telomerase reconstituted with hTERT  $\Delta$ V144 was devoid of enzyme activity in the TRAP and CTA (Figures 5.5 and 5.6). This result provides strong evidence that amino acids 1 to 144 are required for the catalytic activity of telomerase *in vitro*. Beattie *et al.* have previously shown that telomerase reconstituted with hTERT  $\Delta$ 200 exhibits low levels of TRAP activity, which indicates that residues 144-200 are required for catalytic activity [148]. We interpret these results as evidence that an intact hTERT TEN domain, and not residues 144-200 *per se*, is required for telomerase activity *in vitro*. Amino acids 1-144 comprise approximately three-quarters of the TEN domain, which has important roles in enzyme function and telomeric ssDNA-binding activity (Chapter 4). However, hTERT  $\Delta$ V144 exhibited wild type levels of telomeric ssDNA-binding activity *in vitro*, suggesting that the first 144 amino acids are dispensable for primer binding (Figure 5.7). Importantly, hTERT  $\Delta$ V144 contains the evolutionarily-conserved anchor region that is located within the TEN domain (Figure 4.1). We speculate that the DNA-binding properties of this mutant are intact because it contains all the regions that are necessary for physical interactions with telomeric ssDNA *in vitro*.

Our TRAP results indicate that hTERT V144M does not negatively impact the ability of telomerase to elongate partially telomeric ssDNA primers *in vitro*, which corroborates the independent work of Garcia and colleagues [352]. Our CTA results show that telomerase reconstituted with the full length V144M hTERT variant exhibits wild type levels of DNA synthesis and RAP when tested with completely telomeric ssDNA primers (Figure 5.6). These observations collectively indicate that the V144M

**Table 5.5: Summary of the *in vitro* DNA synthesis, repeat addition processivity, and ssDNA-binding activities of hTERT mutants associated with IPF.**

<b>hTERT Mutant</b>	<b>TRAP Activity</b>	<b><u>bio-TELO18</u></b>			<b><u>bio-TELO6</u></b>		
		<b>DNA Binding</b>	<b>DNA Synthesis</b>	<b>Repeat Addition Processivity</b>	<b>DNA Binding</b>	<b>DNA Synthesis</b>	<b>Repeat Addition Processivity</b>
<b>ΔV144</b>	ND	↑	ND	ND	WT	ND	ND
<b>V144M</b>	WT	WT	WT	WT	WT	WT	WT
<b>R865C</b>	↓↓	↓	↓↓	↓↓↓	WT	ND	ND
<b>R865H</b>	↓↓	↓↓	↓↓	ND	WT	ND	ND

A wild type (WT) designation is given to mutants that did not show a difference compared to wild type telomerase or hTERT. Not detected (ND) indicates that the signal was below the detection limit of this assay and the data were not quantified. The number of arrows indicates the relative level of change compared to wild type telomerase or hTERT: minor increase (↑), minor decrease (↓), modest decrease (↓↓), and dramatic decrease (↓↓↓).

mutation does not have a significant impact on telomerase function *in vitro*. This is consistent with the semi-conservative nature of the substitution. Whether this mutation has a more severe consequence on enzyme activity *in vivo* is currently unknown.

The hTERT R865C and R865H mutations are located within motif C of the catalytic RT domain and form part of the conserved LhRhhDD motif, where h indicates hydrophobic residues [159]. In hTERT, the sequence of this motif is LLRLVDD. The two Asp residues form part of the catalytic triad that is shared by all RTs and directly participates in nucleotide addition, coordinated by a two metal ion mechanism: mutating these residues ablates telomerase activity *in vitro* and *in vivo* [116,117,119,123,124,137,154-156]. The Val residue forms part of the nucleotide-binding pocket [128] and mutations of this residue lead to significant changes in overall DNA synthesis and nucleotide incorporation fidelity without affecting RAP [159]. Based on these results, we expected that the R865 mutations would impair enzyme activity. The polar character of the Arg side-chain makes it ideal for binding negatively charged groups, which is consistent with high-resolution structural data that place this residue in the nucleotide-binding pocket [128]. Our studies have uncovered novel roles for R865 in enzyme activity and show that R865C and R865H mutations severely impair DNA synthesis and RAP *in vitro* (Figures 5.5 and 5.6). We speculate that the R865C and R865H mutations disrupt nucleotide positioning in the active site and therefore, directly compromise the catalytic reaction.

### ***5.3.3 Perspectives***

Mutations in the human *TRT* gene have been recently identified in patients afflicted with DC and several DC disease-variants, including IPF, AA, and HH syndrome. The common phenotype among these patients is abnormally short telomeres, suggesting that the general mechanism of these disease states is telomerase deficiency. This is interesting because these patients are predisposed to developing cancer, which is associated with an up-regulation of telomerase activity. It is not clear how genetic lesions in *TRT* contribute to such a broad spectrum of disease phenotypes. The prevailing hypothesis is that a combination of telomerase deficiency and additional genetic or stochastic mutations determine the overall phenotype. This emphasizes the need for a detailed description regarding the mechanisms by which specific hTERT mutations affect telomerase function. The study of naturally-occurring hTERT mutants will provide important fundamental insight into protein structure and function and may ultimately translate into novel therapeutic strategies. Our studies are necessary, but not sufficient, for a complete understanding of how specific hTERT mutations contribute to human disease.

## Chapter Six: Future Directions and Conclusions

### 6.1 General Discussion

Telomeres are essential nucleoprotein structures that form a protective cap for chromosome ends. The cap provides an architectural mechanism that enables cells to regulate telomere elongation and distinguish natural chromosome ends from *bona fide* DNA breaks [50]. The proper maintenance of telomere structure and function is crucial for prolonged cell proliferation and genome stability [295]. Importantly, most normal somatic cells have a limited lifespan and exhibit telomere attrition during cell-division because the semi-conservative DNA replication machinery cannot replicate the termini of linear chromosomes [89-91]. The loss of functional genetic information would result in cellular catastrophe and the terminal segments of linear chromosomes have evolved unique strategies to this from occurring. Almost all eukaryotes utilize an enzyme called telomerase to synthesize and maintain telomeric DNA.

Telomerase is a cellular reverse transcriptase complex that minimally contains a catalytic protein subunit (TERT) and an RNA subunit (TR) [110-112]. TERT proteins are structurally defined by conserved RT and telomerase-specific domains [129]. TERT-specific domains in the NTE and CTE contribute to the biochemical properties that distinguish telomerase from prototypical RT's. TERT uses a small RNA template within TR to reverse transcribe telomeric nucleotides onto the ss 3'-ends of chromosomes *in vivo* or certain ssDNA primers *in vitro*. Telomerase is unique in its ability to catalyze processive DNA synthesis, which is facilitated by telomere-specific DNA-binding domains called anchor sites.

Genetic and somatic mutations that disrupt the normal assembly and function of the human telomerase RNP are associated with a spectrum of disease states [338]. Characterization of human telomerase structure and function is required to understand the molecular mechanisms that underlie these disease states. The physiological importance of telomerase is further illustrated by the fact that approximately 85 % of human cancers exhibit up-regulated telomerase activity [169], which prevents telomere shortening and confers these cells with unlimited replicative capacity. This emphasizes the need for therapeutics that can modulate telomerase activity *in vivo*. Unfortunately, the applicability and efficacy of currently available therapeutic strategies is limited because the molecular mechanism(s) that regulate the assembly and activity of human telomerase are poorly understood [314]. Thus, structure-function studies of human telomerase are also necessary for the rational design of novel therapeutic compounds.

## **6.2 Future Directions**

My thesis work has expanded our knowledge of hTERT structure and function and provides a platform for many different avenues of future research, of which three are discussed below.

### ***6.2.1 Contribution of the telomerase RNA subunit and telomerase-associated proteins to ssDNA-binding***

We developed the primer binding assay to investigate interactions between hTERT and ssDNA in the absence of hTR. However, it would be interesting to determine how hTR affects hTERT-ssDNA interactions *in vitro*. One important challenge that needs

to be resolved is the isolation of fully-assembled hTERT/hTR complexes from RRL. Dual-affinity purification of telomerase could theoretically recover fully assembled complexes but whether this purification strategy would recover sufficient amounts of enzyme for the primer binding assay is unknown.

The primer binding assay could also be used to investigate how telomerase- and telomere-associated proteins influence the DNA-binding activity of hTERT *in vitro*. Based on the recent report that Hsp82 mediates the accessibility of telomeric ssDNA to *S. cerevisiae* telomerase [109], it would be very interesting to determine how the human proteins HSP90 and p23 influence the ssDNA-binding activity of hTERT. This could be accomplished by immunodepleting HSP90 and/or p23 from the RRL reconstitution reaction or by the addition of HSP90/p23 inhibitors (e.g. geldanamycin) before or after hTERT synthesis.

Another potential modification of the primer binding assay is the source of the hTERT and/or telomerase that is assayed for DNA-binding. It would be interesting to study the ssDNA-binding properties of hTERT immunoprecipitated from human cells of different lineages. The main challenges associated with this protocol will be: 1) the ability to recover sufficient amounts of protein to perform the primer binding assay; 2) controlling for the heterogeneity of the immunoprecipitated protein complex; and 3) the antibody-based detection of DNA-bound hTERT. Nonetheless, this approach seems warranted in light of the technical difficulties and cellular manipulations associated with detecting telomere-bound hTERT by chromatin immunoprecipitation [353].

### ***6.2.2 Understanding hTERT mutations in relation to the telomerase holoenzyme***

Several proteins are integral or transient components of the telomerase holoenzyme. Based on this observation, it will be important to determine if the composition of the telomerase RNP is altered in cells that ectopically express distinct hTERT mutants. It would be equally informative to investigate if RNP composition varies between telomerase-positive and telomerase-negative cell lines that ectopically express the mutant hTERT proteins. This objective could be addressed using biased and unbiased approaches. For example, the mutant telomerase complex could be immunoprecipitated and probed for specific interacting proteins, such as dyskerin, pontin/reptin, and TCAB1 (*i.e.* biased approach). Alternatively, the immunoprecipitated complex could be analyzed by mass spectrometry, which would provide unbiased information on telomerase-interacting proteins. One important advantage of the latter approach is the potential to uncover novel telomerase-interacting proteins.

### ***6.2.3 Cellular significance of naturally-occurring hTERT mutants***

It will be important to express the naturally-occurring hTERT mutants in telomerase-positive and telomerase-negative human cell lines and determine how these mutations affect telomerase activity, protein-protein interactions, and telomere length maintenance. These experiments will help us understand the biological consequences of hTERT mutations in relation to human disease. The identification of hTERT mutants that do not exhibit defects in telomere length maintenance would be particularly interesting. This would indicate that the accentuated telomere shortening observed in patients harbouring the *TRT* mutation is caused by another telomerase-relevant mutation. The

most likely candidates for additional mutations are genes encoding telomere- and telomerase-associated proteins.

### 6.3 Conclusions and Perspectives

The overall objective of my thesis work was to understand the fundamental mechanisms by which hTERT interacts with telomeric ssDNA and how these interactions contribute to telomerase function. I was especially interested in elucidating hTERT anchor regions since there was limited information about these telomerase-specific DNA-binding regions at the time I started my thesis work. With this in mind, it is worth mentioning some of the biochemical challenges that are associated with the hTERT protein. First, biochemical purification of full length hTERT has been impeded by the fact that the protein is insoluble and/or unstable under various purification schemes. Related to this is the fact that the endogenous protein is expressed at very low levels in human cells (approximately 20-50 molecules per cell) [101], which is further complicated by the lack of high-quality and reliable hTERT antibodies [354]. These issues can be circumvented by reconstituting human telomerase *in vitro* with the RRL transcription-translation system. However, the RRL contains a high concentration of endogenous proteins that interfere with many biochemical techniques, such as UV-cross-linking and electrophoretic mobility-shift assays (T.L. Beattie, personal communication). Thus, although protein-DNA interactions are a fundamental aspect of telomerase activity, limited information was available on this matter when I started my thesis work. Furthermore, the information that was available regarding protein-DNA interactions had

been inferred from activity assays and therefore, it was unknown if TERT could physically bind telomeric ssDNA in the absence of the integral RNA subunit.

We developed a DNA-binding assay to characterize interactions between RRL-reconstituted hTERT and ssDNA primers *in vitro*. Our studies were the first to demonstrate that hTERT could form stable and sequence-specific interactions with telomeric ssDNA in the absence of the telomerase RNA subunit. Through extensive mutational analysis of hTERT, we uncovered novel regions of the protein that are critical for a stable and sequence-specific interaction with telomeric ssDNA. Our studies were also the first to show that the interaction between hTERT and telomeric ssDNA could be functionally uncoupled from telomerase-mediated telomere elongation. Collectively, our data supported a model in which distinct anchor regions in hTERT co-operate to regulate primer binding and extension *in vitro*.

During the course of my thesis work, the first atomic-resolution structure of TERT was determined – the ciliate TEN domain, which encompasses amino acids 2-191 [143]. Phylogenetically conserved amino acids were identified on the surface of this domain and were predicted to form a ssDNA-binding groove. This previously unrecognized ssDNA-binding channel was expected to represent a long-sought after N-terminal anchor region. Consistent with this hypothesis, an evolutionarily-conserved Gln residue was shown to be required for telomerase function in lower eukaryotes [143,278,289]. We provided the first detailed evidence regarding the biochemical and cellular roles of this Gln residue in higher eukaryotes. Our studies were the first to show that this residue is required for human telomerase activity *in vitro* and *in vivo*. We provided the first evidence that this Gln residue is required for conformational changes in

the hTERT N-terminus that are necessary for optimal substrate-enzyme interactions and nucleotide incorporation. We also uncovered a role for this amino acid in sequence-specific interactions between the hTERT NTE and human telomeric ssDNA. Collectively, our results indicate that the Gln residue forms part of a long-sought evolutionarily-conserved anchor region in the TERT NTE.

Another milestone that was reported during my graduate work was the identification of *TRT* mutations in patients afflicted with DC and IPF. These patients have telomeres that are significantly shorter than age-matched controls, suggesting that the underlying disease mechanism is telomerase deficiency [338]. Although the mutations are distributed throughout the hTERT protein, many reside in the RT domain and were anticipated to directly alter the catalytic reaction. Importantly, other mutations are located within poorly understood regions of hTERT (e.g. the linker region and CTE). Thus, we reasoned that characterizing naturally-occurring hTERT mutants would provide important insight into telomerase structure and function in relation to human disease. Our studies have provided novel insight into the functional consequences of these mutations *in vitro*. We are the first to report on how these mutations affect hTERT-telomeric ssDNA interactions. These studies are necessary, but not sufficient, for a complete understanding of how mutations in telomerase contribute to human disease. These insights may ultimately lead to the development of novel treatment options for patients suffering from DC and IPF.

## References

1. Riethman H, Ambrosini A, Castaneda C et al. Mapping and initial analysis of human subtelomeric sequence assemblies. *Genome Res* 2004;14(1):18-28.
2. Riethman H. Human telomere structure and biology. *Annu Rev Genomics Hum Genet* 2008;9:1-19.
3. Bailey JA, Gu Z, Clark RA et al. Recent segmental duplications in the human genome. *Science* 2002;297(5583):1003-1007.
4. Linardopoulou EV, Williams EM, Fan Y, Friedman C, Young JM, Trask BJ. Human subtelomeres are hot spots of interchromosomal recombination and segmental duplication. *Nature* 2005;437(7055):94-100.
5. Conrad B, Antonarakis SE. Gene duplication: a drive for phenotypic diversity and cause of human disease. *Annu Rev Genomics Hum Genet* 2007;8:17-35.
6. Azzalin CM, Reichenbach P, Khoraiuli L, Giulotto E, Lingner J. Telomeric repeat containing RNA and RNA surveillance factors at mammalian chromosome ends. *Science* 2007;318(5851):798-801.
7. Luke B, Panza A, Redon S, Iglesias N, Li Z, Lingner J. The Rat1p 5' to 3' exonuclease degrades telomeric repeat-containing RNA and promotes telomere elongation in *Saccharomyces cerevisiae*. *Mol Cell* 2008;32(4):465-477.
8. Blackburn EH, Gall JG. A tandemly repeated sequence at the termini of the extrachromosomal ribosomal RNA genes in *Tetrahymena*. *J Mol Biol* 1978;120(1):33-53.
9. Jahn CL, Klobutcher LA. Genome remodeling in ciliated protozoa. *Annu Rev Microbiol* 2002;56:489-520.
10. Yu GL, Blackburn EH. Developmentally programmed healing of chromosomes by telomerase in *Tetrahymena*. *Cell* 1991;67(4):823-832.
11. Klobutcher LA, Swanton MT, Donini P, Prescott DM. All gene-sized DNA molecules in four species of hypotrichs have the same terminal sequence and an unusual 3' terminus. *Proc Natl Acad Sci U S A* 1981;78(5):3015-3019.
12. Van der Ploeg LH, Liu AY, Borst P. Structure of the growing telomeres of *Trypanosomes*. *Cell* 1984;36(2):459-468.
13. Ponzi M, Pace T, Dore E, Frontali C. Identification of a telomeric DNA sequence in *Plasmodium berghei*. *EMBO J* 1985;4(11):2991-2995.
14. Shampay J, Szostak JW, Blackburn EH. DNA sequences of telomeres maintained in yeast. *Nature* 1984;310(5973):154-157.
15. Walmsley RW, Chan CS, Tye BK, Petes TD. Unusual DNA sequences associated with the ends of yeast chromosomes. *Nature* 1984;310(5973):157-160.
16. Richards EJ, Ausubel FM. Isolation of a higher eukaryotic telomere from *Arabidopsis thaliana*. *Cell* 1988;53(1):127-136.
17. Allshire RC, Gosden JR, Cross SH et al. Telomeric repeat from *T. thermophila* cross hybridizes with human telomeres. *Nature* 1988;332(6165):656-659.
18. Moyzis RK, Buckingham JM, Cram LS et al. A highly conserved repetitive DNA sequence, (TTAGGG)<sub>n</sub>, present at the telomeres of human chromosomes. *Proc Natl Acad Sci U S A* 1988;85(18):6622-6626.

19. Meyne J, Ratliff RL, Moyzis RK. Conservation of the human telomere sequence (TTAGGG)<sub>n</sub> among vertebrates. *Proc Natl Acad Sci U S A* 1989;86(18):7049-7053.
20. Wang SS, Zakian VA. Sequencing of *Saccharomyces* telomeres cloned using T4 DNA polymerase reveals two domains. *Mol Cell Biol* 1990;10(8):4415-4419.
21. Kipling D, Cooke HJ. Hypervariable ultra-long telomeres in mice. *Nature* 1990;347(6291):400-402.
22. Starling JA, Maule J, Hastie ND, Allshire RC. Extensive telomere repeat arrays in mouse are hypervariable. *Nucleic Acids Res* 1990;18(23):6881-6888.
23. de Lange T, Shiue L, Myers RM et al. Structure and variability of human chromosome ends. *Mol Cell Biol* 1990;10(2):518-527.
24. Harley CB, Futcher AB, Greider CW. Telomeres shorten during ageing of human fibroblasts. *Nature* 1990;345(6274):458-460.
25. Allshire RC, Dempster M, Hastie ND. Human telomeres contain at least three types of G-rich repeat distributed non-randomly. *Nucleic Acids Res* 1989;17(12):4611-4627.
26. Hastie ND, Dempster M, Dunlop MG, Thompson AM, Green DK, Allshire RC. Telomere reduction in human colorectal carcinoma and with ageing. *Nature* 1990;346(6287):866-868.
27. Lansdorp PM, Verwoerd NP, van de Rijke FM et al. Heterogeneity in telomere length of human chromosomes. *Hum Mol Genet* 1996;5(5):685-691.
28. Henderson ER, Blackburn EH. An overhanging 3' terminus is a conserved feature of telomeres. *Mol Cell Biol* 1989;9(1):345-348.
29. Wellinger RJ, Wolf AJ, Zakian VA. *Saccharomyces* telomeres acquire single-strand TG1-3 tails late in S phase. *Cell* 1993;72(1):51-60.
30. Wright WE, Tesmer VM, Huffman KE, Levene SD, Shay JW. Normal human chromosomes have long G-rich telomeric overhangs at one end. *Genes Dev* 1997;11(21):2801-2809.
31. Makarov VL, Hirose Y, Langmore JP. Long G tails at both ends of human chromosomes suggest a C strand degradation mechanism for telomere shortening. *Cell* 1997;88(5):657-666.
32. Hemann MT, Greider CW. G-strand overhangs on telomeres in telomerase-deficient mouse cells. *Nucleic Acids Res* 1999;27(20):3964-3969.
33. Stewart SA, Ben-Porath I, Carey VJ, O'Connor BF, Hahn WC, Weinberg RA. Erosion of the telomeric single-strand overhang at replicative senescence. *Nat Genet* 2003;33(4):492-496.
34. Cimino-Reale G, Pascale E, Battiloro E, Starace G, Verna R, D'Ambrosio E. The length of telomeric G-rich strand 3'-overhang measured by oligonucleotide ligation assay. *Nucleic Acids Res* 2001;29(7):E35.
35. Lee ME, Rha SY, Jeung HC, Kim TS, Chung HC, Oh BK. Variation of the 3' telomeric overhang lengths in human cells. *Cancer Lett* 2008;264(1):107-118.
36. Keys B, Serra V, Saretzki G, Von Zglinicki T. Telomere shortening in human fibroblasts is not dependent on the size of the telomeric-3'-overhang. *Aging Cell* 2004;3(3):103-109.

37. Griffith JD, Comeau L, Rosenfield S et al. Mammalian telomeres end in a large duplex loop. *Cell* 1999;97(4):503-514.
38. Nikitina T, Woodcock CL. Closed chromatin loops at the ends of chromosomes. *J Cell Biol* 2004;166(2):161-165.
39. Munoz-Jordan JL, Cross GA, de Lange T, Griffith JD. t-loops at trypanosome telomeres. *EMBO J* 2001;20(3):579-588.
40. Murti KG, Prescott DM. Telomeres of polytene chromosomes in a ciliated protozoan terminate in duplex DNA loops. *Proc Natl Acad Sci U S A* 1999;96(25):14436-14439.
41. Cesare AJ, Quinney N, Willcox S, Subramanian D, Griffith JD. Telomere looping in *P. sativum* (common garden pea). *Plant J* 2003;36(2):271-279.
42. Raices M, Verdun RE, Compton SA et al. *C. elegans* telomeres contain G-strand and C-strand overhangs that are bound by distinct proteins. *Cell* 2008;132(5):745-757.
43. Tomaska L, Willcox S, Slezakova J, Nosek J, Griffith JD. Taz1 binding to a fission yeast model telomere: formation of telomeric loops and higher order structures. *J Biol Chem* 2004;279(49):50764-50772.
44. Cesare AJ, Groff-Vindman C, Compton SA, McEachern MJ, Griffith JD. Telomere loops and homologous recombination-dependent telomeric circles in a *Kluyveromyces lactis* telomere mutant strain. *Mol Cell Biol* 2008;28(1):20-29.
45. Stansel RM, de Lange T, Griffith JD. T-loop assembly in vitro involves binding of TRF2 near the 3' telomeric overhang. *Embo J* 2001;20(19):5532-5540.
46. Amiard S, Doudeau M, Pinte S et al. A topological mechanism for TRF2-enhanced strand invasion. *Nat Struct Mol Biol* 2007;14(2):147-154.
47. Baker AM, Fu Q, Hayward W, Lindsay SM, Fletcher TM. The Myb/SANT domain of the telomere-binding protein TRF2 alters chromatin structure. *Nucleic Acids Res* 2009.
48. Pisano S, Galati A, Cacchione S. Telomeric nucleosomes: forgotten players at chromosome ends. *Cell Mol Life Sci* 2008;65(22):3553-3563.
49. de Lange T. Shelterin: the protein complex that shapes and safeguards human telomeres. *Genes Dev* 2005;19(18):2100-2110.
50. Palm W, de Lange T. How Shelterin Protects Mammalian Telomeres. *Annu Rev Genet* 2008.
51. Muller HJ. The Remaking of Chromosomes. *The Collecting Net* 1938;13(8):182-195.
52. McClintock B. A Correlation of Ring-Shaped Chromosomes with Variegation in *Zea Mays*. *Proc Natl Acad Sci U S A* 1932;18(12):677-681.
53. McClintock B. The Behavior in Successive Nuclear Divisions of a Chromosome Broken at Meiosis. *Proc Natl Acad Sci U S A* 1939;25(8):405-416.
54. Takai H, Smogorzewska A, de Lange T. DNA damage foci at dysfunctional telomeres. *Curr Biol* 2003;13(17):1549-1556.
55. d'Adda di Fagagna F, Reaper PM, Clay-Farrace L et al. A DNA damage checkpoint response in telomere-initiated senescence. *Nature* 2003;426(6963):194-198.

56. Herbig U, Jobling WA, Chen BP, Chen DJ, Sedivy JM. Telomere shortening triggers senescence of human cells through a pathway involving ATM, p53, and p21(CIP1), but not p16(INK4a). *Mol Cell* 2004;14(4):501-513.
57. Meier A, Fiegler H, Munoz P et al. Spreading of mammalian DNA-damage response factors studied by ChIP-chip at damaged telomeres. *EMBO J* 2007;26(11):2707-2718.
58. Jacobs JJ, de Lange T. Significant role for p16INK4a in p53-independent telomere-directed senescence. *Curr Biol* 2004;14(24):2302-2308.
59. Smogorzewska A, de Lange T. Different telomere damage signaling pathways in human and mouse cells. *EMBO J* 2002;21(16):4338-4348.
60. Karlseder J, Broccoli D, Dai Y, Hardy S, de Lange T. p53- and ATM-dependent apoptosis induced by telomeres lacking TRF2. *Science* 1999;283(5406):1321-1325.
61. Denchi EL, de Lange T. Protection of telomeres through independent control of ATM and ATR by TRF2 and POT1. *Nature* 2007;448(7157):1068-1071.
62. Guo X, Deng Y, Lin Y et al. Dysfunctional telomeres activate an ATM-ATR-dependent DNA damage response to suppress tumorigenesis. *EMBO J* 2007;26(22):4709-4719.
63. Barrientos KS, Kendellen MF, Freibaum BD, Armbruster BN, Etheridge KT, Counter CM. Distinct functions of POT1 at telomeres. *Mol Cell Biol* 2008;28(17):5251-5264.
64. Karlseder J, Hoke K, Mirzoeva OK et al. The telomeric protein TRF2 binds the ATM kinase and can inhibit the ATM-dependent DNA damage response. *PLoS Biol* 2004;2(8):E240.
65. Counter CM, Avilion AA, LeFeuvre CE et al. Telomere shortening associated with chromosome instability is arrested in immortal cells which express telomerase activity. *EMBO J* 1992;11(5):1921-1929.
66. Smogorzewska A, Karlseder J, Holtgreve-Grez H, Jauch A, de Lange T. DNA ligase IV-dependent NHEJ of deprotected mammalian telomeres in G1 and G2. *Curr Biol* 2002;12(19):1635-1644.
67. Konishi A, de Lange T. Cell cycle control of telomere protection and NHEJ revealed by a ts mutation in the DNA-binding domain of TRF2. *Genes Dev* 2008;22(9):1221-1230.
68. Ferreira MG, Cooper JP. The fission yeast Taz1 protein protects chromosomes from Ku-dependent end-to-end fusions. *Mol Cell* 2001;7(1):55-63.
69. Celli GB, de Lange T. DNA processing is not required for ATM-mediated telomere damage response after TRF2 deletion. *Nat Cell Biol* 2005;7(7):712-718.
70. Zhu XD, Niedernhofer L, Kuster B, Mann M, Hoeijmakers JH, de Lange T. ERCC1/XPF removes the 3' overhang from uncapped telomeres and represses formation of telomeric DNA-containing double minute chromosomes. *Mol Cell* 2003;12(6):1489-1498.
71. Celli GB, Denchi EL, de Lange T. Ku70 stimulates fusion of dysfunctional telomeres yet protects chromosome ends from homologous recombination. *Nat Cell Biol* 2006;8(8):885-890.

72. Wu Y, Mitchell TR, Zhu XD. Human XPF controls TRF2 and telomere length maintenance through distinctive mechanisms. *Mech Ageing Dev* 2008;129(10):602-610.
73. Laud PR, Multani AS, Bailey SM et al. Elevated telomere-telomere recombination in WRN-deficient, telomere dysfunctional cells promotes escape from senescence and engagement of the ALT pathway. *Genes Dev* 2005;19(21):2560-2570.
74. Opresko PL, Mason PA, Podell ER et al. POT1 stimulates RecQ helicases WRN and BLM to unwind telomeric DNA substrates. *J Biol Chem* 2005;280(37):32069-32080.
75. Wang RC, Smogorzewska A, de Lange T. Homologous recombination generates T-loop-sized deletions at human telomeres. *Cell* 2004;119(3):355-368.
76. He H, Multani AS, Cosme-Blanco W et al. POT1b protects telomeres from end-to-end chromosomal fusions and aberrant homologous recombination. *EMBO J* 2006;25(21):5180-5190.
77. Wu L, Multani AS, He H et al. Pot1 deficiency initiates DNA damage checkpoint activation and aberrant homologous recombination at telomeres. *Cell* 2006;126(1):49-62.
78. Bae NS, Baumann P. A RAP1/TRF2 complex inhibits nonhomologous end-joining at human telomeric DNA ends. *Mol Cell* 2007;26(3):323-334.
79. Capper R, Britt-Compton B, Tankimanova M et al. The nature of telomere fusion and a definition of the critical telomere length in human cells. *Genes Dev* 2007;21(19):2495-2508.
80. Xu L, Blackburn EH. Human cancer cells harbor T-stumps, a distinct class of extremely short telomeres. *Mol Cell* 2007;28(2):315-327.
81. Dionne I, Wellinger RJ. Processing of telomeric DNA ends requires the passage of a replication fork. *Nucleic Acids Res* 1998;26(23):5365-5371.
82. Marcand S, Brevet V, Mann C, Gilson E. Cell cycle restriction of telomere elongation. *Curr Biol* 2000;10(8):487-490.
83. Rog O, Cooper JP. Telomeres in drag: Dressing as DNA damage to engage telomerase. *Curr Opin Genet Dev* 2008;18(2):212-220.
84. Crabbe L, Verdun RE, Haggblom CI, Karlseder J. Defective telomere lagging strand synthesis in cells lacking WRN helicase activity. *Science* 2004;306(5703):1951-1953.
85. Opresko PL, von Kobbe C, Laine JP, Harrigan J, Hickson ID, Bohr VA. Telomere-binding protein TRF2 binds to and stimulates the Werner and Bloom syndrome helicases. *J Biol Chem* 2002;277(43):41110-41119.
86. Sowd G, Lei M, Opresko PL. Mechanism and substrate specificity of telomeric protein POT1 stimulation of the Werner syndrome helicase. *Nucleic Acids Res* 2008;36(13):4242-4256.
87. Verdun RE, Crabbe L, Haggblom C, Karlseder J. Functional human telomeres are recognized as DNA damage in G2 of the cell cycle. *Mol Cell* 2005;20(4):551-561.
88. Verdun RE, Karlseder J. The DNA damage machinery and homologous recombination pathway act consecutively to protect human telomeres. *Cell* 2006;127(4):709-720.

89. Olovnikov AM. [Principle of marginotomy in template synthesis of polynucleotides]. Dokl Akad Nauk SSSR 1971;201(6):1496-1499.
90. Olovnikov A. A theory of marginotomy. The incomplete copying of template margin in enzymic synthesis of polynucleotides and biological significance of the phenomenon. J Theor Biol 1973;41:181-190.
91. Watson JD. Origin of concatemeric T7 DNA. Nat New Biol 1972;239(94):197-201.
92. Okazaki R, Okazaki T, Sakabe K, Sugimoto K. Mechanism of DNA replication possible discontinuity of DNA chain growth. Jpn J Med Sci Biol 1967;20(3):255-260.
93. Jacob NK, Kirk KE, Price CM. Generation of telomeric G strand overhangs involves both G and C strand cleavage. Mol Cell 2003;11(4):1021-1032.
94. Sfeir AJ, Chai W, Shay JW, Wright WE. Telomere-end processing the terminal nucleotides of human chromosomes. Mol Cell 2005;18(1):131-138.
95. Dionne I, Wellinger RJ. Cell cycle-regulated generation of single-stranded G-rich DNA in the absence of telomerase. Proc Natl Acad Sci U S A 1996;93(24):13902-13907.
96. Huffman KE, Levene SD, Tesmer VM, Shay JW, Wright WE. Telomere shortening is proportional to the size of the G-rich telomeric 3'-overhang. J Biol Chem 2000;275(26):19719-19722.
97. Kelleher C, Kurth I, Lingner J. Human protection of telomeres 1 (POT1) is a negative regulator of telomerase activity in vitro. Mol Cell Biol 2005;25(2):808-818.
98. Lei M, Zaug AJ, Podell ER, Cech TR. Switching human telomerase on and off with hPOT1 protein in vitro. J Biol Chem 2005;280(21):20449-20456.
99. Wang F, Podell ER, Zaug AJ et al. The POT1-TPP1 telomere complex is a telomerase processivity factor. Nature 2007;445(7127):506-510.
100. Xin H, Liu D, Wan M et al. TPP1 is a homologue of ciliate TEBP-beta and interacts with POT1 to recruit telomerase. Nature 2007;445(7127):559-562.
101. Cohen SB, Graham ME, Lovrecz GO, Bache N, Robinson PJ, Reddel RR. Protein composition of catalytically active human telomerase from immortal cells. Science 2007;315(5820):1850-1853.
102. Yi X, Shay JW, Wright WE. Quantitation of telomerase components and hTERT mRNA splicing patterns in immortal human cells. Nucleic Acids Res 2001;29(23):4818-4825.
103. Hemann MT, Strong MA, Hao LY, Greider CW. The shortest telomere, not average telomere length, is critical for cell viability and chromosome stability. Cell 2001;107(1):67-77.
104. Teixeira MT, Arneric M, Sperisen P, Lingner J. Telomere length homeostasis is achieved via a switch between telomerase- extendible and -nonextendible states. Cell 2004;117(3):323-335.
105. Bianchi A, Shore D. Increased association of telomerase with short telomeres in yeast. Genes Dev 2007;21(14):1726-1730.
106. Sabourin M, Tuzon CT, Zakian VA. Telomerase and Tellp preferentially associate with short telomeres in *S. cerevisiae*. Mol Cell 2007;27(4):550-561.

107. Hector RE, Shtofman RL, Ray A et al. Telp preferentially associates with short telomeres to stimulate their elongation. *Mol Cell* 2007;27(5):851-858.
108. Feldser D, Strong MA, Greider CW. Ataxia telangiectasia mutated (Atm) is not required for telomerase-mediated elongation of short telomeres. *Proc Natl Acad Sci U S A* 2006;103(7):2249-2251.
109. Dezwaan DC, Toogun OA, Echtenkamp FJ, Freeman BC. The Hsp82 molecular chaperone promotes a switch between unextendable and extendable telomere states. *Nat Struct Mol Biol* 2009.
110. Greider CW, Blackburn EH. Identification of a specific telomere terminal transferase activity in Tetrahymena extracts. *Cell* 1985;43(2 Pt 1):405-413.
111. Greider CW, Blackburn EH. The telomere terminal transferase of Tetrahymena is a ribonucleoprotein enzyme with two kinds of primer specificity. *Cell* 1987;51(6):887-898.
112. Greider CW, Blackburn EH. A telomeric sequence in the RNA of Tetrahymena telomerase required for telomere repeat synthesis. *Nature* 1989;337(6205):331-337.
113. Yu GL, Bradley JD, Attardi LD, Blackburn EH. In vivo alteration of telomere sequences and senescence caused by mutated Tetrahymena telomerase RNAs. *Nature* 1990;344(6262):126-132.
114. Lendvay TS, Morris DK, Sah J, Balasubramanian B, Lundblad V. Senescence mutants of *Saccharomyces cerevisiae* with a defect in telomere replication identify three additional EST genes. *Genetics* 1996;144(4):1399-1412.
115. Lingner J, Cech TR. Purification of telomerase from *Euplotes aediculatus*: requirement of a primer 3' overhang. *Proc Natl Acad Sci U S A* 1996;93(20):10712-10717.
116. Lingner J, Hughes TR, Shevchenko A, Mann M, Lundblad V, Cech TR. Reverse transcriptase motifs in the catalytic subunit of telomerase. *Science* 1997;276(5312):561-567.
117. Nakamura TM, Morin GB, Chapman KB et al. Telomerase catalytic subunit homologs from fission yeast and human. *Science* 1997;277(5328):955-959.
118. Meyerson M, Counter CM, Eaton EN et al. hEST2, the putative human telomerase catalytic subunit gene, is up-regulated in tumor cells and during immortalization. *Cell* 1997;90(4):785-795.
119. Harrington L, Zhou W, McPhail T et al. Human telomerase contains evolutionarily conserved catalytic and structural subunits. *Genes Dev* 1997;11(23):3109-3115.
120. Bryan TM, Sperger JM, Chapman KB, Cech TR. Telomerase reverse transcriptase genes identified in *Tetrahymena thermophila* and *Oxytricha trifallax*. *Proc Natl Acad Sci U S A* 1998;95(15):8479-8484.
121. Collins K, Gandhi L. The reverse transcriptase component of the Tetrahymena telomerase ribonucleoprotein complex. *Proc Natl Acad Sci U S A* 1998;95(15):8485-8490.
122. Greenberg RA, Allsopp RC, Chin L, Morin GB, DePinho RA. Expression of mouse telomerase reverse transcriptase during development, differentiation and proliferation. *Oncogene* 1998;16(13):1723-1730.

123. Weinrich SL, Pruzan R, Ma L et al. Reconstitution of human telomerase with the template RNA component hTR and the catalytic protein subunit hTERT. *Nat Genet* 1997;17(4):498-502.
124. Beattie TL, Zhou W, Robinson MO, Harrington L. Reconstitution of human telomerase activity in vitro. *Curr Biol* 1998;8(3):177-180.
125. Osanai M, Kojima KK, Futahashi R, Yaguchi S, Fujiwara H. Identification and characterization of the telomerase reverse transcriptase of *Bombyx mori* (silkworm) and *Tribolium castaneum* (flour beetle). *Gene* 2006;376(2):281-289.
126. Malik HS, Burke WD, Eickbush TH. Putative telomerase catalytic subunits from *Giardia lamblia* and *Caenorhabditis elegans*. *Gene* 2000;251(2):101-108.
127. Figueiredo LM, Rocha EP, Mancio-Silva L, Prevost C, Hernandez-Verdun D, Scherf A. The unusually large *Plasmodium* telomerase reverse-transcriptase localizes in a discrete compartment associated with the nucleolus. *Nucleic Acids Res* 2005;33(3):1111-1122.
128. Gillis AJ, Schuller AP, Skordalakes E. Structure of the *Tribolium castaneum* telomerase catalytic subunit TERT. *Nature* 2008.
129. Autexier C, Lue NF. The Structure and Function of Telomerase Reverse Transcriptase. *Annu Rev Biochem* 2006.
130. Arai K, Masutomi K, Khurts S, Kaneko S, Kobayashi K, Murakami S. Two independent regions of human telomerase reverse transcriptase are important for its oligomerization and telomerase activity. *J Biol Chem* 2002;277(10):8538-8544.
131. Beattie TL, Zhou W, Robinson MO, Harrington L. Functional multimerization of the human telomerase reverse transcriptase. *Mol Cell Biol* 2001;21(18):6151-6160.
132. Wang L, Dean SR, Shippen DE. Oligomerization of the telomerase reverse transcriptase from *Euplotes crassus*. *Nucleic Acids Res* 2002;30(18):4032-4039.
133. Hammond PW, Cech TR. *Euplotes* telomerase: evidence for limited base-pairing during primer elongation and dGTP as an effector of translocation. *Biochemistry* 1998;37(15):5162-5172.
134. Forstemann K, Lingner J. Telomerase limits the extent of base pairing between template RNA and telomeric DNA. *EMBO Rep* 2005;6(4):361-366.
135. Hossain S, Singh S, Lue NF. Functional analysis of the C-terminal extension of telomerase reverse transcriptase. A putative "thumb" domain. *J Biol Chem* 2002;277(39):36174-36180.
136. Bosoy D, Lue NF. Functional analysis of conserved residues in the putative "finger" domain of telomerase reverse transcriptase. *J Biol Chem* 2001;276(49):46305-46312.
137. Haering CH, Nakamura TM, Baumann P, Cech TR. Analysis of telomerase catalytic subunit mutants in vivo and in vitro in *Schizosaccharomyces pombe*. *Proc Natl Acad Sci U S A* 2000;97(12):6367-6372.
138. Lue NF, Lin YC, Mian IS. A conserved telomerase motif within the catalytic domain of telomerase reverse transcriptase is specifically required for repeat addition processivity. *Mol Cell Biol* 2003;23(23):8440-8449.

139. Huard S, Moriarty TJ, Autexier C. The C terminus of the human telomerase reverse transcriptase is a determinant of enzyme processivity. *Nucleic Acids Res* 2003;31(14):4059-4070.
140. Banik SS, Guo C, Smith AC et al. C-terminal regions of the human telomerase catalytic subunit essential for in vivo enzyme activity. *Mol Cell Biol* 2002;22(17):6234-6246.
141. Friedman KL, Cech TR. Essential functions of amino-terminal domains in the yeast telomerase catalytic subunit revealed by selection for viable mutants. *Genes Dev* 1999;13(21):2863-2874.
142. Xia J, Peng Y, Mian IS, Lue NF. Identification of functionally important domains in the N-terminal region of telomerase reverse transcriptase. *Mol Cell Biol* 2000;20(14):5196-5207.
143. Jacobs SA, Podell ER, Cech TR. Crystal structure of the essential N-terminal domain of telomerase reverse transcriptase. *Nat Struct Mol Biol* 2006;13(3):218-225.
144. Rouda S, Skordalakes E. Structure of the RNA-binding domain of telomerase: implications for RNA recognition and binding. *Structure* 2007;15(11):1403-1412.
145. Miller MC, Liu JK, Collins K. Template definition by Tetrahymena telomerase reverse transcriptase. *EMBO J* 2000;19(16):4412-4422.
146. Bosoy D, Peng Y, Mian IS, Lue NF. Conserved N-terminal motifs of telomerase reverse transcriptase required for ribonucleoprotein assembly in vivo. *J Biol Chem* 2003;278(6):3882-3890.
147. Bachand F, Autexier C. Functional regions of human telomerase reverse transcriptase and human telomerase RNA required for telomerase activity and RNA-protein interactions. *Mol Cell Biol* 2001;21(5):1888-1897.
148. Beattie TL, Zhou W, Robinson MO, Harrington L. Polymerization defects within human telomerase are distinct from telomerase RNA and TEP1 binding. *Mol Biol Cell* 2000;11(10):3329-3340.
149. Bryan TM, Goodrich KJ, Cech TR. Telomerase RNA bound by protein motifs specific to telomerase reverse transcriptase. *Mol Cell* 2000;6(2):493-499.
150. Lai CK, Mitchell JR, Collins K. RNA binding domain of telomerase reverse transcriptase. *Mol Cell Biol* 2001;21(4):990-1000.
151. Lai CK, Miller MC, Collins K. Template boundary definition in Tetrahymena telomerase. *Genes Dev* 2002;16(4):415-420.
152. Moriarty TJ, Huard S, Dupuis S, Autexier C. Functional multimerization of human telomerase requires an RNA interaction domain in the N terminus of the catalytic subunit. *Mol Cell Biol* 2002;22(4):1253-1265.
153. O'Connor CM, Lai CK, Collins K. Two purified domains of telomerase reverse transcriptase reconstitute sequence-specific interactions with RNA. *J Biol Chem* 2005;280(17):17533-17539.
154. Counter CM, Meyerson M, Eaton EN, Weinberg RA. The catalytic subunit of yeast telomerase. *Proc Natl Acad Sci U S A* 1997;94(17):9202-9207.
155. Nakayama J, Tahara H, Tahara E et al. Telomerase activation by hTERT in human normal fibroblasts and hepatocellular carcinomas. *Nat Genet* 1998;18(1):65-68.

156. Bryan TM, Goodrich KJ, Cech TR. A mutant of Tetrahymena telomerase reverse transcriptase with increased processivity. *J Biol Chem* 2000;275(31):24199-24207.
157. Peng Y, Mian IS, Lue NF. Analysis of telomerase processivity: mechanistic similarity to HIV-1 reverse transcriptase and role in telomere maintenance. *Mol Cell* 2001;7(6):1201-1211.
158. Wyatt HD, Lobb DA, Beattie TL. Characterization of physical and functional anchor site interactions in human telomerase. *Mol Cell Biol* 2007;27(8):3226-3240.
159. Drosopoulos WC, Prasad VR. The active site residue Valine 867 in human telomerase reverse transcriptase influences nucleotide incorporation and fidelity. *Nucleic Acids Res* 2007;35(4):1155-1168.
160. Seimiya H, Sawada H, Muramatsu Y et al. Involvement of 14-3-3 proteins in nuclear localization of telomerase. *Embo J* 2000;19(11):2652-2661.
161. Counter CM, Hahn WC, Wei W et al. Dissociation among in vitro telomerase activity, telomere maintenance, and cellular immortalization. *Proc Natl Acad Sci U S A* 1998;95(25):14723-14728.
162. Armbruster BN, Banik SS, Guo C, Smith AC, Counter CM. N-terminal domains of the human telomerase catalytic subunit required for enzyme activity in vivo. *Mol Cell Biol* 2001;21(22):7775-7786.
163. Moriarty TJ, Ward RJ, Taboski MA, Autexier C. An anchor site-type defect in human telomerase that disrupts telomere length maintenance and cellular immortalization. *Mol Biol Cell* 2005;16(7):3152-3161.
164. Ji H, Platts MH, Dharamsi LM, Friedman KL. Regulation of telomere length by an N-terminal region of the yeast telomerase reverse transcriptase. *Mol Cell Biol* 2005;25(20):9103-9114.
165. Armbruster BN, Etheridge KT, Broccoli D, Counter CM. Putative telomere-recruiting domain in the catalytic subunit of human telomerase. *Mol Cell Biol* 2003;23(9):3237-3246.
166. Armbruster BN, Linaudic CM, Veldman T, Bansal NP, Downie DL, Counter CM. Rescue of an hTERT mutant defective in telomere elongation by fusion with hPot1. *Mol Cell Biol* 2004;24(8):3552-3561.
167. Lee SR, Wong JM, Collins K. Human telomerase reverse transcriptase motifs required for elongation of a telomeric substrate. *J Biol Chem* 2003;278(52):52531-52536.
168. Wright WE, Piatyszek MA, Rainey WE, Byrd W, Shay JW. Telomerase activity in human germline and embryonic tissues and cells. *Dev Genet* 1996;18(2):173-179.
169. Kim NW, Piatyszek MA, Prowse KR et al. Specific association of human telomerase activity with immortal cells and cancer. *Science* 1994;266(5193):2011-2015.
170. Etheridge KT, Banik SS, Armbruster BN et al. The nucleolar localization domain of the catalytic subunit of human telomerase. *J Biol Chem* 2002;277(27):24764-24770.

171. Yang Y, Chen Y, Zhang C, Huang H, Weissman SM. Nucleolar localization of hTERT protein is associated with telomerase function. *Exp Cell Res* 2002;277(2):201-209.
172. Lin J, Jin R, Zhang B et al. Nucleolar localization of TERT is unrelated to telomerase function in human cells. *J Cell Sci* 2008;121(Pt 13):2169-2176.
173. Khurts S, Masutomi K, Delgermaa L et al. Nucleolin interacts with telomerase. *J Biol Chem* 2004;279(49):51508-51515.
174. Banik SS, Counter CM. Characterization of interactions between PinX1 and human telomerase subunits hTERT and hTR. *J Biol Chem* 2004;279(50):51745-51748.
175. Lin J, Jin R, Zhang B et al. Characterization of a novel effect of hPinX1 on hTERT nucleolar localization. *Biochem Biophys Res Commun* 2007;353(4):946-952.
176. Wong JM, Kusdra L, Collins K. Subnuclear shuttling of human telomerase induced by transformation and DNA damage. *Nat Cell Biol* 2002;4(9):731-736.
177. Zhu Y, Tomlinson RL, Lukowiak AA, Terns RM, Terns MP. Telomerase RNA accumulates in Cajal bodies in human cancer cells. *Mol Biol Cell* 2004;15(1):81-90.
178. Tomlinson RL, Ziegler TD, Supakorndej T, Terns RM, Terns MP. Cell cycle-regulated trafficking of human telomerase to telomeres. *Mol Biol Cell* 2006;17(2):955-965.
179. Romero DP, Blackburn EH. A conserved secondary structure for telomerase RNA. *Cell* 1991;67(2):343-353.
180. Lingner J, Hendrick LL, Cech TR. Telomerase RNAs of different ciliates have a common secondary structure and a permuted template. *Genes Dev* 1994;8(16):1984-1998.
181. Singer MS, Gottschling DE. TLC1: template RNA component of *Saccharomyces cerevisiae* telomerase. *Science* 1994;266(5184):404-409.
182. Blasco MA, Funk W, Villeponteau B, Greider CW. Functional characterization and developmental regulation of mouse telomerase RNA. *Science* 1995;269(5228):1267-1270.
183. McCormick-Graham M, Romero DP. Ciliate telomerase RNA structural features. *Nucleic Acids Res* 1995;23(7):1091-1097.
184. Tsao DA, Wu CW, Lin YS. Molecular cloning of bovine telomerase RNA. *Gene* 1998;221(1):51-58.
185. Feng J, Funk WD, Wang SS et al. The RNA component of human telomerase. *Science* 1995;269(5228):1236-1241.
186. McEachern MJ, Blackburn EH. Runaway telomere elongation caused by telomerase RNA gene mutations. *Nature* 1995;376(6539):403-409.
187. Chen JL, Blasco MA, Greider CW. Secondary structure of vertebrate telomerase RNA. *Cell* 2000;100(5):503-514.
188. Dandjinou AT, Levesque N, Larose S, Lucier JF, Abou Elela S, Wellinger RJ. A phylogenetically based secondary structure for the yeast telomerase RNA. *Curr Biol* 2004;14(13):1148-1158.

189. Leonardi J, Box JA, Bunch JT, Baumann P. TER1, the RNA subunit of fission yeast telomerase. *Nat Struct Mol Biol* 2008;15(1):26-33.
190. Webb CJ, Zakian VA. Identification and characterization of the *Schizosaccharomyces pombe* TER1 telomerase RNA. *Nat Struct Mol Biol* 2008;15(1):34-42.
191. Tzfati Y, Knight Z, Roy J, Blackburn EH. A novel pseudoknot element is essential for the action of a yeast telomerase. *Genes Dev* 2003;17(14):1779-1788.
192. ten Dam E, van Belkum A, Pleij K. A conserved pseudoknot in telomerase RNA. *Nucleic Acids Res* 1991;19(24):6951.
193. Chappell AS, Lundblad V. Structural elements required for association of the *Saccharomyces cerevisiae* telomerase RNA with the Est2 reverse transcriptase. *Mol Cell Biol* 2004;24(17):7720-7736.
194. Lin J, Ly H, Hussain A et al. A universal telomerase RNA core structure includes structured motifs required for binding the telomerase reverse transcriptase protein. *Proc Natl Acad Sci U S A* 2004.
195. Zappulla DC, Cech TR. Yeast telomerase RNA: a flexible scaffold for protein subunits. *Proc Natl Acad Sci U S A* 2004;101(27):10024-10029.
196. Theimer CA, Feigon J. Structure and function of telomerase RNA. *Curr Opin Struct Biol* 2006;16(3):307-318.
197. Chen JL, Greider CW. Telomerase RNA structure and function: implications for dyskeratosis congenita. *Trends Biochem Sci* 2004;29(4):183-192.
198. Vulliamy T, Marrone A, Goldman F et al. The RNA component of telomerase is mutated in autosomal dominant dyskeratosis congenita. *Nature* 2001;413(6854):432-435.
199. Autexier C, Pruzan R, Funk WD, Greider CW. Reconstitution of human telomerase activity and identification of a minimal functional region of the human telomerase RNA. *EMBO J* 1996;15(21):5928-5935.
200. Tesmer VM, Ford LP, Holt SE et al. Two inactive fragments of the integral RNA cooperate to assemble active telomerase with the human protein catalytic subunit (hTERT) in vitro. *Mol Cell Biol* 1999;19(9):6207-6216.
201. Martin-Rivera L, Blasco MA. Identification of functional domains and dominant negative mutations in vertebrate telomerase RNA using an in vivo reconstitution system. *J Biol Chem* 2001;276(8):5856-5865.
202. Chen JL, Greider CW. Template boundary definition in mammalian telomerase. *Genes Dev* 2003;17(22):2747-2752.
203. Chen JL, Greider CW. Determinants in mammalian telomerase RNA that mediate enzyme processivity and cross-species incompatibility. *Embo J* 2003;22(2):304-314.
204. Ly H, Blackburn EH, Parslow TG. Comprehensive structure-function analysis of the core domain of human telomerase RNA. *Mol Cell Biol* 2003;23(19):6849-6856.
205. Ly H, Xu L, Rivera MA, Parslow TG, Blackburn EH. A role for a novel 'trans-pseudoknot' RNA-RNA interaction in the functional dimerization of human telomerase. *Genes Dev* 2003;17(9):1078-1083.

206. Chen JL, Greider CW. Functional analysis of the pseudoknot structure in human telomerase RNA. *Proc Natl Acad Sci U S A* 2005;102(23):8080-8085; discussion 8077-8089.
207. Theimer CA, Blois CA, Feigon J. Structure of the human telomerase RNA pseudoknot reveals conserved tertiary interactions essential for function. *Mol Cell* 2005;17(5):671-682.
208. Moriarty TJ, Marie-Egyptienne DT, Autexier C. Functional organization of repeat addition processivity and DNA synthesis determinants in the human telomerase multimer. *Mol Cell Biol* 2004;24(9):3720-3733.
209. Qiao F, Cech TR. Triple-helix structure in telomerase RNA contributes to catalysis. *Nat Struct Mol Biol* 2008;15(6):634-640.
210. Kim NK, Zhang Q, Zhou J, Theimer CA, Peterson RD, Feigon J. Solution structure and dynamics of the wild-type pseudoknot of human telomerase RNA. *J Mol Biol* 2008;384(5):1249-1261.
211. Mitchell JR, Collins K. Human telomerase activation requires two independent interactions between telomerase RNA and telomerase reverse transcriptase. *Mol Cell* 2000;6(2):361-371.
212. Chen JL, Opperman KK, Greider CW. A critical stem-loop structure in the CR4-CR5 domain of mammalian telomerase RNA. *Nucleic Acids Res* 2002;30(2):592-597.
213. Drosopoulos WC, Drenzo R, Prasad VR. Human telomerase RNA template sequence is a determinant of telomere repeat extension rate. *J Biol Chem* 2005;280(38):32801-32810.
214. Ueda CT, Roberts RW. Analysis of a long-range interaction between conserved domains of human telomerase RNA. *RNA* 2004;10(1):139-147.
215. Mitchell JR, Cheng J, Collins K. A box H/ACA small nucleolar RNA-like domain at the human telomerase RNA 3' end. *Mol Cell Biol* 1999;19(1):567-576.
216. Mitchell JR, Wood E, Collins K. A telomerase component is defective in the human disease dyskeratosis congenita. *Nature* 1999;402(6761):551-555.
217. Lukowiak AA, Narayanan A, Li ZH, Terns RM, Terns MP. The snoRNA domain of vertebrate telomerase RNA functions to localize the RNA within the nucleus. *RNA* 2001;7(12):1833-1844.
218. Fu D, Collins K. Distinct biogenesis pathways for human telomerase RNA and H/ACA small nucleolar RNAs. *Mol Cell* 2003;11(5):1361-1372.
219. Jady BE, Bertrand E, Kiss T. Human telomerase RNA and box H/ACA scaRNAs share a common Cajal body-specific localization signal. *J Cell Biol* 2004;164(5):647-652.
220. Theimer CA, Jady BE, Chim N et al. Structural and functional characterization of human telomerase RNA processing and cajal body localization signals. *Mol Cell* 2007;27(6):869-881.
221. Cristofari G, Adolf E, Reichenbach P et al. Human telomerase RNA accumulation in Cajal bodies facilitates telomerase recruitment to telomeres and telomere elongation. *Mol Cell* 2007;27(6):882-889.

222. Avilion AA, Piatyszek MA, Gupta J, Shay JW, Bacchetti S, Greider CW. Human telomerase RNA and telomerase activity in immortal cell lines and tumor tissues. *Cancer Res* 1996;56(3):645-650.
223. Narayanan A, Lukowiak A, Jady BE et al. Nucleolar localization signals of box H/ACA small nucleolar RNAs. *EMBO J* 1999;18(18):5120-5130.
224. Morris GE. The Cajal body. *Biochim Biophys Acta* 2008;1783(11):2108-2115.
225. Tomlinson RL, Abreu EB, Ziegler T et al. Telomerase Reverse Transcriptase Is Required for the Localization of Telomerase RNA to Cajal Bodies and Telomeres in Human Cancer Cells. *Mol Biol Cell* 2008.
226. Meier UT. The many facets of H/ACA ribonucleoproteins. *Chromosoma* 2005;114(1):1-14.
227. Matera AG, Terns RM, Terns MP. Non-coding RNAs: lessons from the small nuclear and small nucleolar RNAs. *Nat Rev Mol Cell Biol* 2007;8(3):209-220.
228. Hoareau-Aveilla C, Bonoli M, Caizergues-Ferrer M, Henry Y. hNaf1 is required for accumulation of human box H/ACA snoRNPs, scaRNPs, and telomerase. *RNA* 2006;12(5):832-840.
229. Darzacq X, Kittur N, Roy S, Shav-Tal Y, Singer RH, Meier UT. Stepwise RNP assembly at the site of H/ACA RNA transcription in human cells. *J Cell Biol* 2006;173(2):207-218.
230. Trahan C, Dragon F. Dyskeratosis congenita mutations in the H/ACA domain of human telomerase RNA affect its assembly into a pre-RNP. *RNA* 2009;15(2):235-243.
231. Fu D, Collins K. Purification of human telomerase complexes identifies factors involved in telomerase biogenesis and telomere length regulation. *Mol Cell* 2007;28(5):773-785.
232. Venteicher AS, Meng Z, Mason PJ, Veenstra TD, Artandi SE. Identification of ATPases pontin and reptin as telomerase components essential for holoenzyme assembly. *Cell* 2008;132(6):945-957.
233. Baek SH. When ATPases pontin and reptin met telomerase. *Dev Cell* 2008;14(4):459-461.
234. Venteicher AS, Abreu EB, Meng Z et al. A human telomerase holoenzyme protein required for Cajal body localization and telomere synthesis. *Science* 2009;323(5914):644-648.
235. Tycowski KT, Shu MD, Kukoyi A, Steitz JA. A conserved WD40 protein binds the Cajal body localization signal of scaRNP particles. *Mol Cell* 2009;34(1):47-57.
236. Cristofari G LJ, editor. The telomerase ribonucleoprotein particle. 2 ed: Cold Spring Harbor Laboratory Press; 2006. 21-47 p.
237. Nowak T, Januszkiewicz D, Zawada M et al. Amplification of hTERT and hTERC genes in leukemic cells with high expression and activity of telomerase. *Oncol Rep* 2006;16(2):301-305.
238. Andersson S, Wallin KL, Hellstrom AC et al. Frequent gain of the human telomerase gene TERC at 3q26 in cervical adenocarcinomas. *Br J Cancer* 2006;95(3):331-338.

239. Zaug AJ, Linger J, Cech TR. Method for determining RNA 3' ends and application to human telomerase RNA. *Nucleic Acids Res* 1996;24(3):532-533.
240. Collins K. Physiological assembly and activity of human telomerase complexes. *Mech Ageing Dev* 2008;129(1-2):91-98.
241. Zhang A, Zheng C, Lindvall C et al. Frequent amplification of the telomerase reverse transcriptase gene in human tumors. *Cancer Res* 2000;60(22):6230-6235.
242. Fan X, Wang Y, Kratz J et al. hTERT gene amplification and increased mRNA expression in central nervous system embryonal tumors. *Am J Pathol* 2003;162(6):1763-1769.
243. Telomeres and telomerase in cancer. New York, NY: Humana press; 2009.
244. Kilian A, Bowtell DD, Abud HE et al. Isolation of a candidate human telomerase catalytic subunit gene, which reveals complex splicing patterns in different cell types. *Hum Mol Genet* 1997;6(12):2011-2019.
245. Ulaner GA, Hu JF, Vu TH, Giudice LC, Hoffman AR. Telomerase activity in human development is regulated by human telomerase reverse transcriptase (hTERT) transcription and by alternate splicing of hTERT transcripts. *Cancer Res* 1998;58(18):4168-4172.
246. Yi X, White DM, Aisner DL, Baur JA, Wright WE, Shay JW. An alternate splicing variant of the human telomerase catalytic subunit inhibits telomerase activity. *Neoplasia* 2000;2(5):433-440.
247. Colgin LM, Wilkinson C, Englezou A, Kilian A, Robinson MO, Reddel RR. The hTERT $\alpha$  splice variant is a dominant negative inhibitor of telomerase activity. *Neoplasia* 2000;2(5):426-432.
248. Kim JH, Park SM, Kang MR et al. Ubiquitin ligase MKRN1 modulates telomere length homeostasis through a proteolysis of hTERT. *Genes Dev* 2005;19(7):776-781.
249. Prathapam R, Witkin KL, O'Connor CM, Collins K. A telomerase holoenzyme protein enhances telomerase RNA assembly with telomerase reverse transcriptase. *Nat Struct Mol Biol* 2005;12(3):252-257.
250. Stone MD, Mihalusova M, O'Connor C M, Prathapam R, Collins K, Zhuang X. Stepwise protein-mediated RNA folding directs assembly of telomerase ribonucleoprotein. *Nature* 2007;446(7134):458-461.
251. O'Connor CM, Collins K. A novel RNA binding domain in tetrahymena telomerase p65 initiates hierarchical assembly of telomerase holoenzyme. *Mol Cell Biol* 2006;26(6):2029-2036.
252. Holt SE, Aisner DL, Baur J et al. Functional requirement of p23 and Hsp90 in telomerase complexes. *Genes Dev* 1999;13(7):817-826.
253. Forsythe HL, Jarvis JL, Turner JW, Elmore LW, Holt SE. Stable association of hsp90 and p23, but not hsp70, with active human telomerase. *J Biol Chem* 2001;276(19):15571-15574.
254. Keppler BR, Grady AT, Jarstfer MB. The biochemical role of the heat shock protein 90 chaperone complex in establishing human telomerase activity. *J Biol Chem* 2006;281(29):19840-19848.
255. Toogun OA, Dezwaan DC, Freeman BC. The hsp90 molecular chaperone modulates multiple telomerase activities. *Mol Cell Biol* 2008;28(1):457-467.

256. Toogun OA, Zeiger W, Freeman BC. The p23 molecular chaperone promotes functional telomerase complexes through DNA dissociation. *Proc Natl Acad Sci U S A* 2007;104(14):5765-5770.
257. Bachand F, Boisvert FM, Cote J, Richard S, Autexier C. The product of the survival of motor neuron (SMN) gene is a human telomerase-associated protein. *Mol Biol Cell* 2002;13(9):3192-3202.
258. Wenz C, Enenkel B, Amacker M, Kelleher C, Damm K, Lingner J. Human telomerase contains two cooperating telomerase RNA molecules. *Embo J* 2001;20(13):3526-3534.
259. Fouche N, Moon IK, Keppler BR, Griffith JD, Jarstfer MB. Electron microscopic visualization of telomerase from *Euplotes aediculatus* bound to a model telomere DNA. *Biochemistry* 2006;45(31):9624-9631.
260. Prescott J, Blackburn EH. Functionally interacting telomerase RNAs in the yeast telomerase complex. *Genes Dev* 1997;11(21):2790-2800.
261. Ren X, Gavory G, Li H, Ying L, Klenerman D, Balasubramanian S. Identification of a new RNA:RNA interaction site for human telomerase RNA (hTR): structural implications for hTR accumulation and a dyskeratosis congenita point mutation. *Nucleic Acids Res* 2003;31(22):6509-6515.
262. Alves D, Li H, Codrington R et al. Single-molecule analysis of human telomerase monomer. *Nat Chem Biol* 2008;4(5):287-289.
263. Errington TM, Fu D, Wong JM, Collins K. Disease-associated human telomerase RNA variants show loss of function for telomere synthesis without dominant-negative interference. *Mol Cell Biol* 2008;28(20):6510-6520.
264. Bryan TM, Goodrich KJ, Cech TR. Tetrahymena telomerase is active as a monomer. *Mol Biol Cell* 2003;14(12):4794-4804.
265. Wright WE, Tesmer VM, Liao ML, Shay JW. Normal human telomeres are not late replicating. *Exp Cell Res* 1999;251(2):492-499.
266. Jady BE, Richard P, Bertrand E, Kiss T. Cell cycle-dependent recruitment of telomerase RNA and Cajal bodies to human telomeres. *Mol Biol Cell* 2006;17(2):944-954.
267. Morin GB. Recognition of a chromosome truncation site associated with alpha-thalassaemia by human telomerase. *Nature* 1991;353(6343):454-456.
268. Zahler AM, Williamson JR, Cech TR, Prescott DM. Inhibition of telomerase by G-quartet DNA structures. *Nature* 1991;350(6320):718-720.
269. Oganessian L, Moon IK, Bryan TM, Jarstfer MB. Extension of G-quadruplex DNA by ciliate telomerase. *EMBO J* 2006;25(5):1148-1159.
270. Oganessian L, Graham ME, Robinson PJ, Bryan TM. Telomerase recognizes G-quadruplex and linear DNA as distinct substrates. *Biochemistry* 2007;46(40):11279-11290.
271. Greider CW. Telomerase is processive. *Mol Cell Biol* 1991;11(9):4572-4580.
272. Morin GB. The human telomere terminal transferase enzyme is a ribonucleoprotein that synthesizes TTAGGG repeats. *Cell* 1989;59(3):521-529.
273. Cohn M, Blackburn EH. Telomerase in yeast. *Science* 1995;269(5222):396-400.

274. Prowse KR, Avilion AA, Greider CW. Identification of a nonprocessive telomerase activity from mouse cells. *Proc Natl Acad Sci U S A* 1993;90(4):1493-1497.
275. Prescott J, Blackburn EH. Telomerase RNA mutations in *Saccharomyces cerevisiae* alter telomerase action and reveal nonprocessivity in vivo and in vitro. *Genes Dev* 1997;11(4):528-540.
276. Chang M, Arneric M, Lingner J. Telomerase repeat addition processivity is increased at critically short telomeres in a Tel1-dependent manner in *Saccharomyces cerevisiae*. *Genes Dev* 2007;21(19):2485-2494.
277. Lue NF. A physical and functional constituent of telomerase anchor site. *J Biol Chem* 2005;280(28):26586-26591.
278. Lue NF, Li Z. Modeling and structure function analysis of the putative anchor site of yeast telomerase. *Nucleic Acids Res* 2007;35(15):5213-5222.
279. Zaug AJ, Podell ER, Cech TR. Mutation in TERT separates processivity from anchor-site function. *Nat Struct Mol Biol* 2008;15(8):870-872.
280. Collins K, Greider CW. Tetrahymena telomerase catalyzes nucleolytic cleavage and nonprocessive elongation. *Genes Dev* 1993;7(7B):1364-1376.
281. Wang H, Blackburn EH. De novo telomere addition by Tetrahymena telomerase in vitro. *Embo J* 1997;16(4):866-879.
282. Harrington LA, Greider CW. Telomerase primer specificity and chromosome healing. *Nature* 1991;353(6343):451-454.
283. Lee MS, Blackburn EH. Sequence-specific DNA primer effects on telomerase polymerization activity. *Mol Cell Biol* 1993;13(10):6586-6599.
284. Wallweber G, Gryaznov S, Pongracz K, Pruzan R. Interaction of human telomerase with its primer substrate. *Biochemistry* 2003;42(2):589-600.
285. Hammond PW, Lively TN, Cech TR. The anchor site of telomerase from *Euplotes aediculatus* revealed by photo-cross-linking to single- and double-stranded DNA primers. *Mol Cell Biol* 1997;17(1):296-308.
286. Finger SN, Bryan TM. Multiple DNA-binding sites in Tetrahymena telomerase. *Nucleic Acids Res* 2008;36(4):1260-1272.
287. Lue NF, Peng Y. Negative regulation of yeast telomerase activity through an interaction with an upstream region of the DNA primer. *Nucleic Acids Res* 1998;26(6):1487-1494.
288. Baran N, Haviv Y, Paul B, Manor H. Studies on the minimal lengths required for DNA primers to be extended by the Tetrahymena telomerase: implications for primer positioning by the enzyme. *Nucleic Acids Res* 2002;30(24):5570-5578.
289. Romi E, Baran N, Gantman M et al. High-resolution physical and functional mapping of the template adjacent DNA binding site in catalytically active telomerase. *Proc Natl Acad Sci U S A* 2007;104(21):8791-8796.
290. Friedman KL, Heit JJ, Long DM, Cech TR. N-terminal domain of yeast telomerase reverse transcriptase: recruitment of Est3p to the telomerase complex. *Mol Biol Cell* 2003;14(1):1-13.
291. Hayflick L, Moorhead PS. The serial cultivation of human diploid cell strains. *Exp Cell Res* 1961;25:585-621.

292. Hayflick L. The Limited In Vitro Lifetime of Human Diploid Cell Strains. *Exp Cell Res* 1965;37:614-636.
293. Allsopp RC, Vaziri H, Patterson C et al. Telomere length predicts replicative capacity of human fibroblasts. *Proc Natl Acad Sci U S A* 1992;89(21):10114-10118.
294. Counter CM, Gupta J, Harley CB, Leber B, Bacchetti S. Telomerase activity in normal leukocytes and in hematologic malignancies. *Blood* 1995;85(9):2315-2320.
295. Stewart SA, Weinberg RA. Telomeres: cancer to human aging. *Annu Rev Cell Dev Biol* 2006;22:531-557.
296. Smogorzewska A, van Steensel B, Bianchi A et al. Control of human telomere length by TRF1 and TRF2. *Mol Cell Biol* 2000;20(5):1659-1668.
297. Loayza D, De Lange T. POT1 as a terminal transducer of TRF1 telomere length control. *Nature* 2003;423(6943):1013-1018.
298. Dimri GP, Lee X, Basile G et al. A biomarker that identifies senescent human cells in culture and in aging skin in vivo. *Proc Natl Acad Sci U S A* 1995;92(20):9363-9367.
299. Narita M, Nunez S, Heard E et al. Rb-mediated heterochromatin formation and silencing of E2F target genes during cellular senescence. *Cell* 2003;113(6):703-716.
300. Campisi J, d'Adda di Fagagna F. Cellular senescence: when bad things happen to good cells. *Nat Rev Mol Cell Biol* 2007;8(9):729-740.
301. Blasco MA, Lee HW, Hande MP et al. Telomere shortening and tumor formation by mouse cells lacking telomerase RNA. *Cell* 1997;91(1):25-34.
302. Lee HW, Blasco MA, Gottlieb GJ, Horner JW, 2nd, Greider CW, DePinho RA. Essential role of mouse telomerase in highly proliferative organs. *Nature* 1998;392(6676):569-574.
303. Rudolph KL, Chang S, Lee HW et al. Longevity, stress response, and cancer in aging telomerase-deficient mice. *Cell* 1999;96(5):701-712.
304. Samper E, Flores JM, Blasco MA. Restoration of telomerase activity rescues chromosomal instability and premature aging in *Terc*<sup>-/-</sup> mice with short telomeres. *EMBO Rep* 2001;2(9):800-807.
305. Bodnar AG, Ouellette M, Frolkis M et al. Extension of life-span by introduction of telomerase into normal human cells. *Science* 1998;279(5349):349-352.
306. Counter CM, Meyerson M, Eaton EN et al. Telomerase activity is restored in human cells by ectopic expression of hTERT (hEST2), the catalytic subunit of telomerase. *Oncogene* 1998;16(9):1217-1222.
307. Vaziri H, Benchimol S. Reconstitution of telomerase activity in normal human cells leads to elongation of telomeres and extended replicative life span. *Curr Biol* 1998;8(5):279-282.
308. Zhu J, Wang H, Bishop JM, Blackburn EH. Telomerase extends the lifespan of virus-transformed human cells without net telomere lengthening. *Proc Natl Acad Sci U S A* 1999;96(7):3723-3728.
309. Halvorsen TL, Leibowitz G, Levine F. Telomerase activity is sufficient to allow transformed cells to escape from crisis. *Mol Cell Biol* 1999;19(3):1864-1870.

310. Kiyono T, Foster SA, Koop JI, McDougall JK, Galloway DA, Klingelutz AJ. Both Rb/p16INK4a inactivation and telomerase activity are required to immortalize human epithelial cells. *Nature* 1998;396(6706):84-88.
311. Hahn WC, Counter CM, Lundberg AS, Beijersbergen RL, Brooks MW, Weinberg RA. Creation of human tumour cells with defined genetic elements. *Nature* 1999;400(6743):464-468.
312. Hahn WC, Stewart SA, Brooks MW et al. Inhibition of telomerase limits the growth of human cancer cells. *Nat Med* 1999;5(10):1164-1170.
313. Zhang X, Mar V, Zhou W, Harrington L, Robinson MO. Telomere shortening and apoptosis in telomerase-inhibited human tumor cells. *Genes Dev* 1999;13(18):2388-2399.
314. Zimmermann S, Martens UM. Telomeres and telomerase as targets for cancer therapy. *Cell Mol Life Sci* 2007;64(7-8):906-921.
315. Bryan TM, Englezou A, Dalla-Pozza L, Dunham MA, Reddel RR. Evidence for an alternative mechanism for maintaining telomere length in human tumors and tumor-derived cell lines. *Nat Med* 1997;3(11):1271-1274.
316. Bryan TM, Englezou A, Gupta J, Bacchetti S, Reddel RR. Telomere elongation in immortal human cells without detectable telomerase activity. *EMBO J* 1995;14(17):4240-4248.
317. Cesare AJ, Reddel RR. Telomere uncapping and alternative lengthening of telomeres. *Mech Ageing Dev* 2008;129(1-2):99-108.
318. Muntoni A, Neumann AA, Hills M, Reddel RR. Telomere elongation involves intra-molecular DNA replication in cells utilizing alternative lengthening of telomeres. *Hum Mol Genet* 2009;18(6):1017-1027.
319. Londono-Vallejo JA, Der-Sarkissian H, Cazes L, Bacchetti S, Reddel RR. Alternative lengthening of telomeres is characterized by high rates of telomeric exchange. *Cancer Res* 2004;64(7):2324-2327.
320. Kirwan M, Dokal I. Dyskeratosis congenita, stem cells and telomeres. *Biochim Biophys Acta* 2009;1792(4):371-379.
321. Vulliamy T, Marrone A, Szydlo R, Walne A, Mason PJ, Dokal I. Disease anticipation is associated with progressive telomere shortening in families with dyskeratosis congenita due to mutations in TERC. *Nat Genet* 2004;36(5):447-449.
322. Armanios M, Chen JL, Chang YP et al. Haploinsufficiency of telomerase reverse transcriptase leads to anticipation in autosomal dominant dyskeratosis congenita. *Proc Natl Acad Sci U S A* 2005;102(44):15960-15964.
323. Wong JM, Collins K. Telomerase RNA level limits telomere maintenance in X-linked dyskeratosis congenita. *Genes Dev* 2006;20(20):2848-2858.
324. Walne AJ, Vulliamy T, Marrone A et al. Genetic heterogeneity in autosomal recessive dyskeratosis congenita with one subtype due to mutations in the telomerase-associated protein NOP10. *Hum Mol Genet* 2007;16(13):1619-1629.
325. Vulliamy T, Beswick R, Kirwan M et al. Mutations in the telomerase component NHP2 cause the premature ageing syndrome dyskeratosis congenita. *Proc Natl Acad Sci U S A* 2008;105(23):8073-8078.

326. Vulliamy TJ, Walne A, Baskaradas A, Mason PJ, Marrone A, Dokal I. Mutations in the reverse transcriptase component of telomerase (TERT) in patients with bone marrow failure. *Blood Cells Mol Dis* 2005;34(3):257-263.
327. Xin ZT, Beauchamp AD, Calado RT et al. Functional characterization of natural telomerase mutations found in patients with hematologic disorders. *Blood* 2007;109(2):524-532.
328. Kirwan M, Beswick R, Vulliamy T et al. Exogenous TERC alone can enhance proliferative potential, telomerase activity and telomere length in lymphocytes from dyskeratosis congenita patients. *Br J Haematol* 2009;144(5):771-781.
329. Walne AJ, Vulliamy T, Beswick R, Kirwan M, Dokal I. TINF2 mutations result in very short telomeres: analysis of a large cohort of patients with dyskeratosis congenita and related bone marrow failure syndromes. *Blood* 2008;112(9):3594-3600.
330. Savage SA, Giri N, Baerlocher GM, Orr N, Lansdorp PM, Alter BP. TINF2, a component of the shelterin telomere protection complex, is mutated in dyskeratosis congenita. *Am J Hum Genet* 2008;82(2):501-509.
331. Chiang YJ, Kim SH, Tessarollo L, Campisi J, Hodes RJ. Telomere-associated protein TIN2 is essential for early embryonic development through a telomerase-independent pathway. *Mol Cell Biol* 2004;24(15):6631-6634.
332. Knight SW, Heiss NS, Vulliamy TJ et al. Unexplained aplastic anaemia, immunodeficiency, and cerebellar hypoplasia (Hoyeraal-Hreidarsson syndrome) due to mutations in the dyskeratosis congenita gene, DKC1. *Br J Haematol* 1999;107(2):335-339.
333. Marrone A, Walne A, Tamary H et al. Telomerase reverse-transcriptase homozygous mutations in autosomal recessive dyskeratosis congenita and Hoyeraal-Hreidarsson syndrome. *Blood* 2007;110(13):4198-4205.
334. Yamaguchi H, Calado RT, Ly H et al. Mutations in TERT, the gene for telomerase reverse transcriptase, in aplastic anemia. *N Engl J Med* 2005;352(14):1413-1424.
335. Vulliamy T, Marrone A, Dokal I, Mason PJ. Association between aplastic anaemia and mutations in telomerase RNA. *Lancet* 2002;359(9324):2168-2170.
336. Marrone A, Sokhal P, Walne A et al. Functional characterization of novel telomerase RNA (TERC) mutations in patients with diverse clinical and pathological presentations. *Haematologica* 2007;92(8):1013-1020.
337. Armanios MY, Chen JJ, Cogan JD et al. Telomerase mutations in families with idiopathic pulmonary fibrosis. *N Engl J Med* 2007;356(13):1317-1326.
338. Garcia CK, Wright WE, Shay JW. Human diseases of telomerase dysfunction: insights into tissue aging. *Nucleic Acids Res* 2007.
339. Morgenstern JP, Land H. Advanced mammalian gene transfer: high titre retroviral vectors with multiple drug selection markers and a complementary helper-free packaging cell line. *Nucleic Acids Res* 1990;18(12):3587-3596.
340. Naviaux RK, Costanzi E, Haas M, Verma IM. The pCL vector system: rapid production of helper-free, high-titer, recombinant retroviruses. *J Virol* 1996;70(8):5701-5705.

341. Hardy CD, Schultz CS, Collins K. Requirements for the dGTP-dependent repeat addition processivity of recombinant *Tetrahymena* telomerase. *J Biol Chem* 2001;276(7):4863-4871.
342. Jacques PS, Wohrl BM, Ottmann M, Darlix JL, Le Grice SF. Mutating the "primer grip" of p66 HIV-1 reverse transcriptase implicates tryptophan-229 in template-primer utilization. *J Biol Chem* 1994;269(42):26472-26478.
343. Wilson IA, Haft DH, Getzoff ED, Tainer JA, Lerner RA, Brenner S. Identical short peptide sequences in unrelated proteins can have different conformations: a testing ground for theories of immune recognition. *Proc Natl Acad Sci U S A* 1985;82(16):5255-5259.
344. Snow BE, Erdmann N, Cruickshank J et al. Functional conservation of the telomerase protein est1p in humans. *Curr Biol* 2003;13(8):698-704.
345. Benjamin S, Baran N, Manor H. Interference footprinting analysis of telomerase elongation complexes. *Mol Cell Biol* 2000;20(12):4224-4237.
346. Fletcher TM, Sun D, Salazar M, Hurley LH. Effect of DNA secondary structure on human telomerase activity. *Biochemistry* 1998;37(16):5536-5541.
347. Zaug AJ, Podell ER, Cech TR. Human POT1 disrupts telomeric G-quadruplexes allowing telomerase extension in vitro. *Proc Natl Acad Sci U S A* 2005;102(31):10864-10869.
348. Kim NW, Wu F. Advances in quantification and characterization of telomerase activity by the telomeric repeat amplification protocol (TRAP). *Nucleic Acids Res* 1997;25(13):2595-2597.
349. Cramer P. Multisubunit RNA polymerases. *Curr Opin Struct Biol* 2002;12(1):89-97.
350. Cramer P. RNA polymerase II structure: from core to functional complexes. *Curr Opin Genet Dev* 2004;14(2):218-226.
351. Canard B, Chowdhury K, Sarfati R, Doublet S, Richardson CC. The motif D loop of human immunodeficiency virus type 1 reverse transcriptase is critical for nucleoside 5'-triphosphate selectivity. *J Biol Chem* 1999;274(50):35768-35776.
352. Tsakiri KD, Cronkhite JT, Kuan PJ et al. Adult-onset pulmonary fibrosis caused by mutations in telomerase. *Proc Natl Acad Sci U S A* 2007;104(18):7552-7557.
353. Cristofari G, Lingner J. Telomere length homeostasis requires that telomerase levels are limiting. *EMBO J* 2006;25(3):565-574.
354. Wu YL, Dudognon C, Nguyen E et al. Immunodetection of human telomerase reverse-transcriptase (hTERT) re-appraised: nucleolin and telomerase cross paths. *J Cell Sci* 2006;119(Pt 13):2797-2806.